Astrophysics and Space Science Proceedings 35

J.M. Trigo-Rodriguez
François Raulin
C. Muller
Conor Nixon *Editors*

# The Early Evolution of the Atmospheres of Terrestrial Planets

Springer

Astrophysics and Space Science Proceedings
Volume 35

For further volumes:
http://www.springer.com/series/7395

J.M. Trigo-Rodriguez • François Raulin
Christian Muller • Conor Nixon
Editors

# The Early Evolution of the Atmospheres of Terrestrial Planets

Springer

*Editors*
J.M. Trigo-Rodriguez
Campus UAB, Sciences Faculty
Institute of Space Sciences
(CSIC-IEEC)
Bellaterra, Spain

François Raulin
Université Paris Est Créteil
LISA, UMR CNRS/UPEC/UPD/IPSL
Créteil CX, France

Christian Muller
Earth and Space Science Coordination
B.USOC
Brussels, Belgium

Conor Nixon
Department of Astronomy
University of Maryland
Greenbelt, MD, USA

ISSN 1570-6591
ISBN 978-1-4614-5190-7
DOI 10.1007/978-1-4614-5191-4
Springer New York Heidelberg Dordrecht London

ISSN 1570-6605 (electronic)
ISBN 978-1-4614-5191-4 (eBook)

Library of Congress Control Number: 2013937721

# Contents

# Chapter 1
# Introduction: On the Early Evolution of the Atmosphere of Terrestrial Planets: COST Action CM#0805

**Josep M. Trigo-Rodríguez, Christian Muller, Conor Nixon, and François Raulin**

**Abstract** The early setting and evolution of planetary atmospheres of rocky planets is a hot, but still immature research topic. A better understanding of the processes at work at that early epoch in the history of our solar system is certainly required, particularly at this historical juncture when we are just discovering the first exoplanets similar to Earth. These new worlds need to be put in their astrophysical and cosmochemical context, as we understand stars in the Cosmos as physical entities similar to the Sun, but with different masses, composition, and distinctive evolutionary stages. Exoplanets discovered so far exhibit large diversity as a direct consequence of having experienced differing births, evolutionary stages, and being subjected to stochastic processes in the early stages of their growth and evolution. To understand what is going on in the first stages of planetary evolution we must promote interdisciplinary research. That should yield better answers about the role played in planetary setting and evolution by processes such as accretion, chemical differentiation, outgassing, impacts, and the different energy fluxes from their host stars. Our current knowledge regarding the initial atmospheric evolution of the Earth is scarce. State-of-the-art analyses of primitive meteorites, together with returned

J.M. Trigo-Rodríguez (✉)
Institute of Space Sciences (CSIC-IEEC), Campus UAB, Facultat de Ciències, Torre C5-pares, 08193 Bellaterra, Barcelona, Spain
e-mail: trigo@ieec.uab.es

C. Muller
B.USOC Earth and Space Science Coordination, Brussels, Belgium

C. Nixon
Planetary Systems Laboratory, University of Maryland and NASA Goddard Space Flight Center, Greenbelt, MD 20771, USA
e-mail: conor.a.nixon@nasa.gov

F. Raulin
LISA, UMR CNRS 7583, Université Paris Est-Créteil Val de Marne (UPEC) & Université Paris Diderot (UPD), Paris, France

J.M. Trigo-Rodriguez et al. (eds.), *The Early Evolution of the Atmospheres of Terrestrial Planets*, Astrophysics and Space Science Proceedings 35,
DOI 10.1007/978-1-4614-5191-4_1, © Springer Science+Business Media New York 2013

asteroidal and cometary materials will be able to offer us more realistic starting chemical compositions for the primordial building blocks of terrestrial planets. Searching for chemical signatures in Earth-like exoplanets could be an interesting future field of research, and the matches found will provide new points to be compared with increasingly sophisticated atmospheric models. Then, new evidence in other worlds can contribute to a better understanding of the transition point from a hostile to a habitable world. To define the role of N in such context was one of the main goals to promote this COST CM0805 workshop.

## Introduction: The Earliest Setting of Planetary Atmospheres

The origin, and evolution of the atmospheres of terrestrial planets is of crucial importance to understand many cosmochemical, and astrobiological related issues (Holland 1962; Kasting 1993, 1997). We asked ourselves if the contents of the (Lewis and Prinn 1984) book or of the review chapters published in Atreya et al. (1989) compilation should be revisited in the context of recent computational capabilities, and geochemical evidence. After several space missions devoted to gain insight on remote solar system objects we know much more, for example, on the composition of comets and primitive meteorites. Also a significant progress has been made in photochemistry of planetary atmospheres since Yung and DeMore (1999) book dedicated to that issue. Consequently, we think that this proceedings book is making a significant contribution to these fields because different researchers have put all the effort in providing new clues in their respective fields on aspects scarcely treated in scientific literature. This book provides an interesting update to different research areas concerning the origins and the early evolution of planetary atmospheres.

Exoplanet research might provide additional clues for our understanding of the Earth transition from a hot accretionary phase to become a habitable world. Solar system planets have evolved with time to the present stage, and we have lost part of this information during their evolutionary way. Clues on the first stages in planetary evolution can be obtained from new discoveries around other stars as the exoplanets can be in different evolutionary stages, and be the product of similar or different formation processes. Many questions arise in the interpretation of these findings as e.g.: what is the potential role of $N_2$ in these atmospheres? How complex can be the organics formed in N-rich planetary environments? What are the processes involved in this chemical evolution?

In this context, the abundance of N and other volatile elements in planetary atmospheres can provide highly valuable information about the processes that brought them to terrestrial planets. $N_2$ is assumed to be a by-product after the release of $NH_3$ during outgassing, but it can be easily dissociated by EUV solar radiation in the upper atmosphere. An example of how important is assessing the depletion mechanisms of chemical species in planetary atmospheres. In any case, our current knowledge of the initial atmospheric composition of the Earth is scarce because we still have not identified paleosols older than 3.8 Gyr. Despite this, zircon grains suggest that liquid water, and probably other volatiles, were present on the

Earth's surface about 4.3 Gyr ago, even though we initially imagined our early world marked by volcanic activity (Valley et al. 2001).

Nitrogen is also one of the atoms of life and its delicate balance with oxygen in the Earth's atmosphere conditions the habitability of the surface. Cyanhydric acid, and nitric oxide, among other N-bearing compounds, could have played roles in the chemical evolution of early life. The biomarker character of nitrogen containing molecules in planetary systems was a theme of this meeting. Nitric oxide is also one of the main elements of the formation of the Earth's ionosphere and thus contributes, together with the magnetic field, to the habitability of the planet. These are some of the main issues that motivate us to organize this workshop.

## Book Contributions in These Proceedings

The book starts with a general overview on the origin of N, and the role of Solar System minor bodies in the delivery of volatiles to Earth. This review chapter is written by Trigo-Rodríguez (2013). Oxygen isotopic data is particularly suggestive that enstatite and ordinary chondrites were the main primordial building blocks of the Earth (Wasson 2000). Such meteorites host several orders of magnitude less abundance in volatiles than those contained in some water-rich asteroids and comets. Does this suggest that the atmospheres of N-rich planetary bodies like Earth and Titan are the consequence of post-accretional delivery of volatile-rich bodies as predicted by recent models of the migration of giant planets?

Probably existed different pathways for massive delivery of N at early times. N-rich planetary atmospheres like Earth and Titan are consequence of the continuous delivery of volatiles along their evolutionary histories. Our current scenario for the delivery of volatiles is quite different from the envisioned by Chyba et al. (1990) and Chyba and Sagan (1992) as a byproduct of more complete, but still naïve, understanding of the bulk chemistry of undifferentiated asteroids and comets: authentic planetary building survivors.

The following chapter by Delgado-Bonal and Martín Torres (2013) deals with the abiotic sources of nitrogen fixation in early Earth, and their role in triggering a selection pressure favoring the evolution of nitrogenase and an increase in the nitrogen fixation rate. They introduce a mathematic method to analyze the amount of fixed nitrogen, both biotic and abiotic, through Earth's history.

In the field of exoplanets this book compiles very relevant contributions. Lammer et al. (2013) discuss the stability of Earth-like $N_2$-rich atmospheres and the main implications that such gaseous environments have for atmospheric, and planetary evolution and habitability. Evidence for such type of atmospheres in recently discovered exoplanets is discussed. Miguel and Kaltenegger (2013) introduce the reader into the fascinating topic of the new exoplanets called as super-Earths. These are planets with less than ten Earth masses that are very close to the Sun, that are unknown in our Solar System. A general review of the nitrogen chemistry in hot Jupiters atmosphere is given in the chapter by Venot et al. (2013).

It is usually considered that the earliest atmosphere of the Earth was produced by mantle outgassing, but it seems obvious that impacts participated in its evolution, as discussed in the Trigo-Rodríguez and Martín-Torres (2013) chapter. Impacts delivered water and organic compounds to a world mostly formed by anhydrous building blocks and even promoted catalytic reactions in the atmospheres of rocky planets. The authors invoke the need to accurately evaluate endogenous and exogenous sources of volatiles according to the geological and lunar evidence. They also discuss how laboratory experiments could be crucial to explain the evolution of the terrestrial atmosphere in that period.

Muller (2013) chapter deals with the intriguing presence in the Earth's atmosphere of $N_2O$. Since the discovery of this compound in 1938, $N_2O$ sources and sinks have been a puzzle. $N_2O$ has now been identified as produced by anaerobic bacteria's in soils which are sufficiently acid. The chapter also discusses the possible importance of $N_2O$ as a biomarker in the characterization of exoplanet atmospheres.

The book starts a section with several chapters on Titan. The chapter by Sekine (2013) reviews pre- and post-Cassini-Huygens theories for the formation of a $N_2$ atmosphere in Titan. Before the arrival of Cassini, it was considered that Titan's $N_2$ atmosphere formed as a result of a major differentiation during accretion and subsequent chemical reactions (such as shock heating and photolysis) in a hot and prolonged proto-atmosphere, mainly composed of $NH_3$ and $CH_4$. However, the new gravitational data provided by Cassini has revealed that Titan's core consists of a low-density material, suggesting that it remains relatively cold throughout its history.

Another fascinating result of the Cassini-Huygens (NASA-ESA) mission was to identify different common features among the atmospheres of Earth and Titan. An example is the assessment that molecular nitrogen is the major component of Titan's dense atmosphere, and is the basis for a very complex chemistry (Nixon et al. 2013). This chemically inert molecule is activated in the upper atmosphere by VUV radiations and particle impact ionization, causing its partial dissociation and ionization. The chapter by Carrasco et al. (2013) describes laboratory analyses performed with the goal of explaining the way in which nitrogen is retained in Titan's organic aerosols. As $N_2$ is a rather chemically inert molecule, the processes leading to the high nitrogen content of Titan's aerosols are far from being understood. Recent laboratory analogues and experimental results are then presented. Balucani et al. (2013) are discussing N fixation by photochemical processes in the atmosphere of Titan and the implications for prebiotic chemistry. Titan upper atmosphere chemistry involving nitrogen active forms and hydrocarbons is discussed, and the plausible intermediate molecular species that, via addition reactions, polymerization and copolymerization form the N-rich organic aerosols are presented.

The Moyano-Cambero et al. (2013) chapter describes the applications of Martian meteorite studies to assess the atmospheric composition of Mars over time. Most Martian meteorites have experienced significant shock during the impact that released them from the red planet, and during the flight through the Martian atmosphere some of the gases were retained in the shock-altered glasses. As different radiogenic systems allow dating such processes, these meteorites can be considered

as time capsules capable of providing valuable information on the atmospheric evolution of Mars. Different SNCs were released by impacts at different times, having then different atmosphere-implantation ages, so in practice we can obtain clues on the composition of Mars' atmosphere at different times. Taking this information into account, they have developed a simple model of the evolution of Mars' atmosphere.

Finally, four authors (Moyano-Cambero, Martín-Torres, Serrano and Trigo-Rodríguez) contributed to the text by writing the book glossary. This quite exhaustive compilation will make general concepts and definitions accessible to students, and researchers of other areas. It is particularly useful for making this book understandable to a general reader, one of our main goals after all.

## Putting the COST CM#0805 Workshop in Context

The scientific meeting that has led to these proceedings was organized by the Institute of Space Sciences (CSIC) and the Institut d'Estudis Espacials de Catalunya (IEEC) with the collaboration of the Scientific Secretariat of the Institute for Catalan Studies (IEC). Spanish Ministry of Science funded the complementary action called AYA2011-13250-E that has allowed the publication of this book. The workshop took place from 21 to 23 September, 2011 in the IEC historical building located in Carme street 47, nearby the famous Ramblas. A memorable poster session took place at IEC historical cloister on Wednesday 21st (see Fig. 1.1).

**Fig. 1.1** A general view of workshop participants in the IEC historical cloister during the coffee break preceding the poster session (Alina Hirschman/CSIC-IEEC)

**Fig. 1.2** A group picture of workshop participants in the IEC historical cloister during the coffee break preceding the poster session (Helmut Lammer/AAS)

All participants agreed that the meeting location was a perfect place to discuss many interdisciplinary issues concerning the formation and the evolution of planetary atmospheres. Consequently, this meeting resulted in a rewarding experience for all participants (Fig. 1.2), most of them granted by an European COST action.

## The Proceedings Book

This interdisciplinary book is fruit of a common effort of authors and editors for promoting research on these disciplines. The book is published with funds received on 2011 from the Spanish Ministry of Science in a complementary action called

AYA2011-13250-E. We are all grateful to Spanish government for being sensitive to our research on the first stages in the evolution of planetary atmospheres.

As editors of this volume we are also especially grateful to all distinguished authors for preparing texts of high quality despite having long peer-review publication duties ahead in their agendas. We also thank the additional effort made by internal reviewers to read and correct the book contributions. They deserve all the credit to produce this comprehensive and enthusiastic book of proceedings that compiles most of the work presented during the COST CM#0805 workshop of Barcelone. We sincerely hope that all this common effort is useful for having many readers keeping the track on this fascinating research area.

**Acknowledgements** Workshop attendance was financially supported by COST action CM0805. We also thank the Spanish Ministry of Science for funding this book as part of the complementary action called AYA2011-13250-E. We are very grateful to the Scientific Secretary of the Institute for Catalan Studies (IEC), Prof. Ricard Guerrero, who give us access to IEC facilities where the workshop took place with big success. Finally, the Institute of Space Sciences (CSIC) and the Institut d'Estudis Espacials de Catalunya (IEEC) provided the needed logistics.

## References

Atreya, S.K., Pollack, J.B., Matthews, M.S. (eds.): Origin and evolution of planetary and satellite atmospheres. The University of Arizona Press, Tucson (1989)

Balucani, N., et al.: Nitrogen fixation by photochemistry in the atmosphere of Titan and implications for prebiòtic chemistry. In: The Early Evolution of the Atmospheres of Terrestrial Planets. Springer (2013, this volume)

Carrasco, N., et al.: Nitrogen in Titan's atmospheric aerosol factory. In: The Early Evolution of the Atmospheres of Terrestrial Planets. Springer (2013, this volume)

Chyba, C., Sagan, C.: Endogenous production, exogenous delivery and impact-shock synthesis of organic molecules: an inventory for the origins of life. Nature **355**, 125–132 (1992)

Chyba, C., Thomas, P.J., Brookshaw, L., Sagan, C.: Cometary delivery of organic molecules to the early Earth. Science **249**, 366–373 (1990)

Delgado-Bonal, A., Martín Torres, F.J.: A mathematic approach to nitrogen fixation through Earth history. In: The Early Evolution of the Atmospheres of Terrestrial Planets. Springer (2013, this volume)

Holland, H.D.: Model for the evolution of the Earth's atmosphere. In Petrologic Studies: A volume to honor A.F. Buddington, Geological Society of America. pp. 447–477 (1962)

Kasting, J.F.: Earth's early atmosphere. Science **259**, 920–926 (1993)

Kasting, J.F.: Warming early Earth and Mars. Science **276**, 1213–1215 (1997)

Lammer, H., et al.: Stability of Earth-like $N_2$ atmospheres: implications for habitability. In: The Early Evolution of the Atmospheres of Terrestrial Planets. Springer (2013, this volume)

Lewis, J.S., Prinn, R.G.: Planets and Their Atmospheres: Origin and Evolution. Academic, Orlando (1984)

Miguel, Y., Kaltenegger, L.: Hot super-Earth atmospheres. In: The Early Evolution of the Atmospheres of Terrestrial Planets. Springer (2013, this volume)

Moyano-Cambero, C.E., et al.: SNC meteorites: atmosphere implantation ages and the climatic evolution of Mars. In: The Early Evolution of the Atmospheres of Terrestrial Planets. Springer (2013, this volume)

Muller, C.: $N_2O$ as a biomarker, from the Earth and solar system to exoplanets. In: The Early Evolution of the Atmospheres of Terrestrial Planets. Springer (2013, this volume)
Nixon, C.A., et al.: Nitrogen in the stratosphere of Titan from Cassini CIRS infrared spectroscopy. In: The Early Evolution of the Atmospheres of Terrestrial Planets. Springer (2013, this volume)
Sekine, Y.: Formation of a nitrogen-rich atmosphere on Titan: a review of pre- and post- Cassini-Huygens knowledge. In: The Early Evolution of the Atmospheres of Terrestrial Planets. Springer (2013, this volume)
Trigo-Rodríguez, J.M.: Nitrogen in solar system minor bodies: delivery pathways to primeval Earth. In: The Early Evolution of the Atmospheres of Terrestrial Planets. Springer (2013, this volume)
Trigo-Rodríguez, J.M., Martín-Torres, F.J.: Implication of impacts in the young Earth Sun paradox and the evolution of Earth's atmosphere. In: The Early Evolution of the Atmospheres of Terrestrial Planets. Springer (2013, this volume)
Valley, J.W., King, E.M., Peck, W.H., Graham, C.M., Wilde, S.A.: The cool early Earth: oxygen isotope evidence for continental crust and oceans on Earth at 4.4 Ga. In: Abstract in the American Geophysical Union Spring Meeting, Boston (2001)
Venot, O., et al.: The nitrogen chemistry in hot Jupiters atmosphere. In: The Early Evolution of the Atmospheres of Terrestrial Planets. Springer (2013, this volume)
Wasson, J.T.: Oxygen-isotopic evolution of the Solar Nebula. Rev. Geophys. **38**, 491–512 (2000)
Yung, Y.L., DeMore, W.B.: Photochemistry of planetary atmospheres. Oxford University Press, Oxford (1999)

# Chapter 2
# Nitrogen in Solar System Minor Bodies: Delivery Pathways to Primeval Earth

**Josep M. Trigo-Rodríguez**

**Abstract** Oxygen isotope data point towards enstatite and ordinary chondrites as presumable building blocks of primordial Earth. Nitrogen was incorporated as nitrides to these first building blocks and was outgassed in the early stages of chemical segregation. However, giant impacts with planetesimals played an important role in partially eroding the atmosphere of Earth, and promoting thermal escape of diverse components. As a consequence, the Earth's atmospheric composition could have been subjected to important changes along the eons. A last, and probably less massive, delivery of volatiles took place at the time of a gigantic cataclysm known as Late Heavy Bombardment. During a short interval roughly between 3.9 and 3.8 Gyr ago, a gravitational migration inwards of Jupiter and Saturn occurred, that perturbed hundreds of small bodies rich in water, ammonia, methane and organic compounds that were stored until then in the outer regions. Current atmospheric signatures suggest that by that mechanism a continuous shower of outer-disk primordial components enriched the volatile inventory of terrestrial planets. The relevance of such contribution is still debated, but significant progress has been made in the last decades from the study of undifferentiated bodies. Consequently, planetary scattering of undifferentiated bodies delivered to Earth a significant fraction of minerals, and light elements that could have played a key role in the volatile enrichment the terrestrial crust. I suggest some unexplored pathways to allow a safe delivery of organics to Earth's surface, following recent evidence on meteoroid fragmentation, fireball spectra and Antarctic micrometeorite discoveries. Recent compositional studies of asteroids, comets and meteorites corroborate the need of having more precise data on the abundance and isotopic ratios of N in these minor bodies. Future space missions to primitive bodies like Rosetta, OSIRIS-

J.M. Trigo-Rodríguez (✉)
Institute of Space Sciences (CSIC-IEEC), Campus UAB, Facultat de Ciències, Torre C5-parells, 08193, Bellaterra, Barcelona, Spain
e-mail: trigo@ieec.uab.es

J.M. Trigo-Rodriguez et al. (eds.), *The Early Evolution of the Atmospheres of Terrestrial Planets*, Astrophysics and Space Science Proceedings 35,
DOI 10.1007/978-1-4614-5191-4_2, 

Rex, Hayabusa II, or Marco Polo-R could help us to complete the big picture, and this chapter tries to compile our present knowledge of its delivery to Earth along the eons.

## Introduction: The Sources of Terrestrial Nitrogen

Oxygen isotope ratios demonstrate a distinctive origin of meteorites in different parent bodies (Alexander et al. 2012). Such evidence points towards a differentiated accretion of planetary bodies from ring-like populations of building blocks mostly located at well-constrained solar distances, and then inheriting distinctive O isotope ratios. Oxygen isotope clues, and bulk chemistry point towards enstatite and ordinary chondrites as presumable building blocks of primordial Earth (Anders and Grevesse 1989; Wasson 2000; Lodders 2010). Such components were poor in volatile elements, but N was probably incorporated as nitrides (Rubin and Choi 2009). The primordial solar N and O isotopic composition has been inferred from first condensates (Meibom et al. 2007). This evidence allows the comparison of different sources of volatile elements, and helps establish plausible pathways for their delivery to Earth (Marty and Yokochi 2006). It seems likely there was an N-rich early atmosphere from direct outgassing. Despite this, during the late accretionary period large impacts eroded significant amounts of the Earth's volatile inventory. In this sense, a depletion in N and Xe has been noted with respect to other volatiles that are in chondritic proportions (Marty 2012). Such depletion could be explained as a consequence of large impacts producing a thermal escape and affecting the atmospheric components. In fact, a giant impact probably originated the Moon and eroded the early atmosphere of Earth (Cameron and Ward 1976).

Urey (1952) treated the origin of planets and their atmospheres in great detail for his time. Bukvic (1979) and Zahnle et al. (1988) and more recently Schaefer and Fegley (2007) and Schaefer et al. (2012) have modeled the equilibrium gas chemistry of an outgassed chondritic-vaporized reducing atmosphere, but several processes that can take place in the aftermatch of the impacts are scarcely known (Trigo-Rodríguez and Martín-Torres 2013). Other authors have an opposite view where the outgassed vapors (Delano 2001), or the degassed vapors during impacts (Ahrens et al. 1989) produced oxidizing products ($H_2O + CO_2$). It is even possible that the degassed products varied significantly depending on variability of Earth's surface redox properties along the eons (Kasting and Catling 2003). Relative abundances of bioelements are in Table 2.1.

Current models accounting for the growth of terrestrial planets support the existence of a gigantic cataclysm over the entire solar system as the cause of the Late Heavy Bombardment (Gomes et al. 2005). Then, roughly between 3.9 and 3.8 Gyr ago, an inwards migration of Jupiter and Saturn occurred that gravitationally perturbed hundreds of minor bodies rich in water, ammonia, methane and organic compounds. That mechanism probably delivered to Earth a significant fraction of nitrogen and other bioelements currently present in the terrestrial hydrosphere, and

**Table 2.1** Relative abundances of bioelements in the Sun, some Earth reservoirs and simple life forms (Adapted from Golsmith and Owen 2003))

| Element | Sun | Earth crust | Earth's atmosphere | Ocean | Microbium |
|---|---|---|---|---|---|
| H | 91 | 0.14 | $< 0.001$ | 11 | 63 |
| O | 0.08 | 46 | 21 | 86 | 26 |
| C | 0.03 | 0.02 | 0.04 | 0.003 | 6.4 |
| N | 0.010 | 0.002 | 78 | $5 \times 10^{-5}$ | 1.4 |
| S | 0.002 | 1.6 | $< 0.001$ | 0.09 | 0.06 |
| P | $3 \times 10^{-5}$ | 0.11 | $< 0.001$ | $6 \times 10^{-6}$ | 0.12 |

**Table 2.2** Distinctive N isotopic composition of chondritic meteorites (According to data compiled by Rubin and Choi (2009)

| Chondrite classes | $\delta^{15}$N | N location |
|---|---|---|
| Enstatite | $\approx -20$ | Forming nitrides |
| Ordinary | $-5$ to 20 | In chondrules |
| Carbonaceous | 20–190 | Mostly in matrix, and minor in chondrules |

biosphere. Recent discoveries in minor bodies emphasize the enriching role of this late veneer population, and this chapter tries to compile current evidence in this regard. However, future sample-return missions like e.g. OSIRIS-Rex, Hayabusa II, or Marco Polo-R could provide a significant breakthrough in our knowledge (Barucci et al. 2012).

## The D/H, and the $^{15}$N/$^{14}$ N Ratios in Transitional Bodies

The most primitive materials arriving to Earth come from undifferentiated comets and asteroids. A continuous flux of low-strength aggregates associated with comets are preferentially disrupted in the upper atmosphere (Trigo-Rodríguez and Llorca 2006, 2007; Trigo-Rodríguez and Blum 2009a). Some arrive with the right geometry and velocity to survive as Interplanetary Dust Particles, but most are ablated and or disaggregated in the upper atmosphere as a consequence of their aerodynamic deceleration. Stardust studies of comet 81P/Wild 2 demonstrated that most of the N was present in the micron-sized matrix that was preferentially sputtered during aerogel capture in the tracks walls (Brownlee et al. 2006). In any case, in some surviving 81P/Wild 2 particles (e.g. shown by Febo) had matrix contained $^{15}$N hotspots with isotopic signatures typical of the interstellar medium (Matrajt et al. 2008). This is not so surprising as carbonaceous chondrites also have distinctive heavy bulk N($20 < \delta^{15}\text{N} < 190$) that are suggestive of a significant flux of interstellar materials moving inwards towards the disk regions where these primitive meteorites accreted. Consistent this picture and with the origin of the different chondrite classes, the amount of $^{15}$N decreased going inwards in the disk (see Table 2.2).


**Fig. 2.1** A large specimen of the Murchison CM2 chondrite fell in Australia in 1969. The dark appearance of the matrix is due to its C content. *Grey* chondrules, and *white* Ca-Al rich inclusions (CAIs) are clearly distinguishable even at this naked-eye resolution (This picture made by the author is from a specimen belonging to the Leonard collection (IGPP/UCLA))

Chondritic meteorites are undifferentiated materials (e.g. non metamorphosed in large bodies) that comprise carbonaceous, ordinary and enstatite classes that are subdivided into 15 groups (Weisberg et al. 2006). All chondrites are considered chemically primitive by the fact that the ratios of their major, non-volatile elements (Fe, Si, Mg, Al, Ca, etc…) are close to those observed in the Sun (Anders and Grevesse 1989). It is thought that the different groups formed at different heliocentric distances, and slightly different times. Consequently, they inherited important chemical differences from the environment. Among chondrites, the carbonaceous chondrite (CC) class is thought to be especially pristine (Zolensky and McSween 1988). Inside CCs, several groups (mainly CI, CM, CO and CRs) exhibit important water contents and are formed by hydrated or aqueously-altered minerals (see e.g. Brearley 2006). Other volatile elements, e.g. N, are mainly located in the fine grained dust (so called *matrix*) that is cementing these rocks with typical grain sizes of 1 μm or less (see Fig. 2.1).

In summary, the different chondrite classes are basically conglomerates of fine dust (a mixture of silicates, oxides, metal, sulfides and organic constituents, see Fig. 2.2), chondrules, and refractory or mafic inclusions (Brearley and Jones 1998).

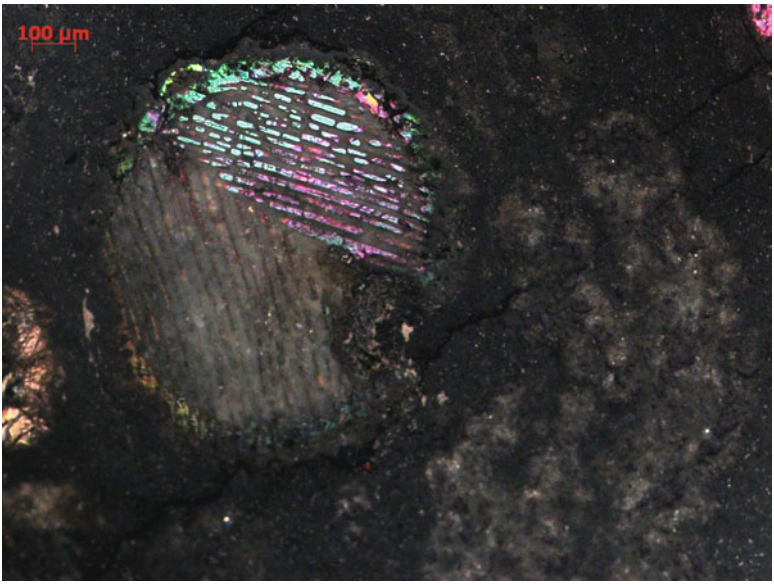


**Fig. 2.2** A thin section of the Allende CV3 chondrite fell in Mexico in 1969. A barred olivine chondrule is seen in the *center*, and a CAI in the *bottom-right* quadrant. Notice the dark fine-grained matrix compacting the structure all around (J.M.Trigo/CSIC-IEEC)

The primordial water content in the different groups is difficult to assess, but those chondrites containing Fe-metal are indicative of being anhydrous in origin. We also know that many carbonaceous chondrite groups are unprocessed because they exhibit unequilibrated minerals, and also contain interstellar grains with isotopic anomalies that survived processing in the solar nebula and accretionary processes when incorporated to these rocks (Anders and Zinner 1993; Huss et al. 2006; Trigo-Rodríguez and Blum 2009b). Aqueous alteration plays against pristinity as there is clear evidence that some isotopic ratios (like e.g. D/H) are altered during parent body aqueous alteration processes (Alexander et al. 2012). Secondary minerals produced as consequence of aqueous alteration in carbonaceous chondrite parent bodies suggest that these processes occurred during the first 10 million of years after the birth of the solar system (Fujiya et al. 2013)

On the other hand, the N abundances and isotopic ratios in comets are poorly known. A significant achievement was obtained when the PIA mass spectrometer onboard Giotto (ESA) spacecraft was able to infer the composition of 1P/Halley dust particles. A big surprise was having most of the particles in the coma formed by light elements (H, C, N and O), the so-called CHON component (Kissel et al. 1986, see Fig. 2.3). Despite this, obtaining information about the light component is not trivial. For example, molecular nitrogen cannot be directly detected by remote spectroscopic techniques, and the usual inferences regarding N isotopic ratios are come directly from other species, such as $NH_3$ and HCN (Bockelée-Morvan

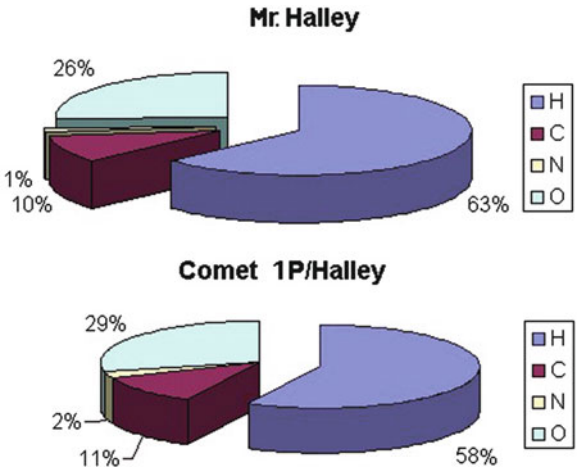


**Fig. 2.3** A comparative view of the similitude between the proportions in the CHON elemental distribution found in comet 1P/Halley and humans

et al. 2004). All these species from which reasonable isotopic information is extracted are observed in cometary comae (see e.g. review by Rauer 2008). To have a better idea of the N content in comets we must wait for in situ studies of comets as precognized (Oró 1961). The Rosetta spacecraft is an ESA mission that plans to perform accurate studies of the isotopic composition of the CHON component in comet 67P/Churyumov-Gerasimenko by using *Ptolemy*: a gas chromatograph coupled to a mass spectrometer (Morse et al. 2008).

Calculations by Marty and Meibom (2007) suggest that a cometary contribution capable of fitting the abundances of noble gases is unable to produce more than ∼6 % of the nitrogen inventory in the terrestrial atmosphere. A similar amount is obtained in the review made by Marty (2012). Obviously we do not know the exact composition, and neither do we know the nature of the bodies that were able to reach the Earth during the LHB. Despite this, it is reasonable to consider the relevance of two still remaining water-rich populations. One is represented by the recently discovered Main-Belt comets (Hsieh and Jewitt 2006), and the other is represented by the Jupiter Family Comets that are collisionally generated fragments of Kuiper Belt Objects or KBOs (Jewitt 2008). In coming decades, we must explore those transitional objects that could be of interest for understanding this additional source of water and organics. An example is comet 29P/Schwassmann-Wachmann 1 that is considered the archetype of comets exhibiting outbursts and subsequent changes in their coma appearance and brightness (Sekanina 1982). This comet is defined as a Centaur due to its movement along a quasi-circular orbit that crosses the orbits of giant planets with eccentricity $e \sim 0.044$ and semimajor axis $a \sim 6$ AU. To get new clues on the structure, composition, and physical processes causing outbursts at these heliocentric distances we have promoted more than a decade of multiband photometric monitoring (Trigo-Rodríguez et al. 2008, 2010). During


**Fig. 2.4** A thin section of GRA95229 from the NASA Antarctic collection that shows several silicate chondrules and the dark fine-grained matrix compacting the structure (J.M.Trigo/CSIC-IEEC)

an outburst its nuclear magnitude typically increases by 2 or 5 magnitudes in a behavior that seems unusual, but that would be typical for primitive objects like e.g. Centaurs, that evolve from Trans-Neptunian Objects (TNOs) located at the appropriated heliocentric distances.

Recent studies have identified a population of N-rich chondrites in the CR group of carbonaceous chondrites like e.g. GRA95229 (Fig. 2.4), suggesting that some regions in the protoplanetary disk had N-rich environments (Martins et al. 2007; Martins 2011; Pizzarello and Williams 2012). This enrichment in N and organics could be explained by gas drag effects that will transport inwards ice-rich bodies accreted in the trans-Neptunian region. A continuous disruption of such bodies at the particular time in which CR chondrites accreted could be envisioned as the source of N. In fact, high-eccentricity TNOs are probably the source of Jupiter Family comets (Emel'yanenko et al. 2004). Water and ammonia-rich TNO surfaces (covered by complex ice mixtures) have been found in the TNO population (DeMeo et al. 2010; Barucci et al. 2010). TNOs exhibiting such ices on their surfaces, could feasibly have experienced exhalation, perhaps by regular hydrothermal activity.

The contribution of the previously mentioned sources to the Earth's atmosphere and hydrosphere could be better explored when we acquire samples from primitive solar system objects. Future progress in modeling large impacts and the dynamic routes of minor bodies through solar system history could also be crucial (Kaula 1979; Wetherill 1985). For example, it has been recently demonstrated

that the cataclysmic impact forming the Moon probably did not completely erode the atmosphere of the Earth as previously thought (Genda and Abe 2003, 2005: Newman et al. 1999). This huge impact was probably an inflexion point followed by less massive impacts that brought volatile-rich materials and released reduced gases when subjected to subduction. Bukvic (1979) and more recently Schaefer and Fegley (2007) have modeled the equilibrium gas chemistry of an outgassed chondritic-vaporized reducing atmosphere, but several processes that can take place in the aftermath of the impacts are scarcely known. Other authors have an opposite view where the outgassed vapors (Delano 2001), or the degassed vapors during impacts (Ahrens et al. 1989) produced oxidizing products ($H_2O + CO_2$). Both scenarios are briefly explored, together with the influence of an enhanced shortwave solar activity during the early Hadean in Trigo-Rodríguez and Martín-Torres chapter (2013).

## Ammonia, and Aqueous Alteration in Pristine Transitional Bodies

The chemical and structural differences observed in the different groups of carbonaceous chondrites are suggestive of their accretion in different outer regions of the protoplanetary disk where a moderate gas pressure and temperature allowed the ices and organics to remain in solid form. These aggregates formed the matrix in which the rest of components were accumulating. When the free-floating materials encountered each other under moderate relative velocities, progressive growth occurred until completion of the accretionary stage (Blum et al. 2006). Comets and carbonaceous asteroids were formed in the same way, but with different ice:dust ratios. As a direct consequence of their origin, the volatile elements were mostly retained in the fine-grained matrix.

Once the undifferentiated bodies completed their growing, some internal heat was released from the accreted radionuclides. Of particular interest in our discussion is the role of hydrostatic compaction in hydrous chondritic asteroids/comets. In other words, compaction due to the body's own gravity. In the last decade the idea of having a continuum of bodies with variable ice:rock ratio has received considerable support (see e.g. Gounelle 2011). In fact, accretionary models suggest that initial chondritic building blocks had porosities larger than 60 % (Blum et al. 2006; Trigo-Rodríguez and Blum 2009a). Depending on the ice:rock ratio and the final size of the body formed, they could have experienced hydrostatic inner pressures of the order of 0.1–3 MPa (Warren 2011). Under such hydrostatic pressure the water initially available as ice or as hydrated phases would be released, soaking the body. This type of aqueous alteration could be consistent with the observed typically static alteration features in hydrated groups like the CM chondrites (Trigo-Rodríguez et al. 2006, Rubin et al. 2007). Another clear type example are the Fe-rich aureoles found in the same group by Hanowski and Brearley (2000).

Significant progress has been made concerning the CM group of carbonaceous chondrites. The members of this group have experienced aqueous alteration to different degrees (Rubin et al. 2007). We infer that a large variety of mineral phases (e.g. phyllosilicates, sulfides, carbonates, oxides, and other poorly characterized phases or "PCP") contained in these meteorites were produced via alteration of primitive materials by the pervasive action of water. The source of this water is unknown but could include water of hydration in phyllosilicates within the chondrites (Petaev and Wood 1998) or accreted ice (Stevenson and Lunine 1988). Parent-body processing like e.g. the produced primordially by radionuclide decay, or the induced by compaction of the materials due to gravity-sintering or impacts occurred along the eons caused water to be released from the initial host phases and produced aqueous alteration of primitive CM materials. Petrographic observations and the mineralogy of CM matrices are consistent with aqueous alteration at temperatures $<400$K (Bunch and Chang 1980). The presence of PCP clumps in CM matrices and the absence of glassy mesostases in CM chondrules attest to microscopic-scale aqueous alteration.

The presence of ice could have promoted hydro cryogenic alteration of anhydrous material through the action of unfrozen water over long time scales, but other processes involved soaking some regions of the CM parent body over shorter time scales. Obviously, an extended period of aqueous alteration would require the presence of liquid water and would imply a heating mechanism. As a consequence of heating, water exhalation or convection could be generated on the CM parent body (Young et al. 2003). The examination of newly discovered CM chondrites from Antarctica and hot desert regions provides new evidence bearing on the nature of aqueous alteration on the CM parent asteroid. We examined a suite of CM chondrites spanning the aqueous alteration sequence and found that one of these chondrites (MET 01070) contains cm-long, PCP-rich lenses that appears to be a product of aqueous flow on the parent body (Trigo-Rodríguez and Rubin 2006; Rubin et al. 2007). This is the first evidence of aqueous flow in CM chondrites (Fig. 2.5).

## Discussion and Conclusions

N and other biogenic elements arrived at the Earth affected by different evolutionary cycles experienced in the inner solar system. The big picture is complex, but we are starting to understand the main evolutionary pathways. Current space missions are producing a large amount of information on the composition of comets and asteroids, which is paradoxical considering our scarce knowledge of the interaction of cometary materials with the atmosphere of Earth. However, Pierazzo and Chyba (2010) have recently made a significant computational progress developing a high-resolution hydrocode capable to predict shock temperatures and amino acids survival under particular entry conditions. The idea is not new, the delivery of organic compounds from comets was revisited in a couple of pioneering papers

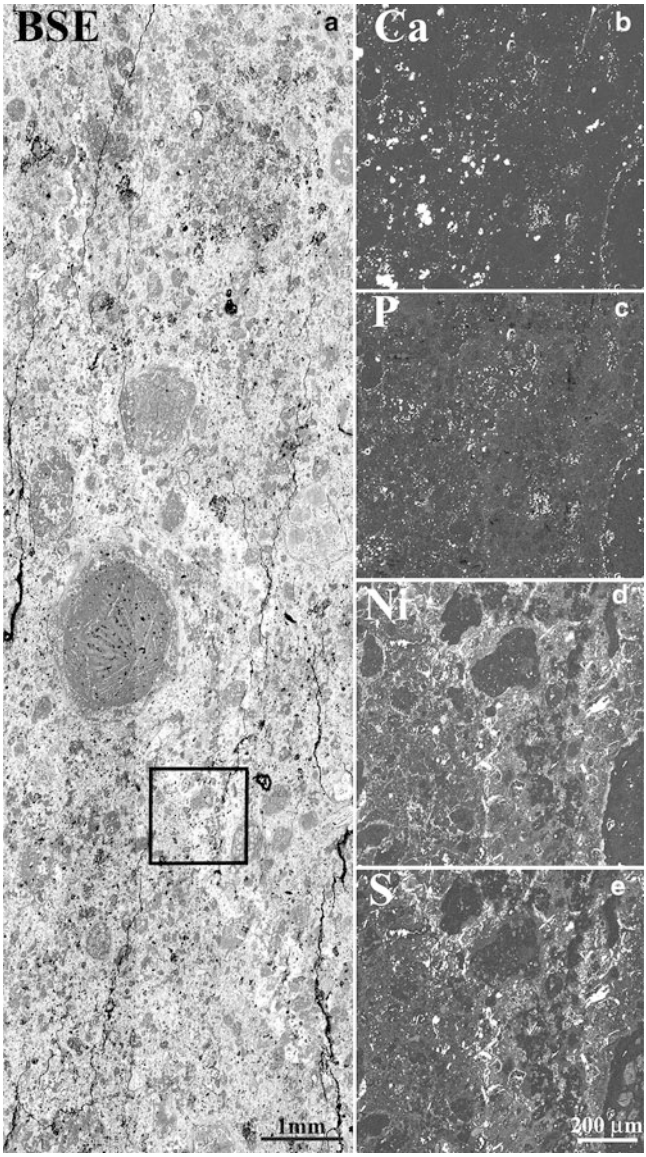


**Fig. 2.5** A PCP lens identified in the SEM image of the Antarctic CM chondrite MET 01070. A X-ray mapping of the *black square* shows in the right images the presence of different elements mobilized by aqueous alteration (From Rubin et al. 2007)

(Chyba et al. 1990; Chyba and Sagan 1992). Current models suggest that water-rich asteroids and comets impacting the atmosphere of Earth are delivering volatile elements during the bolide phase, but the amounts of surviving organic species

are scarce if the impact geometry and velocity are not favorable for an efficient deceleration and settling of the materials in the atmosphere (Blank et al. 2001). With this in mind, other direct pathways should be explored. For example, during the LHB period the scattered asteroids/comets should be fragile and could be efficiently disrupted during close approaches to terrestrial planets. If this is correct, the dense dust trails produced could efficiently deliver pristine materials with lower entry velocities. Fireball spectroscopy of cm- to mm-sized meteoroids suggests that catastrophic disruptions in the atmosphere can disperse dust far away from the shock wave frontal region where the bolide experiences higher temperatures (Trigo-Rodríguez et al. 2003; Trigo-Rodríguez and Blum 2006). Consequently, the exposure to heat is minimized and there is room for a percentage of body survival, at least as small fragments that are slowly setting down towards the surface. Such a scenario could be consistent with the recent discovery of ultracarbonaceous micrometeorites in Antarctica (Duprat et al. 2010).

Consequently, the main conclusions of this brief review are:

1. Current evidence suggests that N, and other light elements are abundant in undifferentiated bodies e.g. chondritic asteroids, comets, and TNOs. They are present in the fine-grained matrix forming these bodies, but probably also associated with aqueous alteration minerals.
2. Mobilization of light elements during aqueous alteration processes occurred at early times in the evolution of minor bodies. Such alteration processes provide a way to avoid outgassing of volatiles.
3. Due to the intrinsic difficulties associated with the remote detection of N and its isotopic ratio in minor bodies, the best way to proceed is by promoting future sample return missions like OSIRIS Rex, Hayabusa II or Marco Polo-R. Developing new technology to achieve a cryogenic return of cometary samples could also be the following step after them.
4. A significant part of Earth's atmosphere could have been delivered at the time of the Late Heavy Bombardment. However, a better knowledge of the volatile abundances in comets will allow us to revisit current models.
5. Fragmentation of meteoroids in the upper atmosphere of Earth could have provided a significant pathway for the delivery of the CHON component to primeval Earth.

**Acknowledgements** This work was financially supported by CSIC grant #201050I043 and AYA2011-26522 grants.

## References

Ahrens, T.J., O'Keefe, J.D., Lange, M.A.: Formation of atmospheres during accretion of the terrestrial planets, In: Origin and evolution of planetary and satellite atmospheres (A89-43776 19-90). Tucson, AZ, University of Arizona Press, pp. 328–385 (1989)

Alexander, C.M.O'D., Bowden, R., Fogel, M. L., Howard, K.T., Herd, C.D.K., Nittler, L.R.: The provenance of asteroids, and their contributions to the volatile inventories of the terrestrial planets. Sci. Express **337**, 721–723 (2012). doi:10.1126/science.1223474

Anders, E., Grevesse, N.: Abundances of the elements: meteoric and solar. Geochim. Cosmochim. Acta **53**, 197–214 (1989)

Anders, E., Zinner, E.: Interstellar grains in primitive meteorites - Diamond, silicon carbide, and graphite. Meteo. **28**, 490–514 (1993)

Barucci, M.A., Morea Dalle Ore, C., Älvarez-Candal, A., de Bergh, C., Merlin, F., Dumas, C., Cruikshank, D.: (90377) Sedna: investigation of surface compositional variation. Astron. J. **140**, 2095–2100 (2010)

Barucci, M.A., et al.: Marco Polo-R near Earth asteroid sample return mission. Exp. Astron. **33**, 645–684 (2012)

Blank, J.G., Miller, G.H., Ahrens, M.J., Winans, R.E.: Experimental Shock Chemistry of Aqueous Amino Acid Solutions and the Cometary Delivery of Prebiotic Compounds, Origins of Life and Evolution of the Biosphere, **31**(1/2), 15–51 (2001)

Blum, J., Schräpler, R., Davidson, B.J.R., Trigo-Rodríguez, J.M.: The physics of protoplanetesimal dust agglomerates. I. Mechanical properties and relations to primitive bodies in the solar system. Astrophys J. **652**, 1768–1781 (2006)

Bockelée-Morvan, D., Crovisier, J., Mumma, M.J., Weaver, H.A.: The composition of cometary volatiles. In: Festou, M.C., Keller, H.U., Weaver, H.A. (eds.) Comets II, pp. 391–423. University of Arizona Press, Tucson (2004)

Brearley, A.J.: The action of water. In: Lauretta, D.S., McSween, H.Y. (eds.) Meteorites and the Early Solar System II, pp. 587–624. University of Arizona Press, Tucson (2006)

Brearley, A., Jones, R.H.: Chondritic meteorites. In: Papike, J.J. (ed.) Planetary Materials, Reviews in Mineralogy 36, Chapter 3, pp. 1–398 (1998)

Brownlee, D., et al.: Comet Wild 2 under a microscope. Science **314**, 1711–1716 (2006)

Bukvic, D.S.: Outgassing of chondritic planets. M.S: Thesis, MIT (1979)

Bunch T. Chang S.: Carbonaceous chondrites – II: carbonaceous chondrite phyllosilicates and light element geochemistry as indicators of parent body processes and surface conditions. Geochim. Cosmochim. Acta **44**, 1543–1577 (1980)

Cameron, A.G.W., Ward, W.R.: The origin of the Moon. In: 7th LPS Conference, Houston, p. 120. Lunar and Planetary Institute (1976)

Chyba, C., Sagan, C.: Endogenous production, exogenous delivery and impact-shock synthesis of organic molecules: an inventory for the origins of life. Nature **355**, 125–132 (1992)

Chyba, C., Thomas, P.J., Brookshaw, L., Sagan, C.: Cometary delivery of organic molecules to the early Earth. Science **249**, 366–373 (1990)

Delano, J.W.: Redox history of the Earth's interior since ∼3,900 Ma: implications for prebiotic molecules. Orig. Life **31**, 311–341 (2001)

DeMeo, F., Barucci, M.A., Álvarez-Candal, A., de Bergh, C., Fornasier, S., Merlin, F., Perna, D., Belskaya, I.: A spectroscopic analysis of Jupiter-coupled object (52872) Okyrhoe, TNOs (90482) Orcus and (73480) 2002 $PN_{34}$. Astron. Astrophys. **521**, 9 (2010). id.A35

Duprat, J., et al.: Extreme deuterium excesses in ultracarbonaceous micrometeorites from Central Antarctic snow. Science **328**, 742–745 (2010)

Emel'yanenko, V.V., Asher, D.J., Bailey, M.E.: High-eccentricity trans-Neptunian objects as a source of Jupiter-family comets. Mon. Not. R. Astron. Soc. **350**, 161–166 (2004)

Fujiya W., Sugiura N., Sano Y., and Hiyagon H.: Mn-Cr ages of dolomites in CI chondrites and the Tagish Lake ungrouped carbonaceous chondrite. Earth and Planetary Sci. Lett. **362**, 130–142 (2013)

Genda, H., Abe, Y.: Survival of a proto-atmosphere through the stage of giant impacts: the mechanical aspects. Icarus **164**, 149–162 (2003)

Genda, H., Abe, Y.: Enhanced atmospheric loss on protoplanets at the giant impact phase in the presence of oceans. Nature **433**, 842–844 (2005)

Golsmith, D., Owen, T.: The Search for Life in the Universe. University Science Books, Herndon (2003)

Gomes, R., Levison, H.F., Tsiganis, K., Morbidelli, A.: Origin of the cataclysmic Late Heavy Bombardment period of the terrestrial planets. Nature **435**, 466–469 (2005)
Gounelle, M.: The asteroid-comet continuum: in search of lost primitivity. Elements **7**(1), 29–34 (2011)
Hanowski, N.P., Brearley, A.J.: Iron-rich aureoles in the CM carbonaceous chondrites Murray, Murchison, and Allan Hills 81002: evidence for in situ aqueous alteration. Meteor. Planet. Sci. **35**, 1291–1308 (2000)
Hsieh, H.H, Jewitt, D.: A population of comets in the main asteroid belt. Science **312**, 561–563 (2006)
Huss, G.R., Rubin, A.E., Grossman, J.N.: Thermal metamorphism in chondrites. In: Lauretta, D.S., McSween, H.Y. (eds.) Meteorites and the Early Solar System II, pp. 567–586. University of Arizona Press, Tucson (2006)
Jewitt, D.: Kuiper Belt and comets: an observational perspective. In: Altwegg, K., Benz, W., Thomas, N. (eds.) Trans-Neptunian Objects and Comets, pp. 1–78. Springer, Berlin (2008)
Kaula, W.M.: Thermal evolution of earth and moon growing by planetesimal impacts. J. Geophys. Res. **84**, 999–1008 (1979)
Kasting, J.F., Catling, D.: Evolution of a habitable planet. Annu. Rev. Astron. Astrophys. **41**, 429–463 (2003)
Kissel, J., et al.: Composition of comet Halley dust particles from Giotto observations. Nature **321**, 336–337 (1986)
Lodders, K.: Solar system abundances of the elements. In: Goswami, A., Reddy, B.E. (eds.) Principles and Perspectives in Cosmochemistry, pp. 379–417. Springer, Berlin/Heidelberg (2010)
Martins, Z.: Organic chemistry of carbonaceous meteorites. Elements **7**, 35–40 (2011)
Martins, Z., Alexander, C.M.O.D., Orzechowska, G.E., Fogel, M.L., Ehrenfreund, P.: Indigenous amino acids in primitive CR meteorites. Meteor. Planet. Sci. **42**, 125–136 (2007)
Marty, B.: The origins and concentrations of water, carbon, nitrogen and noble gases on Earth. Earth Planet. Sci. Lett. **313–314**, 56–66 (2012)
Marty, B., Meibom, A.: Noble gas sigmature of the Late Heavy Bombardment in the Earth's atmosphere. eEarth **2**, 43–49 (2007)
Marty, B., Yokochi, R.: Water in the early Earth. Rev. Mineral. Geochem. **62**, 421–450 (2006)
Matrajt, G., Ito, M., Wirick, S., Messenger, S., Brownlee, D.E., Joswiak, D., Flynn, G., Sandford, S., Snead, S., Westphal, A.: Carbon investigation of two Stardust particles: a TEM, NanoSIMS, and XANES study. Meteor. Planet. Sci. **43**, 315–334 (2008)
Meibom, A., Krot, A.N. Robert, F., Mostefaoui, S., Russell, S.S., Peatev, M.I., Gounelle, M.: Nitrogen and carbon isotopic composition of the Sun inferred from a high-temperature solar nebula condensate. Astrophys. J. **656**, L33–L36 (2007)
Morse, A.D., Morgan, G.H., Andrews, D.J., Barber, S.J., Leese, M.R., Sheridan, S., Wright, I.P., Pillinger, C.T.: Ptomely – a GCMS to measure the chemical and stable isotopic composition of a comet. In: Schulz, R., Alexander, C., Boehnhardt, H., Glassmeier, K.-H. (eds.) Rosetta: ESA's Mission to the Origin of the Solar System, pp. 669–686. Springer, New York (2008)
Newman, W.I., Symbalisty, E.M.D., Ahrens, T.J., Jones, E. M.: Impact erosion of planetary atmospheres: some surprising results. Icarus **138**, 224–240 (1999)
Oró, J.: Comets and the formation of biochemical compounds on the primitive Earth. Nature **190**, 389–390 (1961)
Petaev M.I. Wood J.A.: The condensation with partial isolation (CWPI) model of condensation in the solar nebula. Meteor. Planet. Sci **33**, 1123–1137 (1998)
Pierazzo E. Chyba C.F.: Amino acid survival in large cometary impacts. Meteor. Planet. Sci **34**, 909–918 (2010)
Pizzarello, S., Williams, L.B.: Ammonia in the early solar system; an account from carbonaceous chondrites. Astrophys. J. **749** (2012). id. 161
Rauer, H.: Comets. In: Altwegg, K., Benz, W., Thomas, N. (eds.) Trans-Neptunian Objects and Comets, pp. 165–254. Springer, Berlin (2008)
Rubin, A.E., Choi, B.-G.: Origin of halogens and nitrogen in enstatite chondrites. Earth Moon Planets **105**, 41–53 (2009)

Rubin, A.E., Trigo-Rodríguez, J.M., Huber, H., Wasson, J.T.: Progressive aqueous alteration of CM carbonaceous chondrites. Geochim. Cosmochim. Acta **71**, 2361–2382 (2007)
Schaefer, L., Fegley, B., Jr.: Outgassing of ordinary chondritic material and some of its implications for the chemistry of asteroids, planets and satellites. Icarus **186**, 462–483 (2007)
Schaefer, L., Lodders, K., Fegley, B., Jr.: Vaporization of the Earth: application to exoplanet atmospheres. Astrophys. J. **755**, 41, 16 pp (2012)
Sekanina, Z.: The problem of split comets in review, In: Comets, Univ. Arizona Press, Tucson, AZ, pp. 251–287 (1982)
Stevenson, D.J., Lunine, J.I.: Rapid formation of Jupiter by diffuse redistribution of water vapor in the solar nebula. Icarus **75**, 146–155 (1988)
Trigo-Rodríguez, J.M., Blum, J.: Tensile strength as an indicator of the degree of primitiveness of undifferentiated bodies. Planet. Space Sci. **57**, 243–249 (2009a)
Trigo-Rodríguez, J.M., Blum, J.: The effect of aqueous alteration and metamorphism in the survival of presolar silicate grains in chondrites. Publ. Astron. Soc. Aust. **26**, 289–296 (2009b)
Trigo-Rodríguez, J.M., Llorca, J.: The strength of cometary meteoroids: clues to the structure and evolution of comets. Mon. Not. R. Astron. Soc. **372**, 655–660 (2006)
Trigo-Rodríguez, J.M., Llorca, J.: Erratum: the strength of cometary meteoroids: clues to the structure and evolution of comets. Mon. Not. R. Astron. Soc. **375**, 415 (2007)
Trigo-Rodríguez, J.M., Martín-Torres, F.J.: Implication of impacts in the young Earth Sun paradox and the evolution of Earth's atmosphere. In: The Early Evolution of the Atmospheres of Terrestrial Planets. Springer (2013, this volume)
Trigo-Rodríguez, J.M., Rubin, A.E.: Evidence for parent-body aqueous flow in the MET 01070 CM carbonaceous chondrite. In: 37th LPS Conference, League City. Lunar and Planetary Institute (2006). abstract #1104
Trigo-Rodríguez, J.M., Llorca, J., Borovicka, J., Fabregat, J.: Chemical abundances determined from meteor spectra: I. Ratios of the main chemical elements. Meteor. Planet. Sci. **38**, 1283–1294 (2003)
Trigo-Rodríguez, J.M., Rubin, A.E., Wasson, J.T.: Non-nebular origin of dark mantles around chondrules and inclusions in CM chondrites. Geochim. Cosmochim. Acta **70**, 1271–1290 (2006)
Trigo-Rodríguez, J.M., García-Melendo, E., Davidsson, B.J.R., Sánchez, A., Rodríguez, D., Lacruz, J., De los Reyes, J. A., Pastor, S.: Outburst activity in comets: I. Continuous monitoring of comet 29P/Schwassmann-Wachmann 1. Astron. Astrophys. **485**, 599–606 (2008)
Trigo-Rodríguez, J.M., García-Hernández, D.A., Sánchez, A., Lacruz, J., Davidsson, B.J.R., Rodríguez, D., Pastor, S., De los Reyes, J.A.: Outburst activity in comets. II. A multiband photometric monitoring of comet 29P/Schwassmann-Wachmann 1. Mon. Not. R. Astron. Soc. **409**, 1682–1690 (2010)
Urey, H.: The Planets: Their Origin and Development. Yale University Press, New Haven (1952)
Warren, P.H.: Ejecta-megaregolith accumulation on planetesimals and large asteroids. Meteor. Planet. Sci. **46**, 53–78 (2011)
Wasson, J.T.: Oxygen-isotopic evolution of the Solar Nebula. Rev. Geophys. **38**, 491–512 (2000)
Weisberg, M.K., McCoy, T.J., Krot, A.N.: Systematics and evaluation of meteorite classification. In: Lauretta, D.S., McSween, H.Y. (eds.) Meteorites and the early Solar System II, pp.19–52. University of Arizona Press, Tucson (2006)
Wetherill, G.W.: Occurrence of giant impacts during the growth of the terrestrial planets. Science **228**, 877–879 (1985)
Young, E.D., Zhang, K.K., Schubert, G.: Conditions for pore water convection within carbonaceous chondrite parent bodies: implications for planetesimal size and heat production. Earth Planet. Sci. Lett. **213**, 249–259 (2003)
Zahnle, K., Kasting, J., Pollack, J.B.: Evolution of a steam atmosphere during Earth's accretion. Icarus **74**, 62–97 (1988)
Zolensky, M.E., Sween, Mc.: Aqueous alteration. In: Kerridge, J.F., Matthews, M.S., (eds.) Meteorites and the early solar system, Univ. of Arizona, Tucson, **114**, (1988)

# Chapter 3
# A Mathematic Approach to Nitrogen Fixation Through Earth History

**Alfonso Delgado-Bonal and F. Javier Martín-Torres**

**Abstract** Nitrogen is essential for life as we know it. According to phylogenetic studies, all organisms capable of fixing nitrogen are prokaryotes, both bacteria and archaea, suggesting that nitrogen fixation and ammonium assimilation were metabolic features of the Last Universal Common Ancestor of all organisms. At present time the amount of biologically fixed nitrogen is around $2 \times 10^{13}$ g/year (Falkowski 1997), an amount much larger than the corresponding to the nitrogen fixed abiotically (between $2.6 \times 10^{9}$ and $3 \times 10^{11}$ g/year) (Navarro-González et al. 2001). The current amount of nitrogen fixed is much higher than it was on Earth before the Cambrian explosion, where the symbiotic associations with *leguminous* plants, the major nitrogen fixer currently, did not exist and nitrogen was fixed only by free-living organisms as cyanobacteria. It has been suggested (Navarro-González et al. 2001) that abiotic sources of nitrogen fixation during Early Earth times could have an important role triggering a selection pressure favoring the evolution of nitrogenase and an increase in the nitrogen fixation rate. In this study we present briefly a method to analyze the amount of fixed nitrogen, both biotic and abiotic, through Earth's history.

## Introduction

Nitrogen is an essential component of all living organisms on Earth (Fig. 3.1). It is a basic component of aminoacids and nucleobases, and therefore of proteins and nucleic acids. In the human body, the quantity of nitrogen in our cells is about a 3%, i.e. around 1.860 Kg of the average mass. In prokariotic cells, present nowadays in a quantity of $4–6 \times 10^{30}$ cells, i.e., around $85–130 \times 10^{30}$ g of Nitrogen (Whitman

A. Delgado-Bonal • F.J. Martín-Torres (✉)
Centro de Astrobiología (CSIC-INTA), 28850 Torrejón de Ardoz, Madrid, Spain
e-mail: adelgado@cab.inta-csic.es; javiermt@cab.inta-csic.es

J.M. Trigo-Rodriguez et al. (eds.), *The Early Evolution of the Atmospheres of Terrestrial Planets*, Astrophysics and Space Science Proceedings 35,
DOI 10.1007/978-1-4614-5191-4_3, 

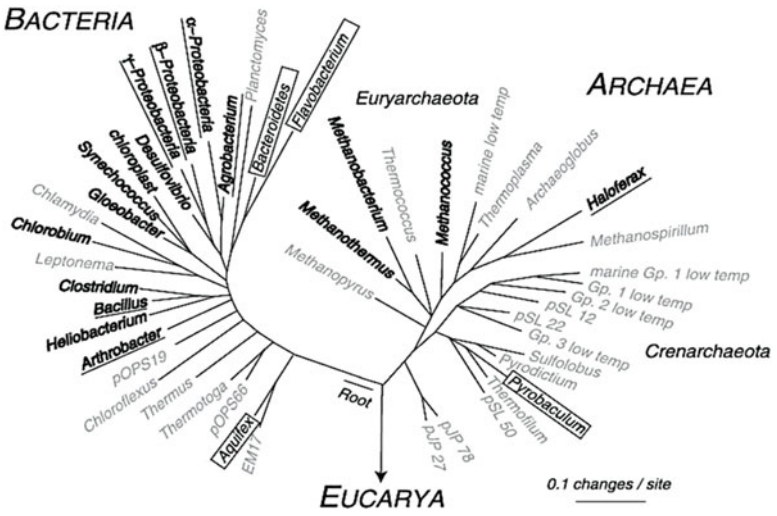


**Fig. 3.1** Phylogenetic tree of the three domains of life (*Bacteria*, *Archaea*, and *Eucarya*) (Adapted from Barns et al. (1996)). Members of the *Eucarya* are omitted for clarity. The genera listed are representative of major lineages of the two domains

et al. 1998), more than a half of the biomass. That this is an outstanding number can be easly seen when we compare it with the total amount of nitrogen content in the atmosphere ($1.3 \times 10^{16}$ g (Ehrlich 1996)).

Nitrogen is not a basic component of the Lithosphere, (although it can be found on clay minerals as $NH_4^+$ occuping the interlayer place of $K^+$), and then can be assumed that the source of the nitrogen incorporated to the biomass is the atmosphere. A relevant fact is that nitrogen in its molecular stable form, $N_2$, cannot be used generally as nutrient. This is because the strong triple bond between the N atoms of $N_2$ molecule makes it relatively inert. In fact, in order for plants and animals to be able to use nitrogen, $N_2$ gas must first be converted to more a chemically available form such as ammonium $(NH_4^+)$, nitrate $(NO_3^-)$, or organic nitrogen $(\text{e.g.urea} - (NH_2)_2CO)$. The inert nature of $N_2$ means that biologically available nitrogen is often in short supply in natural ecosystems, limiting plant growth and biomass accumulation. This need to convert $N_2$ before beeing incorporated to organisms is an important difference with respect to other elements like Carbon (C) or Hydrogen (H).

If nitrogen atoms incorporated in living organisms have their origin in Earth's atmosphere then the atmosphere must be different now from the one present before the origin of life. Nowadays Nitrogen is the main compound in the Earth's atmosphere with a 78.1%, and current models of the composition of Early Earth's atmosphere conclude that nitrogen abundance was more than 98% (Kasting 1993). In this paper we present a simple method to estimate the effects of life in the fixation and uptaken of nitrogen from Earth atmosphere through history.

## Nitrogen Fixation

Nitrogen fixation is the process wherein $N_2$ is converted to ammonium. It is essential because it is the only way that organisms attain nitrogen directly from the atmosphere. It is not a static process, because although there are abiotic methods (lightning) and biotic (nitrogen fixers) to fix nitrogen to the ground, there are several processes that give back nitrogen to the atmosphere.

We describe abiotic and biotic nitrogen fixation briefly:

– *Abiotic nitrogen Fixation*

High-energy natural events such as lightning, forest fires, and even hot lava flows can cause the fixation of smaller, but significant amounts of nitrogen. The high energy of these natural phenomena can break the triple bonds of $N_2$ molecules, thereby making individual N atoms available for chemical transformation.

In particular the enormous energy of lightning breaks nitrogen molecules and enables their atoms to combine with oxygen in the air forming nitrogen oxides. These oxides dissolve in rain, forming nitrates, that are carried to the surface. Lightning plays a minor part in the fixation of atmospheric nitrogen. Atmospheric nitrogen fixation probably contributes some 5–8% of the total nitrogen fixed. Nevertheless in the early stages of emergence of life its role could have been very important (Navarro-González et al. 2001).

In the abiotic fixation, $N_2$ would have been oxidized with $CO_2$ by lightning:

$$N_2 + 2CO_2 - - > 2NO + 2CO$$

After this process, NO then gets converted to soluble nitrosyl hydride (HNO). An important point is that the fixed nitrogen depends on the abundance of $CO_2$. According to Navarro-González et al. (2001), for $CO_2$ mixing ratios from 0.04 to 0.5, the rate of fixation would be $2.6 \times 10^9$ to $3 \times 10^{11}$ g N year $^{-1}$(Catling and Kasting 2007), and references there in Hill et al. (1980).

In the Ocean, dissolved $N_2$ would have been converted into $NO_3^-$ and $NO_2^-$, according to Mancinelli and McKay (1998). However, the cycle of nitrogen also works in the Ocean, and ferrous iron $Fe^{2+}$ can reduce the dissolved forms to produce ammonia, $NH_3$, some of which would flux to the atmosphere, where it would be photolyzed to $N_2$ and $H_2$.

Another way that nitrogen could have been fixed abiotically was through HCN synthesis in atmospheres containing trace levels of $CH_4$.HCN is hydrolyzed in solution to form ammonium, $NH_4^+$.

– *Biological Nitrogen Fixation*

Between living beings the ability to fix nitrogen is found only in certain bacteria and archaea:

– Certain bacteria, for example those among the genus *Rhizobium*, are the only organisms that fix nitrogen through metabolic processes.

- Some live in a symbiotic relationship with plants of the legume family (e.g., soybeans, alfalfa). Symbiotic nitrogen fixation occurs in plants that harbor nitrogen-fixing bacteria within their tissues. Each of these is able to survive independently (soil nitrates must then be available to the legume), but life together is clearly beneficial to both. In this relationship, nitrogen fixing bacteria inhabit legume root nodules and receive carbohydrates and a favorable environment from their host plant in exchange for some of the nitrogen they fix. Only together can nitrogen fixation take place.
- Some establish symbiotic relationships with plants other than legumes (e.g., alders).
- Some establish symbiotic relationships with animals, e.g., termites and "shipworms" (wood-eating bivalves).
- Some nitrogen-fixing bacteria live free in the soil.
- Nitrogen-fixing cyanobacteria are essential to maintaining the fertility of semi-aquatic environments like rice paddies. In aquatic environments, blue-green algae (really a bacteria called cyanobacteria) is an important free-living nitrogen fixer.
- Within the last century, human activities have become as important a source of fixed nitrogen equivalent to all natural sources combined. Burning fossil fuels, using synthetic nitrogen fertilizers, and cultivation of legumes all fix nitrogen. Through these activities, humans have more than doubled the amount of fixed nitrogen that is pumped into the biosphere every year

In order to model the amount of nitrogen taken from the atmosphere and biologically reduced we need to know the population of bacteria at each time since life appeared on Earth.

## Nitrogen Cycle

The nitrogen cycle is the set of biogeochemical processes by which nitrogen undergoes chemical reactions, changes form, and moves through difference reservoirs on earth, including living organisms. The nitrogen cycle has changed through Earth's history (Fig. 3.2). For example it is believed that during the Archean there was no-denitrification, which means that all the nitrogen fixed remained in that way. After that period of time, denitrification is a fact and nitrogen cycle started, coupled to other biochemical cycles such as Carbon cycle and Phosphate cycle.

In this work, we assume a rate of denitrification about 11% (Do-Hee Kim et al. 1997). This value is similar to the denitrification rate at present day, knowing that, although is very probable that during that time the denitrification rate was smaller, we are trying to estimate the minimum value of the nitrogen fixed. Also, the organic nitrogen formed in the atmosphere is photodissociated with a rate of 25% (Kasting and Walker 1981).

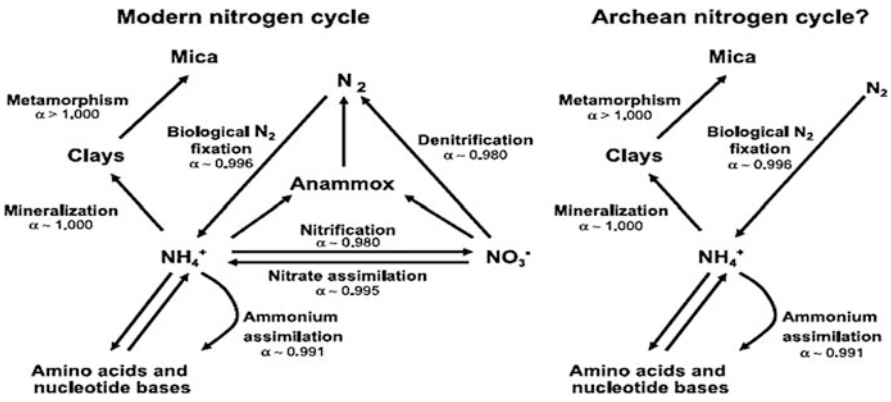


**Fig. 3.2** *Left*: A simplified modern nitrogen cycle with known fraction effects for the nitrogenous reaction product. *Right*: The proposed nitrogen cycle operating during the Archean (From Papineau et al. (2005))

## The Population of Bacteria

It is usually attributed to Malthus (1798) the merit to propose the first model for population growth based on a geometrical equation. Its mathematical expression is an exponential dependent of one parameter, $\mu$, called the growth factor:

$$\mathbf{P} = \mathbf{P}_0 \cdot \mathbf{e}^{\mu t}$$

Other more sophisticated models of growth have been proposed in the past, as for example the logistical model proposed by Verhust (1838), dependent on three-parameters: $k$ (maximum of the population), $\mu$ (the growth constant), and $\tau$ (the instant in which the population is k/2):

$$\mathrm{P} = \mathrm{k}/[1 + \mathrm{e} - \mu(\mathrm{t} - \tau)]$$

More detailed formulations of the population growth have been done increasing the number of parameters of the equation. Independently of the model, the fundamental parameter that determine the population at one instant of time will be the growth constant, $\mu$.

The population growth depends mainly on temperature and nutrients (Ratkowsky et al. 1982; Savage et al. 2004). During the glaciations periods for instance, the growth constant was near zero due to the fact that most known bacteria need a range of temperature very limited, and if it goes below 0°C, it cannot grow properly. Also, the availability of nutrients is a very big limitation for the population of bacteria, nitrogen and carbon being the main compounds affecting the growth constant (Demoling and Figueroa 2007).

In this work, the influence of these parameters is not taken into account directly but it is actually included in the formulation, as we have taken stromatolites as a reference, and the natural conditions at any time are having influence in the number of cells and therefore in the growth constant we obtain from the fit.

## Stromatolites as a Test for the Model

The arrow of time goes in one unique direction and it is not possible to have direct proof of the validity of a model estimating the evolution. A source of information from the past that can help us to test our model is the fossile record, particulary stromatolites. Stromatolites are the fossiles that bacteria and archea left behind after their dead. This fossilized microbial mat changes their abundance with time as showed in Table 3.1. Although the different opinions about the appearance of metazoa and the decline of stromatolites are well explained, there seems to exist in fact a relation, due to the change of sediments by metazoa and the possible fossilization of microbial mats associated to it (Awramik 1984; Walter and Heys 1985).

Although stromatolites are not only composed of cyanobacteria but other organisms such as Planctomycetes, Proteobacteria or Archea, and their abundance is only about 5% of the total number of cells (Papineau et al. 2005), it can be used as a marker for estimating the cyanobacteria growth factor. We understand that this is a good assumption, even when the % of cyanobacteria is different from one fossil to another.

Taking into account the amount of stromatolites, we can fit the data to an exponential function since 3,500 Myr until approximately 0.600 Ma (Fig. 3.3), the time in which the Cambrian explosion modified the fossil record. The parameters of this fit are:

$$\mu = 2.1319 + / - 0.06374 (2.99\,\%)$$

and the data are plotted in Fig. 3.4.

**Table 3.1** Abundance of stromatolites classified as function of geological epoch (Adapted from Walter and Heys (1985))

| Boundary | Interval | Duration (Ga) | Abundance |
|---|---|---|---|
| 0.5 | Cambrian | 0.07 | 86 |
| 0.57 | Vendian | 0.11 | 140 |
| 0.68 | Late Riphean | 0.38 | 357 |
| 1.05 | Middle Riphean | 0.3 | 274 |
| 1.35 | Early Riphean | 0.3 | 170 |
| 1.65 | Late Proterozoic | 0.55 | 153 |
| 2.2 | Early Proterozoic | 0.3 | 8 |
| 2.5 | Archean | | |

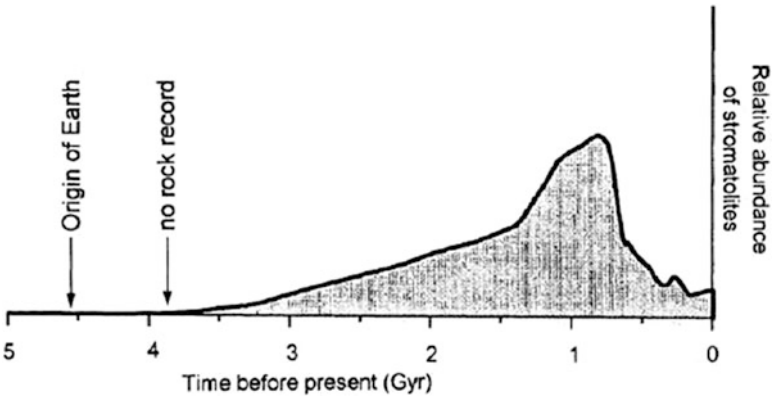


**Fig. 3.3** Relative abundance of stromatolites (Adapted from "The Ecology of Cyanobacteria; Their diveristy in time and space", Whitton and Potts (2002))

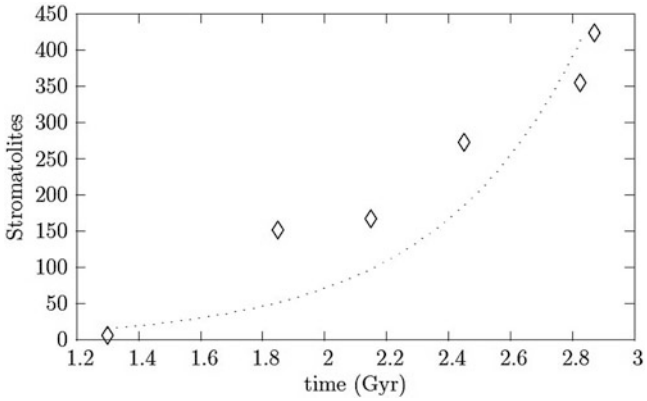


**Fig. 3.4** Exponential fit for stromatolites in time

## Summary and Conclusions

We have developed a very simple model to estimate the effect of nitrogen fixation and uptaken from life in the abundance of atmospheric nitrogen through Earth's history.

Although the first cyanobacteria fossiles found in stromatolites are dated back from 3.5 Gyr ago there are evidences for the existence of life on Earth before 3.8 Gry ago based on Carbon isotopes studies (Mojzsis et al. 1996), although this is still debated. Assuming that only one living cell was present at that time, we have modelled the evolution of a population of cells based on a realistic value for the growth constant from stromatolites and estimated the amount of cells during the evolution of Earth till the Cambrian Explosion. This calculation provides a

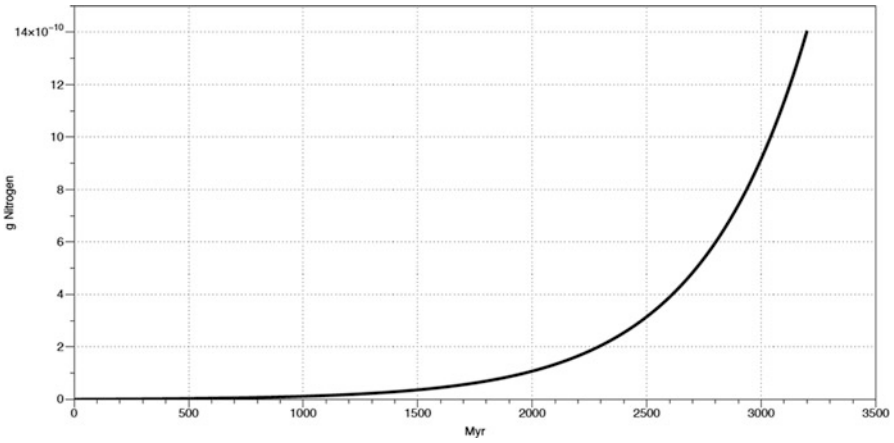


**Fig. 3.5** Biological nitrogen fixed since the origin of life until the Cambrian explosion

minimum value for the number of cells present at each instant of time and, with that value, it is possible to estimate the biological fixation during the Precambrian epoch. Therefore, this is not a very precise model for the estimation of biological fixation, but it is useful to understand the relative importance of lighting and abiotical fixation with respect to the biological fixation.

From the data showed in Table 3.1 and Fig. 3.5 we conclude that the nitrogen biological fixed at the time of the Cambrian explosion was about $1.4 \times 10^{-9}$ g

Considering that 3% of a cell is nitrogen, and an average cell weight is about $10^{-12}$ g, the amount on nitrogen present in a cell is $3 \times 10^{-14}$ g. By the time of the cambrian explosion, our model provides a value for the number of cells around 900,000 cells, which means $2.7 \times 10^{-8}$ g of nitrogen needed to maintain the population.

This estimated number of cells needs more biological nitrogen than the amount they can fix, so this result indicates that an additional source of abiotic nitrogen fixation was needed during the Precambrian to substain this amount of living systems.

This additional source could be, for example lightning, as proposed by Navarro-González et al. (2001). According to these authors, lightning could be a source of nitrogen fixation of about $10^{12}$ g N year$^{-1}$, which means that can be fixed abiotically in a year more than bioticaly in all the Precambrian.

Nevertheless, today the biological fixation is many times bigger than the abiotical one, and this is not because the number of cells increased, but because of the associations between different organisms. A symbiotic association of leguminous can fix nitrogen thousand times more efficiently than a free-living organism.

**Acknowledgements** ADB acknowledges INTA grant TD 04/10 and JMT acknowledges Spanish Government PIE201050I025 and AYA2011-25720 grant.

## References

Awramik, S.M.: Ancient stromatolites and microbial mats. In: Cohen, Y, Castenholz, R.W., Halvoson, H.O. (eds.) Microbial Mats: Stromatolites, pp. 1–22. Alan R. Liss Inc., New York (1984)

Barns, S.M., Delwiche, C.F., Palmer, J.D., Pace, N.R.: Perspectives on archaeal diversity, thermophily and monophyly from environmental rRNA sequences. Proc. Natl. Acad. Sci. USA **93**, 9188–9193 (1996)

Catling, D.C., Kasting, J.F.: Planetary atmospheres and life. In: Sullivan, W., Baross, J. (eds.) Planets and Life: The Emerging Science of Astrobiology, pp. 91–116. Cambridge University Press, Cambridge (2007)

Demoling, F., Figueroa, D.: Comparison of factors limiting bacterial growth in different soils. Soil Biol. Biochem. **39**(10), 2485–2495 (2007)

Ehrlich, H.L.: Geomicrobiology. Marcel Dekker Inc, Basel (1996)

Falkowski, P.G.: Evolution of the nitrogen cycle and its influence on the biological sequestration of CO2 in the ocean. Nature **387**, 272–275 (1997)

Hill, R.D., Rinker, R.G., Wilson, H.D.: Atmospheric nitrogen fixation by lightning. J. Atmos. Sci. **37**, 179–192 (1980)

Kasting, J.F.: Earth's early atmosphere. Science **259**(5097), 920–926 (1993)

Kasting, J.F., Walker, J.C.G.: Limits on oxygen concentrations in the prebiological atmosphere and rate of abiotic fixation of nitrogen. J. Geophys. Res. **86**, 1147–1158 (1981)

Do-Hee Kim, Osamu Matsuda, Tamiji Yakamoto: Nitrification, Denitrification and Nitrate Reduction Rates in the Sediment of Hiroshima Bay, Japan. J. Oceanogr. **53**, 317–324 (1997)

Malthus, T.R.: An Essay on the Principle Population. J. Johnson, London (1798)

Mancinelli, R.L., McKay, C.P.: Evolution of nitrogen cycling. Orig. Life **18**, 311–325 (1998)

Mojzsis, S.J., Arrhenius, G., McKeegan, K.D., Harrison, T.M., Nutman, A.P., Friend, C.R.L.: Evidence for life on Earth before 3,800 million years ago. Nature **384**, 55–59 (1996)

Navarro-González, R., McKay, C.P., Mvondo, D.N.: A possible nitrogen crisis for Archaean life due to reduced nitrogen fixation by lightning. Nature **412**, 61–64 (2001)

Papineau, D., Mojzsis, S.J., Karhu, J.A., Marty, B.: Nitrogen isotopic composition of ammoniated phyllosilicates: case studies from Precambrian metamorphosed sedimentary rocks. Chem. Geol. **216**(1–2), 37–58 (2005)

Papineau, D., Walker, J.J., Mojzsis, S.J., Pace, N.R.: Composition and structure of microbial communities from stromatolites of Hamelin Pool in Shark Bay, Western Australia. Appl. Environ. Microbiol. **71**(8), 4822–4832 (2005)

Ratkowsky, D.A., Olley, J., McMeekin, T.A., Ball, A.: Relationship between temperature and growth rate of bacterial cultures. J. Bacteriol. **149**(1), 1–5 (1982)

Savage, V.M., Gillooly, J.F., Brown, J.H., West, G.B., Charnov, E.L.: Effects of body size and temperature on population growth. Am. Nat. **163**, 429–441 (2004)

Verhust, P.F.: Notice sur la loi que la population suit dans son accroissement. Corr. Math. Phys. **10**, 113 (1838)

Walter, M.R., Heys, G.R.: Links between the rise of the metazoa and the decline of stromatolites. Precambrian Res. **29**(1–3), 149–174 (1985)

Whitton, B.A., Potts, M. (eds.): The Ecology of Cyanobacteria; Their Diveristy in Time and Space. Kluwer Academic Publishers, New York, **39**(3), 466 (2001). doi10.1023/A:1015127720748

Whitman, W.B., Coleman, D.C., Wiebe, W.J.: Prokaryotes: the unseen majority. Proc. Natl. Acad. Sci. **95**, 6578–6583 (1998)

# Chapter 4
# Stability of Earth-Like $N_2$ Atmospheres: Implications for Habitability

**Helmut Lammer, Kristina G. Kislyakova, Manuel Güdel, Mats Holmström, Nikolai V. Erkaev, Petra Odert, and Maxim L. Khodachenko**

**Abstract** According to recent studies related to the EUV heating by the young Sun of Earth's nitrogen atmosphere, upper atmosphere temperatures could rise up to several thousand Kelvin. For fluxes larger $\geq 7$ times that of today's Sun the thermosphere changes from a hydrostatic to a dynamically expanding non-hydrostatic regime, adiabatically cools but expands beyond the magnetopause so that the magnetosphere is not able to protect the upper atmosphere from solar wind erosion. A $N_2$-rich terrestrial atmosphere would have been lost within a few million years during the EUV active period of the young Sun $\geq 4$ Ga ago. These results indicate that a hydrogen-rich gaseous envelope, which could have remained from Earths protoatmosphere and/or higher atmospheric $CO_2$ amounts may have protected Earth's atmospheric nitrogen inventory against efficient escape to space.

H. Lammer (✉) • K.G. Kislyakova • M.L. Khodachenko
Austrian Academy of Sciences, Space Research Institute, Graz, Austria
e-mail: helmut.lammer@oeaw.ac.at; kristina.kislyakova@oeaw.ac.at; maxim.khodachenko@oeaw.ac.at

M. Güdel
Institute of Astrophysics, University of Vienna, Vienna, Austria
e-mail: manuel.guedel@univie.ac.at

M. Holmström
Swedish Institute of Space Physics, Kiruna, Sweden
e-mail: matsh@irf.se

N.V. Erkaev
Russian Academy of Sciences, and Siberian Federal University, Institute for Computational Modelling, Krasnoyarsk, Russian Federation
e-mail: erkaev@icm.krasn.ru

P. Odert
Institute of Physics, IGAM, University of Graz, Austria

Austrian Academy of Sciences, Space Research Institute, Graz, Austria
e-mail: petra.odert@oeaw.ac.at

J.M. Trigo-Rodriguez et al. (eds.), *The Early Evolution of the Atmospheres of Terrestrial Planets*, Astrophysics and Space Science Proceedings 35,
DOI 10.1007/978-1-4614-5191-4_4, © Springer Science+Business Media New York 2013

An alternative scenario would be that the nitrogen in Earth's early atmosphere was degassed or delivered during the late heavy bombardment period, where the solar EUV flux decreased to values <7 times of the modern value. Finally, we discuss how EUV heated and extended upper atmospheres and their interaction with the host star's plasma environment could be observed around transiting Earth-like exoplanets at dwarf stars by space observatories such as the WSO-UV. Such future observations could be used to test the discussed atmospheric evolution scenarios and would enhance our understanding on the impact on the activity of the young Sun/star on the early atmospheres of Venus, Earth, Mars and exoplanets.

## Introduction

The evolution of planetary atmospheres can only be studied properly by taking into account that the radiation and particle environment of the Sun or a planet's host star is changing with time (e.g., Güdel et al. 1997; Ribas et al. 2005; Güdel 2007; Lundin et al. 2007). The total radiative output of the young Sun can be assessed from two sources: First, the theory of stellar evolution indicates that the young Sun at a time when it started core hydrogen burning on the main sequence emitted 30% less electromagnetic radiation than at present (e.g., Sackmann and Boothroyd 2003). Second, the total luminosity of stars with known masses and ages can in principle be derived from observations; stellar masses and ages are, difficult to infer accurately.

However, geologic evidence on Earth (Peck et al. 2001; Valley et al. 2002) and Mars (e.g., Phillips et al. 2011; Smith et al. 2001; Carr and Head 2003; Head and Marchant 2009; Barrat and Bollinger 2010) indicate that both planets maintained early environmental conditions allowing liquid water – a prerequisite for the formation of life as we know it – to exist on the surface. This mystery is called Faint Young Sun Paradox (FYSP), because according to the standard solar evolution model and the lower luminosity which increased only slowly during the next billion years both planetary surfaces would thus have been completely frozen. To solve this apparent paradox, various hypotheses have been tested although a conclusive answer is still outstanding. The most popular theory assumes higher admixtures of greenhouse gases in the atmospheres of Earth and Mars; such gases include carbon monoxide, ammonia, and methane ($CO_2$, $NH_3$, and $CH_4$, respectively). A more radical remedy of the FYSP would be a young Sun that was significantly more massive than at present, losing the excess mass during its main-sequence life in an enhanced ionized wind (Whitmire et al. 1995; Sackmann and Boothroyd 2003). The bolometric luminosity of main-sequence stars scales approximately with stellar mass to the third power; further, the radius of the Earth's orbit would have been smaller for a more massive Sun because the orbital radius scales inversely with the solar mass. Both effects combine to a scaling of the received flux with the fifth power of the solar mass. Constraints on this model come from the requirement that the young Martian atmosphere was warm enough to maintain water in liquid form, but the Earth's atmospheric temperature was moderate enough to prevent loss of the water oceans in a runaway greenhouse. The appropriate mass range for the young Sun was thus 1.03–1.07 $M_{Sun}$. Corresponding solar models are in acceptable

agreement with helioseismology results (Sackmann and Boothroyd 2003) but the observational evidence is presently unclear (Gaidos et al. 2000; Wood et al. 2005; Minton and Malhotra 2007).

Multi-wavelength satellite observations at short wavelengths of solar proxies with ages covering a time span between ∼0.1–7 Ga indicate that young Sun-like stars rotate more than 10 times faster compared to the present Sun and have much stronger dynamo-driven high energy photon emissions. Astrophysical observations suggest that the coronal X-ray, soft X-ray (SXR) and EUV emissions of the young main-sequence Sun might have been ∼100–1,000 times stronger than at present (e.g. Güdel et al. 1997; Ribas et al. 2005; Güdel 2007).

The extreme radiation in short wavelengths together with the plasma environment of the young Sun or star has important implications for the evolution of the planetary atmospheres both in our solar and in extrasolar planetary systems. The solar/stellar radiation and the particle flux have a tremendous influence on the energy budget, thermal structure, and photochemistry of the upper atmosphere and can result in significant thermospheric expansion and enhanced erosion (Kulikov et al. 2006; 2007; Lammer et al. 2007; Lichtenegger et al. 2010). Depending on atmospheric composition and planetary mass, when the solar/stellar SXR and EUV flux exceeds a critical value, the outward flow of the bulk upper thermosphere starts cooling due to adiabatic expansion. This cooling results in a decrease of the temperature in the upper atmosphere and acts against further expansion of the thermosphere (Tian et al. 2008a, b).

Thus, an upper atmosphere can transit from a hydrostatic to a hydrodynamic outflow state, depending on the solar/stellar SXR/EUV flux and planetary and atmospheric parameters. Such expanded thermosphere-exosphere regions are expected to suffer high non-thermal atmospheric loss rates (Lundin et al. 2007; Tian et al. 2008a, b; Lichtenegger et al. 2010). If the early Earth's nitrogen atmosphere would have indeed experienced strong thermal or non-thermal escape to space we would expect that the present atmosphere would be enriched by heavier $^{15}N$ isotopes compared to the lighter $^{14}N$ isotope, as observed on Mars and Titan (Lammer and Bauer 2003).

However, from $^{15}N/^{14}N$ isotope observations in Earth's atmosphere there is no indication that Earth's nitrogen experienced strong escape during the planet's history (Lammer and Bauer 2003). In this work we will briefly address the expected atmospheric response of Earth's nitrogen atmosphere to high EUV fluxes of the young Sun. Then we discuss several possibilities which may have protected the atmospheric nitrogen abundance against efficient thermal and non-thermal escape during the extreme EUV activity of the young Sun. Furthermore, we present an idea how we can test the atmospheric evolution hypotheses by future UV observations during transits of terrestrial exoplanets around M-type dwarf stars.

## Atmospheric Response to High Solar/Stellar EUV Radiation

In recent studies Tian et al.(2008a, b) investigated the response of Earth's upper atmosphere to extreme solar EUV conditions and discovered that the upper atmosphere of an Earth-mass planet with the present Earth atmospheric composition

**Table 4.1** Upper atmosphere response modeled for an Earth-size and mass planet by hydrodynamic upper atmosphere models based on Penz et al. (2008) for the hydrogen-rich thermosphere (see also Tian et al. 2005) and for the nitrogen-rich thermosphere from Tian et al. (2008a). The EUV response of the $CO_2$ atmosphere is calculated from a diffusive-gravitational equilibrium and thermal balance model described in Kulikov et al. (2006). The exobase temperature $T_{exo}$ and exobase distance $r_{exo}$ is given in units of Kelvin and planetary radius $r_{pl}$ to atomic hydrogen-, nitrogen-, and $CO_2$-rich upper atmospheres as a function of solar/stellar EUV flux

| | 1 $EUV_{Sun}$ | | 5 $EUV_{Sun}$ | | 10 $EUV_{Sun}$ | | 20 $EUV_{Sun}$ | |
|---|---|---|---|---|---|---|---|---|
| | $T_{exo}$[K] | $r_{exo}/r_{pl}$ | $T_{exo}$ [K] | $r_{exo}/r_{pl}$ | $T_{exo}$ [K] | $r_{exo}/r_{pl}$ | $T_{exo}$/[K] | $r_{exo}/r_{pl}$ |
| H | 240 | 7.5 | 360 | 9.5 | 485 | 10.5 | 850 | 12 |
| $H_2$ | 460 | 6 | 525 | 7 | 625 | 7.7 | 790 | 8.5 |
| N | 900 | 0.078 | 7,500 | 2.5 | 5,600 | 5 | 2,500 | 12.7 |
| $CO_2$ | 280 | 0.028 | 550 | 0.03 | 620 | 0.036 | 1,000 | 0.047 |

would start to rapidly expand if the thermospheric temperatures exceeded 7,000–8,000 K. If these temperatures are reached, the upper part of the thermosphere is cooled adiabatically due to the outflow of the dominant dissociated atoms such as O, N, etc. From these studies a problem to the evolution of early Earth's atmosphere occurs. Similar to hydrogen-rich upper atmospheres, a nitrogen dominated thermosphere of the early Earth would also experience a rapid transition to a hydrodynamic expansion, which is affected by adiabatic cooling. However, for EUV fluxes >10 EUV the location of the exobase which separates the collisional regime from the collisionless regime will move above the present average geocentric subsolar magnetopause stand-off distance of $\sim$10 $R_{Earth}$, so that the neutral constituents beyond the magnetopause can be ionized and picked up by the solar wind. This mechanism is capable to erode a $\sim$1 bar nitrogen atmosphere during $\sim$10 Ma (Lichtenegger et al. 2010; Lammer et al. 2012).

Table 4.1 compares hydrogen-rich, nitrogen-rich and Venus-type $CO_2$ thermosphere responses for an Earth-analogue planet which is exposed to solar/stellar EUV flux which is 1, 5, 10 and 20 times that of the present solar value. One can see in Table 4.1 that hydrogen- and nitrogen-rich atmospheres may expand to several Earth-radii, while Venus-type $CO_2$-dominated atmospheres remain close to the planet surface. The reason for this low expansion is related to the fact that $CO_2$ molecules are good IR-coolers so that a large fraction of the incoming EUV radiation is emitted back to space due to emissions in the 15 µm band (e.g., Kulikov et al. 2006; 2007).

One can also see from Table 4.1 that the exobase temperature $T_{exo}$ remains relatively cool for hydrogen-rich upper atmospheres compared to one which is dominated by nitrogen. The reason for this behavior is that an upper atmosphere which is dominated by atomic hydrogen starts to change from a hydrostatic to a non-hydrostatic dynamically expanding regime at lower temperatures compared to a nitrogen-rich thermosphere. This can be also seen in the $T_{exo}$ for N atoms which are hydrostatic until $\sim$5 EUV and began to expand but adiabatically cool for higher EUV values. In the case of a nitrogen dominated atmosphere and in the absence of strong IR-cooling molecules the gas can be heated up to a few thousand Kelvin

before the thermosphere changes from hydrostatic to hydrodynamic conditions (Tian et al. 2008a, b).

According to Lichtenegger et al. (2010) the non-thermal nitrogen escape rates corresponding to EUV periods with fluxes $\geq$7 EUV times that of the present Sun, would result in the loss of the entire current nitrogen atmosphere within a few million years. Although there are uncertainties in the solar wind parameters, these authors showed that even if one assumes a present-day solar wind $\sim$4.2 Ga ago, the Earth would have lost its present nitrogen atmosphere during about 10 Ma.

After the late heavy bombardment (LHB) period, the EUV flux and also the solar wind ram pressure decreased, which resulted in a decreasing exobase distance and an increasing magnetopause standoff location. Then, the atmosphere eventually became protected by the magnetosphere and the nitrogen escape rate substantially decreased. Because there is no evidence that Earth's atmospheric nitrogen inventory experienced strong escape it remains an aeronomical mystery how the planet could keep its nitrogen dominated atmosphere during the first $\sim$500 Ma after the planets origin. In the following sections we discuss several scenarios which may help to shed some light on this complex problem.

## Formation of Protoatmospheres

For understanding how planetary atmospheres originated and evolved it is important to know the potential sources and sinks, which contributed to their initial formation. The earliest protoatmospheres of terrestrial planets can be linked to three formation scenarios which are illustrated in Fig. 4.1. The first protoatmosphere may originate by the accumulation of a hydrogen- and He-rich gaseous envelope from the nebula around the growing protoplanet before its accretion is finished (e.g. Hayashi et al. 1979; Ahrens et al. 1989; Ikoma and Hori 2012). A second protoatmosphere is produced after the young planet finished its accretion. By using bulk compositions related to primitive and differentiated meteorite compositions, outgassing alone can create a wide range of masses of initial planetary atmospheres.

According to Elkins-Tanton and Seager (2008) these protoatmospheres can range from $\leq$1 % of the planet's total mass up to $\sim$6 % by mass of hydrogen, to $\sim$20 mass % of $H_2O$, and/or $\sim$5 mass % of carbon compounds. Hydrogen-rich atmospheres can be outgassed as a result of oxidizing metallic iron with water, and excess water and carbon can produce atmospheres through simple degassing. During the solidification of the planet's magma ocean, dense water dominated $H_2O/CO_2$-rich steam atmospheres build up (e.g., Elkins-Tanton and Seager 2008; Elkins-Tanton and Seager 2008, 2011). $CH_4$ and $NH_3$ should also be outgassed and/or produced via mineralogical reactions in the crust on top of the lava ocean. Due to the dissociation of these molecules by the high X-ray flux of the young and active star additionally hydrogen atoms will contribute to the water-related content in the upper atmosphere, while C, O and N are converted into $CO_2$ and $N_2$ in the lower atmosphere (Rosenqvist and Chassefière 1995).

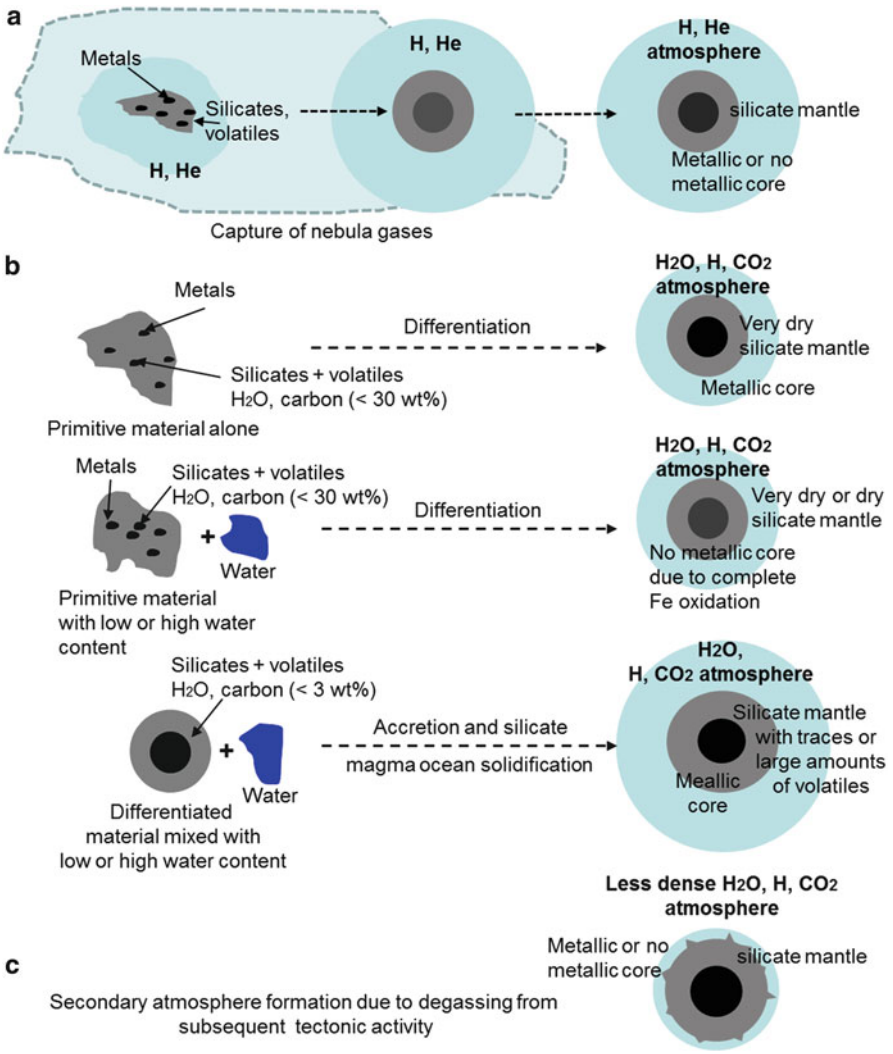


**Fig. 4.1** Illustration of the three primary sources for the formation of terrestrial planetary atmospheres. (**a**) Illustrates the capture of nebula gases and the accumulation of hydrogen-rich protoatmospheric layers around a rocky planet (e.g., Ikoma and Hori 2012). (**b**) Illustrates protoatmosphere formation scenarios during accretion and the solidification of a magma ocean. Depending on the impact history, and the initial water content dense steam atmospheres will be catastrophically outgassed (e.g., Elkins-Tanton and Seager 2008). (**c**) Illustrates the subsequent formation of secondary atmospheres related to tectonic activity on a terrestrial planet. As soon as the outgassing flux of the volatiles is higher than their escape flux a secondary atmosphere will accumulate (e.g., Rubey 1951)

Finally the third formation process is related to the later growth of a secondary atmosphere which builds up by tectonic activity such as volcanos (e.g. Rubey 1951; Schaefer and Fegley 2009; Grott et al. 2011). All three atmosphere formation scenarios are strongly linked to the impact history of the individual system, and the delivered or integrated volatiles during the formation process of a particular planet or system. Terrestrial planets may obtain their initial atmosphere by a mixture of all three scenarios but may originate most likely with dense hydrogen-, $H_2O$- and $CO_2$-rich atmospheres with $CH_4$ and $NH_3$ contents. As a byproduct these atmospheric outgassing models indicate that modest initial water contents can create planets with deep surface liquid water oceans soon after accretion is complete (Elkins-Tanton and Seager 2008; Elkins-Tanton 2011). This scenario is also consistent with the zircon evidence supporting the presence of liquid water on Earth's surface about 4.2 Ga ago (Peck et al. 2001).

However, there is also evidence from K/U ratio inventories that Earth accreted dry via stepwise growth from planetary embryos which lost their water and volatile inventories due to their lower gravity to space (Albarède and Blicher-Toft 2007). In this scenario Earth would have obtained its volatiles and water inventory by impacts during the late veneer (Albarède 2009).

## Early Hydrogen Envelopes and Steam Atmospheres

From the brief discussion before it becomes clear that the upper atmosphere of early terrestrial planets, including the early Earth may have been dominated by dense hydrogen-dominated gaseous envelopes either nebula based or produced from dissociated $H_2O$ molecules of the catastrophically outgassed and/or impact related steam atmospheres. In such a scenario one can assume that a dense and extended hydrogen envelope, could have acted as a protecting shield against the loss of heavier atmospheric species such as $N_2$. On the other hand if early Earth's initial $N_2$ inventory was indeed protected by hydrogen envelopes, such remnant gases must have escaped until today.

As shown in Lammer et al. (2012) during this early period a hydrogen-dominated upper atmosphere of an Earth-like planet experienced the most efficient atmospheric escape process, namely so called blow off, which develops if the mean thermal energy of the upper atmosphere gases at the exobase level exceeds the gravitational energy. Under this extreme condition the atmospheric escape is very efficient because the whole exosphere evaporates and will be refilled as long as enough gas is delivered from below. For estimating how much hydrogen and dragged oxygen atoms can be lost from a planet during its blow off phase, one can apply a blow off escape formula of Erkaev et al. (2007), which is based on Hunten (1993). The average escape flux $F_H$ of hydrogen atoms from the planetary dayside can then be written as

$$F_H = \frac{3\eta I_{EUV} F_{EUV}}{4\pi r_{\rm pl}^2 {\rm G}\rho_{\rm pl} {\rm m_H}}. \tag{4.1}$$

with $r_{\rm pl}$ the planetary radius. $I_{\rm EUV} = [t/t_{\rm Sun}]^{-1.23}$ is the EUV enhancement factor as a function of time $t (t \geq 0.1\,{\rm Ga})$ and solar age $t_{\rm Sun}$ in units of Ga according to Ribas et al. (2005), $F_{\rm EUV}$ is today's solar EUV flux averaged over the planetary sphere, $G$ is the gravitational constant and $\rho_{\rm pl}$ the mean planetary density, $\eta$ is the heating efficiency which is defined as a ratio of the net local gas heating rate to the rate of stellar radiative energy absorption. For hydrogen this value is often assumed to be 10–25 % (Lammer et al. 2009). Because $\eta$ is altitude dependent it could also be higher but is most likely <60 % (Yelle 2004; Penz et al. 2008). A value of 100 % is unrealistic and would correspond to the energy limited approach which certainly overestimates the escape rates.

In a steam atmosphere, the $H_2O$ molecules will be dissociated by the high EUV flux of the young Sun or star and by frequent meteorite impacts (Trigo-Rodriguez and Martin-Torres 2012a). Under such an extreme environment, oxygen atoms are most likely the main form of oxygen in the upper atmosphere, which can be dragged by the hydrogen atom flux $F_{\rm H}$, according to the formula given by Hunten et al. (1987)

$$F_{\rm O} = \frac{X_{\rm O}}{X_{\rm H}} F_{\rm H} \left[ \frac{\left(m_{\rm H} + \frac{kTF_{\rm H}}{bgX_{\rm H}}\right) - m_{\rm O}}{\left(m_{\rm H} + \frac{kTF_{\rm H}}{bgX_{\rm H}}\right) - m_{\rm H}} \right], \tag{4.2}$$

where $F_{\rm O}$ is the flux of the dragged oxygen atoms, $X_{\rm O}$ and $X_{\rm H}$ are the mole mixing ratios of atomic hydrogen and oxygen, $m_{\rm O}$ and $m_{\rm H}$ the particle masses, $b$ is a molecular diffusion parameter for oxygen atoms in a hydrogen atmosphere (Zahnle and Kasting 1986; Chassefière 1996a), $g$ is the gravity acceleration, and $T$ is the average atmospheric temperature in the thermosphere.

Figure 4.2a shows the maximum amount of atomic hydrogen that could escape during blow off from an Earth-like hydrogen-rich planet estimated from the formulas shown in Eqs. (4.1) and (4.2) for a heating efficiencies $\eta$ of 15, 30, 60 and 100 % in units of Earth ocean ($\rm EO_H$) equivalent amounts, since the end of the expected accretion of the Earth at ~50 Myr (Allègre et al. 1995; Touboul et al. 2007), during 450 Myr corresponding to the EUV-enhancement factor of Ribas et al. (2005).

Depending on the assumed $\eta$ one can see from Fig. 4.2a that Earth could have lost hydrogen atoms of an amount which was $<40\,{\rm EO_H}$ during 0.5 Ga after the planet finished its accretion. By assuming that not 100 % of the EUV energy is used to power the escape more realistic estimates for $\eta$ = 15–40 % yield $\leq 15\,{\rm EO_H}$. This would mean that if the early Earth would have accumulated more hydrogen it would not get rid of it. However, we note that our estimated loss could be slightly higher because the protoplanet started to lose its nebula-based hydrogen envelope after the nebula evaporated. It is expected that about 80 % of Earth's mass was accreted at ~20 Myr and ~90 % at ~30 Myr after the origin of the Sun (Zahnle et al. 1988; Lammer et al. 2012).

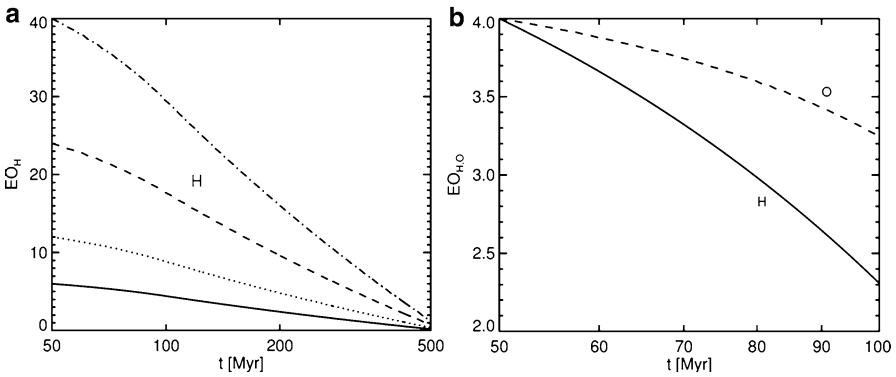


**Fig. 4.2** Amount of hydrogen atoms in units of Earth ocean ($EO_H$) equivalents that can escape via blow off from an Earth-analogue planet after its accretion as a function of heating efficiency $\eta$. *Solid line*:$\eta = 15\,\%$, *dotted line*:$\eta = 30\,\%$, dashed line: $\eta = 60\,\%$, *dashed dotted line*: $\eta = 100\,\%$. (**b**) Escape and accumulation of atomic hydrogen and oxygen for an Earth-like planet in units of $EO_{H,O}$, equivalents, which outgassed a 1,000 bar steam atmosphere during the magma ocean solidification. The dense gaseous hydrogen and oxygen envelopes cannot escape to space and most likely surround the planet during its whole lifetime (Lammer et al. 2012)

One should also note that dense hydrogen gas envelopes would rise the temperature of the planet's surface and lower atmosphere so that the homopause level would expand. In such a case the lower thermosphere would be hotter, resulting in much higher escape rates which may be up to a factor 10 higher compared to that estimated above and shown in Fig. 4.2. Because of these uncertainties the estimated escape rates should be considered as a conservative lower value. On the other hand if a terrestrial planet had acquired a steam atmosphere after its accretion of more than 1,000 bar a huge fraction of its dissociated hydrogen and oxygen atoms would not have escaped during the EUV-active phase of a solar-like G star. Such a scenario is shown in Fig. 4.2b. A dense hydrogen envelope and oxygen remnant might remain after the active phase of the planet's host star ended. An Earth-like planet would retain $\geq$2.3 EOs of hydrogen and $\geq$3.2 EO equivalents of oxygen. These results are in agreement with Kasting (1995) and Chassefière (1996a, b) in the sense that there should be planets, depending on their size, mass, orbital distance, as well as their host star's EUV flux evolution, which may accumulate huge amount of abiotic oxygen. The presence of abiotic oxygen could be also reinforced by the delivery of O from minor bodies' impacts (Ahrens et al. 1989; Trigo-Rodriguez and Martin-Torres 2012a, this volume).

In case a dense hydrogen envelope surrounded the very early Earth, the scale height of the H atoms would be much larger compared to molecular nitrogen, which would be populated in the mixed lower atmosphere close to the planetary surface so that nitrogen would not reach the stellar wind interaction region, similar as on present Earth. As long as enough hydrogen is in the thermosphere the extended upper atmosphere would act as a shield against the loss of heavier particles.

If early Earth's nitrogen inventory and other heavy trace gases were indeed protected by such extended hydrogen dominated gaseous envelopes these envelopes should have been lost during Earth's history. As discussed before and researched in detail by Elkins-Tanton and Seager (2008) and Elkins-Tanton and Seager (2008) the second abundant species besides $H_2O$ which is outgassed during the magma ocean solidification period is $CO_2$.After the EUV flux of the young Sun or young star decreased to values below 30 times the present EUV flux $CO_2$ becomes due to its IR-cooling capability also an efficient protector of planetary atmospheres. In the following section we will discuss the possible role of $CO_2$ during the early phase of Earth's atmosphere evolution in comparison with a nitrogen dominated atmosphere.

## $CO_2$- Versus $N_2$ -Rich Atmospheres and the Role of the Faint Young Sun Paradox

The average effective temperature $T_{\rm eff}$ of a planetary surface in the absence of an atmosphere can be estimated from the energy balance between the optical/near-IR emission, which irradiates a planet and the mid-IR thermal radiation that is lost to space. The incoming power $P_{\rm in}$ from the Sun/star to a planet can be written as

$$P_{\rm in} = \pi r_{\rm pl}^2 S (1 - A)\,, \tag{4.3}$$

were $S$ is the solar radiative energy flux at the orbital location of the planet, $A$ is the bond Albedo which corresponds to the fraction of the reflected radiation, $r_{\rm pl}$ is the planetary radius. The power which is leaving the Earth's upper atmosphere $P_{\rm out}$ is given by

$$P_{\rm out} = 4\pi r_{\rm pl}^2 \varepsilon \sigma T_{\rm eff}^4 \tag{4.4}$$

with $\sigma$ the Stefan Boltzmann constant and surface mid-IR emissivity $\varepsilon$. By equating both powers one obtains

$$P_{\rm in} = P_{\rm out} = \sigma T^4 = \frac{S(1-A)}{4\varepsilon}, \tag{4.5}$$

If one uses the present solar energy flux $S = 1{,}366\,{\rm W\,m^{-2}}$, $\varepsilon$ of 0.9 which corresponds to a solid rock and an albedo $A$ of $\sim$0.29 for the Earth one obtains a $T_{\rm eff}$ of $\sim$260 K (Sagan and Mullen 1972) which is below the freezing point. From a planet which has an atmosphere, $T_{\rm eff}$ is always lower than the surface temperature $T_{\rm s}$ and also lower than to the exobase temperature $T_{\rm exo}$. The reason is that an atmosphere produces a greenhouse effect so that $T_{\rm s} > T_{\rm eff}$.

Assuming the same atmospheric composition for the Earth as today but a solar constant reduced by about 30 % calculations show that under such environmental conditions the temperature would have remained below the freezing point until

2 Ga ago (e.g., Sagan and Mullen 1972; Kasting and Catling 2003). For a planet which is surrounded by an atmosphere, the effective temperature can be raised owing to the presence of greenhouse gases. Considering the greenhouse effect for a present-day atmosphere leads to a somewhat elevated average temperature of 288 K, in agreement with measurements (e.g., Sagan and Mullen 1972; Kasting and Catling 2003). These facts lead to the suggestion that the early Earth may have had greenhouse gases such as $CO_2$ or $CH_4$ in its atmosphere so that the lower solar energy flux of the young Sun could be compensated.

Our knowledge of the early climate history of the Earth, relies on geological evidence: oxygen isotopes measured in Jack Hills zircons dated at ∼4.4–4.3 Ga suggested that parent rocks interacted with liquid water; ∼3.8 Ga old sedimentary rocks from Isua (West Greenland) and were clearly deposited in aquatic environments (e.g. Peck et al. 2001); All these pieces of evidence indicate relatively mild climates and the presence of liquid water.

According to Elkins-Tanton and Seager (2008) the Earth may have outgassed up to about 500 bar $H_2O$ and ∼60–100 bar of $CO_2$ after the accretion ended. Such values are in agreement with estimations that the present Earth has an equivalent amount of about 60 bar of $CO_2$ in carbonate rocks (Holland 1978; Kasting and Ackermann 1986). If there were such amounts of $CO_2$ present in the catastrophically outgassed protoatmosphere, after a fraction of the steam condensed and contributed together with impacts to the formation of Earth's water oceans its presence might have confined the upper atmosphere within the shielding magnetosphere also for higher EUV fluxes at least when the solar EUV flux decreased from about 100 times to about 30 times of the present value.

Novoselov and Silantyev (2010) found that the balance of $CO_2$ in the atmosphere–hydrosphere–crustal system depended strongly on the character of the mineral formation during the alteration of the crustal material owing to its interaction with the early seawater. They predict from their studies a sharp depletion of the Earth's early atmosphere in $CO_2$ probably $\sim 10^5$ year after the formation of the hydrosphere and reflected the stage of extensive formation of the earliest carbonates in the hydrothermally altered crust. Thus, depending on the available landmass, the alkalinity of the early ocean water, $CO_2$ might have been weathered efficiently out from the atmosphere. In such a case a substantial amount of $CO_2$ from the primitive atmosphere could have been removed within a short geological time period (e.g., Kempe and Degens 1985; Novoselov and Silantyev 2010). If the $CO_2$ was indeed weathered into carbonates so early and if one assumes no dense hydrogen envelope which surrounded the early planet, the atmospheric nitrogen inventory should have escaped to space efficiently (Lichtenegger et al. 2010; Lammer et al. 2012), but as we know, nitrogen remained.

Because $CO_2$ is a greenhouse gas it has been considered together with $CH_4$ and $NH_3$ as a compensation of the solar heat flux deficiency during the "faint young Sun" period for explaining the evidence for the presence of liquid water on the early Earth's surface (Kasting et al. 1984; Kasting 1996; Kasting and Ono 2006; Haqq-Misra et al. 2008; Von Paris et al. 2008) after the ocean formed ∼4.4 Ga ago. During these early epochs between ∼3.8–4.4 Ga ago the FYSP together with higher

$CO_2$ concentrations could also have played a role in constraining the $CO_2$ amount in the early Earth atmosphere. The required $CO_2$ level to keep liquid water oceans, even if they were covered by an ice shield would be self-regulated by the carbonate-silicate cycle (e.g., Walker et al. 1981; Kasting and Catling 2003).

According to studies of Von Paris et al. (2008) and Lichtenegger et al. (2010) a $CO_2$ amount which is about 180 times higher compared to the present atmospheric value would be necessary to reach the freezing point at about 272 K before ∼4 Ga ago. If Earth's early atmosphere contained higher $CO_2$ levels during this early period and if the $CO_2$ value decreased, afterwards the oceans may have been covered by an ice layer which acted against further $CO_2$ weathering. Thus, higher $CO_2$ contents may have been in Earth's atmosphere during these very early periods but $CO_2$ levels may have been much lower or negligible compared to the nitrogen content about 3.2–3.5 Ga ago.

This evidence can be seen from various geochemical and geological investigations where the results point against very massive $CO_2$ atmospheres in these later epochs, such as the absence of siderite in paleosols (Rye et al. 1995; Rosing et al. 2010, and references therein). Recently, Rosing et al. (2010) found that the mineralogy of Archaean sediments, such the ubiquitous presence of mixed-valence Fe(II–III) oxides in banded iron formations is inconsistent with such high concentrations of greenhouse gases and the metabolic constraints of extant methanogens. These authors concluded that, in the absence of geologic evidence for very high greenhouse-gas concentrations, is expected a lower albedo on the Earth, because assuming a considerably smaller continental area and the lack of biologically induced cloud condensation nuclei, the environmental conditions could be kept above the freezing point of water.

From these studies at time periods ∼3.2–3.5 Ga ago, the solar EUV flux decreased already to values which are $\leq$5 times that of the present Sun so that one may expect lower or even negligible nitrogen escape rates and a stable $N_2$ atmosphere since that time. As illustrated in Fig. 4.3, if the early Earth's atmosphere had low or negligible $CO_2$ levels, or if the young Sun was brighter during the high EUV period of the young Sun, only extended hydrogen envelopes which slowly escaped from the protoatmosphere may have prevented massive losses under the influence of an enhanced early solar wind and enhanced EUV radiation. Besides gravity the thermospheric main constituents such as H, N, O, or $CO_2$ determine the expansion of the exobase level. The detection of EUV heated, non-hydrostatic upper atmospheres around terrestrial exoplanets would constrain the uncertainties related to the discussed atmosphere evolution scenarios addressed in the previous sections.

## Testing Atmosphere Evolution Scenarios

For testing the various possible atmosphere evolution scenarios which have been discussed above numerical modeling techniques together with future UV transit observations of EUV heated extended upper atmospheres which interact with the

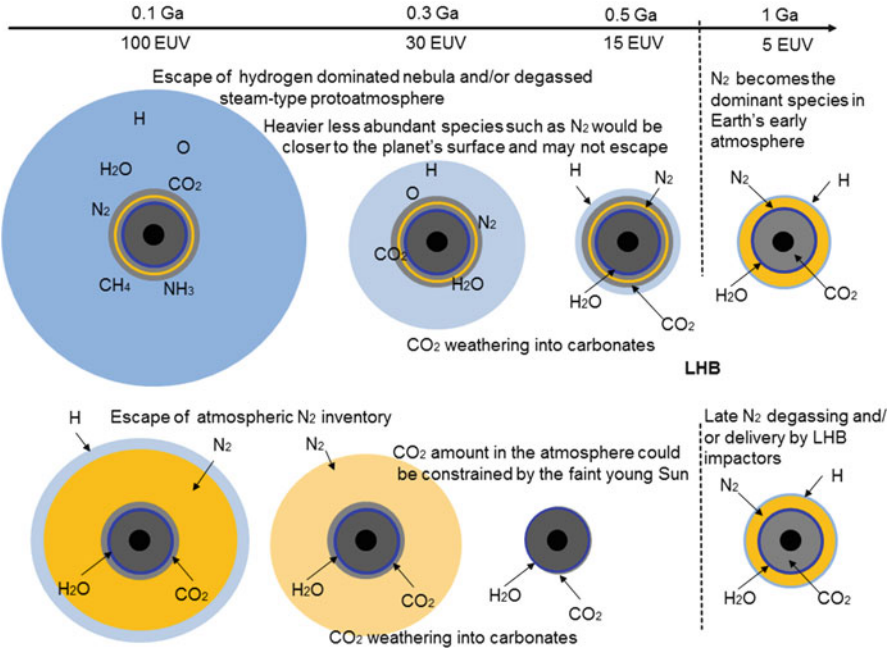


**Fig. 4.3** Illustration of atmosphere evolution scenarios during the first Ga after Earth's origin for a dense hydrogen- and $CO_2$-rich protoatmosphere and for a nitrogen dominated atmosphere before ~4 Ga ago. *Upper evolution scenario*: Dense hydrogen envelopes from Earth's protoatmosphere may act as a shield against the solar wind plasma flow and may protect heavier species such as $N_2$ molecules against fast atmospheric escape. This hydrogen envelope should have been lost during the first Ga after Earth's origin and after the weathering of $CO_2$ into carbonates. Nitrogen become the dominant atmospheric constituent at a time period when the solar EUV flux decreased to values $\leq$7 times that of the present Sun. *Lower evolution scenario*: If one assumes that the early Earth had a nitrogen dominated atmosphere soon after its origin, the atmosphere would have been lost during the first 200 Ma after the planet's formation. If this scenario is real the present nitrogen content in Earth's atmosphere should have been delivered after the solar EUV flux decreased to values which are $\leq$7 times that of the present Sun

stellar wind plasma of the planet's host star may be used. The observational method may be similar to that applied by Vidal-Madjar et al. (2003) who observed the transiting hydrogen-rich gas giant HD 209458b with the HST STIS-instrument and discovered a several percent intensity drop in the stellar Lyman-$\alpha$ line which was larger than for an atmosphere of a planet occulting only 1.5% of the star. From this observation one can suggest that the upper atmosphere of HD 209458b is expanded up to $\sim 4.3\, r_{\mathrm{Jup}}$ (e.g., Vidal-Madjar et al. 2003; Ben-Jaffel and Hosseini 2010; Koskinen et al. 2010). Similar transit observations of extended hydrogen atmospheres or non-hydrostatic upper atmospheres in general around terrestrial exoplanets should be observable if the planet orbits around M-type dwarf stars (Lammer et al. 2011a). Dynamically outward flowing neutral atoms can interact with the stellar plasma flow so that huge hydrogen coronae and energetic neutral

**Table 4.2** Upper atmosphere and solar/stellar wind parameters used in the simulation shown in Fig. 4.4a, b. The planet has in both cases the radius and mass of the Earth

| Parameter | 1EUV \| d=1 AU | M-star:10 EUV \| d=0.24 AU |
|---|---|---|
| $T_{exo}$ [K] | 1,000 | 485 |
| $r_{ib}$ [m] $\|[r_{ib}/r_{Earth}]$ | $1 \times 10^6 \| \sim 0.156$ | $6.6 \times 10^7 \| \sim 10.5$ |
| $n_{exo}[m^{-3}]$ | $7.0 \times 10^{10}$ | $4.85 \times 10^{10}$ |
| $n_{sw}[m^{-3}]$ | $8.0 \times 10^6$ | $2.5 \times 10^8$ |
| $v_{sw}[kms^{-1}]$ | 400 | 330 |
| $T_{sw}$ [K] | 1e6 | 1e6 |

atom (ENA) clouds can be produced via charge exchange. By observing the size and velocity distribution of such hydrogen exospheres and related ENA-clouds one can draw conclusions about the upper atmosphere structure, the involved species, as well as the plasma and magnetic parameters.

As for future observations, the planned WSO-UV space telescope which is expected to be launched around 2016 may be helpful in obtaining information about the upper layers of the planetary atmospheres of various types (Shustov et al. 2009; Lammer et al. 2011a). Below we modeled an expected stellar wind plasma interaction scenario around an Earth-like planet with a H-rich thermosphere which is exposed to a 10 times larger EUV flux compared to that of the Sun, inside the habitable zone (HZ) at ∼0.24 AU of an M-star with a mass of ∼0.45 solar masses. For comparison with the present Earth we modeled also the geo-corona. Table 4.2 shows the upper atmosphere and solar/stellar wind plasma parameters for Earth's present day hydrogen geo-corona and a hydrogen-rich M-star Earth-like planet. The inner boundary distance $r_{ib}$ of the simulation is chosen for the geo-corona (1 EUV) case at the altitude where atomic H becomes the dominant species in Earth's exosphere (Bauer and Lammer 2004), while for the M-star test planet $r_{ib} = r_{exo}$ for H and 10 EUV given in Table 4.1.

Figure 4.4 presents the modeling results of the hydrogen coronae which are formed around our examples. The results of our simulation for the present Earth hydrogen geo-corona are in a good agreement with observations of the hydrogen exosphere and a related production of ENAs around the sub-solar magnetopause location $r_{mp}$ at a distance of $\sim 10 R_{Earth}$ (Fuselier et al. 2010).

The model result allows the estimation of the hydrogen density at that distance of ∼ 10–12 H atoms $cm^{-3}$. This value coincides well with the corresponding observations of NASAs IBEX satellite by Fuselier et al. (2010) who inferred the hydrogen corona density from ENA images at $r_{mp}$ of ∼8 H atoms $cm^{-3}$.

Figure 4.4a shows the hydrogen geo-corona around the present Earth, while Fig. 4.4b shows the modeled hydrogen corona for a terrestrial planet orbiting an M-star. The code used for the model simulations is a further development of a direct simulation Monte Carlo (DSMC) exosphere – stellar wind particle model, which is described in Holmström et al. (2008), Ekenbäck et al. (2010) and Lammer et al. (2011b). The upper atmosphere parameters of the hydrogen-rich exo-Earth

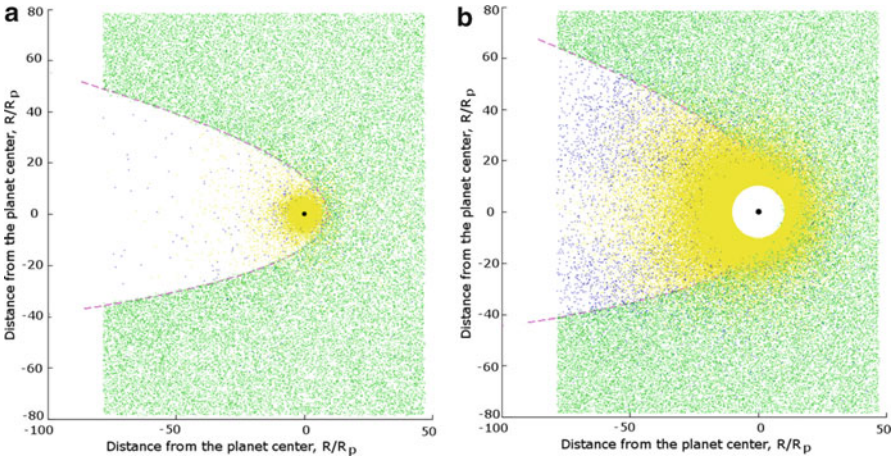


**Fig. 4.4** Projection of the planetary hydrogen and ENA-cloud around present Earth and a hydrogen-dominated Earth-like planet within the orbit of an M-star habitable zone shown in the planetary orbital plane. The coordinate system is centered at the planets with the x-axis pointing towards the star, and the y-axis opposite to their orbital velocity. (**a)** Modeled present Earth hydrogen geo-corona (1 EUV); (**b**) model results of an extended hydrogen corona which surrounds an Earth-like planet with a thermosphere which is dominated by atomic hydrogen inside the HZ of an M-star (10 EUV). The *dashed line* in both cases shows the magnetic obstacle segregating the area dominated by the planetary magnetosphere from the surrounding space

shown in Fig. 4.4b have been obtained by using a hydrodynamic model which is described in Penz et al. (2008). The empty area around the planet which is illustrated as the black dot in the center corresponds to the atmosphere below the exobase level, which is used as the inner boundary for our stellar wind – hydrogen corona interaction model.

The green dots represent the protons, the yellow dots correspond to the slow hydrogen atoms belonging to the planetary exosphere with velocities $\leq 5\,\mathrm{km\,s^{-1}}$ while the blue dots show the fast moving hydrogen atoms – ENAs which originate from charge-exchange between stellar or solar wind protons and neutral particles in the exosphere-stellar wind interaction region. It should be mentioned that in the case if an extended upper atmosphere is not in the blow off regime, it can be eroded by the stellar or solar wind.

Moreover, the interaction between stellar wind protons and neutral planetary hydrogen atoms which leads to charge-exchange reactions between these two species is much more intensive in the case when the exosphere is not protected by the magnetic field. As one can see in Fig. 4.4a, present Earth's exosphere is mainly wrapped and protected by the magnetosphere, while in the 10 EUV case the exosphere expands beyond the magnetopause. In the considered cases the magnetospheric obstacle was assumed to be conic-shaped. The magnetopause distance was assumed 10 planetary radii for the Earth as known from the observations and 10.6 planetary radii for the second terrestrial planed shown in Fig. 4.4b.

It should also be noted that not only the EUV flux but also the plasma environment in the habitable zone near an M-star may differ significantly from that of the present Sun. M-stars may stay longer active and probably have a denser stellar wind at the HZ location which is much closer (0.24 AU in this particular case) at the star compared to the Sun (e.g., Khodachenko et al. 2007; Scalo et al. 2007). As shown from Table 4.2 a 10 times higher EUV flux compared to that of the present Sun causes the expansion of the exobase to a planetocentric distance of $\sim 10.5\, r_{\mathrm{Earth}}$.

As one may see from the presented pictures hydrogen coronae are formed in both cases, but the hydrogen corona of the hydrogen-rich terrestrial test planet on Fig. 4.4b is sufficiently larger and as a result the exosphere is practically not protected by a magnetic field. This leads to intensive charge-exchange so that also a huge amount of ENAs can be produced. We expect that terrestrial planets with huge hydrogen envelopes in orbits around dwarf stars should be observable during the transits by space telescopes in the Lyman-alpha line. Observations of Earth-size planets or super-Earths with this type of upper atmosphere would be strong evidence that hydrogen coronae which may have remained from the protoatmospheres of the particular planet may play a significant role in the protection of the lower atmosphere and species like nitrogen from enhanced EUV fluxes and stellar wind erosion.

## Conclusions and Discussions

We briefly addressed the aeronomical stability problem of Earth-like nitrogen atmospheres against high solar/stellar EUV fluxes. In the absence of a high amount of IR-coolers such as $CO_2$ or $H_3^+$ molecules, nitrogen-dominated thermospheres can be heated to temperatures of a few thousand Kelvin so that the atmosphere structure changes from hydrostatic to hydrodynamic regimes. For a planet with the gravity of the Earth when the solar/stellar EUV flux reaches values which are $\geq$10 times that of the present Sun the exobase level expands beyond the magnetopause distance and non-thermal atmospheric escape processes erode the atmosphere during a few tens of Ma. A nitrogen-rich atmosphere on early Earth should have been lost entirely long before the LHB period. In case Earth's initial nitrogen inventory was not degassed 500 Ma after Earth's origin or delivered during the LHB by impactors (Trigo-Rodriguez and Martin-Torres 2012b) other protection mechanisms should have been at work.

However, based on protoatmosphere hypotheses which expect nebula-based hydrogen-rich and/or catastrophically outgassed or impact related dense $H_2O/CO_2$ steam atmospheres could have protected heavier less abundant species against efficient escape. Due to the high solar/stellar EUV flux ~4–4.5 Ga ago molecular hydrogen gas from an accumulated nebula remnant or $H_2O$, $CH_4$ or $NH_3$ molecules would have been dissociated so that atomic hydrogen envelopes would have formed and surrounded the early planet. As long as such hydrogen envelopes were not

lost they may also have protected heavier species such as nitrogen and other minor species from fast escape. Higher $CO_2$ levels during this early epoch would also act against strong expansion of the upper atmosphere and its escape.

During these extreme early stages an induced magnetic field could have also reduced the efficiency of non-thermal atmospheric loss processes and partially protected the primitive atmosphere from complete destruction. From our discussions one finds that there are indications that many planets within the size and mass range from Earth-type to so called super-Earths may not completely get rid of their initial hydrogen and water inventories so that they may accumulate dense hydrogen and abiotic oxygen-rich upper atmospheres during their lifetime or remain as sub-Neptune-type bodies. In this sense, the role of giant impacts could be determinant and should be addressed by performing additional modeling of the survival of the atmosphere under the eroding effect of giant impacts.

Future UV transit observations of terrestrial exoplanets within orbits of dwarf stars, together with advanced numerical modeling techniques can be used for the study of the stellar wind interaction with EUV heated non-hydrostatic thermospheres. These approaches will be applied during the near future so that the discussed atmospheric evolution hypotheses can be studied and will finally be tested via observations.

**Acknowledgements** H. Lammer, K. G. Kislyakova, M. Güdel and M. L. Khodachenko, acknowledge the support by the FWF NFN project S116 "Pathways to Habitability: From Disks to Active Stars, Planets to Life", and the FWF NFN subprojects, S116 604-N16, S116606-N16, S116607-N16. P. Odert acknowledges the FWF project P22950-N16. N. V. Erkaev acknowledge support from the RFBR grant N 12-05-00152-a. The authors also acknowledge support from the EU FP7 project IMPEx (No.262863) and the EUROPLANET-RI projects, JRA3/EMDAF and the Na2 science WG4 and WG5. H. Lammer, K. G. Kislyakova and P. Odert thank also the Helmholtz Alliance project "Planetary Evolution and Life." The software used for the hydrogen exosphere and stellar wind plasma interaction simulations was in part developed by the DOE-supported ASC/Alliance Center for AstrophysicalThermonuclear Flashes at the University of Chicago, USA. K. G. Kislyakova, M. Holmström and H. Lammer acknowledge also supporting HPC resources of HPC2N, Umeå University, Sweden.

## References

Ahrens, T., O'Keefe, J.D, Lange, M.A.: Formation of atmospheres during accretion of the terrestrial planets. In: Origin and Evolution of Planetary and Satellite Atmospheres, pp. 328–385. University of Arizona Press, Tucson (1989)

Albarède, F.: Volatile accretion history of the terrestrial planets and dynamic implications. Nature **461**, 1227–1232 (2009)

Albarède, F., Blicher-Toft, J.: The split fate of the early Earth, Mars, Venus, and Moon. C. R. Geoscience **339**, 917–927 (2007)

Allègre, C.J., Manhès, G., et al.: The age of the Earth. Geochim Cosmochim Acta **59**, 1445–1456 (1995)

Bauer, S.J., Lammer, H.: Planetary Aeronomy. Springer, Heidelberg/New York (2004)

Barrat, J.-A., Bollinger, C.: Geochemistry of the martian meteorite ALH 84001, revised. Meteorit. Planet. Sci. **45**, 495–512 (2010)

Ben-Jaffel, L., Sona Hosseini, S.: On the existence of energetic atoms in the upper atmosphere of exoplanet HD 209458b. ApJ **709**, 1284–1296 (2010)
Chassefière, E.: Hydrodynamic escape of hydrogen from a hot water-rich atmosphere: the case of Venus. J. Geophys. Res. **101**, 26039–26056 (1996a)
Chassefière, E.: Hydrodynamic escape of oxygen from primitive atmospheres: applications to the cases of Venus and Mars. Icarus **124**, 537–552 (1996b)
Carr, M.H., Head, J.W.: Oceans on Mars: an assessment of the observational evidence and possible fate. J. Geophys. Res. **108** (2003). doi:10.1029/2002JE001963
Ekenbäck, A., Holmström, M., et al.: Energetic neutral atoms around HD 209458b: estimations of magnetospheric properties. ApJ **709**, 670–679 (2010)
Elkins-Tanton, L.T.: Linked magma ocean solidification and atmospheric growth for Earth and Mars. Earth Planet. Sci. Lett. **271**, 181–191 (2008)
Elkins-Tanton, L.T.: Formation of water ocean on rocky planets. Astrophys. Space Sci. **332**, 359–364 (2011)
Elkins-Tanton, L., Seager, S.: Ranges of atmospheric mass and composition of super-Earth exoplanets. ApJ **685**, 1237–1246 (2008)
Erkaev, N.V., Kulikov, Yu.N., et al.: Roche lobe effects on the atmospheric loss from Hot Jupiters. A&A **472**, 329–334 (2007)
Fuselier, S.A., Funsten, H.O., et al.: Energetic neutral atoms from the Earth's subsolar magnetopause. Geophys. Res. Lett. **37,** L13101 (2010). doi:10.1029/2010GL044140
Gaidos, E.J., Güdel, M., et al.: The Faint Young Sun Paradox: an observational test of an alternative solar model. Geophys. Res. Lett. **27**, 501–503 (2000)
Grott, M., Morschhauser, A., et al.: Volcanic outgassing of $CO_2$ and $H_2O$ on Mars. Earth Planet. Sci. Lett. **308**, 391–400 (2011)
Güdel, M.: The Sun in Time: activity and environment. Living Rev. Sol. Phys. **4**(3), 1–137 (2007)
Güdel, M., Guinan, E.F., et al.: The X-ray Sun in Time: a study of the long-term evolution of coronae of solar-type stars. ApJ **483**, 947–960 (1997)
Haqq-Misra, J.D., Domagal-Goldman, S.D., et al.: A revised, hazy methane greenhouse for the Archean Earth. Astrobiology **8**, 1127–1137 (2008)
Hayashi, C., Nakazawa, K. et al.: Earth's melting due to the blanketing effect of the primordial dense atmosphere. Earth Planet. Sci. Lett. **43**, 22–28 (1979)
Head, J.W., Marchant, D.R.: Inventory of ice-related deposits on Mars: evidence for burial and long-term sequestration of ice in non-polar regions and implications for the water budget and climate evolution. In The 40th Lunar and Planetary Science Conference, The Woodlands, TX (2009). abs. 1356
Holland, H. D.: The Chemistry of the Atmosphere and Oceans. Wiley, New York (1978)
Holmström, M., Ekenbäck, A., et al.: Energetic neutral atoms as the explanation for the high-velocity hydrogen around HD 209458b. Nature **451**, 970–972 (2008)
Hunten, D.M.: Atmospheric evolution of the terrestrial planets. Science **259**, 915–920 (1993)
Hunten, D M., Pepin, R.O., et al.: Mass fractionation in hydrodynamic escape. Icarus **69**, 532–549 (1987)
Ikoma, M., Hori, Y.: In-situ accretion of hydrogen-rich atmospheres on short-period super-Earths: implications for the Kepler-11 planets. ApJ (2012). submitted arXiv:1204.5302v1
Kasting, J.F.: $O_2$ concentrations in dense primitive atmospheres: commentary. Planet. Space Sci. **43**, 11–13 (1995)
Kasting, J.F.: Planetary atmosphere evolution: Do other habitable planets exist and can we detect them? Astrophys. Space Sci. **241**, 3–24 (1996)
Kasting, J.F.: Warming Early Earth and Mars. Science **276**, 1213–1215 (1997)
Kasting, J.F., Pollack, J.B., Crisp, D.: Effects of high CO2 levels on surface temperature and atmospheric oxidation state of the early Earth. J. Atmos. Chem. **1**, 403–428 (1984)
Kasting, J.F., Ackermann, T.P.: Climate consequences of very high carbon dioxide levels in the Earth's early atmosphere. Science **234**, 1383–1385 (1986)
Kasting, J.F., Catling, D.: Evolution of a habitable planet. Annu. Rev. Astron. Astrophys. **41**, 429–463 (2003)

Kasting, J.F., Ono, S.: Palaeoclimates: the first two billion years. Philos. Trans. R. Soc. B **361**, 917–929 (2006)

Kempe, S., Degens, E.T.: An early Soda ocean? Chem. Geol. **53**, 95–108 (1985)

Khodachenko, M.L., Ribas, I., et al.: Coronal mass ejection (CME) activity of low mass M-stars as an important factor for the habitability of terrestrial exoplanets. I. CME impact on expected magnetospheres of Earth-like exoplanets in close-in habitable zones. Astrobiology **7**, 167–184 (2007)

Koskinen, T.T., Yelle, R.V., Lavvas, P., Lewis, N.K.: Characterizing the thermosphere of HD209458 b with UV tranist observations. ApJ **723**, 116–128 (2010)

Kulikov, Yu.N., Lammer, H., et al.: Atmospheric and water loss from early Venus. Planet. Space Sci. **54**, 1425–1444 (2006)

Kulikov, Yu.N., Lammer, H., et al.: A comparative study of the influence of the active young Sun on the early atmospheres of Earth, Venus and Mars. Space Sci. Rev. **129**, 207–243 (2007)

Lammer, H.S., Bauer, J.: Isotopic fractionation by gravitational escape. Space Sci. Rev. **106**, 281–291 (2003)

Lammer, H., Lichtenegger, H.I.M., et al.: Coronal mass ejection (CME) activity of low mass stars as an important factor for the habitability of terrestrial exoplanets. II. CME-induced ion pick up of Earth-like exoplanets in close-in habitable zones. Astrobiology **7**, 185–207 (2007)

Lammer H, Odert, P., et al.: Determining the mass loss limit for close-in exoplanets: what can we learn from transit observations? A&A **506**, 399–410 (2009)

Lammer H., Eybl, V., et al.: UV transit observations of EUV-heated expanded thermospheres of Earth-like exoplanets around M-stars: testing atmosphere evolution scenarios. Astrophys. Space Sci. **335**, 39–50 (2011a)

Lammer, H., Kislyakova, K.G., et al.: Hydrogen ENA-cloud observation and modeling as a tool to study star-exoplanet interaction. Astrophys. Space Sci. **335**, 9–23 (2011b)

Lammer, H., Kislyakova, K.G., et al.: Pathways to Earth-like atmospheres: extreme ultraviolet (EUV)-powered escape of hydrogen-rich protoatmospheres. Orig. Life Evol. Biosph. **41**, 503–522 (2012)

Lichtenegger, H.I.M., Lammer, H., et al.: Aeronomical evidence for higher $CO_2$ levels during Earth's Hadean epoch. Icarus **210**, 1–7 (2010)

Lundin, R., Lammer, H., et al.: Planetary magnetic fields and solar forcing: Implications for atmospheric evolution. Space Sci. Rev. **129**, 245–278 (2007)

Minton, D.A., Malhotra, R.: Assessing the massive young Sun hypothesis to solve the warm young Earth puzzle. ApJ **660**, 1700–1706 (2007)

Novoselov, A.A., Silantyev, S.A.: Hydrothermal systems of the Hadean ocean and their influence on the material balance in the crust–hydrosphere–atmosphere system of the early Earth. Geochem. Int. **48**, 643–654 (2010)

Peck W., et al.: O isotope ratios and rare earth elements in 3.3 to 4.4 Ga zircons. Geochem. et Cosm. Acta **65–22**, 4215–4229 (2001)

Penz, T., Erkaev, N.V, et al.: Mass loss from "Hot Jupiters" Implications for CoRoT discoveries, Part II: long time thermal atmospheric evaporation modeling. Planet. Space Sci. **56**, 1260–1272 (2008)

Phillips, R.J., Zuber, M.T., et al.: Ancient geodynamics and global-scale hydrology on Mars. Science **291**, 2587–2591 (2001)

Ribas, I., Guinan, E.F., et al.: Evolution of the solar activity over time and effects on planetary atmospheres. I. High-energy irradiances (1–1700 Å). ApJ **622**, 680–694 (2005)

Rosenqvist J., Chassefière, E.: Inorganic chemistry of $O_2$ in a dense primitive atmosphere. Planet. Space Sci. **43**, 3–10 (1995)

Rosing, M.T., Bird, D.K., et al.: No climate paradox under the faint early Sun. Nature **464**, 744–747 (2010)

Rubey, W.W.: Geological history of seawater. Bull. Geol. Soc. Am. **62**, 1111–1148 (1951)

Rye, R., Kuo, P.H., et al.: Atmospheric carbon dioxide concentrations before 2.2 billion years ago. Nature **378**, 603–605 (1995)

Sackmann, I.-J., Boothroyd, A.I.: Our Sun. V. A bright young Sun consistent with helioseismology and warm temperatures on ancient Earth and Mars. ApJ **583**, 1024–1039 (2003)
Sagan, C., Mullen, G.: Earth and Mars: evolution of atmospheres and surface temperatures. Science **177**, 52–56 (1972)
Scalo, J., Kaltenegger, L., et al.: M-stars as targets for terrestrial exoplanet searches and biosignature detection. Astrobiology **7**, 85–166 (2007)
Schaefer L, Fegley, B., Jr.: Chemistry of silicate atmospheres of evaporating super-Earths. ApJ **703**, L113–L117 (2009)
Shustov, B., Sachov, M., et al.: WSO-UVultraviolet mission for the next decade. Astrophys. Space Sci. **320**, 187–190 (2009)
Smith, D.E., Zuber, M.T., et al.: X. Sun, Mars Orbiter Laser Altimeter: experiment summary after the first year of global mapping of Mars. J. Geophys. Res. **106**, 23689–23722 (2001)
Tian, F., Toon, O.B., et al.: A hydrogen-rich early Earth atmosphere. Science **308**, 1014–1017 (2005)
Tian, F., Kasting, J.F., et al.: Hydrodynamic planetary thermosphere model: 1. The response of the Earth's thermosphere to extreme solar EUV conditions and the significance of adiabatic cooling. J. Geophys. Res. **113** (2008a). doi:10.1029/2007JE002946
Tian, F., Solomon, S.C., et al.: Hydrodynamic planetary thermosphere model: 2. coupling of an electron transport/energy deposition model. J. Geophys. Res. **113**, E07005 (2008b)
Touboul, M., Kleine, T., et al.: Late formation and prolonged differentiation of the Moon inferred from W isotopes in lunar metals. Nature **450**, 1206–1209 (2007)
Trigo-Rodriguez, J.M., Martin-Torres, F.J.: Implication of impacts in the young earth Sun paradox and the evolution of Earth's atmosphere. In: The Early Evolution of the Atmospheres of Terrestrial Planets (2012a), this volume
Trigo-Rodriguez, J.M., Martin-Torres, F.J.: Clues on the importance of comets in the origin and evolution of the atmospheres of Titan and Earth. Planet. Space Sci. **60**, 3–9 (2012b)
Valley, A.M., Peck, W.H., et al.: A cool early Earth. Geology **30**, 351–354 (2002)
Vidal-Madjar, A., Lecavelier des Etangs, A., et al.: An extended upper atmosphere around the extrasolar planet HD209458b. Nature **422**, 143–146 (2003)
Von Paris P., Rauer, H., et al.: Warming the early Earth – $CO_2$ reconsidered. Planet. Space Sci. **45**, 1254–1259 (2008)
Walker, J.C.G., Hays, P.B., et al.: A negative feedback mechanism for the long-tern stabilization of the Earth's surface temperature. J. Geophys. Res. **86**, 9776–9782 (1981)
Whitmire, D.P., Doyle, L.R., et al.: A slightly more massive young Sun as an explanation for warm temperatures on early Mars. J. Geophys. Res. **100**, 5457–5464 (1995)
Wood, B.E., Müller, H.-R., et al.: New mass-loss measurements from astrospheric Ly-$\alpha$ absorption. ApJL **628**, L143–L146 (2005)
Yelle, R.V.: Aeronomy of extra-solar giant planets at small orbital distances. Icarus **170**, 167–179 (2004)
Zahnle, K.J., Kasting, J.F.: Mass fractionation during transonic escape and implications for loss of water from Mars and Venus. Icarus **66**, 462–480 (1986)
Zahnle, K.J., Kasting, J.F., et al.: Evolution of a steam atmosphere during Earth's accreation. Icarus **74**, 62–97 (1988)

# Chapter 5
# Hot Super-Earth Atmospheres

**Yamila Miguel and Lisa Kaltenegger**

**Abstract** The search for extrasolar planets has resulted in the discovery of super-Earths, with masses less than ten Earth masses. Regarding the orbital distances, some of these planets are very close to its star, at distances much less than Mercury to the Sun. Since no such planets exist in our solar system, the atmospheres of these hot rocky planets remains largely unknown. In this work, we present the main characteristics of this hot rocky planet population, with a focus on the potential atmospheric composition obtained by assuming different types of planetary composition and using corresponding model calculations. The vaporization of silicate magma is used in order to explore hot atmospheres above 1,000 K. We present how to estimate the range of atmospheric compositions for rocky planets for different semi-major axis and show an application of the results, to the Kepler February 2011 data release. Our model suggests that hot, rocky super-Earth atmospheres can be divided into five types, whose definition is strongly dependent on the initial composition and the planet's distance to the star. These simple set of parameters provided, can be used to explore atmospheric compositions for current and future candidates provided by the *Kepler* mission and other searches.

Y. Miguel (✉)
Max Planck Institut für Astronomie, Königstuhl 17, 69117, Heidelberg, Germany
e-mail: miguel@mpia-hd.mpg.de

L. Kaltenegger
Max Planck Institut für Astronomie, Königstuhl 17, 69117, Heidelberg, Germany
Harvard Smithsonian Center for Astrophysics, 60 Garden St., Cambridge, 02138 MA, USA
e-mail: kaltenegger@mpia.de

J.M. Trigo-Rodriguez et al. (eds.), *The Early Evolution of the Atmospheres of Terrestrial Planets*, Astrophysics and Space Science Proceedings 35,
DOI 10.1007/978-1-4614-5191-4_5, 

## Introduction

The population of extrasolar planets have grown significantly in the last years. To date more than 750[1] exoplanets and over 2,000 planetary candidates have been detected . Among them, the first rocky planets with minimum masses below $10\,M_\oplus$ and radii less than $2\,R_\oplus$ [2, 18], have been found.

Figures 5.1 and 5.2 show the semimajor axis and stellar effective temperature of confirmed exoplanets and Kepler planetary candidates from the Feb 2011 data release, respectively. In Fig. 5.1 planets with masses less that $10\,M_\oplus$, are shown in black. The planets consistent with rocky planet models (radii below two Earth mass) are shown in red and black in Fig. 5.2. Planets are shown in different point size, according to their mass and radius, respectively. As seen in the Figures, most of these small planets are located extremely close to their stars, at distances much less than $1\,AU$, due to the current detection sensitivity. Some of these planets are exposed to an intense stellar irradiation and can reach equilibrium temperatures high enough to have a magma of melted silicates on their surfaces, assuming they are rocky in composition. Two known hot-exoplanets with these characteristics are Corot 7b and Kepler 10b, shown in red in Fig. 5.1 (see Chap. 2, section "Introduction: The Sources of Terrestrial Nitrogen" for a description).

The *Kepler* mission announced 1,235 planetary candidates in their Feb 2011 data release [3]. Six hundred and fifteen of these *Kepler* objects of interest (KOI) are potentially rocky (radius $<2.5\,R_\oplus$ including the measurement error bars, called Super-Earths here) and a subsample of 193 might have extremely high temperatures on their surfaces ($T_P > 1{,}000\,K$) due to stellar irradiation, assuming an albedo of 0.01 [21]. Such high temperature caused by irradiation can lead to an outgassing and the subsequent formation of the planet's atmosphere.

Our aim in this work is to show the primitive outgassed atmospheric compositions of hot super-Earths, and its dependence on the distance between the planet and its host star, as shown by Miguel et al. [21]. These results are applied to the Kepler planetary candidates sample from February 2011, but this approach can be also applied to current and future candidates provided by the *Kepler* mission and other exoplanet surveys.

## Hot Potentially Rocky Exoplanet Population

The study of small hot exoplanets is raise major question since the discovery of the first super-Earths a few years ago. In this work we focus only on the outgassed primary atmosphere of hot super-Earths. In this section we show the main characteristics of this sample of hot small planets known so far, and also present the population of hot potentially rocky *Kepler* planetary candidates.

[1] http://exoplanet.eu

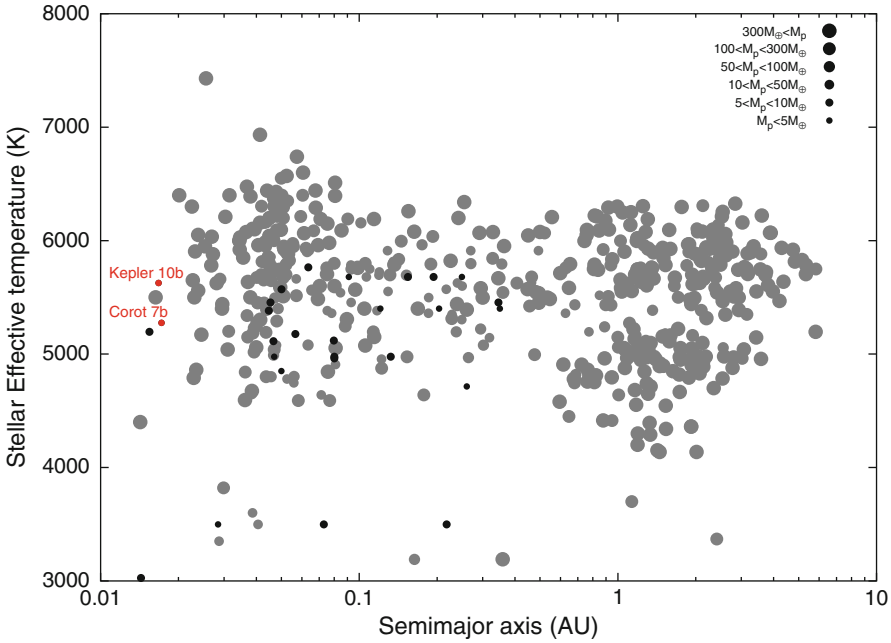


**Fig. 5.1** Stellar effective temperature vs. semi-major axis of the exoplanets confirmed so far. Those planets with masses less that $10\,M_{\oplus}$ are shown in *black*. The two first confirmed hot super-Earths are shown in *red*

## *Confirmed Planets*

The first confirmed strongly irradiated rocky planets discovered were Corot 7b [18] and Kepler 10b [2].

**Corot 7b.** is the first known transiting super-Earth ($1.68\,R_{\oplus}$). It is located very close to its central star, at only $4.3\,R_{\star}$, which suggest a tidally locked planet with a high surface temperature [18]. The extreme physical properties of this planet were analysed in [19], while the composition of the atmosphere was explored by [30], who found that the main gases in the atmosphere are Na, $O_2$, O and SiO with partial pressures of $\sim 1 \times 10^{-3}$ bars. Other atmospheric studies were focused on the interaction between the planet and the star. Due to its proximity to the star Corot 7, it is expected to have undergone a large atmospheric mass loss during its history. Several studies explore the exosphere of this planet and calculate the mass loss rate (e.g., [8, 17, 20, 23]).

**Kepler 10b.** has an observed semimajor axis of $0.01684\,AU$ and a radius of $1.416\,R_{\oplus}$ [2]. The close proximity to its host star indicates a high temperature at its surface and the density suggest that this is a rocky planet, according to interior models [33]. The atmospheric studies performed in Kepler 10b were focus on the escape mechanisms, as is shown by Lammer et al. [17] and Leitzinger et al. [20].

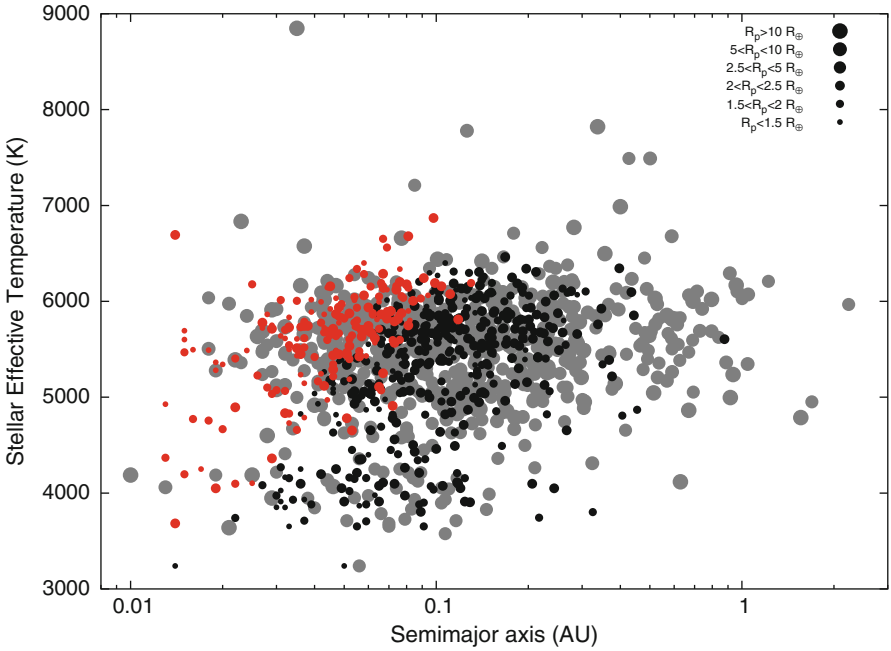


**Fig. 5.2** Effective stellar temperature vs. semi-major axis of *Kepler* planetary candidates released on February 2011, in different point sizes, according to their radii. Candidates with $T_p$ >1,000 K and $R_p \leq 2.5\,R_\oplus$, are shown in *red*. The cooler planets (in the same radius range) are shown in *black*. Those with $R_p$ >2.5 $R_\oplus$ are shown in *grey* (Adapted from Miguel et al. [21])

## *Kepler Planetary Candidates*

The NASA's *Kepler* mission was designed to searching for transiting exoplanets [5, 14, 16]. In the data released in February of 2011 [3], the *Kepler* team presented 997 stars with a total of 1,235 planetary candidates. The stellar effective temperature versus planetary semi-major axis for the 1,235 *Kepler* candidates is shown in Fig. 5.2. In the plot, the different planetary radii are shown as different point sizes.

In this work we focus only on hot rocky planets. As explained in [21], planets located at different distances from the host star will be exposed to different stellar irradiation and will have different surface temperatures (see section "Different Atmospheric Compositions" for details). Figure 5.2 shows planetary candidates with derived $T_p > 1{,}000\,K$ and $R_p \leq 2.5\,R_\oplus$, in red. Cooler planets (in the same radius range) are shown in black. The planet candidates with $R_p > 2.5\ R_\oplus$ are shown in grey.

## Outgassing Model

When a planet reaches temperatures higher than $T_p > 1{,}000$ K, the surface material vaporizes, forming an outgassed atmosphere. Here we present a simple approach to find the relation between the observable data of a planet (radius, semimajor axis and stellar effective temperature) and the potential atmospheric composition, as developed by Miguel et al. [21]. The MAGMA code [7, 29] is used to compute the chemical equilibrium between the melt and vapor in a magma for temperatures higher than 1,000 K [9–12], for Al, Ca, Fe, K, Mg, Na, O, Si, Ti and their compounds.

The initial composition assumed for the magma determines the outgassed atmosphere [30, 34]. Since the composition of a super-Earth is unknown, we based our choice of magma material on the fact that a more massive planet should have a lower composition of FeO in the mantle than a less massive one, a consequence of the solubility of oxygen in liquid iron-alloy, which increases with temperature [28]. Therefore, we adopt as the initial composition for a hot super-Earth planet komatiite rock composition. Komatiites are ultramafic lavas that erupted on Earth during the Archaean period, between 3.8 and 2.5 billion years ago, when Earth had a higher surface temperature. These rocks present a lower FeO content than the one of bulk silicate earth, as seen in Table 5.1.

## Different Atmospheric Compositions

In the work developed by Miguel et al. [21], outgassing simulations for temperatures between 1,000 and 3,500 K are performed, assuming atmospheres free of volatile gases such as H, C, N, S (see discussion). The partial pressures of all the gases vaporized from a Komattite's magma, at different temperatures, are shown in Fig. 5.3.

Figure 5.4 shows that the gases with the larger partial pressures are Fe, FeO, Mg, Na, O, $O_2$, SiO, $SiO_2$ (shown in a wider line), where the order of relevance depends on the planet's surface temperature.

We link the partial pressures to the resulting atmospheric composition, calculating the column density ($\sigma_i$) of each gas $i$, for a 10 $M_\oplus$ planet.

$$\sigma_i = \frac{P_i N_A}{g \mu_i} \tag{5.1}$$

**Table 5.1** Komatiite and bulk silicate earth compositions

| Oxide | $SiO_2$ | MgO | $Al_2O_3$ | $TiO_2$ | $Fe_2O_3$ | FeO | CaO | $Na_2O$ | $K_2O$ |
|---|---|---|---|---|---|---|---|---|---|
| Komatiite (%) | 47.10 | 29.60 | 4.04 | 0.24 | 12.80 | 0.0 | 5.44 | 0.46 | 0.09 |
| Bulk silicate earth (%) | 45.97 | 36.66 | 4.77 | 0.18 | 0.0 | 8.24 | 3.78 | 0.35 | 0.04 |

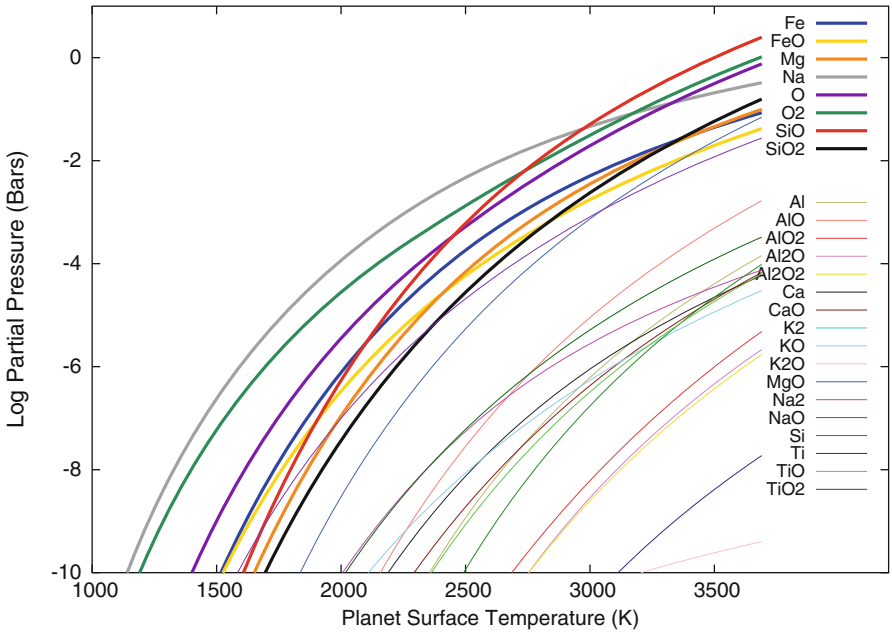


**Fig. 5.3** Partial pressures of the gases as a function of the planet surface temperature of the gases vaporized from a komatiite magma. The gases with the highest partial pressures are shown with a *wider line* (Adapted from Miguel et al. [21])

As seen Eq. 5.1, the column density of each gas is a function of the gas' partial pressure, $P_i$, the Avogadro's number, $N_A$, the molecular weight of the species, $\mu_i$ and the gravitational surface acceleration of the planet $g$.

To explore the effects of initial composition on the results, we adopt a komatiite composition and also Bulk Silicate Earth (B.S.E) as initial composition for hot super-Earths. The results are shown in Fig. 5.4.

Figure 5.4a shows the column densities outgassed from a $10\,M_\oplus$ planet with different surface temperatures, when adopting komatiites rock composition. Figure 5.4b shows the results when assuming a composition of BSE. In both cases the most abundant gases are Fe, Mg, Na, O, $O_2$ and SiO. We note that the abundance of each gas in the atmosphere depends on the surface temperature. Planets with similar surface temperature and composition have similar initial atmospheric composition, in this model. At certain temperatures the order of abundance of the most abundant gases change. These temperatures, indicated in Fig. 5.5, are the limits between the different atmospheric types found by Miguel et al. [21] and change depending on the planetary composition adopted.

The planet equilibrium temperature reached by a planet due to irradiation is given by,

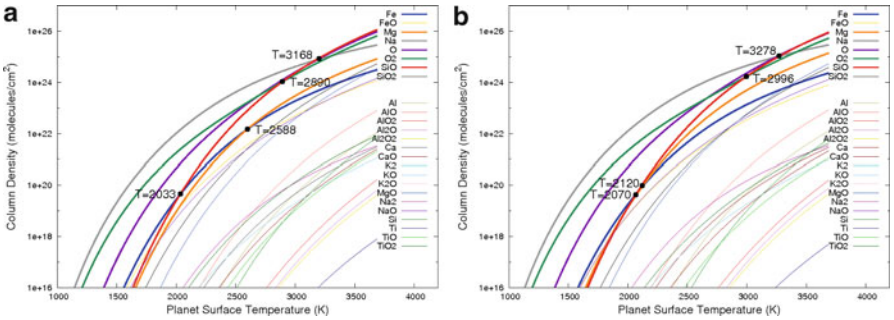


**Fig. 5.4** Column densities of the atmospheric gases vs. planet surface temperature. The column densities were calculated for a planet of 10 $M_{\oplus}$. Different planetary compositions are considered: komatiite (**a**) and bulk silicate of the Earth (**b**). Temperatures where the most abundant gases change are indicated (Adapted from Miguel et al. [21])

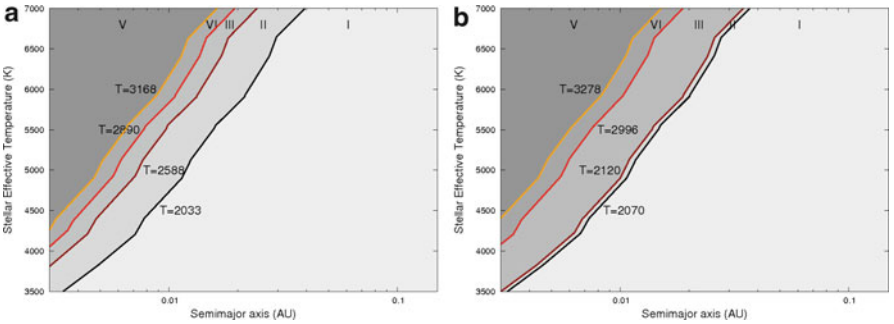


**Fig. 5.5** Stellar effective temperature vs. semi-major axis. The limit temperatures between the different atmospheric types are indicated with lines of different colors. Two different planetary compositions are adopted: komatiite (**a**) and bulk silicate of the Earth (**b**)

$$T_p = T_{eff,\star}\left(\frac{(1-A)R_\star^2}{4a^2}\right)^{\frac{1}{4}} \tag{5.2}$$

where $A$ is the planet bond albedo, that we assumed as 0.01 (see discussion), $a$ is the semimajor axis, $R_\star$ is the stellar radius and $T_{eff,\star}$ is the stellar effective temperature.

As seen in Eq. 5.2 the planetary temperature depends on the semimajor axis and stellar effective temperature. Therefore, we can relate the primitive type of atmosphere with the observable data of the planets: the stellar effective temperature and the distance between the planet and the host star. This relation is shown in Fig. 5.5. Figure 5.5a (komatiite) and Fig. 5.5b (BSE composition) show the stellar effective temperature vs. the planet's distance to the star. Lines show the temperatures that separate the different classes of planetary atmospheres. Areas highlighted in gray scale indicate the regions of different types of atmospheres.

In our model, hot rocky planet atmospheres are separated into five classes. Temperatures that limit each class change when considering different magma compositions. For komatiite composition:

Atmospheres Type I ($T_p < 2{,}033$ K), characterized by the presence of monatomic Na, $O_2$, monatomic O and monatomic Fe in order of abundance.

Atmospheres Type II ($2{,}033 < T_p < 2{,}588$ K), SiO becomes more abundant than monatomic Fe. The atmosphere is characterized by monatomic Na, $O_2$, monatomic O, SiO, monatomic Fe and monatomic Mg from the most to the least abundant.

Atmospheres Type III ($2{,}588 < T_p < 2{,}890$ K), monatomic Mg becomes more abundant than monatomic Fe. The gases with the highest column densities are monatomic Na, $O_2$, monatomic O, SiO, monatomic Mg and monatomic Fe. Note that the column densities of $O_2$, monatomic O and SiO are almost equal in this temperature range.

Atmospheres Type VI ($2{,}890 < T_p < 3{,}168$ K), SiO becomes more abundant than $O_2$ and the atmosphere becomes silicate and monatomic Na dominated.

Atmospheres Type V ($T_p > 3{,}168$ K), dominated by silicate oxide, followed closely by monatomic O, $O_2$ and monatomic Na.

When adopting the BSE composition, the temperature limits between the five classes change slightly to 2,070, 2,120, 2,996 and 3,278 K, respectively.

## An application: Kepler Candidates' Composition

These results are applied to planet candidates in the February 2011 *Kepler* data release with $R_p \leq 2.5\,R_\oplus$ and $T_p > 1{,}000$ K. Figure 5.6 shows the 193 planetary candidates studied in this work, shown in different point sizes according to their radius: 2–2.5 $R_\oplus$ (large points), 1.5–2 $R_\oplus$ (medium points) and candidates with $R_p$ ¡ 1.5 $R_\oplus$ (small points).

Of the 193 *Kepler* candidates (see Fig. 5.6a), 189 are characterized by Type I atmospheres when adopting komatiite as the initial composition. Three planets are characterized by Type II (between the black and the dark-red line in Fig. 5.6a), no planets by Type III (between the dark-red and red lines), only one by Type IV (located between the red and yellow lines) and none by Type V atmospheres (above the yellow line) , if we only consider the irradiation from the star for heating (see discussion).

For a BSE composition, 190 planetary candidates are characterized by Type I atmospheres (located below the black line in Fig. 5.5b), only 1 planet by Type II atmosphere (between the black and the dark-red lines), 1 by Type III (between the

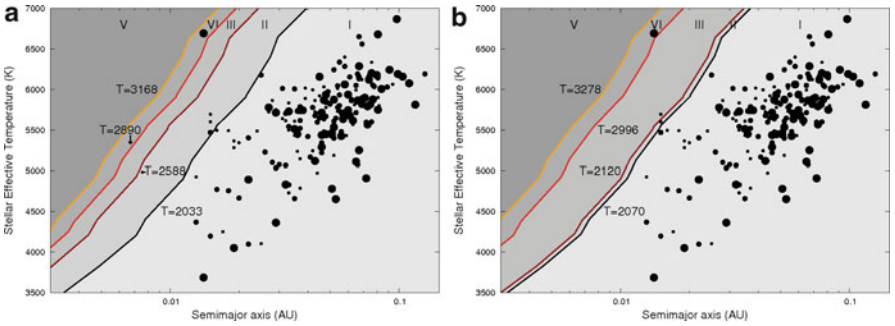


**Fig. 5.6** Stellar effective temperature vs. semi-major axis of Kepler planetary candidates, for the two different planetary compositions adopted: komatiite, shown in (**a**) and bulk silicate of the Earth, shown in (**b**) (Adapted from Miguel et al. [21])

dark-red and red lines), 1 by Type IV (located between the red and yellow lines) and none by Type V (above the yellow line). As a result, note that, for this planetary sample, the initial composition is not important for planets with high temperatures (atmospheres of Type IV and V). Nevertheless, for lower temperatures (Types I, II and III) it becomes an important factor, since a small difference in temperature can change the dominant gases in the planetary atmosphere.

## Discussion

There are many unknown factors that can change the results.

### *Planetary Composition*

The characterization of the initial planetary atmosphere is strongly dependent on the composition. Since the initial composition of the exoplanets remain unknown, two different initial compositions taken from our Solar System are adopted, but substantially different compositions are possible.

### *Volatiles in the Atmosphere*

We followed the work by Schaefer et al. [30] and consider atmospheres produced by the outgassing of a volatile-free magma. For such extreme temperatures, $T_p >$ 1,000 K, elements such as H, C, N and S should escape from the atmosphere in

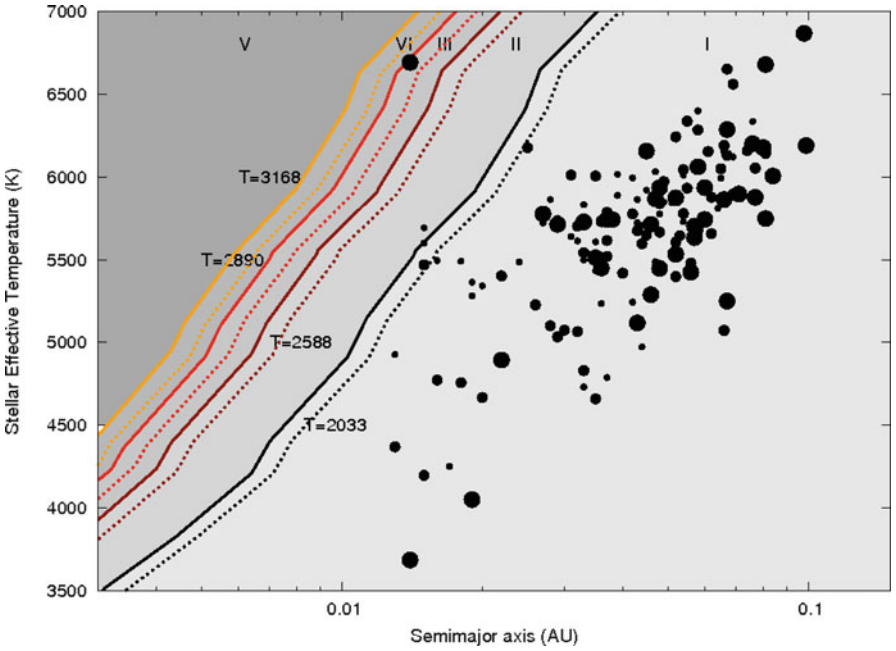


**Fig. 5.7** Stellar effective temperature and semimajor axis for the Kepler candidates. The *dotted lines* are the limit temperatures in the case of adopting 0.2 as the Bond albedo

short timescales. For this reason we do not expect this gases to be present in the atmosphere. We base this assumption on models of volatile loss in hot-Jupiters [1], hot super-Earths [20] and rocky bodies [6, 31]. If the volatiles were not lost, the atmosphere would be dominated by volatiles. For information about cooler planets that could potentially provide habitable conditions see e.g. [15].

## *Albedo*

The planetary bond albedo adopted in this work is $A = 0.01$. The observations [25–27] and modeling [4, 22, 32] of hot exoplanets support this assumption. According to these studies, there are currently no indications that suggest higher albedos for hot rocky planets, nevertheless we study the effect of a higher albedo on our results. For comparison we adopt also the Earth bond albedo (0.2) and analyse the change in the results. For an albedo of 0.2, we find 146 planetary candidates with radius less than $2.5\,R_\oplus$ and $T_p > 1{,}000\,K$. Of these 146 planets, 144 are characterized by atmospheres Type I, 1 by Type II, 1 by Type III, 0 by Type IV and 0 by Type V (adopting komatiite composition). The differences in the limit temperatures and corresponding results can be seen in Fig. 5.7.

### *Heating Source*

In this work we consider irradiation from the central star as the main heating source. Heating sources like short-lived radioisotopes, impacts and tidal effects (among others) can increase the surface temperature. According to [13], the insolation is the most important heating source for planets with periods larger than ∼2 days and for those with shorter periods, with non eccentric orbits. We expect that these planets located so close to their central star have low eccentricities. Nevertheless, we explore the effects of tidal heating in the Kepler planetary candidates with $P < 2$ days, that can be affected by this effect if presenting eccentricities larger than $e > 0.1$. Equation 5.3 shows the planetary temperature when considering both effects: insolation and tides [13, 24],

$$T_{p,tidal+ins} = \left( \frac{\pi R_p^2 (1-A) \frac{L_\star}{4\pi a^2} + \frac{21}{2} \frac{k_2}{Q} \frac{G R_p^5 n e^2}{a^6} M_\star^2}{4\pi R_p^2 \sigma} \right)^{\frac{1}{4}} \tag{5.3}$$

where, $k_2 \simeq 0.3$ is the second-order Love number of super-Earths (Henning personal communication), $Q$ is the quality factor of the planet, $n$ its mean motion and $e$ the eccentricity. Since $e$ and $Q$ are unknown for the Kepler candidates, we test different values. Kepler candidates with periods less than 2 days are expected to have almost circular orbits. Therefore, we adopt $e = 0.001$ and $e = 0.01$ and two different values for $Q$: 200 and 20,000, which represent planets with limited partial melting or significant partial melting in the mantle, respectively [13] . We find no significant change in the planets surface temperatures in the four cases analyzed. The role of tides in these planets, if occurring, will be to increase the convective vigor of the mantle, causing a larger fraction of total mantle volume to be accessible to surface degassing, but should not change the surface temperature significantly.

## Conclusion

In this work we present a simple approach to explore the atmospheric composition of hot super-Earths as a function of the observable data of the planets: its semimajor axis, radius and stellar effective temperature. We model the initial planetary atmospheric compositions due to outgassing assuming komatiite and bulk silicate Earth as magma compositions. The planet equilibrium temperatures were calculated assuming that the main source of heating is irradiation from the central star, and discuss the consequences of adopting different sources of heating. The model results indicate five types of atmospheres, based on the abundance of the dominant gases (Fe, Mg, Na, O, $O_2$ and SiO).

We apply this approach to explore the different atmospheric composition of hot potentially rocky planetary candidates from the February 2011 *Kepler* data release. According to our findings, 615 planetary candidates have radii less than 2.5 $R_\oplus$,

of which 193 have $T_p$ larger than 1,000 K (assuming an albedo of 0.01). When adopting komatiite composition, 189 of 193 *Kepler* candidates present a Type I model atmosphere dominated by monatomic Na, $O_2$, monatomic O and monatomic Fe. Three planetary candidates are characterized by Type II atmospheres, where SiO becomes more abundant than monatomic Fe, no candidates with Type III atmospheres, where monatomic Mg is more abundant than monatomic Fe, and only one planet is characterized by Type IV, with a large abundance of SiO. Finally, there is no Kepler planetary candidate with an atmosphere of Type V, which is completely dominated by SiO.

**Acknowledgements** The authors acknowledge support from DFG funding ENP Ka 3142/1-1 and NASA NAI.

## References

1. Baraffe, I., et al.: Hot-Jupiters and hot-Neptunes: a common origin? A&A **436**, L47 (2005)
2. Batalha, N., et al.: Kepler's first rocky planet: Kepler-10b. ApJ **729**, 27 (2011)
3. Borucki, W.J., et al.: Characteristics of planetary candidates observed by Kepler. II. Analysis of the first four months of data. ApJ **736**, 19 (2011)
4. Burrows, A., Ibgui, L., Hubeny, I.: Optical albedo theory of strongly irradiated giant planets: the case of HD 209458b. ApJ **682**, 1277 (2008)
5. Caldwell, D.A., et al.: Instrument performance in Kepler's first months. ApJ **713**, L92 (2010)
6. Fegley, B. Jr.: In: Davis, A.M., Turekian, K.K., Holland, H.D. (eds.) Meteorites, comets and planets. Treatise on Geochemistry, vol. 1, p. 487. Elsevier, Boston (2004)
7. Fegley, B. Jr., Cameron, A.G.W.: A vaporization model for iron/silicate fractionation in the mercury protoplanet. Earth Planet. Sci. Lett. **82**, 207 (1987)
8. Guenther, E.W., et al.: Constraints on the exosphere of CoRoT-7b. A&A **525**, 24 (2011)
9. Hastie, J.W., Bonnell, D.W.: A predictive phase equilibrium model for multicomponent oxide mixtures. Part II. Oxides of Na-K-Ca-Mg-Al-Si. High Temp. Sci. **19**, 275 (1985)
10. Hastie, J.W., Bonnell, D.W.: A predictive thermodynamic model of oxide and halide glass phase equilibria. J. Non-Crystalline Solids **84**, 151–158 (1986)
11. Hastie, J.W., Horton, W.S., Plante, E.R., Bonnell, D.W.: Thermodynamic models of alkali-metal vapor transport in silicate systems. High Temp. High Press. **14**, 669–679 (1982)
12. Hastie, J.W., Bonnell, D.W., Plante, E.R., Horton, W.S.: Thermodynamic activity and vapor pressure models for silicate systems including coal slags. In: Ribeiro da Silva, M.A.V. (ed.) Thermochemistry and Its Applications to Chemical and Biochemical Systems, pp. 235–251. Reidel, Dordrecht (1984)
13. Henning, W.G., Connell, R.J.O., Sasselov, D.D.: Tidally heated terrestrial exoplanets: viscoelastic response models. ApJ **707**, 1000 (2009)
14. Jenkins, J.M., et al.: Overview of the Kepler science processing pipeline. ApJ **713**, L87 (2010)
15. Kaltenegger, L., Sasselov, D.D.: Exploring the habitable zone for Kepler planetary candidates. ApJ **736**, L25 (2011)
16. Koch, D.G., et al.: Kepler mission design, realized photometric performance, and early science. ApJ **713**, L79 (2010)
17. Lammer, H., et al.: Determining the mass loss limit for close-in exoplanets: what can we learn from transit observations? A&A **506**, 399 (2009)
18. Leger, A., et al.: Transiting exoplanets from the CoRoT space mission. VIII. CoRoT-7b: the first super-Earth with measured radius. A&A **506**, 287L (2009)

19. Leger, A., et al.: The extreme physical properties of the CoRoT-7b super-Earth. Icarus **213**, 1L (2011)
20. Leitzinger, M., et al.: Could CoRoT-7b and Kepler-10b be remnants of evaporated gas or ice giants? Planet. Space Sci. **59**, 1472 (2011)
21. Miguel, Y., Kaltenegger, L., Fegley, B. Jr., Schaefer, L.: Compositions of hot super-earth atmospheres: exploring Kepler candidates. ApJ **742**, L19 (2011)
22. Miller-Ricci, E., Fortney, J.J.: The nature of the atmosphere of the transiting Super-Earth GJ 1214b. ApJ **716**, 74 (2010)
23. Mura, A., et al.: Comet-like tail-formation of exospheres of hot rocky exoplanets: possible implications for CoRoT-7b. Icarus **211**, 1 (2011)
24. Murray, C.D., Dermott, S.F.: Solar Systema Dynamics. Cambridge University Press, New York (2005)
25. Rogers, J.C., Apai, D., Lpez-Morales, M., Sing, D.K., Burrows, A.: Ks-Band detection of thermal emission and color constraints to corot-1b: a low-albedo planet with inefficient atmospheric energy redistribution and a temperature inversion. ApJ **707**, 1707 (2009)
26. Rowe, J.F., et al.: An upper limit on the albedo of HD 209458b: direct imaging photometry with the MOST satellite. ApJ **646**, 1241 (2006)
27. Rowe, J.F., et al.: The very low albedo of an extrasolar planet: MOST space-based photometry of HD 209458. ApJ **689**, 1345 (2008)
28. Rubie, D.C., Gessmann, C.K., Frost, D.J.: Partitioning of oxygen during core formation on the Earth and Mars. Nature **429**, 58 (2004)
29. Schaefer, L., Fegley, B. Jr.: A thermodynamic model of high temperature lava vaporization on Io. Icarus **169**, 216 (2004)
30. Schaefer, L., Fegley, B. Jr.: Chemistry of silicate atmospheres of evaporating Super-Earths. ApJ **703**, 113 (2009)
31. Spencer, J.R., Schneider, N.M.: Io on the eve of the Galileo mission. Ann. Rev. Earth Planet. Sci. **24**, 125 (1996)
32. Sudarsky, D., Burrows, A., Pinto, P.: Albedo and reflection spectra of extrasolar giant planets. ApJ **538**, 885 (2000)
33. Valencia, D., Sasselov, D.D., O' Connell, R.: Detailed models of Super-Earths: how well can we infer bulk properties? ApJ **665**, 1413 (2007)
34. Valencia, D., Ikoma, M., Guillot, T., Nettelmann, N.: Composition and fate of short-period super-Earths. The case of CoRoT-7b. A&A **516**, 20 (2010)

# Chapter 6
# The Nitrogen Chemistry in Hot Jupiters Atmosphere

**Olivia Venot, Eric Hébrard, Marcelino Agúndez, Michel Dobrijevic, Franck Selsis, Franck Hersant, Nicolas Iro, and Roda Bounaceur**

**Abstract** The atmosphere of hot Jupiters can be probed by primary transit and secondary eclipse spectroscopy. In order to constrain the atmospheric thermal structure and composition from observables, chemical models are necessary. Due to the intense UV irradiation, mixing and circulation, the chemical composition is maintained out of equilibrium and kinetic photochemical models must be applied with kinetics valid at the high temperatures prevailing in hot Jupiters atmospheres. We study the steady state atmospheric composition of HD 189733b one of the most observed hot Jupiters by implementing a new kinetic network in a 1D time-dependent chemical model including photodissociations and vertical diffusion. We confirm that the atmospheric composition of the planet is maintained out of the equilibrium by photodissociations and vertical quenching. The core and novelty of this study is the chemical scheme. It was produced in close collaboration with experts of applied high-temperature kinetics and methodically validated over a range of temperatures and pressures typical of the atmospheric layers influencing the observations of hot Jupiters. In addition to our nominal chemical scheme, we implemented other reaction sub-networks for nitrogen-bearing species that are

O. Venot (✉) • E. Hébrard • M. Agúndez • M. Dobrijevic • F. Selsis • F. Hersant
University of Bordeaux, LAB, UMR 5804, F-33270, Floirac, France
CNRS, LAB, UMR 5804, F-33270, Floirac, France
e-mail: venot@obs.u-bordeaux1.fr; hebrard@obs.u-bordeaux1.fr; agundez@obs.u-bordeaux1.fr; dobrijevic@obs.u-bordeaux1.fr; selsis@obs.u-bordeaux1.fr; hersant@obs.u-bordeaux1.fr

N. Iro
Astrophysics Group, Keele University, Keele, Staffordshire, ST5 5BG, UK
LESIA, Observatoire de Paris, 5 Place Jules Janssen, F-92195 Meudon, France
e-mail: nicolas.iro@zmaw.de

R. Bounaceur
Laboratoire Réactions et Génie des Procédés, LRGP UPR 3349 CNRS, Université de Lorraine, 1 rue Grandville, BP 20401, F-54001, Nancy, France
e-mail: roda.bounaceur@univ-lorraine.fr

J.M. Trigo-Rodriguez et al. (eds.), *The Early Evolution of the Atmospheres of Terrestrial Planets*, Astrophysics and Space Science Proceedings 35,
DOI 10.1007/978-1-4614-5191-4_6, 

commonly used in the field of combustion, and investigate the sensitivity of the predicted abundances and spectra to the network. We found that the abundances of $NH_3$ and HCN can vary by 2 orders of magnitude. A spectral feature of $NH_3$ at 10.5 µm is sensitive to these abundance variations and thus to the chemical scheme.

## Introduction

So far, more than 700 exoplanets have been confirmed and thousands of transiting candidates have been identified by the space telescope Kepler [4]. Among them, hot Jupiters are a class of gas giants with orbital periods of a few days or less. They are found around ∼0.5% of KGF stars [29, 30]. About 10% of them transit their host star and their atmospheric composition and physical structure can be studied by transit spectroscopy [12, 13, 31, 52, 58, 62–66]. Photochemical models have been developed to interpret these observations [44–46, 50, 73].

Because of their short orbital distance, hot Jupiters receive a high UV flux (typically 10,000 times the flux received on the top of the atmosphere of Jupiter) and their equilibrium temperature is very high (ranging from 600 to 3,000 K). Thus, the atmospheric composition of these planets is potentially influenced by both photochemistry and thermochemistry [73].

In Solar System atmospheres, photolyses due to solar UV photon occur at low temperature and chemical models can neglect endothermic reactions. In the hot lower atmospheres of gas giants, icy giants, and Venus, temperature is high enough for endothermic reactions to take place but no UV radiation is present. Therefore, we cannot use the same models to describe correctly hot Jupiter atmospheres, since it is necessary to consider chemical reactions in both the exothermic and endothermic directions, with rate coefficients specific to the relevant temperature range, as well as UV photolyses. To that purpose, we have implemented a chemical scheme that is new in the field of astrochemistry, but initially developed for industrial applications (mainly combustion in car engines). Chemical models based on this scheme have been the subject of a comprehensive validation against experiments.

## Chemical Modeling

### *Kinetics and Thermodynamic Equilibrium*

An elementary reversible reaction $i$ involving $J$ chemical species can be represented in the following general form:

$$\sum_{j=1}^{J} \nu'_{ji} \chi_j \Leftrightarrow \sum_{j=1}^{J} \nu''_{ji} \chi_j \tag{6.1}$$

where $\nu'_{ji}$ are the forward stoichiometric coefficients, and $\nu''_{ji}$ are the reverse ones. $\chi_j$ is the chemical symbol of the $j$th species. The kinetic data associated to each reaction are expressed with a modified Arrhenius law $k(T) = A \times T^n \exp^{-\frac{E_a}{RT}}$ where $T$ is the temperature, $R$ the universal gas constant, $E_a$ is the activation energy of the reaction, $A$ the pre-exponential factor and $n$ a coefficient which allows the temperature dependence of the pre-exponential factor. If the rate constant associated to the forward reaction is $k_{fi}(T)$, then the one associated to the reverse reaction is $k_{ri}(T)$, verifying:

$$K_i = \frac{k_{fi}(T)}{k_{ri}(T)} \left( \frac{P^0}{k_B T} \right)^{\Sigma_{j=1}^{J} \nu_{ji}} \tag{6.2}$$

where $K_i$ is the equilibrium constant (with the activity of the reactants expressed in pressure units) [7]:

$$K_i = \exp\left( \frac{\Delta S_i^0}{R} - \frac{\Delta H_i^0}{RT} \right) \tag{6.3}$$

where $\Delta S_i^0$ and $\Delta H_i^0$ are the variation of entropy and enthalpy occurring when passing from reactants to products in the reaction $i$, $P^0$ is the standard pressure ($P^0 = 1{,}01325$ bar), $k_B$ is the Boltzmann's constant and $\nu_j$ are the stoichiometric coefficients of the $J$ species involved in reaction $i$: $\nu_j = \nu''_{ji} - \nu'_{ji}$. The enthalpy and the entropy are expressed in therms of NASA polynomials as described in Venot et al. [71]. By reversing all the reactions, the kinetic system will evolved towards the thermodynamic equilibrium.

The equilibrium composition of a system at a defined temperature and pressure can also be determined by finding the composition that minimizes the Gibbs energy of the system. Indeed, a system always evolves in order to reduce its Gibbs energy. This energy is given by:

$$G = \sum_{j=1}^{J} \overline{g_j} N_j \tag{6.4}$$

where $J$ is the total number of species, $\overline{g_j}$ is the partial free energy of the species $j$ and $N_j$ is the number of moles of the species $j$. The partial free energy of a compound $j$, behaving as an ideal gas, is given by:

$$\overline{g_j} = g_j(T,P) + RT \ln N_j \tag{6.5}$$

where $g_j(T,P)$ is the free energy of the species $j$ at the temperature $T$ and the pressure $P$ of the system and $R$ is the ideal gas constant. For an ideal gas, $g_j(T,P)$ is given by:

$$g_j(T,P) = h_j^0(T) - T s_j^0(T) + RT \ln\left( \frac{P}{P^0} \right) \tag{6.6}$$

where $h_j^0(T)$ and $s_j^0(T)$ are respectively, the standard-state enthalpy and entropy of the species $j$ at the temperature $T$ of the system. As we said, these quantities are calculated with the NASA coefficients. Using only these coefficients, one can determine the equilibrium composition of a system.

## *Kinetic Network: From Car Engine to Hot Jupiters*

Significant progress has been done during the past decade in the development of combustion mechanisms.[1] In the context of limiting the environmental impact of transportation, there is indeed a need in the development of detailed chemical kinetic models more predictive and more accurate for the combustion of fuels. One part of the studies undertaken in the LRGP (Laboratoire Réactions et Génie des Procédés, Nancy, France) concerns engine-fuel adaptation in order to improve the efficiency of engines and to limit the emission of pollutants. Most of these kinetic models were developed for industrial applications and have been validated in a range of temperatures, from 300 to approximately 2,500 K, and for pressures from 0.01 bar to some hundreds of bar. What is worth noticing is the similarity of these temperature and pressure ranges with the conditions prevailing in hot Jupiters atmospheres, in the very layers where they influence the observed molecular features. In addition, combustion mechanisms mainly deal with molecules made of C, H, O and N, which are also the main constituents of the molecules and radicals in these atmospheres. For this reason, we have decided to implement such a mechanism, which has already been applied successfully to many cases and systematically validated [8], to study the atmosphere of hot Jupiters.

We have used a C/H/O/N mechanism, whose core is a $C_0$–$C_2$ mechanism that includes all the reactions required to model the kinetic evolution of radicals and molecules containing less than three carbon atoms. This mechanism is described in Venot et al. [71]. The originality of this scheme, is that it includes experimental data for both exothermic and endothermic directions for three important reactions, instead of reversing them with the equilibrium constant. Indeed, we have explained in section "Kinetics and Thermodynamic Equilibrium" that it was necessary to reverse all the reactions of a system to reproduce the thermodynamical equilibrium, but it does not ensure that the kinetic evolution is realistic. Decade of study and experiments in the field of combustion have shown that the kinetic evolution was more realistic using experimental data for some reactions for both directions.

As nitrogen species, such as $N_2$, $NH_3$, HCN, are expected to be important constituents of hot Jupiter atmospheres, we completed this $C_0$–$C_2$ base with a validated sub-mechanism specifically constructed to model nitrogen species and all the cross-term reactions involved (for instance, reactions between alkanes and $NO_X$). These mechanisms do not use rate coefficients that have been adjusted by optimization procedures in order to fit experiments. Their values are those recommended for the individual processes by the main kinetics databases for combustion [6, 49, 59, 67]. The list of the reactions and their rate coefficients are

[1] In the field of combustion, a *mechanism* or reaction base is a network of reactions able to describe the kinetic evolution of a given pool of species. The mechanism includes the list of reactions and the associated rate coefficients, in a modified Arrhenius form, as well as the thermodynamic data for all the species involved in these reactions, which are required to calculate the equilibrium constants of the reactions and the rates of the reverse reactions.

available in the online database KIDA: KInetic Database for Astrochemistry[2] [72]. The final mechanism includes 957 reversible and 6 irreversible reactions, involving 105 neutral species (molecule or radical). Helium is also included in this mechanism and plays the role of third body in some reactions.

#### Nitrogen Reaction Base

In our nominal model, the sub-network for the nitrogen bearing species is derived from Konnov [35, 36] and Coppens et al. [14]. It is based on a comprehensive analysis of the combustion chemistry of nitrogen oxides [38], ammonia [40], hydrazine [42], and modeling of nitrogen oxides formation in different combustion systems [37, 39, 41]. In addition, we consider a few additional pathways for HCN oxidation from Dagaut et al. [15].

Validations of our nominal sub-network for nitrogen bearing species have been made on the basis of experimental data obtained, for instance, by oxidation of HCN in a silica jet-stirred reactor (JSR) at atmospheric pressure and from 1,000 to 1,400 K [15], or studying laminar flame speeds in $NH_3$ – $N_2O$ mixtures [9]. The nitrogen mechanism includes 42 species: $NO_3$, $HONO_2$, $CH_3ONO$, $CH_3NO_2$, $HNO_2$, $CH_3NO$, $NO_2$, HONO, HCNN, HCNO, $N_2O$, NCO, HNO, HOCN, NNH, $H_2CN$, $N(^4S)$, CN, HNCO, NO, NH, $NH_2$, HCN, $NH_3$, $N_2$, $N_2O_4$, $N_2O_3$, $N_2H_2$, $N_2H_3$, $N_2H_4$, HNNO, HNOH, $HNO_3$, $NH_2OH$, $H_2NO$, CNN, $H_2CNO$, $C_2N_2$, HCNH, HNC, HON and NCN. For comparison, we have also used other nitrogen sub-mechanisms, which are presented in section "Nitrogen Reaction Base" with the corresponding results.

Because the mechanism we use was created from individual processes and validated without any optimization of their reaction coefficients, its application outside the condition range of validation is not problematic. This is an issue, for instance, with the well-known combustion mechanism GRI-Mech V3.0[3] [59], proposed by Gas Research Institute, which is an optimized mechanism designed to model natural gas combustion. Optimization makes the model extremely accurate within the optimization domain but its application beyond is risky [5].

### *Photochemistry*

We add to the thermochemical scheme a set of 34 photodissociations. In hot Jupiters, UV flux penetrates down to a pressure of about 1 bar, where the temperature is higher than 1,500 K. At these temperatures and pressures, endothermic reactions do matter, which implies that photochemistry and thermochemistry are coupled

[2] http://kida.obs.u-bordeaux1.fr.

[3] http://www.me.berkeley.edu/gri_mech/.

in such highly irradiated atmospheres. We used absorption cross section at the highest available temperature (i.e. 370 K at maximum, which is low compared to the temperatures in the atmosphere of hot Jupiters (see Fig. 6.1)). To tackle this issue, we have decided to measure absorption cross section at high temperature for important molecules such as $CO_2$ and $H_2O$. These measurements and their impact on the results given by our model are presented in Venot et al. [70].

Photodissociations produce excited states of oxygen ($O(^1D)$) and nitrogen ($N(^2D)$) that are not treated in the original combustion mechanisms. Therefore, we added to the C/H/O/N mechanism, 19 reversible reactions which describe the kinetics of $O(^1D)$ and $N(^2D)$, including radiative and collisional desexcitation. These reactions rates are taken (or have been estimated) from Okabe [51], Herron [28], Umemoto et al. [69], Balucani et al. [2], Sato et al. [55], Balucani et al. [3] and Sander et al. [54].

### *1D Numerical Model*

We use this chemical network in a 1D model that includes photolyses and vertical transport, which has been previously used to study the atmospheric photochemistry of various objects of the Solar System: Neptune [19], Titan [26, 27], Saturn [11, 18], and Jupiter [10] as well as extrasolar terrestrial planets [56]. This model has been adapted to hot Jupiters and is described in Dobrijevic et al. [19] and Venot et al. [71].

To calculate the photodissociation rates in all the layers of the atmosphere, we compute the stellar UV flux as a function of pressure and wavelength, taking into account molecular absorption by 22 species and Rayleigh scattering. Actinic fluxes are calculated with a resolution of 1 nm (which is also the resolution we adopted for the absorption cross-sections), assuming a plane parallel geometry and an incidence angle $\theta$ of 48° (because $< \cos\theta >= 2/3$ ($\theta \simeq 48°$) is the projected-areaweighted average of the cosine of the stellar zenith angle over the planetary disk at secondary-eclipse conditions). Multiple Rayleigh scattering is coupled with absorption through a simple two-stream iterative algorithm [34].

## Application to HD 189733b

HD 189733b transits around a nearby bright star. Its atmosphere has been studied by the transmission spectrum obtained during the primary transit and the day-side emission spectrum measured at the secondary eclipse. These observations can be used to constrain the thermal profile [47] and to detect the spectral signature of atmospheric compounds [24, 63, 65, 66].

The physical properties used for HD 189733b and HD 189733 come from Southworth [60, 61]. We use the temperature (Fig. 6.1) and eddy diffusion profiles published in Moses et al. [50]. These profiles are derived from the general

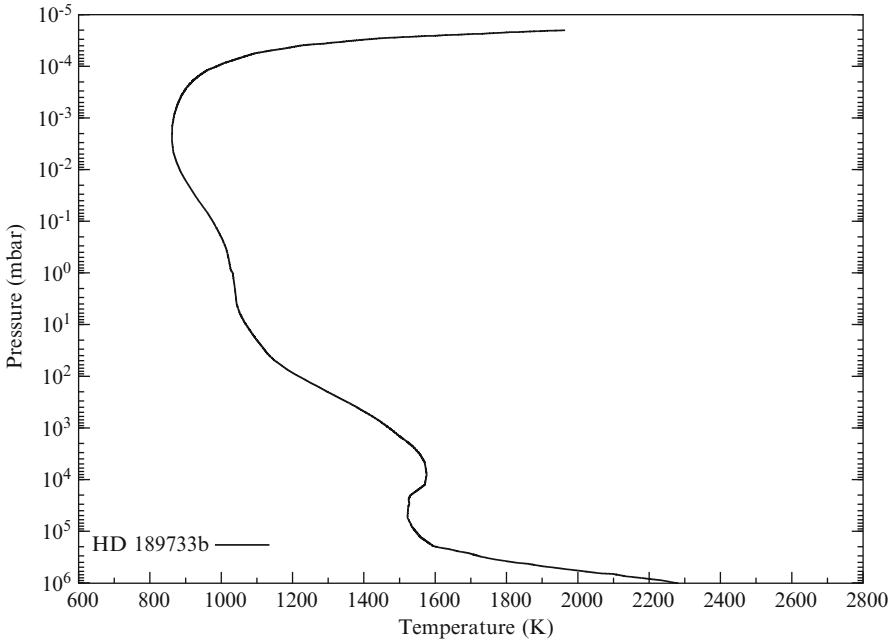


**Fig. 6.1** Pressure-temperature profiles of HD 189733b (From [50])

circulation model of Showman et al. [57] (for $K(z)$ and $PT$ profiles) and the 1-D model of Fortney et al. [21, 22] (for $PT$ profile only). Also following Moses et al. [50], we assume solar elemental abundances for this planet, with 20 % of depletion for oxygen (sequestered along with silicates and metals). We start our time-dependent modeling with the thermodynamic equilibrium abundances calculated with TECA (an equilibrium model described in Venot et al. [71]) at each level of the atmosphere.

For the star HD 189733, a K1–K2 star, the UV spectrum has been provided to us by Ignasi Ribas (private communication). It is based on FUSE and HST observations of the star $\varepsilon$ Eridani, a proxy of HD 189733 (similar type, age and metallicity), in the 90–330 nm range and on scaling laws between 0.5 and 90 nm. Above 330 nm, we use a synthetic spectrum calculated with the stellar atmosphere code Phoenix [25].

## *Nominal Model*

First of all, we checked that our kinetic model reproduces the thermodynamic equilibrium, in the absence of vertical mixing and photodissociation. We obtained differences lower than a few percent. The homopause is found above the $1 \times 10^{-5}$ mbar level, which is beyond the range of pressure that we model. As a consequence, and although it is included, molecular diffusion does not affect our results.

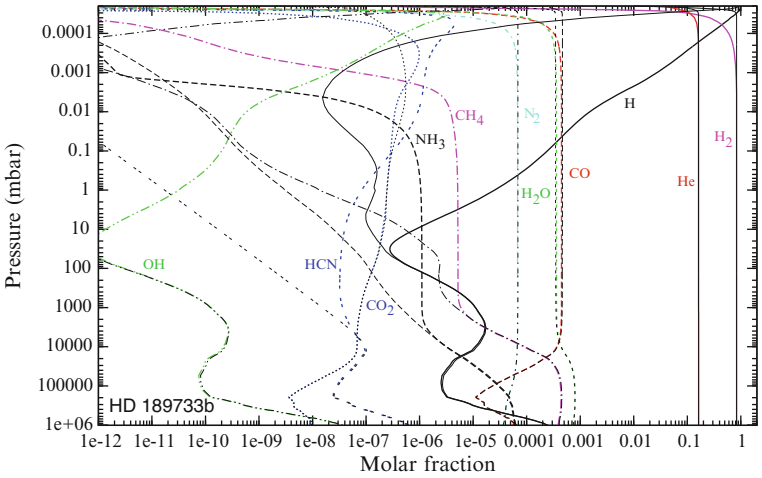


**Fig. 6.2** Steady-state composition of HD 189733b calculated with our nominal model (*color lines*), compared to the thermodynamic equilibrium (*thin black lines*)

Figure 6.2 shows the steady-state composition of the atmosphere of HD 189733b, with vertical transport and photodissociations. The vertical quenching has an effect on a large part of the atmosphere of HD 189733b. $NH_3$ and HCN are quenched at 5 bar, $CH_4$ at 1 bar, H at 40 mbar and $CO_2$ at 20 mbar. Quenching contaminates the composition up to very low-pressure levels ($10^{-4}$ mbar).

Photodissociations affect the composition down to about the 10 mbar level. The production of H is dominated by the photolysis of $H_2$ for pressures lower than 1 µbar. Below this level, and for pressures higher than 0.1 mbar, H is produced by the photodissociation of $H_2O$, with a minor contribution of the photodissociations of $NH_3$ and HCN. The abundance of OH follows the profile of H, and increases for pressures lower than 10 mbar. There is a photochemical enhancement of HCN above the 10 mbar pressure level, as discussed in Moses et al. [50]. $CH_4$ is destroyed by photolyses for pressures lower than 0.01 mbar. $NH_3$ is photodissociated down to levels as deep as 1 bar, but vertical transport compensates this destruction for pressures higher than 0.1 mbar. Above that level, the amount of $NH_3$ decreases with altitude due to photolyses. Photochemistry has a negligible effect on $CO_2$, as noted by Zahnle et al. [73].

## *Other Networks for Nitrogen Species*

The chemistry of some nitrogen compounds is not well constrained. However, $NO_X$, HCN, CN and $NH_3$ are important species in applied combustion (gas fuel, for instance, can contain high concentrations of ammonia), and should be well

reproduced within the temperature and pressure range of the validation. Quenching is found to occur within 100 to a few hundred bars, a pressure range at which our nominal mechanism has been validated. Other sub-mechanisms are available to model the kinetics of nitrogen-bearing species. In order to test how our results are sensitive to the nitrogen scheme, we replaced our nitrogen reaction base by other nitrogen sub-mechanisms:

- *GRIMECH*, mechanism based on GRI-Mech 3.0 [59] with several reactions involving $NO_X$ compounds added with respect to the mechanisms of Glaude et al. [23] as recommended and done by Anderlohr et al. [1]. It includes 162 reversible reactions involving 26 nitrogen compounds. The GRI-Mech 3.0 is a mechanism designed to model natural gas combustion, including NO formation and reburn chemistry. As already mentioned in section "Nitrogen Reaction Base", it has been optimized as a global mechanism, i.e., some rate coefficients have been modified (compared to the literature) in order to fit the results of a pool of experiments with conditions and compositions specific to combustion. The individual processes have not been studied separately in all the pressure and temperature range. Applying this mechanism beyond its domain of optimization/validation is a risky extrapolation. Mixing ratios of oxidants, for instance, are very low in hot Jupiter atmospheres compared with the experiments used to optimize/validate GRI-Mech 3.0.
- *GDF-Kin*, mechanism for natural gas combustion modeling [16, 68] that includes 180 reversibles reactions involving 22 nitrogen species. Several experimental data on natural gas combustion have been acquired in partnership with *Gaz de France* to develop and optimize this mechanism. $NO_X$ chemistry has been included in GDF-Kin 3.0 [20]. We use the update version GDF-Kin 5.0 [43], in which five reactions involving NCN have been refined in order to better reproduce the kinetics of this species.
- *DEAN*, taken from Dean and Bozzelli [17]. This book that presents a catalog of reactions is used by Moses et al. [50], at least for some reactions. The mechanism derived from this work includes 370 reversible reactions involving 49 nitrogen species and one C/H/O species that is not included in our $C_0$–$C_2$ scheme: HCOH. The purpose of the work of Dean and Bozzelli was to list gas phase reactions involving nitrogen-bearing species that could be important for high temperature combustion modeling and to provide the associated rate coefficients based on an analysis of elementary reaction data, when available, or on estimations from thermochemical kinetics principles otherwise. This mechanism was developed on the basis of analysis of individual reactions rather than by attempting to reproduce any specific set of experiments. It is clearly written in this book that: "Although we show in the chapter that this mechanism provides a reasonable description of some aspects of high-temperature nitrogen chemistry, we have not attempted a comprehensive comparison". Therefore, this kinetic network should be viewed as a database of reaction rate constants rather than a real validated mechanism.

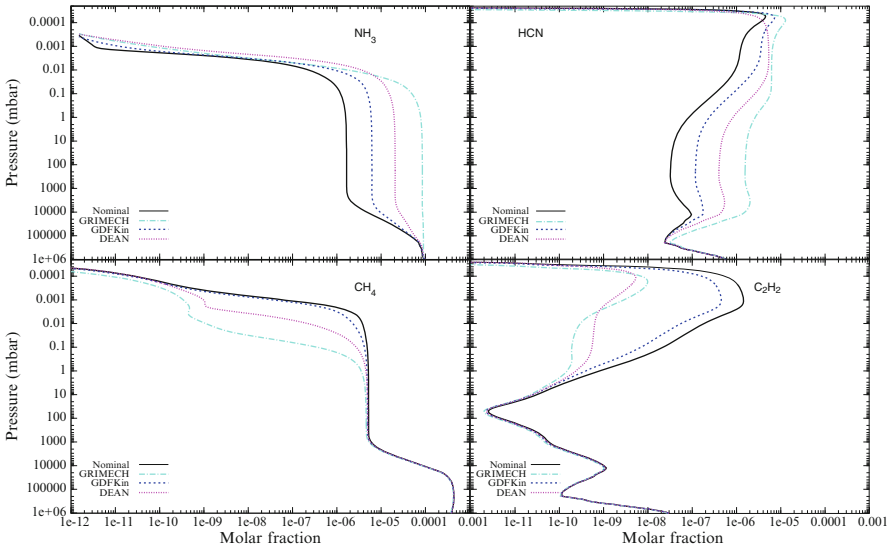


**Fig. 6.3** Abundances of $NH_3$, HCN, $CH_4$ and $C_2H_2$ in HD 189733b with the four different models

The impact of the different nitrogen sub-mechanisms on the abundance profiles of various species is illustrated in Fig. 6.3. Thermodynamic equilibrium is the same for all schemes (for the species in common).

The main species that are significantly affected at these pressure levels by the change of nitrogen scheme are HCN and $NH_3$. This is not surprising as these are the only ones departing from equilibrium due to quenching, and the pressure level at which the quenching occurs depends on the kinetic network adopted. For both HCN and $NH_3$, profiles obtained with *GDF-Kin* are bracketed by those from the nominal model and *DEAN*, while *GRIMECH* gives significantly higher abundances than all other models in the quenching region. With *GRIMECH*, we also notice that $NH_3$ becomes the main nitrogen-bearing species from the bottom of the atmosphere up to 0.03 mbar because of vertical mixing, whereas thermodynamics predicts that $N_2$ should be the main nitrogen-bearing species.

For hydrocarbons (see Fig. 6.3) all the models we tested cluster to the same profiles for pressures below 1 mbar. This shows that N-bearing species have little influence on hydrocarbon chemistry at these altitudes (This would no longer be true at higher temperature and for higher C/O ratios as HCN would become a major reservoir of both N and C).

At lower pressure, Fig. 6.3 shows large differences that are no longer due to quenching. When comparing our nominal model with our alternative ones, departures can be due to differences in the kinetic network (different rates, different minor species included) and in photochemistry, as some absorbing species are not included in all the models. The difference is particularly striking for $C_2H_2$, where

*DEAN* and *GRIMECH*, on the one hand, and the nominal model and *GDF-Kin*, on the other hand, seem to cluster in two different regimes, exhibiting 2 to 3 order of magnitude differences at 0.1–0.001 mbar.

### *Corresponding Emission and Transmission Spectra*

In order to calculate the planetary transmission and emission+reflection spectra of HD 189733b (Fig. 6.4), we use a line-by-line radiative transfer model from 0.3 to 25 µm [32, 33]. The opacity sources included in the model are the main molecular constituents: $H_2O$, CO, $CH_4$, $NH_3$, Na, K and TiO; Collision Induced Absorption by $H_2$ and He; Rayleigh diffusion and $H^-$ bound-free and $H_2^-$ free-free. For absorbing species not included in our kinetic model (Na, K and TiO), chemical equilibrium is assumed. The current model does not account for clouds. For the reflected component, we use synthetic stellar spectra generated from ATLAS.[4] The main difference from the static model described in Iro et al. [33] is the addition of $NH_3$ for which we used the HITRAN 2008 database [53].

We applied this model for the compositions obtained with the two nitrogen mechanisms, which give the most opposite results (Nominal and *GRIMECH*), as well as for chemical equilibrium. The *GRIMECH* scheme gives the highest abundance for ammonia: 100 times more $NH_3$ than the nominal model. As a consequence, features of this molecule become noticeable on both the emission and transmission spectra at 1.9, 2.3, 3.0, 4.0, 6.1 and 10.5 µm. The most prominent feature is found at 10.5 µm.

At the moment, our radiative transfer model does not include the contribution of HCN to the opacities. Based on the HCN abundances and associated spectra found by Moses et al. [50], we can expect the spectra to be also sensitive to the HCN abundance. Indeed, at the altitudes probed by the observations, there is nearly 2 orders of magnitude less HCN with our nominal model than with *GRIMECH*, and *GRIMECH* gives HCN abundances similar to that of Moses et al. [50]. Therefore, the signature of HCN found by Moses et al. [50] at 14 µm should also become noticeable with the *GRIMECH* version of our scheme.

## Discussion

The modeled abundances of nitrogen-bearing species (in particular $NH_3$ and HCN) differ significantly depending on the reaction network that we use. Deviations are also found for hydrocarbons in the upper atmosphere. To study the chemical composition of hot atmospheres, we recommend to use, as far as possible, chemical

[4] http://kurucz.harvard.edu/stars.html.

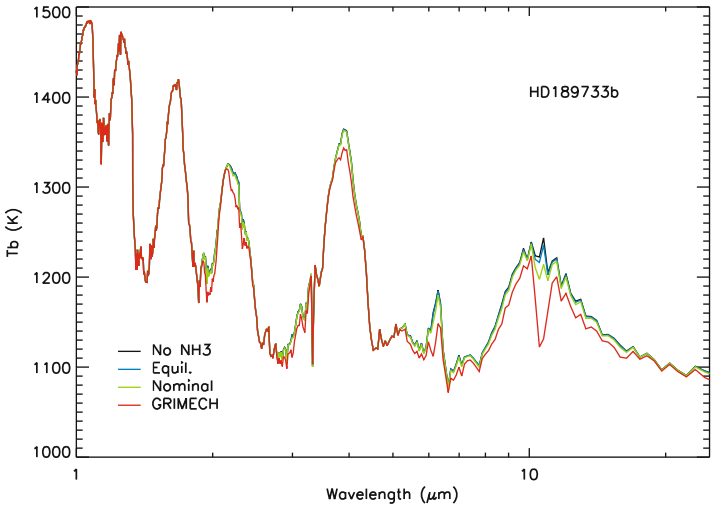


**Fig. 6.4** Synthetic day-side spectra of HD 189733b with the nominal mechanism (*green curve*) compared to the one corresponding to the *GRIMECH* mechanism (*red curve*) and to the thermochemical equilibrium (*blue curve*). The *dark curve* is obtained when $NH_3$ is removed from the model. The day-side fluxes are given as brightness temperatures ($T_b$). Because of the reflection component, note that the link between $T_b$ and the atmospheric thermal profile is altered below 2 μm

schemes validated against experiments, like ours. We do not claim that it is a definite chemical scheme, it will certainly evolve in the same time as our knowledge about nitrogen chemistry. Indeed, kinetics of reactions between nitrogen-bearing species is not as well known as for carbon-bearing species. Nitrogen mechanisms are expected to be improved and completed to study exoplanet atmospheres. For instance, in our chemical scheme we note the absence of several species (such as $CH_3CN$, $HC_3N$, ...), which have observable abundances in some planetary atmospheres of the Solar System (Titan and Earth). With solar elemental abundances and in the range of pressures and temperatures that we considered for the planet studied, HCN and $NH_3$ remain minor species, and it is likely that the departures that we find have little influence on the thermal profile and the spectra of this planet. However, hot Jupiters are certainly significantly enriched in heavy elements if formed by core accretion. A possible signature of that is the high abundance of $CO_2$ found by observations [64, 65], that requires a high metallicity [73]. In addition, C/O ratios could be altered during planet formation and a high C/O ratio could explain the high observed abundances of both $CH_4$ and $CO_2$ [48]. If this is correct, then HCN should be a key species and a main reservoir of both C and N in atmospheric layers probed by observations. New observations able to constrain the abundance of $NH_3$ and/or HCN would be extremely useful.

## Conclusion

Since decades, the field of combustion deals with high temperatures and pressures, similar to the ones found in hot Jupiters. Models used for industrial applications (such as car engine simulations) have been developed and validated over a broad range of temperatures, pressures and compositions. An important work of experiments have been required to obtain such a chemical scheme. We can benefit from this expertise and use the same chemical scheme to study the atmospheric composition of planets with warm atmospheres, as hot Jupiters and hot Neptunes. Despite this hard work, nitrogen chemistry is still not well constrained. Different schemes exist and are commonly used in the combustion field to study different purposes. Using these schemes in a photochemical model give a large range of possible results. This confirms the fact that chemical networks, in particular for N-bearing species, will have to be tested experimentally in conditions that are closer to those prevailing in hot exoplanet atmospheres. These planets represent a real laboratory to study nitrogen chemistry. We can hope that future, more accurate observations obtained for instance with EChO and JWST, will provide constraints allowing us to improve our mechanisms.

**Acknowledgements** We thank Ignasi Ribas for providing us the UV flux of $\varepsilon$ Eridani, proxy of HD 189733 and Anthony M. Dean for providing us the list of rate coefficients from his book in an electronic form. F. S., O. V., E. H. and M. A. acknowledge support from the European Research Council (ERC Grant 209622: $E_3$ARTHs).

## References

1. Anderlohr, J., Bounaceur, R., Pires Da Cruz, A., Battin-Leclerc, F.: Modeling of autoignition and no sensitization for the oxidation of ic engine surrogate fuels. Combust. Flame **156**(2), 505–521 (2009)
2. Balucani, N., Alagia, M., Cartechini, L., Casavecchia, P., Volpi, G.G., Sato, K., Takayanagi, T., Kurosaki, Y.: Cyanomethylene formation from the reaction of excited nitrogen atoms with acetylene: a crossed beam and ab initio study. J. Am. Chem. Soc. **122**(18), 4443–4450 (2000a)
3. Balucani, N., Cartechini, L., Alagia, M., Casavecchia, P., Volpi, G.: Observation of nitrogen-bearing organic molecules from reactions of nitrogen atoms with hydrocarbons: a crossed beam study of N($^2$D)+ ethylene. J. Phys. Chem. A **104**(24), 5655–5659 (2000b)
4. Batalha, N.M., Rowe, J.F., Bryson, S.T., Barclay, T., Burke, C.J., Caldwell, D.A., Christiansen, J.L., Mullally, F., Thompson, S.E., Brown, T.M., Dupree, A.K., Fabrycky, D.C., Ford, E.B., Fortney, J.J., Gilliland, R.L., Isaacson, H., Latham, D.W., Marcy, G.W., Quinn, S., Ragozzine, D., Shporer, A., Borucki, W.J., Ciardi, D.R., Gautier, T.N., III, Haas, M.R., Jenkins, J.M., Koch, D.G., Lissauer, J.J., Rapin, W., Basri, G.S., Boss, A.P., Buchhave, L.A., Charbonneau, D., Christensen-Dalsgaard, J., Clarke, B.D., Cochran, W.D., Demory, B.O., Devore, E., Esquerdo, G.A., Everett, M., Fressin, F., Geary, J.C., Girouard, F.R., Gould, A., Hall, J.R., Holman, M.J., Howard, A.W., Howell, S.B., Ibrahim, K.A., Kinemuchi, K., Kjeldsen, H., Klaus, T.C., Li, J., Lucas, P.W., Morris, R.L., Prsa, A., Quintana, E., Sanderfer, D.T., Sasselov, D., Seader, S.E., Smith, J.C., Steffen, J.H., Still, M., Stumpe, M.C., Tarter, J.C., Tenenbaum, P., Torres, G., Twicken, J.D., Uddin, K., Van Cleve, J., Walkowicz, L., Welsh, W.F.: Planetary candidates observed by Kepler, III: analysis of the first 16 months of data. ArXiv e-prints (2012)

5. Battin-Leclerc, F., Blurock, E., Bounaceur, R., Fournet, R., Glaude, P.A., Herbinet, O., Sirjean, B., Warth, V.: Towards cleaner combustion engines through groundbreaking detailed chemical kinetic models. Chem. Soc. Rev. **40**(9), 4762–4782 (2011)
6. Baulch, D.L., Bowman, C.T., Cobos, C.J., Cox, R.A., Just, T., Kerr, J.A., Pilling, M.J., Stocker, D., Troe, J., Tsang, W., et al.: Evaluated kinetic data for combustion modeling: supplement II. J. Phys. Chem. Ref. Data **34**(3), 757–1398 (2005)
7. Benson, S.W.: Thermochemical Kinetics: Methods for the Estimation of Thermochemical Data and Rate Parameters, 2nd edn. Wiley, New York (1976)
8. Bounaceur, R., Glaude, P., Fournet, R., Battin-Leclerc, F., Jay, S., Cruz, A.: Kinetic modeling of a surrogate diesel fuel applied to 3D auto-ignition in HCCI engines. Int. J. Veh. Des. **44**(1), 124–142 (2007)
9. Brown, M.J., Smith, D.B.: Aspects of nitrogen flame chemistry revealed by burning velocity modeling. Symp. (Int.) Combust. **25**(1), 1011–1018 (1994). 25th symposium (international) on combustion
10. Cavalié, T., Billebaud, F., Biver, N., Dobrijevic, M., Lellouch, E., Brillet, J., Lecacheux, A., Hjalmarson, Å., Sandqvist, A., Frisk, U., et al.: Observation of water vapor in the stratosphere of Jupiter with the odin space telescope. Planet. Space Sci. **56**(12), 1573–1584 (2008)
11. Cavalié, T., Billebaud, F., Dobrijevic, M., Fouchet, T., Lellouch, E., Encrenaz, T., Brillet, J., Moriarty-Schieven, G., Wouterloot, J., Hartogh, P.: First observation of CO at 345 GHz in the atmosphere of Saturn with the JCMT: new constraints on its origin. Icarus **203**(2), 531–540 (2009)
12. Charbonneau, D., Brown, T., Latham, D., Mayor, M.: Detection of planetary transits across a sun-like star. Astrophys. J. Lett. **529**, L45 (2000)
13. Charbonneau, D., Knutson, H., Barman, T., Allen, L., Mayor, M., Megeath, S., Queloz, D., Udry, S.: The broadband infrared emission spectrum of the exoplanet HD 189733b. Astrophys. J. **686**, 1341 (2008)
14. Coppens, F.H.V., De Ruyck, J., Konnov, A.: The effects of composition on burning velocity and nitric oxide formation in laminar premixed flames of $CH_4$+ $H_2$+ $O_2$+ $N_2$. Combust. Flame **149**(4), 409–417 (2007)
15. Dagaut, P., Glarborg, P., Alzueta, M.: The oxidation of hydrogen cyanide and related chemistry. Prog. Energy Combust. Sci. **34**(1), 1–46 (2008)
16. De Ferrieres, S., El Bakali, A., Lefort, B., Montero, M., Pauwels, J.: Experimental and numerical investigation of low-pressure laminar premixed synthetic natural gas/$O_2$/$N_2$ and natural gas/ $H_2$/$O_2$/$N_2$/ flames. Combust. Flame, **154**(3), 601–623 (2008)
17. Dean A., Bozzelli, J.: Gas-Phase Combustion Chemistry, pp. 125–341. Springer, New York (2000)
18. Dobrijevic, M., Ollivier, J., Billebaud, F., Brillet, J., Parisot, J.: Effect of chemical kinetic uncertainties on photochemical modeling results: application to Saturn's atmosphere. Astron. Astrophys. **398**(1), 335–344 (2003)
19. Dobrijevic, M., Cavalié, T., Hébrard, E., Billebaud, F., Hersant, F., Selsis, F.: Key reactions in the photochemistry of hydrocarbons in Neptune's stratosphere. Planet. Space Sci. **58**, 1555–1566 (2010)
20. El Bakali, A., Pillier, L., Desgroux, P., Lefort, B., Gasnot, L., Pauwels, J.F., da Costa, I.: No prediction in natural gas flames using gdf-kin® 3.0 mechanism ncn and hcn contribution to prompt-no formation. Fuel **85**(7), 896–909 (2006)
21. Fortney, J., Cooper, C., Showman, A., Marley, M., Freedman, R.: The influence of atmospheric dynamics on the infrared spectra and light curves of hot Jupiters. Astrophys. J. **652**, 746 (2006)
22. Fortney, J., Shabram, M., Showman, A., Lian, Y., Freedman, R., Marley, M., Lewis, N.: Transmission spectra of three-dimensional hot Jupiter model atmospheres. Astrophys. J. **709**, 1396 (2010)
23. Glaude, P., Marinov, N., Koshiishi, Y., Matsunaga, N., Hori, M.: Kinetic modeling of the mutual oxidation of no and larger alkanes at low temperature. Energy Fuels **19**(5), 1839–1849 (2005)

24. Grillmair, C., Burrows, A., Charbonneau, D., Armus, L., Stauffer, J., Meadows, V., Van Cleve, J., Von Braun, K., Levine, D.: Strong water absorption in the dayside emission spectrum of the planet hd 189733b. Nature **456**(7223), 767–769 (2008)
25. Hauschildt, P., Allard, F., Baron, E.: The nextgen model atmosphere grid for $3000 \leq T_{eff} \leq 10{,}000$ k. Astrophys. J. **512**, 377 (1999)
26. Hébrard, E., Dobrijevic, M., Bénilan, Y., Raulin, F.: Photochemical kinetics uncertainties in modeling Titan's atmosphere: a review. Photochem. Photobiol. C **7**(4), 211–230 (2006)
27. Hébrard, E., Dobrijevic, M., Bénilan, Y., Raulin, F.: Photochemical kinetics uncertainties in modeling Titan's atmosphere: first consequences. Planet. Space Sci. **55**(10), 1470–1489 (2007)
28. Herron, J.: Evaluated chemical kinetics data for reactions of $N(^2D)$, $N(^2P)$, and $N_2$ ($a^3\sigma u+$) in the gas phase. J. Phys. Chem. Ref. Data **28**(5), 1453–1483 (1999)
29. Howard, A., Marcy, G., Johnson, J., Fischer, D., Wright, J., Isaacson, H., Valenti, J., Anderson, J., Lin, D., Ida, S.: The occurrence and mass distribution of close-in super-earths, Neptunes, and Jupiters. Science **330**(6004), 653 (2010)
30. Howard, A., Marcy, G.W., Bryson, S.T., Jenkins, J.M., Rowe, J.F., Batalha, N.M., Borucki, W.J., Koch, D.G., Dunham, E.W., Gautier, T.N., III, Van Cleve, J., Cochran, W.D., Latham, D.W., Lissauer, J.J., Torres, G., Brown, T.M., Gilliland, R.L., Buchhave, L.A., Caldwell, D.A., Christensen-Dalsgaard, J., Ciardi, D., Fressin, F., Haas, M.R., Howell, S.B., Kjeldsen, H., Seager, S., Rogers, L., Sasselov, D.D., Steffen, J.H., Basri, G.S., Charbonneau,D., Christiansen, J., Clarke, B., Dupree, A., Fabrycky, D.C., Fischer, D.A., Ford, E.B., Fortney J.J., Tarter, J., Girouard, F.R., Holman, M.J., Johnson, J.A., Klaus, T.C., Machalek, P., Moorhead, A.V., Morehead, R.C., Ragozzine, D., Tenenbaum, P., Twicken, J.D., Quinn, S.N., Isaacson, H., Shporer, A., Lucas, P.W., Walkowicz, L.M., Welsh, W.F., Boss, A., Devore, E., Gould, A., Smith, J.C., Morris, R.L., Prsa, A., Morton, T.D.: Planet Occurrence within 0.25 AU of Solar-type Stars from Kepler. ArXiv e-prints (2011)
31. Huitson, C.M., Sing, D.K., Vidal-Madjar, A., Ballester, G.E., Lecavelier des Etangs, A., Désert, J.M., Pont, F.: Temperature-pressure profile of the hot Jupiter HD 189733b from HST sodium observations: detection of upper atmospheric heating. ArXiv e-prints (2012)
32. Iro N., Deming, L.D.: A time-dependent radiative model for the atmosphere of the eccentric exoplanets. Astrophys. J. **712**, 218–225 (2010)
33. Iro, N., Bézard, B., Guillot, T.: A time-dependent radiative model of HD 209458b. Astron. Astrophys. **436**, 719–727 (2005)
34. Isaksen, I.S.A., Midtbo, K.H., Sunde, J., Crutzen, P.J.: A simplified method to include molecular scattering and reflection in calculations of photon fluxes and photodissociation rates. Geophys. Nor. **31**, 11–26 (1977)
35. Konnov, A.A.: Development and validation of a detailed reaction mechanism for the combustion of small hydrocarbons. In: 28th Symposium (International) on Combustion Abstract Symposium Paper, Edinburgh, p. 317 (2000)
36. Konnov, A.A.: Implementation of the ncn pathway of prompt-No formation in the detailed reaction mechanism. Combust. Flame **156**(11), 2093–2105 (2009)
37. Konnov, A.A., De Ruyck, J.: Upper limit rate constants for the reactions of NH and $NH_2$ radicals with $N_2O$ derived from the kinetic modeling of hydrogen oxidation by nitrous oxide. In: Mediterranean Combustion Symposium, Antalya, pp. 679–690 (1999a)
38. Konnov, A.A., De Ruyck, J.: Kinetic modeling of nitrogen oxides decomposition at flame temperatures. Combust. Sci. Technol. **149**(1–6), 53–78 (1999b)
39. Konnov, A.A., and De Ruyck, J.: Temperature dependent rate constant for the reaction NNH + O = NH + NO. 16th International Symposium on Gas Kinetics, Cambridge, Abstr. Symp. Pap. PC10 (2000a)
40. Konnov, A.A., De Ruyck, J.: Kinetic modeling of the thermal decomposition of ammonia. Combust. Sci. Technol. **152**(1), 23–37 (2000b)
41. Konnov, A.A., and De Ruyck, J.: Temperature-dependent rate constant for the reaction NNH + O − > NH + NO. Combust. Flame **125**, 1258–1264 (2001a).
42. Konnov, A.A., De Ruyck, J.: Kinetic modeling of the decomposition and flames of hydrazine. Combust. Flame **124**(1–2), 106–126 (2001b)

43. Lamoureux, N., Desgroux, P., El Bakali, A., Pauwels, J.: Experimental and numerical study of the role of ncn in prompt-no formation in low-pressure $CH_4$-$O_2$-$N_2$ and $C_2H_2$-$O_2$-$N_2$ flames. Combust. Flame **157**(10), 1929–1941 (2010)
44. Liang, M., Parkinson, C., Lee, A., Yung, Y., Seager, S.: Source of atomic hydrogen in the atmosphere of HD 209458b. Astrophys. J. Lett. **596**, L247 (2003)
45. Liang, M., Seager, S., Parkinson, C., Lee, A., Yung, Y.: On the insignificance of photochemical hydrocarbon aerosols in the atmospheres of close-in extrasolar giant planets. Astrophys. J. Lett. **605**, L61 (2004)
46. Line, M., Liang, M., Yung, Y.: High-temperature photochemistry in the atmosphere of HD 189733b. Astrophys. J. **717**, 496 (2010)
47. Madhusudhan, N., Seager, S.: A temperature and abundance retrieval method for exoplanet atmospheres. Astrophys. J. **707**, 24 (2009)
48. Madhusudhan, N., Mousis, O., Johnson, T., Lunine, J.: Carbon-rich giant planets: atmospheric chemistry, thermal inversions, spectra, and formation conditions. Astrophys. J. **743**, 191 (2011)
49. Manion, J. A., Huie, R. E., Levin, R. D., Burgess D. R., Jr., Orkin, V. L., Tsang, W., McGivern, W. S., Hudgens, J. W., Knyazev, V. D., Atkinson, D. B., Chai, E., Tereza, A. M., Lin, C.-Y., Allison, T. C., Mallard, W. G., Westley, F., Herron, J. T., Hampson, R. F., and Frizzell, D. H.: NIST Chemical Kinetics Database, NIST Standard Reference Database, National Institute of Standards and Technology, Gaithersburg, Maryland, **17**, 20899–8320 (2008). http://kinetics.nist.gov/
50. Moses, J., Visscher, C., Fortney, J., Showman, A., Lewis, N., Griffith, C., Klippenstein, S., Shabram, M., Friedson, A., Marley, M., et al.: Disequilibrium carbon, oxygen, and nitrogen chemistry in the atmospheres of HD 189733b and hd 209458b. Astrophys. J. **737**, 15 (2011)
51. Okabe, H.: Photochemistry of Small Molecules. Wiley, New York (1978)
52. Richardson, L., Deming, D., Horning, K., Seager, S., Harrington, J.: A spectrum of an extrasolar planet. Nature **445**(7130), 892–895 (2007)
53. Rothman, L.S., Gordon, I.E., Barbe, A., Benner, D.C., Bernath, P.F., Birk, M., Boudon, V., Brown, L.R., Campargue, A., Champion, J.P., Chance, K., Coudert, L.H., Dana, V., Devi, V.M., Fally, S., Flaud, J.M., Gamache, R.R., Goldman, A., Jacquemart, D., Kleiner, I., Lacome, N., Lafferty, W.J., Mandin, J.Y., Massie, S.T., Mikhailenko, S.N., Miller, C.E., Moazzen-Ahmadi, N., Naumenko, O.V., Nikitin, A.V., Orphal, J., Perevalov, V.I., Perrin, A., Predoi-Cross, A., Rinsland, C.P., Rotger, M., Šimečková, M., Smith, M.A.H., Sung, K., Tashkun, S.A., Tennyson, J., Toth, R.A., Vandaele, A.C., Vander Auwera, J.: The HITRAN 2008 molecular spectroscopic database. J. Quant. Spectrosc. Radiat. Transf. **110**, 533–572 (2009)
54. Sander, S. P., Abbatt, J., Barker, J. R., Burkholder, J. B., Friedl, R. R., Golden, D. M., Huie, R. E., Kolb, C. E., Kurylo, M. J., Moortgat, G. K., Orkin, V. L., Wine, P. H.: Chemical Kinetics and Photochemical Data for Use in Atmospheric Studies, Evaluation. JPL Publication, Jet Propulsion Laboratory, Pasadena, **17**, 10–6 (2011)
55. Sato, K., Misawa, K., Kobayashi, Y., Matsui, M., Tsunashima, S., Kurosaki, Y., Takayanagi, T.: Measurements of thermal rate constants for the reactions of $N(^2D, ^2P)$ with $C_2H_4$ and $C_2D_4$ between 225 and 292. J. Phys. Chem. A **103**(43), 8650–8656 (1999)
56. Selsis, F., Despois, D., Parisot, J.: Signature of life on exoplanets: can Darwin produce false positive detections? Astron. Astrophys. **388**(3), 985–1003 (2002)
57. Showman, A., Fortney, J., Lian, Y., Marley, M., Freedman, R., Knutson, H., Charbonneau, D.: Atmospheric circulation of hot Jupiters: coupled radiative-dynamical general circulation model simulations of HD 189733b and 209458b. Astrophys. J. **699**, 564 (2009)
58. Sing, D., Vidal-Madjar, A., Désert, J., Etangs, A., Ballester, G.: Hubble space telescope STIS optical transit transmission spectra of the hot Jupiter HD 209458b. Astrophys. J. **686**, 658 (2008)
59. Smith, G., Golden, D., Frenklach, M., Moriarty, N., Eiteneer, B., Goldenberg, M., Bowman, C., Hanson, R., Song, S., Gardiner W. Jr., Lissianski, V.V., Qin, Z.: Gri-mech 3.0. http://www.me.berkeley.edu/gri_mech (1999)

60. Southworth, J.: Homogeneous studies of transiting extrasolar planets–i. Light-curve analyses. Mon. Not. R. Astron. Soc. **386**(3), 1644–1666 (2008)
61. Southworth, J.: Homogeneous studies of transiting extrasolar planets–iii. Additional planets and stellar models. Mon. Not. R. Astron. Soc. **408**(3), 1689–1713 (2010)
62. Swain, M., Bouwman, J., Akeson, R., Lawler, S., Beichman, C.: The mid-infrared spectrum of the transiting exoplanet HD 209458b. Astrophys. J. **674**, 482 (2008a)
63. Swain, M., Vasisht, G., Tinetti, G.: The presence of methane in the atmosphere of an extrasolar planet. Nature **452**(7185), 329–331 (2008b)
64. Swain, M., Tinetti, G., Vasisht, G., Deroo, P., Griffith, C., Bouwman, J., Chen, P., Yung, Y., Burrows, A., Brown, L., et al.: Water, methane, and carbon dioxide present in the dayside spectrum of the exoplanet HD 209458b. Astrophys. J. **704**, 1616 (2009a)
65. Swain, M., Vasisht, G., Tinetti, G., Bouwman, J., Chen, P., Yung, Y., Deming, D., Deroo, P.: Molecular signatures in the near-infrared dayside spectrum of hd 189733b. Astrophys. J. Lett. **690**, L114 (2009b)
66. Tinetti, G., Vidal-Madjar, A., Liang, M., Beaulieu, J., Yung, Y., Carey, S., Barber, R., Tennyson, J., Ribas, I., Allard, N., et al.: Water vapour in the atmosphere of a transiting extrasolar planet. Nature **448**(7150), 169–171 (2007)
67. Tsang W., Hampson, R.: Chemical kinetic data base for combustion chemistry. part i. Methane and related compounds. J. Phys. Chem. Ref. Data **15**(3), 1087 (1986)
68. Turbiez, A., Pauwels, J., Desgroux, P., Sochet, L., Poitou, S., Perrin, M.: Gdf-kin® a detailed kinetic mechanism for natural gas combustion modeling. In: 27th Symposium (International) on Combustion, Boulder (1998)
69. Umemoto, H., Nakae, T., Hashimoto, H., Kongo, K.: Reactions of N($^2$D) with methane and deuterated methanes. J. Chem. Phys. **109**(14), 5844–5848 (1998)
70. Venot, O., Fray, N., Bénilan, Y., Gazeau, M.-C., Hébrard, E., Dobrijevic, M., Selsis, F.: High-temperature measurements of VUV-absorption cross sections of $CO_2$ and application to exoplanets. Astron. Astrophys. **551**, A131 (2013)
71. Venot, O., Hébrard, E., Agúndez, M., Dobrijevic, M., Selsis, F., Hersant, F., Iro, N., Bounaceur, R.: A chemical model for the atmosphere of hot Jupiters. Astron. Astrophys. **546**, A43 (2012)
72. Wakelam, V., Herbst, E., Loison, J.C., Smith, W., Chandrasekaran, V., Pavone, B., Adams, N., Bacchus-Montabonel, M.C., Bergeat, A., Beroff, K., Bierbaum, V.M., Chabot, M., Dalgarno, A., van Dishoeck, E.F., Faure, A., Geppert, W.D., Gerlich, D., Galli, D., Hebrard, E., Hersant, F., Hickson, K.M., Honvault, P., Klippenstein, S.J., Le Picard, S., Nyman, G., Pernot, P., Schlemmer, S., Selsis, F., Sims, I.R., Talbi, D., Tennyson, J., Troe, J., Wester, R., Wiesenfeld, L.: A kinetic database for astrochemistry (kida). Astrophys. J. Suppl. Ser. **199**, 21 (2012)
73. Zahnle, K., Marley, M., Freedman, R., Lodders, K., Fortney, J.: Atmospheric sulfur photochemistry on hot Jupiters. Astrophys. J. Lett. **701**, L20 (2009)

# Chapter 7
# Implication of Impacts in the Young Earth Sun Paradox and the Evolution of Earth's Atmosphere

**Josep M. Trigo-Rodríguez and F. Javier Martín-Torres**

**Abstract** The role of impacts in the evolution of the Earth's atmosphere is discussed. Impacts could have been significant heating sources during the Hadean eon, and likely promoted thermal escape of atmospheric species to differing degrees. Large impacts, that are regularly delivering enough energy to Earth's atmosphere to cause significant erosion, can also bring metal particles with catalytic properties in the right conditions. That impact-induced chemistry is poorly known, but recent laboratory studies emphasize its key role in the production of greenhouse gases and organic compounds. A better understanding of the phases associated with re-entry and cooling phases of a bolide plume evolving in the aftermatch of a huge impact is needed. In the right range of temperature and pressure conditions, impacts can produce ammonia, methane and other organic compounds through the Haber and Fischer-Tropsch catalytic processes, but mixing and decay of those compounds in different models of the atmosphere needs to be explored. Hadean-atmosphere models proposed so far are reviewed also discussing the scarcely available geological evidence. Simple thermodynamic equilibrium calculations for probable Hadean atmosphere conditions are presented. Several scenarios of reducing ($H_2$-rich) and oxidizing ($CO_2$-rich) atmospheres are considered to study the stability of $CH_4$ and $NH_3$ and the formation of organic compounds. Searching for chemical signatures in similar evolutionary stages of recently formed Earth-like exoplanets could be an interesting future field of research. New evidence in this regard can contribute to a better understanding of the transition point to a habitable world.

J.M. Trigo-Rodríguez (✉)
Facultat de Ciències, Institute of Space Sciences (CSIC-IEEC), Campus UAB, Torre C5-pares, 08193 Bellaterra, Barcelona, Spain
e-mail: trigo@ieec.uab.es

F.J. Martín-Torres
Centro de Astrobiología (INTA-CSIC), Ctra. Ajalvir Km.4, Torrejón de Ardoz, 28850, Madrid, Spain
e-mail: javiermt@cab.inta-csic.es

J.M. Trigo-Rodriguez et al. (eds.), *The Early Evolution of the Atmospheres of Terrestrial Planets*, Astrophysics and Space Science Proceedings 35,
DOI 10.1007/978-1-4614-5191-4_7, 

## Introduction

Oparin (1924) was one of the first authors to speculate about the composition of the primeval atmosphere and its implications on the origin of life. He proposed a strongly reducing atmosphere rich in hydrogen ($H_2$), ammonia ($NH_3$), methane ($CH_4$) and other hydrocarbons, and suggested that the reactions between those compounds led to the production of organic compounds with increasing complexity, which then rained into the primordial ocean. A few years later Haldane (1928) proposed that carbon dioxide ($CO_2$) was the dominant carbon source in the early atmosphere, on the basis that volcanic degassing formed the primeval atmosphere. Despite being speculative, Oparin's scenario was innovative for his time because, not only did it propose an early atmosphere based on quite reasonable assumptions, but also provided a direct link between its evolution and the origin of life. Nowadays, many authors share this view and make the study of the origin of the atmosphere an interdisciplinary and exciting subject.

The first author to give a theoretical foundation to Oparin's ideas was Urey (1952) who developed the first relatively quantitative model of the primeval atmosphere. The successful synthesis of amino acids in laboratory by Miller (1953) and later by Miller and Urey (1959) gave additional value to Oparin and Urey's hypothesis of the reducing conditions of the early atmosphere. Practically at the same time Rubey (1951, 1955) challenged this hypothesis proposing instead an oxidizing atmospheric composition. According to this author the first atmosphere came from degassing of the Earth's interior and the volcanic gases would have released oxidized species, but quite different to those observed nowadays. Rubey proposed that the major hydrogen species was $H_2O$ rather than $H_2$, $CO_2$ rather than CO and $N_2$ rather than $NH_3$. In this scenario the bulk of the early atmosphere would have been in a neutral oxidation state due to the presence of small amounts of reduced compounds (Table 7.1).

Although both hypotheses are difficult to reconcile, Holland (1962) tried it by proposing that the primitive atmosphere passed through both stages: in a first period the Earth would have a reducing atmosphere because the volcanic gases released prior to core formation would have been rich in metallic iron; then progressively it evolved to a more neutral atmosphere but still anoxic. The absence of oxygen in the early atmosphere is usually granted (cf. Holland 1984).

Now we know that all these first models about the origin and evolution of the early atmosphere are unrealistic, because we have additional information about some processes that happened in on the surface of the primeval Earth and,

**Table 7.1** Main chemical species depending on the oxidation state of an early-Earth atmosphere

| Atmosphere | H species | C species | N species | O species |
|---|---|---|---|---|
| Reducing | $H_2$ | $CH_4$ | $NH_3$ | CO |
| Oxidized | $H_2O$ | $CO_2/CO$ | $N_2$ | $CO_2$ |

moreover, we know that the Earth formed in a shorter accretion process than proposed in the past (Safronov 1969). Taking into account a period for Earth's accretion close to the actual calculations (10–100 Ma, with a preferred value of 50 Ma), the planet's interior probably was heated to several thousand Kelvin by gravitational energy released during impacts with planetesimals (Kaula 1979). In consequence core formation occurred probably at a faster rate than assumed in preliminary models, and differentiation was essentially complete in a short time scale (Stevenson 1983; Lammer et al. 2011). It is usually considered that the earliest atmosphere of the Earth was produced by primitive mantle outgassing, but it seems obvious that stochastic massive impacts could have also been an important factor in its composition. Impacts probably delivered organic compounds promoting catalytic reactions as consequence of the disruption in the atmosphere of metal-rich chondritic bodies. Endogenous and exogenous sources need to be evaluated and balanced in accordance with the geological and lunar evidence, but also laboratory experiments could be crucial for explaining the evolution of the terrestrial atmosphere in that period. This is a complex puzzle because such an atmosphere would have contained $H_2$, $H_2O$, CO, $CO_2$, $CH_4$, and $NH_3$, but also because of the scarce geological evidence available for that period.

A very dense primitive atmosphere, containing $CO_2$ and $H_2O$ may have efficiently trapped the heat from the Sun (weaker at visible and longer wavelengths) and also participated in retaining the primordial accretionary energy. Consequently, it has been envisioned that the surface temperature of the proto-Earth rose to above 1,500 K creating a "magma ocean" on the surface (Matsui and Abe 1986; Zahnle et al. 1988). These authors suggested that such conditions prevailed because a massive atmosphere prevented the rapid freezing of the magma ocean during the first tens of Ma in the Earth surface, coinciding with the period of high accretion. A stable magma ocean requires that the volatile outgassing together with the exogenous delivery be of at least of the same order as the atmospheric mass loss by Jeans escape. Kaula (1979) obtained the Earth's thermal evolution taking into account the impactor's frequency. He found that the surface's temperature probably stayed between 2,000 and 3,500 K during the Earth's accretion period (about 50 Ma). The upper mantle was probably more reduced than today, although progressively became more oxidized as a result of the release of reduced volcanic gases and the subduction of hydrated, oxidized seafloor (Kasting et al. 1993).

It has been shown that the cataclysmic impact forming the Moon probably did not completely erode the atmosphere of the Earth (Genda and Abe 2003, 2005; Newman et al. 1999). This inflexion point was followed by other less massive impacts bringing volatile-rich materials that could have released reduced gases when subjected to subduction. Bukvic (1979) and more recently Schaefer and Fegley (2007) have modeled the equilibrium gas chemistry of an outgassed chondritic-vaporized reducing atmosphere, but several processes that can take place in the aftermath of the impacts are scarcely known. Other authors have an opposite view where the outgassed vapors (Delano 2001), or the degassed vapors during impacts (Ahrens et al. 1989) produced oxidizing products ($H_2O + CO_2$). Both scenarios are explored here, and also the influence of an enhanced shortwave solar activity during the early Hadean.

## Composition of Impactors and Their Impact in the Chemistry

In this section we analyze the role of impacts inducing significant compositional changes in the terrestrial atmosphere. We will particularly focus on the key role of carbon- and water-rich bodies that, due to their relative low bulk density, tensile strength, and volatile abundance experience catastrophic disruption in the upper atmosphere. Typically, about 60% of the large fireballs recorded and measured by the Prairie Network experience one or several fragmentations along their path, and in about 20% of the cases the bolide practically ends up in a sudden overwhelming fragmentation (Ceplecha et al. 2003). In simple terms, it happens because when the meteoroid penetrates the atmosphere it feels an increasing dynamic pressure ($p = \rho \cdot v^2$). When the loading pressure surpasses the material strength required for fragmentation the body breaks apart and, as consequence of the flight and the shock wave shaking, disruption is imminent. The properties of the above-mentioned large meteoroids are probably not identical to volatile-rich asteroids or comets because, among other things, meter-sized meteoroids arriving at our planet are biased towards high-strength materials that have survived an excavating impact in their parent bodies and long-exposures to interplanetary space. It is well known, for example that Near Earth Objects (NEO) are delivered to near-Earth space from the Main Belt in typical periods of millions of years. Blum et al. 2006) reasoned from accretionary and evolutionary arguments that hundred- to km-sized primitive asteroids and comets should exhibit a fragile nature: extremely low bulk density, and high porosity.

Water-rich asteroids and comets impacting the atmosphere of Earth are directly delivering volatile species as consequence of the disruption behavior, but the amounts of surviving materials are scarce if the impact geometry and velocity are not favorable for a moderate deceleration and settling of the materials in the atmosphere (Blanck et al. 2001). On the basis of fireball spectroscopy it is suspected that catastrophic disruptions can disperse dust far from the shock wave frontal region where bolide experiences higher temperatures (Borovicka 1993, 1994; Trigo-Rodríguez et al. 2003). Consequently, the peak temperature and the exposure to heat are both minimized and there is room for a percentage of the body to survive, at least, as small fragments that are slowly settling down towards the surface.

Other important aspect to consider is the thermal processing that affects the materials subjected to ablation in the fireball column. As a consequence of the heat associated with the collision with atmospheric gases, meteoric minerals are ablated, vaporized and dissociated. Elemental lines and molecular bands are remarkable features in bolide spectra (Fig. 7.1). It has been demonstrated that most of the fireball chemistry behind radiating light can be perfectly fit with a thermodynamic equilibrium model (Borovicka 2001; Trigo-Rodríguez et al. 2003). This behavior is probably a consequence of the quick mixing of air and meteoric plasma promoted by the supersonic movement, meteoroid spinning, and subsequent induced turbulence around the bolide. In this work we are assuming thermodynamic equilibrium to study some of the processes that could take place in bolide plumes.

It is important to remark, however, that the production of different gases can be avoided in environments with different chemistry and radiative flux. Results are then preliminary, with the main aim of exploring unknown aspects of the delivery of pristine materials to Earth's atmosphere.

The reentry and ablation of cometary dust was studied thanks to the accurate spectroscopic study of the impact plumes produced in Jupiter's atmosphere as a consequence of the impact of comet Shoemaker-Levy 9 in July 1994 (Fitzsimmons et al. 1996). Interestingly these authors found that most of the light emission came from silicate grains ablated in the different phases. In the case of a chondritic (asteroidal) body with larger metal abundance at least two key processes are envisioned to participate in greenhouse gas production in the aftermath of the bolide interaction:

1. A rapid conversion of $N_2$ to $NH_3$ is feasible in the aftermatch of impacts, particularly during the final stage in which the bolide plume stops its adiabatic expansion, and falls back to the surface. The catalysis producing abundant ammonia, known as the Haber process, requires the surface of metal grains acting as catalyzers.
2. At the same time, metal grains can catalyze a plethora of different organic compounds when abundant CO and $H_2$ are available via Fischer-Tropsch catalysis (Sekine et al. 2003, 2006). This has been found to be a key process occurring in impact plumes produced by comets and carbonaceous asteroids atmospheric disruptions.

*Survival of Greenhouse Gases: $CH_4$ and $NH_3$*

The tendency of $NH_3$ and $CH_4$ to decompose has been the main criticism against the long-term stability of these compounds and the possibility of having a strongly reduced Hadean environment. Sagan and Chyba (1997) attempted to solve the faint young Sun dilemma by proposing the formation of particles of organic polymers (tholins) by the action of UV light in an atmosphere with $CO_2/CH_4 < 1$. Suspended in the stratosphere, those polymers would protect the lower atmosphere from UV photolysis, acting as a screen capable of avoiding the photodecomposition of these greenhouse gases. Protected by tholins from ultraviolet radiation, they would have enhanced the early greenhouse in an amount enough to keep warm temperatures despite the weakness of the young Sun.

The proportions of C and O in the atmosphere are also important. This is because a C/O $> 1$ ratio promotes polymerization of $CH_4$ whereas C/O $< 1$ led primarily to oxidation (Sagan and Chyba 1997). In an anoxic atmosphere the primary reservoirs of oxygen are $CO_2$ and $H_2O$. Probably $CO_2$ outgassing was important in the Hadean. However, Kasting (1997) and Sleep and Zahnle (2001) proposed that the rapid weathering of the ejecta from frequent large impacts could have provided a sink for atmospheric $CO_2$. According to their model, methane and ammonia participated in a kind of feedback cycle, working together in two main ways: (i) methane's presence produced an organic haze due its capacity to polymerize and (ii) this haze protected ammonia from UV photodissociation. This cycle could yield longer lifetimes for these gases, in turn allowing the greenhouse effect in the primeval atmosphere

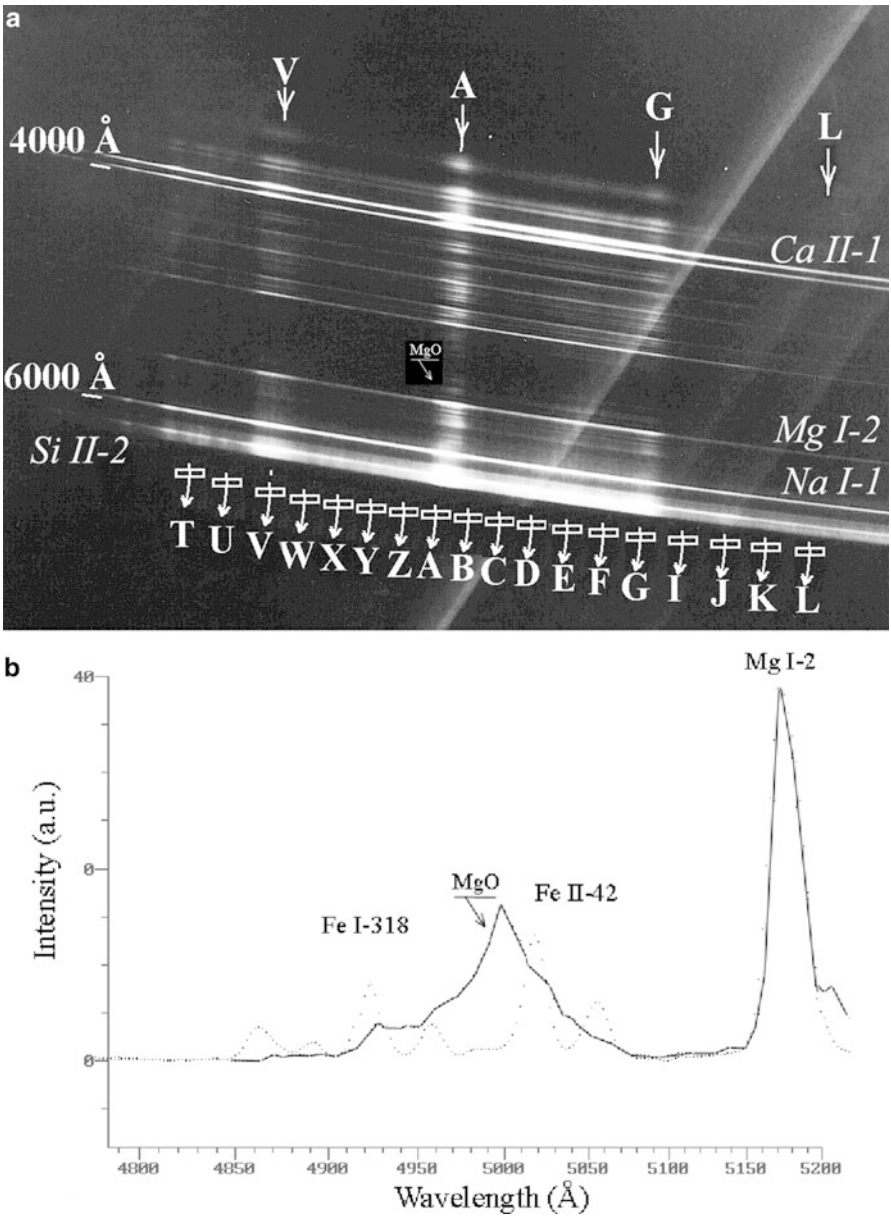


**Fig. 7.1** A photographic spectrum of a Perseid fireball associated with comet 109P/Swift-Tuttle recorded in photographic plate from Ondrejov Observatory. The meteoroid producing this bolide was about 30 g in mass, and appeared on Aug. 11, 1969 at 21h06m UTC. (**a**) Detailed image of the ending part of the fireball luminous path showing the scanned slots with a microdensitometer as discussed in Trigo-Rodríguez (2002) and Trigo-Rodríguez et al. (2003). The main emission lines are shown: the Ca II-1 doublet, the Mg I-2, the Na I-1, and finally the Si II-2 line associated with the high temperature component. (**b**) A small part of the *center* image shows a MgO band that cannot be fitted to elemental emission lines. The scanned signal in this graph appears discontinuous, while a *darker, continuous line* shows the modeled spectrum (Original image courtesy of Jiri Borovicka (Ondrejov Observatory, Czech Republic))

during longer time scales than when each is considered separately. Such a high amounts of these greenhouse gases are supported by evidence for a $CH_4$ mixing ratio of $10^{-4}$ (100 ppmv) in paleosol data 2.8 Ga old (see e.g. Pavlov et al. 2000). In fact, Catling, Zahnle and McKay (2001) suggested that the concentration of methane in the Archean atmosphere was even larger than this given by Pavlov et al. (2000). The main pros and cons of these arguments are given on Table 7.2.

## Discussion and Conclusions

Today most researchers seem to prefer a mildly reducing atmosphere based on mantle degassing and bolide impact but there is still controversy. The different components considered in the literature are compiled in Table 7.2. Stellar evolution models show that the solar luminosity has increased through time, with the solar constant (S) around 30% smaller 4 Ga ago than nowadays. At the same time, the integrated high-energy emission was about one order of magnitude higher than in the present about 3.9 Gyrs ago (Ribas et al. 2005). All these changes probably had important consequences for the Earth's atmosphere, like the non-thermal escape processes produced by magnetic-induced solar forcing (Lundin et al. 2007).

*Was the Hadean atmosphere anoxic?* Several authors have widely presented the rise of oxygen in the Earth's atmosphere as an evolutionary process. Walker et al. (1983) and Kasting (1987) developed simple models involving the atmosphere-ocean system. They proposed the evolution of oxygen in three main stages. During the first stage (stage I), the entire atmosphere/ocean system was essentially devoid of free oxygen under reducing conditions. The main basis of this argument is that the supply rate of reduced substances as $H_2$, CO and $H_2S$ from volcanoes and $Fe^{2+}$ from seawater/basalt interaction exceeded the production of $O_2$ from photolysis followed by the escape of hydrogen to space. A few authors do not share that view (e.g Towe 1981) and support the presence of $O_2$ in the primeval environment. According to Kasting et al. (1992) at some point during the Archean or the Early Proterozoic, the supply of reduced substances decreased or the oxygen rate increased. As volcanic activity and impact plumes were the principal sources of reducing gases, the transition to an $O_2$-rich atmosphere probably happened when the LHB ceased at the end of the Hadean. The process was probably slow, induced by stromatolitic bacteria near the surface where local oxic conditions can be reached. The deep ocean remained anoxic, carrying ppm abundances of ferrous iron in solution. Such conditions are necessary to create banded iron sediments formed until the mid-Proterozoic. The presence of an oxidized surface and a reduced deep ocean identifies the Stage II of Walter-Kasting model for the early Proterozoic (Kasting and Chang 1992) under increasing $O_2$ abundance originated from photosynthetic organisms. Finally in Stage III is characterized by extended oxic conditions.

The geological evidence for an anoxic Archean (and presumably late Hadean) environment has been recently obtained. Farquhar et al. (2001) presented recently the evidence of Mass Independent Fractionation (MIF) of sulfur isotopes in sediment deposited prior to 2.3 Ga. By MIF we understand that sulfur isotopes do

**Table 7.2** Main pros and cons for the presence of two greenhouse gases, $NH_3$ and $CH_4$ in the primeval atmosphere

| | Pros | Cons |
|---|---|---|
| $NH_3$ | 1. A small quantity $[NH_3] \sim 10^{-5}$ in a 1 bar atmosphere can increase the global temperature enough to avoid a glacial era | 1. Soluble in water and subject to rapid rainout |
| | 2. Can come from different endogenous and exogenous sources | 2. The proposed amount of $NH_3$ can be photodissociated by UV light to produce $N_2$ in a few decades |
| | 3. Produced by cometary impacts (Lellouch 1996) | 3. $NH_3$ can be destroyed by reaction with OH to produce $N_2$ |
| | 4. If $CH_4$ was present forming an organic haze, the $NH_3$ could substantially shield from photolysis | 4. $NH_3$ constitutes less than 1% of the volatile mass of comets |
| $CH_4$ | 1. Photodissociation is only produced by $\lambda < 1,450$ Å photons | |
| | 2. It's possible to polymerize the methane with UV photons (oxidation is replaced by polymerization happens when C/O ratio passes unity) | 1. The $CH_4$ lifetime (under present conditions) is of the order of centuries |
| | 3. Endogenous source: some $CH_4$ is produced by serpentinization in mid ocean ridge basalts | 2. No probable exogenous source is known; $CH_4$ constitutes less than 1% of the mass of comets |
| | 4. Possible production of $CH_4$ during cometary impacts (Zahnle 1996; Lellouch 1996) | |
| | 5. In the low $O_2$ Archean atmosphere $CH_4$ is not oxidized | |

not obey the standard mass-dependent relationship of S isotopes in aqueous solution. The penetration of UV radiation in the 190–220 nm spectral region can produce MIF as was demonstrated by Farquhar et al. (2001). In order for this radiation to penetrate deep into the atmosphere the columns of $O_2$ and $O_3$ must have been

much lower than at present. In this way, under reduced atmospheric conditions S can be removed from the terrestrial atmosphere in a variety of different oxidation states. Additional evidence for an anoxic Archean atmosphere is the presence of sedimentary deposits (red beds) more than 2.45 Ga ago containing uraninite, siderite and pyrite, the reduced shallow-water facies of Fe formations, the presence of highly carbonaceous shales not enriched in redox-sensitive elements and, in general, the general observation than the older palaeosols are not oxidized (Pavlov and Kasting 2002).

*Where is the outgassed $CO_2$?* The total amount of carbon dioxide tied up in carbonate rocks today is some $3 \times 10^{20}$ kg, the equivalent of about 60 bar if introduced in the atmosphere. Ronov and Yaroshevskiy (1967) initially used this evidence for suggesting a massive $CO_2$ early atmosphere, and the idea was also adopted by other authors (Holland 1978; Kasting 1983). They proposed that this carbon, along with other volatile elements reached the Earth during planetesimals' accretion, with carbonaceous chondrites and comets being the main sources of this carbon (see also Chyba et al. 1990; Chyba and Sagan 1992). This simple view of an extraordinary amount of carbon in the primeval atmosphere is unrealistic based in two arguments. First, the carbon-rich bodies reached the Earth separated by large time intervals, therefore gradually incorporating this carbon directly into the Earth crust, where it was retained (Oró 1961; Sagan and Khare 1971). Second, the presence of a global water ocean, supported by the isotopic studies of a 4.4 Ga zircon (Valley et al. 2001), makes it possible that the injection of large quantities of $CO_2$ into the atmosphere during impacts or degassing was quickly removed by the ocean feedback. Probably the Earth developed a mechanism to remove efficiently the excess of carbon in its atmosphere as evidence that nowadays the oceans are able to absorb $6 \times 10^{15}$, g C/year as estimated Keeling (1983, 1993). Nowadays it depends on biological sequestering of $CO_2$ as carbonates, but if one inorganic sink existed in the past producing a similar rate, the oceans would be capable to remove this carbon from the atmosphere in only 50 Ma. This is just an upper limit because seems reasonable that not all this carbon was brought to the atmosphere at the same time and, moreover, the presumed overabundance of water in the primeval environment could participate accelerating the absorption rate of $CO_2$ by the ocean.

The absence of glacial deposits prior to 3 Ga was the main reason argued by Owen et al. (1978) and Kasting (1993) to support a dense primeval $CO_2$ atmosphere. This greenhouse gas had increased the temperature of the Earth to keep water in liquid state. Sagan and Chyba (1997) cast doubt on these arguments by suggesting the presence of other greenhouse gases capable to solve the "early faint-Sun dilemma" without the necessity to invoke a massive $CO_2$ atmosphere. Probably the carbonate-silicate geochemical cycle (Schidlowski et al. 1983) had an inorganic counterpoint in the early Earth by over-saturation of the oceans because silicate minerals were also common from that epoch. Currently the task to precipitate $CaCO_3$ is being mainly performed by living organisms, producing the isotopic fractionation of carbon. Support for this process is found in the data on C-isotopic compositions; transformation of inorganic carbon into living matter entails a marked bias towards the light isotope ($^{12}C$) with the heavy one ($^{13}C$)

retained in the inorganic reservoir (Schidlowski 1987, 1988). The first evidence for organic production of carbonate rocks comes from mat-forming bacteria, producing sedimentary rocks and stromatolites around 3.8 Ga ago (Maher and Stevenson 1988; Kasting and Chang 1992). Moreover sedimentary rocks rich in oxidized iron containing smaller quantities of carbon also formed in abundance in the Archean when the atmosphere was anaerobic (Walker 1987). Nowadays principally living organisms, particularly by calcareous plankton, performs this task.

Biogenic sinks of $CO_2$ were probably not present during the Hadean, but water was abundant as inferred from zircon data (Peck et al. 2001). Sleep and Zahnle (2001) proposed as a solution that the dynamic mantle buffer dominated over the crustal one on the early Earth. As a consequence, the mantle cycle would maintain low atmospheric and oceanic $CO_2$ levels, capable to produce a cold climate unless another greenhouse gas was important. The Hadean was also marked by collisions that participate in the sink of $CO_2$. For example, Sleep and Zahnle (2001) proposed that the huge production of basaltic glass ejecta in these impacts was weathered in a similar way as modern mafic and ultramafic volcanic glasses producing *palagonite*. After it, the hydration of such minerals progresses very quickly, being a direct sink for $CO_2$. The efficiency of this reaction depends of the access of reactable seawater or rainwater to the ejecta grains. This process is even plausible at temperatures close to the freezing point of water although are expected to be higher at temperate conditions (Brady and Gislason 1997).

To summarize, we think that an open view to explore different plausible scenarios for the Hadean terrestrial environment is needed. Physico-chemical processes associated with impacts must be taken into account in future models. Consequently, we wish to encourage new theoretical and laboratory approaches to get a more complete picture of the first stages in atmospheric evolution, also considering the role of impacts in an environment marked by a very different solar irradiance flux than nowadays (Ribas et al. 2005).

**Acknowledgements** This work was financially supported by CSIC grant #201050I043 and AYA2011-26522 and AYA2011-25720 grants.

## References

Ahrens, T., O'Keefe, J.D., Lange, M.A.: Formation of atmospheres during accretion of the terrestrial planets. In: Origin and Evolution of Planetary and Satellite Atmospheres, pp. 328–385. University of Arizona Press, Tucson (1989)

Borovicka, J.: A fireball spectrum analysis. Astron. Astrophys. **279**, 627–645 (1993)

Borovicka, J.: Two components in meteor spectra. Planet. Space Sci. **42**, 145–150 (1994)

Borovicka, J. (1994b) "Line identifications in a fireball spectrum", Astronomy & Astrophysics Supl. Series 103, 83-96.

Brady, P.V., Gislason, S.R.: Seafloor weathering controls on atmospheric CO2 and global climate. Geochim. Cosmochim. Acta **61**, 965–973 (1997)

Bukvic, D.S.: Outgassing of chondritic planets, M.S: thesis, MIT (1979)

Catling, D.C., Zahnle, K.J., McKay, C.P.: Biogenic methane, hydrogen escape, and the irreversible oxidation of the early Earth. Science **293**, 839–843 (2001)
Ceplecha Z., Borovika, Ji; Elford, W.G., Revelle, D.O.., Hawkes, R.L., Poruban, V., imek, M. (1998) Meteor Phenomena and Bodies, Space Science Reviews, **84**, 3/4, 327–471.
Chyba, C., Sagan, C.: Endogenous production, exogenous delivery and impact-shock synthesis of organic molecules: an inventory for the origins of life. Nature **355**, 125–132 (1992)
Chyba, C., Thomas, P.J., Brookshaw, L., Sagan, C.: Cometary delivery of organic molecules to the early Earth. Science **249**, 366–373 (1990)
Delano, J.W.: Redox history of the Earth's interior since ∼3900 Ma: implications for prebiotic molecules. Orig. Life **31**, 311–341 (2001)
Farquhar, J.; Savarino, J., Airieau, S., Thiemens, M.H. (2001) "Observation of wavelength-sensitive mass-independent sulfur isotope effects during SO2 photolysis: Implications for the early atmosphere", Journal of Geophysical Research, **106** E12, 32829–32840
Farquhar, J., Wing, B.A.: Multiple sulfur isotopes and the evolution of the atmosphere. Earth Planet. Sci. Lett. **213**, 1–13 (2003)
Fitzsimmons, A., Andrews, P.J., et al.: Re-entry and ablation of cometary dust in the impact plumes of Shoemaker-Levy 9. Nature **379**, 801–804 (1996)
Genda, H, Abe, Y.: Survival of a proto-atmosphere through the stage of giant impacts: the mechanical aspects. Icarus **164**, 149–162 (2003)
Genda, H., Abe, Y.: Enhanced atmospheric loss on protoplanets at the giant impact phase in the presence of oceans. Nature **433**, 842–844 (2005)
Haldane, J.B.: The origin of life. Ration. Annu. **148**, 3–10 (1928)
Holland, H.D.: Model for the evolution of the Earth's atmosphere. In Petrologic Studies: A volume to honor A.F. Buddington, Geological Society of America, pp. 447–477 (1962)
Kasting J.F. (1984) "The Evolution of the Prebiotic Atmosphere", Origins of Life, **14** 1–4, 75–82
Kasting J.F., Pollack, J.B., Ackerman, T.P. (1984) "Response of Earth's atmosphere to increases in solar flux and implications for loss of water from Venus", Icarus 57, 335–355.
Kasting, J.F.: Earth's early atmosphere. Science **259**, 920–926 (1993)
Kasting, J.F.: Warming early Earth and Mars. Science **276**, 1213–1215 (1997)
Kasting, J.F.: Earth history: the rise of atmospheric oxygen. Science **293**, 819–820 (2001)
Kasting, J.F., Chang, S.: Formation of the Earth and the origin of life. In: Schopf, J.W., Klein, C. (eds.) The Proterozoic Biosphere: A Multidisciplinary Study, pp. 9–12. Cambridge University Press, Cambridge/New York (1992)
Kasting, J.F., Eggler, D.H., Raeburn, S.P.: Mantle redox evolution and the oxidation state of the Archean atmosphere. J. Geol. **101**, 245–258 (1993)
Kasting J.F. and Catling D. (2003) "Evolution of a habitable planet", Annu. Rev. Astron. Astrophys. 41, 429-463.
Kaula, W.M.: Thermal evolution of earth and moon growing by planetesimal impacts. J. Geophys. Res. **84**, 999–1008 (1979)
Keeling, C.D.: The global carbon cycle: what we know and could know from atmospheric, biospheric and oceanic observations. In: Proceedings Carbon Dioxide Research Conference: $CO_2$, Science and Consensus, Conf #820970. US Department of energy, Washington (1983)
Keeling, C.D.: Global observations of atmospheric $CO_2$. In: Heimann, M. (ed.) The Global Carbon cycle, pp. 1–29. Springer, New York (1993)
Lammer, H., Kislyakova, K.G., Odert, P., Leitzinger, M., Schwarz, R., Pilat-Lohinger, E., Kulikov, Y.N., Khodachencko, M.L., Güdel, M., Hanslmeier, A.: Pathways to Earth-like atmospheres. Orig. Life Evol. Biosph. **41**, 503–522 (2011)
Lellouch, E.: Chemistry induced by the impacts: observations. In: Noll, K.S., Weaver, H.A., Feldman, P.D. (eds.) The Collision of Comet Shoemaker-Levy 9 and Jupiter, pp. 213–242. Cambridge University Press, Cambridge/New York (1996)
Lundin, R., Lammer, H., Ribas, I.: Planetary magnetic fields and solar forcing: implications for atmospheric evolution. Space Sci. Rev. **129**, 245–278 (2007)
Maher, K.A., Stevenson, D.J.: Impact frustration of the origin of life. Nature **331**, 612–614 (1988)
Matsui, T., Abe, Y.: Evolution of an impact-induced atmosphere and magma ocean on the accreting Earth. Nature **319**, 303–305 (1986)

Miller, S.L.: A production of amino acids under possible primitive earth conditions. Science **117**, 528–529 (1953)
Miller, S.L., Urey, H.C.: Organic compound synthesis on the primitive Earth. Science **130**, 245–251 (1959)
Newman, W.I., Symbalisty, E.M.D., Ahrens, T.J., Jones, E.M.: Impact erosion of planetary atmospheres: some surprising results. Icarus **138**, 224–240 (1999)
Oparin A.: "The origin of life", Moscow Worker Publisher, Moscow, in Russian.
Oparin, A.I.: Origin of Life. Macmillan, New York (1938)
Oró, J.: Comets and the formation of biochemical compounds on the primitive Earth. Nature **190**, 389–390 (1961)
Pavlov, A.A., Kasting, J.F.: Mass independent fractionation of sulfur isotopes in archean sediments: strong evidence for an anoxic Archean atmosphere. Astrobiology **2**, 27–41 (2002)
Pavlov, A.A., Kasting, J.F., Brown, L.L., Rages, K.A., Freedman, R.: Greenhouse warming by $CH_4$ in the atmosphere of early Earth. J. Geophys. Res. **105**, 11981–11990 (2000)
Peck, W., et al.: O isotope ratios and rare earth elements in 3.3 to 4.4 Ga zircons. Geochem. et Cosm. Acta **65**(22), 4215–4229 (2001)
Pepin, R.O., Porcelli, D.: Origin of noble gases in the terrestrial planets. In: Noble Gases in Geochemistry and Cosmochemistry. Reviews in Mineralogy & Geochemistry, vol. 47. Mineralogical Society of America Washington, (2002)
Prather, M.J., Derwent, R., Ehhalt, D., Fraser, P., Sanhueza, E., Zhou, X.: Other trace gases and atmospheric chemistry. In: Houghton, J.T., Meira Filho, L.G., Bruce, J., Lee, H., Callender, B.A., Haites, E., Harris, N., Maskell, K. (eds.) Climate Change 1994, pp. 73–126. Cambridge University Press, Cambridge (1995)
Ribas, I., Guinan, E.F., Güdel, M., Audard, M.: Evolution of the solar activity over time and effects on planetary atmospheres. I. High-energy irradiances (1–1700 Å). Ap. J. **622**, 680–694 (2005)
Ronov, A.B., Yaroshevskiy, A.A.: The chemical nature of the earth's crust. Geokhimiya **11**, 1285–1309 (1967)
Rubey, W.W.: Geological history of seawater. An attempt to state the problem. Geol. Soc. Am. Bull. **62**, 1111–1148 (1951)
Rubey, W.W.: Development of the hydrosphere and atmosphere, with special reference to probable composition of the early atmosphere. In: Poldervaart, A. (ed.) Crust of the Earth, pp. 631–650. Geological Society of America, New York (1955)
Sagan, C., Chyba, C.: The early faint Sun Paradox. Science **276**, 1217–1221 (1997)
Sagan, C., Khare, B.N.: Experimental Jovian Photochemistry: initial results. Ap.J. **168**, 563 (1971)
Schaefer, L., Fegley, B. Jr.: Outgassing of ordinary chondritic material and some of its implications for the chemistry of asteroids, planets and satellites. Icarus **186**, 462–483 (2007)
Schidlowski, M.: Application of stable carbon isotopes to early biochemical evolution on earth. Annu. Rev. Earth Planet. Sci. **15**, 47–72 (1987)
Schidlowski, M.: A 3800-million year isotopic record of life from carbon in sedimentary rocks. Nature **333**, 313–318 (1988)
Schidlowski, M., Hayes, J.M., Kaplan, I.R.: Isotopic inferences of ancient biochemistries: carbon, sulfur, hydrogen, and nitrogen. In: Schopf, J.W. (ed.) Earth's Earliest Atmosphere: Its Origin and Evolution, pp. 149–187. Princeton University Press, Princeton (1983)
Sekine, Y., Sugita, S., Kadono, T., Matsui, T.: Methane production by large iron impacts on early Earth. J. Geophys. Res. **108**, 6 (2003)
Sekine Y., Sugita, S., Shido, T., Yamamoto, T., Iwasawa, Y., Kadono, T., Matsui, T.: An experimental study on Fischer-Tropsch catalysis: implications for impact phenomena and nebular chemistry. Meteor. Planet. Sci. **41**, 715–729 (2006)
Shaw, D.M.: Development of the early continental crust. Part 2. Prearchean, Protoarchean and later eras. In: Windley, B.F. (ed.) The Early History of the Earth, pp. 33–54. Wiley, New York (1976)
Sleep, N.H., Zahnle, K.: Carbon dioxide cycling and implications for climate on ancient Earth. J. Geophys. Res. **106**, 1373–1399 (2001)

Stevenson, D.J.: The nature of the Earth prior to the oldest known rock record: the Hadean Earth. In: J.W. Schopf (ed.) Earth's Earliest Atmosphere: Its Origin and Evolution, pp. 32–40. Princeton University Press, Princeton (1983)

Towe K.M. (1981) "Biochemical Keys to the Emergence of Complex Life", Life in the Universe. Proceedings of the Conference on Life in the Universe, held at NASA Ames Research Center, June 19-20, 1979. Editor, John Billingham; Publisher, MIT Press, Cambridge, Massachusetts, 1981. ISBN # 0-262-52062-1

Trenberth, K.E., Guillemot, C.J.: The total mass of the atmosphere. J. Geophys. Res. **99**, 23079–23088 (1994)

Trigo-Rodríguez, J.M.: Spectroscopic analysis of cometary and asteroidal fragments during their entry to the terrestrial atmosphere. Ph.D. thesis (In Spanish), Servei Publicacions de la Universitat de Valencia, pp. 356 (2002). Online at: http://hdl.handle.net/10803/9481

Trigo-Rodríguez, J.M., Llorca, J., Borovicka, J., Fabregat, J.: Chemical abundances determined from meteor spectra: I. Ratios of the main chemical elements. Meteor. Planet. Sci. **38**, 1283–1294 (2003)

Trigo-Rodríguez, J.M., Martín-Torres, F.J.: Clues on the importance of comets in the origin and evolution of the atmospheres of Titan and Earth. Planet. Space Sci. **60**, 3–9 (2012)

Urey, H.: The Planets: Their Origin and Development. Yale University Press, New Haven (1952)

Valley, J.W., King, E.M., Peck, W.H., Graham, C.M., Wilde, S.A.: The cool early Earth: oxygen 236 isotope evidence for continental crust and oceans on Earth at 4.4Ga. In: Abstract in the 237 American Geophysical Union Spring Meeting, Boston (2001)

Valley, J.W., King, E.M., Peck, W.H., Grham, C.M., Wilde, S.A.: The cool early Earth: oxygen isotope evidence for continental crust and oceans on Earth at 4.4 Ga. In: Abstract in the American Geophysical Union Spring Meeting (2001)

Wetherill, G.W.: Occurrence of giant impacts during the growth of the terrestrial planets. Science **228**, 877–879 (1985)

Walker, J.C.G.; Klein,C.; Schidlowski,M.; Schopf, J.W.; Stevenson, D.J.; Walter, M.R. (1983) "Environmental evolution of the Archean-Early Proterozoic Earth", In Earth's earliest biosphere: Its origin and evolution (A84-43051 21-51). Princeton, NJ, Princeton University Press, 260–290. (1983)

Zahnle, K.: Dynamics and chemistry of SL9 plumes. In: Noll, K.S., Weaver, H.A., Feldman, P.D. (eds.) The Collision of Comet Shoemaker-Levy 9 and Jupiter, pp. 183–212. Cambridge University Press, Cambridge/New Rork (1996)

Zahnle, K., Kasting, J., Pollack, J.B.: Evolution of a steam atmosphere during Earth's accretion. Icarus **74**, 62–97 (1988)

# Chapter 8
# $N_2O$ as a Biomarker, from the Earth and Solar System to Exoplanets

**Christian Muller**

**Abstract** Since its discovery in the earth's atmosphere in 1938, $N_2O$ sources and sinks have been a puzzle. $N_2O$ has now been identified as produced by anaerobic bacteria's in soils which are sufficiently acid. The influence of agriculture is still to be determined as the nitrogen cycle is broken by both the addition of inorganic fertilizers and the simultaneous oxygenation of soils by mechanized agriculture. The situation was even complicated recently by the discovery of an abiotic $N_2O$ production in the Antarctic brines (Samarkin et al. 2010). In the last 10 years, a global increase has been observed and $N_2O$ is considered as a greenhouse gas in the current IPCC report. It is destroyed by direct oxidation by oxygen atoms in the stratosphere where it is also sensitive to photodissociation. The observation of $N_2O$ from space is possible as several of its bands are in infrared atmospheric windows, especially the strong 7.8, 4.5 and the weaker 3.7 μm bands. Terrestrial $N_2O$ would be both a by-product of a subterranean biosphere and of the current agricultural practices. Its oxidation produces also tropospheric nitric oxide in the unpolluted troposphere, in limited quantities, No also plays an important role for biological processes.

$N_2O$ on the contrary to methane and formaldehyde has never been even tentatively identified nor on Mars nor on another planet. Martian methane still awaits a definitive confirmation from the EXOMARS orbiter payload in 2016 but its most probable origin would be the release of methane pockets produced under the surface by a deep biosphere while the new earth Antarctic process could also be a possibility. By analogy with the earth model, a similar mechanism would apply to the production of nitrous oxide, however, the absence of a blocking ozone layer is a sufficient reason to make the observation of $N_2O$ impossible because of its

C. Muller (✉)
Belgian User Support and Operation Centre, Brussels, Belgium
e-mail: christian.muller@busoc.be

J.M. Trigo-Rodriguez et al. (eds.), *The Early Evolution of the Atmospheres of Terrestrial Planets*, Astrophysics and Space Science Proceedings 35,
DOI 10.1007/978-1-4614-5191-4_8, 

sensitivity to UV radiation, however UV bands of NO are observed in the upper Martian atmosphere since Mariner 6 and 7 and confirmed by SPICAM on Mars-Express (Bertaux et al. 2005).

These considerations show the necessity of a better understanding of the nitrogen cycles on Mars in order to point to uncharted sources in the Martian subsurface which could prove Martian nitrogen compounds to be biomarkers.

## Introduction: What Is a Biomarker?

A biomarker is essentially a proxy for the existence of life; the typical biomarker is the fossil. A fossil is an inert artefact which only life could produce and which allows the identification of the life form that produced it, as they age fossils deteriorate and finally, the oldest fossils require extensive analysis to prove their biological origin. In the case of astronomical objects, the main source of information is the light that originates from them and it is thus tempting to look for spectral traces of life which are essentially the signatures of the gases usually associated with life or some very specific signatures of surface life forms as for example the chlorophyll "red edge" of earth vegetation. The exercise began with spectroscopy in 1867 when Pierre Janssen, the founder of the Meudon observatory, found a difference between the spectra of Mars and the moon obtained at the Etna summit and attributed it to absorption by water vapour and oxygen, it took 20 years to prove (Campbell 1894) that this observation was not possible with the instruments used during the Mount Etna expedition. However, most of the astronomical community and educated public accepted in the early twentieth century that colour changes, polar caps and the presence of an atmosphere were biomarkers for Mars and took the habitability of the planet for granted (Jouan 1900). This situation dramatically changed when the few images returned by Mariner 4, together with the first measurements of the pressure showed a moon-like landscape where a pressure of 6 hPa made the triple point of water difficult to attain (Anderson 1965). The situation changed again when the extensive cartography of Mars by the missions MARINER 9 and VIKING 1 and 2 showed that Mars had traces of liquid erosion and deposition basins hinting that earlier it had been habitable, reviving thus the interest for search of life on the planets. I was in this context that Sagan et al. (1993) made the exercise of attempting to detect earth's life from space using a flyby of the GALILEO payload aimed at the study of the Jupiter system (Fig. 8.1). The same exercise was repeated with most planetary spacecrafts including VIRTIS on VENUS-EXPRESS (Fig. 8.2). The molecules detected on earth are water vapour, ozone, methane and nitrous oxide. The detection of oxygen in the infrared is not easy and as well, the instrumental quality and the configuration of the instruments do not allow the detection of other oxides of nitrogen and related acids, life related carbon molecules as formaldehyde and glyoxal now routinely monitored by earth observation satellites are also too weak to appear on these spectra.

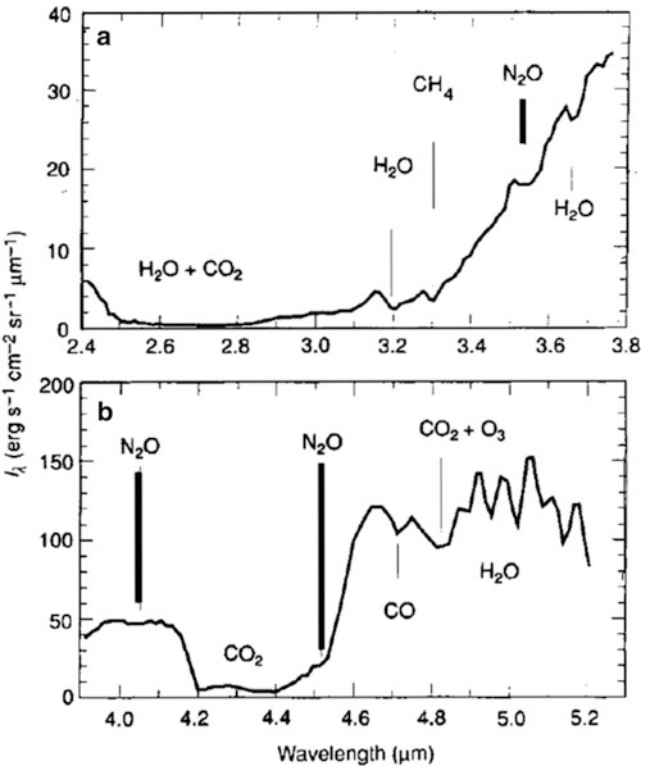


**Fig. 8.1** Nadir spectrum obtained by the GALILEO payload (Sagan et al. 1993), all the molecules identified have a relation with life, $N_2O$ is one of them

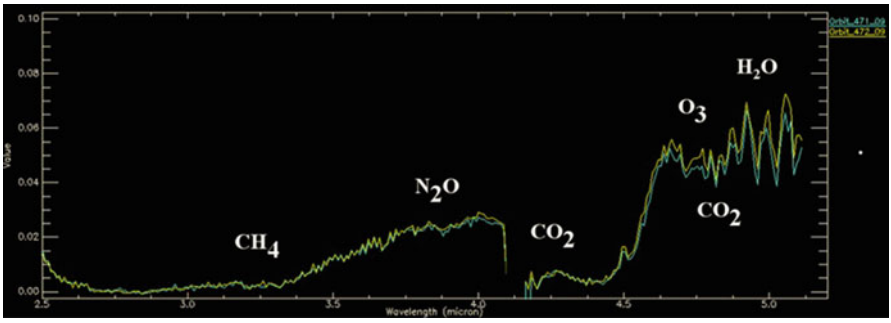


**Fig. 8.2** Earth observed in 2007 from the Venus orbit by the VIRTIS instrument on board VENUS-EXPRESS (ESA/VIRTIS/INAF-IASF/Obs. de Paris-LESIA, http://www.esa.int/esaSC/SEMUOW4N0MF_index_0.html) The difference between the two curves comes from a change in the configuration of continents, the same complement of gases appear on both images

The biomarker name used for the first time by Sagan et al. (1993) applies perfectly to this set of molecules taken as a whole: water and especially liquid water is necessary for life membranes mobility, ozone is both an indication of oxygen and an effective UV shield for DNA molecules, methane on the earth is produced at 95% by contemporary bacteria's and the same analysis has been applied to nitrous oxide. Also, the earth's DNA of composed of only five atoms: hydrogen, carbon, oxygen, nitrogen and more marginally phosphorous. The recent discovery that a life form adapted by substituting DNA phosphorous with arsenic in the California Mono Lake (Wolfe-Simon et al. 2011) is only a small step towards the extension of the definition of life. This paper when it appeared in print was accompanied in the same SCIENCE issue by eight technical comments starting a debate on the nature of the observed adaptation, these criticisms which were also peer reviewed address both the method used by the authors and fundamental arsenic and phosphorus biochemistry properties. The authors clarified their printed text and added a response to these technical comments, they also made their strains available to researchers for further analysis. The Mono lake itself will continue to be studied as its pH of 10 and increasing salinity make it a unique eco-system.

## $N_2O$ Specificities as a Biomarker on Earth

Nitrogen oxides on earth form a very important family of gases, extending to all domains of biological and atmospheric physics. $N_2O$ is however very specific as it is the only one for which no production in the gaseous phase on the earth have ever been observed in situ, it photodissociates extremely easily and its presence in the earth's troposphere is only possible under the protection of the ozone layer, in the absence of industrial pollution, it is the main source of stratospheric nitric oxide. Theoretically, gaseous phase production mechanisms could exist beginning with the direct reaction: $N2 + O(1D) + M$ producing $N_2O + M$, in the current upper atmosphere, the nitrous oxide produced than would rapidly react with O(3P) to produce NO. It is however not excluded that exceptional situations in earth history could have led to a measurable $N_2O$ atmospheric source. In the present mesosphere and higher, however, NO is produced by the reaction of the photodissociation products of oxygen and nitrogen containing molecules, its photoionization leads to the ionospheric layers so important for radio-propagation.

The $N_2O$ biological production has been linked to anaerobic bacteria's in acid soils with low level of oxygen. The denitrification of soils is a complex process that produces according to conditions $N_2O$, NO and $N_2$ (Hénault and Germon 1995). On earth, $N_2O$ was only discovered on infrared solar spectra by Adel in 1938 (Adel 1939, 1951), its value at various ground stations was measured during the 50s and showed considerable fluctuations around an average mixing ratio of 2.5 E-7 between 1955 and 1975. Since 1975 this value has increased to about 3.2 E-7 according to the current WMO report on greenhouse gases: (http://www.wmo.int/pages/prog/arep/gaw/ghg/documents/GHG_bull_6en.pdf). $N_2O$ constitutes now 6%

of the greenhouse gases forcing on climate, the current increase being related to the development of artificial fertilization while ploughs cannot introduce more oxygen in the soil that they already did 20 years ago.

NO in an unpolluted troposphere is not only produced by the denitrification of soils but also by the oxidation of $N_2O$, in limited quantities, it has an important biological role as a neuro-transmitter and also plays a regulation role in the UV resistance of deinococcus radiodurans, the most*** resistant life-form known to exist (Patel et al. 2009). Deinococcus radiodurans was first isolated by Anderson et al. (1956) while studying the sterilisation of food by irradiation, it has been studied since and it is thought now that its resistance comes from an exceptional DNA repair capability which mechanism is still not fully known.

## Abiotic Production of $N_2O$ on Earth

The eighteenth century identification by Priestley (Davy 1800) was made through the analysis of the decomposition of ammonium nitrate:

$$NH_4NO_3 \rightarrow N_2O + 2H_2O$$

This process was later used to produce $N_2O$ for anaesthetic uses in the nineteenth century "As nitrous oxide ... appears capable of destroying physical pain, it may probably be used with advantage during surgical operations in which no great effusion of blood takes place..."(Davy 1800). The process is very unlikely to be reproduced naturally as it requires a controlled high temperature. More recently, an inorganic source of nitrous oxide was identified in a hypersaline pond of the dry valleys of Antarctica (Samarkin et al. 2010). This source is completely marginal compared to the biological source and does not reflect itself in the satellite observations of $N_2O$ in the earth's troposphere. These Antarctic dry valleys are interesting as they can be viewed as a Mars analogue.

The atmospheric direct production mechanisms have already been discussed and are negligible in the present earth atmosphere.

## Nitrogen Oxides on Mars

Nitrogen oxide has been observed in day glow and night glow by UV instruments since MARINER 6-7 in the upper atmosphere of Mars, the observation is still performed in 2012 by the SPICAM instrument on Mars-Express (Bertaux et al. 2005), NO is produced in the most simple inorganic way by direct reactions between nitrogen and oxygen atoms. It is in no way a biomarker. Nitrogen exists on Mars, it has been observed by VIKING and in trapped gas on Martian meteorites, its mixing ratio is of 2.7% (Viking value). Enrichment in $^{15}N$ leads to think that most

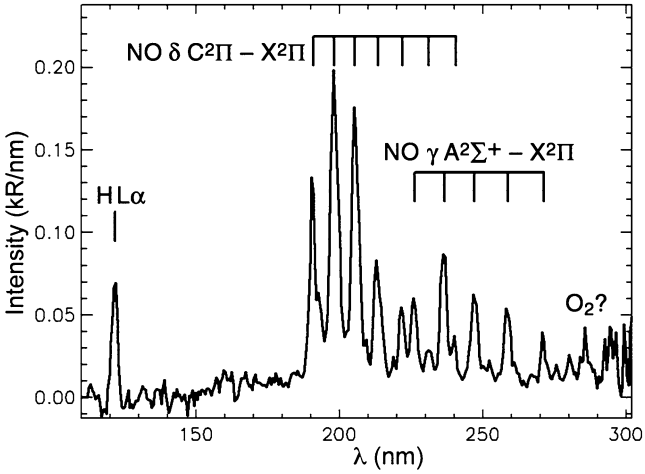


**Fig. 8.3** Observation of nightglow of NO by the SPICAM instrument on the ESA Mars Express satellite, the figure corresponds to a NO layer centred at the altitude of 117 km (Bertaux et al. 2005)

of Mars nitrogen has escaped a long time ago. It is not consistent with an active biological source which would produce fresh nitrogen continuously, more striking also is the fact that this mixing ratio is similar in meteorites which have formed at least million years before present, this would point to a very old escape of nitrogen from Mars and is in contradiction with the current reports of methane atmospheric releases from a submartian production hypothesized to be biospheric. The most instrumentally sound of these communications is the Mumma et al. (2009) mapping of a release in the Terras Sabeas region of Mars. This and other observations of Martian methane are now controversial as they are not reproducible and as the observed large space and time fluctuations have until now no clear explanations. Alternative spectroscopic interpretations of the data have been proposed but as they depend on either terrestrial methane or carbon dioxide isotopologues, they do not explain either the observed variations. Anyway, no observation makes mention of a nitrous oxide line in either ground based of space-borne data (Fig. 8.3).

Other oxides of nitrogen than NO have still to be observed, the presence of strong UV due to the absence of an ozone layer and the effects of strong oxidants make this observation difficult with the current spacecraft instrumentation. The payload of the ESA EXOMARS trace gas orbiter should be able to perform an inventory of the Martian atmospheric composition in both limb and nadir and put an end to the current controversies.

## The Future: Exoplanets and Conclusions

The infrared observation of $N_2O$ will never be easy as its bands overlap with the infrared bands of other likely molecules as HDO, methane, ozone and of course unknown bands of molecules which are less abundant in earth conditions, including isotopologues. However, $N_2O$ has its chances in the planets of UV weak stars where it could accumulate and be destroyed neither by direct UV radiation nor by reactive photodissociation products. These effects as well as the production of nitrogen oxides by galactic cosmic rays have been envisaged by Grenfell et al. (2007). The review of potential gaseous signatures by Des Marais et al. (2002) indicates also $N_2O$ as a quasi-sure biomarker but puts a lot of restrictions on observational possibilities, the worse being possibly the contamination by water vapour. On the contrary of methane, only the middle infrared is usable for $N_2O$ detection. In view of the contamination possibilities, the design of a specialized instrument could be envisaged with as first application the thematic mapping of $N_2O$ on earth which has until now received a lower priority compared to methane.

**Acknowledgements** This work has been made possible by the COST action CM-0805, the Chemical Cosmos.

B.USOC is funded by the Belgian Science Policy Office, ESA PRODEX and ESA-HSO to support the manned exploration programme.

## References

Adel, A.: Note on the atmospheric oxides of nitrogen. Astrophys. J. **90**, 627 (1939)

Adel, A.: Atmospheric nitrous oxide and the nitrogen cycle. Science **113**, 624–625 (1951)

Anderson, H.R.: Mariner 4 measurements near Mars, initial results, spacecraft description and encounter sequence. Science **149**, 1226–1228 (1965)

Anderson, A.W., Nordan, H.C., Cain, R.F., Parrish, G., Duggan, D.: Studies on a radio-resistant Micrococcus. I. isolation, morphology, cultural characteristics, and resistance to gamma radiation. Food Technol. **10**, 575–578 (1956) s

Bertaux, J.L., Leblanc, F., Perrier, S., Quemerais, E., Korablev, O., Dimarellis, E., Reberac, A., Forget, F., Simon, P.C., Stern, S.A., Sandel, B., the SPICAM team: Nightglow in the upper atmosphere of Mars and implications for atmospheric transport. Science **307**, 566–569 (2005)

Campbell, W.W.: The spectrum of Mars. Publ. Astron. Soc. Pac. **6**, 228–236 (1894)

Davy, H.: Researches, Chemical and Philosophical; Chiefly Concerning Nitrous Oxide. Johnson, London (1800). Available from GOOGLE books

Des Marais, D.J., Harwit, M.O., Jucks, K.W., Kasting, J.F., Lin, D.N., Lunine, J.I., Schneider, J., Seager, S., Traub, W.A., Woolf, N.J.: Remote sensing of planetary properties and biosignatures on extrasolar terrestrial planets. Astrobiology **2**, 153–181 (2002)

Grenfell, J.L., Griessmeier, J.M., Patzer, B., Rauer, H., Segura, A, Stadelmann, A., Stracke, B., Titz, R., Von Paris, P.: Biomarker response to galactic cosmic ray-induced NOx and the methane greenhouse effect in the atmosphere of an Earth-like planet orbiting an M dwarf star. Astrobiology **7**, 208–221 (2007)

Hénault, C., Germon, J.C.: Quantification de la dénitrification et des émissions de protoxyde d'azote $N_2O$ par les sols. Agronomie **15**, 321–355 (1995)

Patel, M., Moreau, M., Widom, J., Huan Chen, Longfei Yin, Yuejin Hua, Crane, B.R.: Endogenous nitric oxide regulates the recovery of the radiation-resistant bacterium Deinococcus radiodurans from exposure to UV light. PNAS **106**, 18183–18188 (2009)

Jouan, R.: La question de l'habitabilité des mondes étudiée au point de vue de l'histoire, de la science, de la raison et de la foi. Publication, Saint-Ilan, par Yffiniac (1900). (available from Gallica)

Mumma, M.J., Geronimo L., Villanueva, R. E., Novak, E., Hewagama, T., Bonev, B.P., DiSanti, M.A., Mandell, A.M., Smith, M.D.: Strong release of methane on Mars in Northern summer 2003. Science **323**, 1041–1045 (2009)

Sagan, C., Thompson, W.R., Carlson, R., Gurnett, D.,Hord, C.: A search for life on Earth from the Galileo spacecraft. Nature **365**, 715–721 (1993)

Samarkin, V.A., Madigan, M.T., Bowles, M.W., Casciotti, K.L., Priscu, J.C., McKay C.P., Joye, S.B.: Abiotic nitrous oxide emission from the hypersaline Don Juan Pond in Antarctica. Nat. Geosci. **3**, 341–344 (2010)

Wolfe-Simon, F., Blum, J.S., Kulp, T.R., Gordon, G.W., Hoeft, S.E., Pett-Ridge, J., Webb, S.M., Weber, P.K.: A Bacterium that can grow by using arsenic instead of phosphorus. Science **332**, 1163–1166 (2011)

# Chapter 9
# Formation of a Nitrogen-Rich Atmosphere on Titan: A Review of Pre- and Post-Cassini-Huygens Knowledge

**Yasuhito Sekine**

**Abstract** This paper reviews pre- and post-Cassini-Huygens knowledge on the formation mechanisms of a $N_2$ atmosphere on Titan. Before the arrival of Cassini, it has been generally considered that Titan's $N_2$ was formed as a result of a major differentiation during accretion and subsequent chemical reactions (such as shock heating and photolysis) in a hot and prolonged proto-atmosphere, mainly composed of $NH_3$ and $CH_4$. However, gravitational data provided by Cassini has revealed that Titan's core consists of a low-density material, suggesting that it remains relatively cold throughout its history. In this case, Titan's proto-atmosphere would have been only tenuous and short-lived, implying that the formation of $N_2$ may not have occurred effectively during accretion. Furthermore, the direct measurements of Enceladus' plumes suggest that the chemical composition of planetesimals that formed the Saturnian satellites was highly likely comet-like, namely large amounts of $CO_2$ rather than $CH_4$. This implies that primordial $CO_2$ in Titan's proto-atmosphere would have been converted into abundant CO via all of the proposed mechanisms that converted $NH_3$ to $N_2$. Recent experiments suggest that even if early Titan was relatively cold, cometary impacts during the late heavy bombardment can produce sufficient amounts of $N_2$ from $NH_3$ contained in Titan. Nevertheless, impacts also could have produced lots of CO as well as $N_2$. Although the recent findings by Cassini-Huygens support the idea that Titan was formed in a gas-starved Saturnian subnebula, there is no scenario that can account for both the formation of the Saturnian satellites in a gas-starved disk and the generation of a thick $N_2$–rich atmosphere on Titan. We discuss the unanswered problems arisen by Cassini and future studies that attempt to resolve them.

Y. Sekine (✉)
Department of Complexity Science and Engineering, The University of Tokyo,
5-1-5 Kashiwanoha, Kashiwa, Chiba 277-8561, Japan
e-mail: sekine@k.u-tokyo.ac.jp

J.M. Trigo-Rodriguez et al. (eds.), *The Early Evolution of the Atmospheres of Terrestrial Planets*, Astrophysics and Space Science Proceedings 35,
DOI 10.1007/978-1-4614-5191-4_9, 

## Introduction

Nitrogen molecule is the major component of the atmospheres of Titan and other large icy bodies in the outer solar system, such as Triton and Pluto. However, the origins of these $N_2$ remain largely unknown. Although it is considered that $N_2$ has been the principle form of nitrogen-bearing species in the solar nebula, recent observations of comets suggest that $N_2$ may have been depleted in icy planetesimals in the outer solar nebula (e.g., Bockelée-Morvan et al. 2004), and less volatile $NH_3$ was probably the principle form of nitrogen-bearing species trapped in ice at least in the Saturn-forming region of the solar nebula (e.g., Iro et al. 2003). The low abundance of primordial $^{36}Ar$ in Titan's atmosphere ($^{36}Ar/N_2 = 2.8 \times 10^{-7}$) suggests that Titan's $N_2$ is not direct capture of $N_2$ from the nebular material but is of secondary origin (Niemann et al. 2005) as well as that of Earth. This is because a large amount of primordial $^{36}Ar$ (nearly 11 % by volume) should have been trapped in the icy planetesimals that formed Titan under the nebular conditions where $N_2$ was trapped as clathrate hydrate and/or condensed as ices (e.g., Lunine and Stevenson 1985). These facts suggest that physical and chemical processes occurred on Titan may have played an important part for converting primordial $NH_3$ to $N_2$ forming the current atmosphere. Knowledge on the physics and chemistry of these processes would be essential for understanding the formation of $N_2$ on terrestrial planets and icy bodies in the solar system and beyond.

In this paper, we first review the scenarios for the origin of Titan's $N_2$ atmosphere before the arrival of Cassini. Although it is still unclear how Titan has developed the atmosphere, the Cassini-Huygens mission has provided important clues and, at the same time, serious dilemmas for understanding its origin and evolution. Then we discuss the new observational constrains on the origin of Titan's atmosphere as well as recent progresses in our understanding of physical and chemical processes responsible for forming atmospheric $N_2$. Finally, we discuss the unanswered questions remaining after the Cassini-Huygens mission and describe future missions, experiments, and modeling to resolve them.

## Pre-Cassini View of the Origin of Titan's Atmosphere

**Accretion and proto-atmosphere:** Our understanding of the origin and evolution of large icy satellites, including Titan, was greatly improved in 1980–1990s owing to knowledge on both the formation theory of Earth's atmosphere (e.g., Matsui and Abe 1986; Zahnle et al. 1988) and observations of these satellites by the Voyager spacecraft (e.g., Smith et al. 1979, 1981). Regular large icy satellites around a gas planet usually formed in a circumplanetary subnebula by accretion of icy planetesimals (e.g., Lunine and Stevenson 1982). The formation and early evolution of large icy satellites strongly depends on the timescale of accretion (Fig. 9.1) (Kuramoto and Matsui 1994). When Titan formed on the order of $10^4$ years or

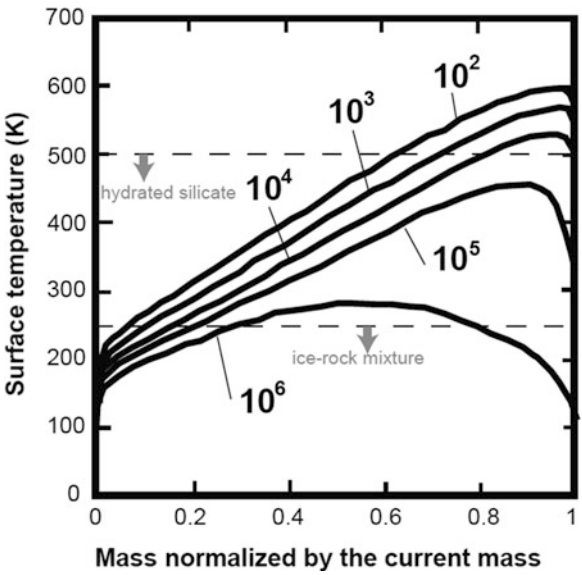


**Fig. 9.1** Evolution of the surface temperature as a function of mass of accreting Titan for different accretion time (years) (original data from Kuramoto and Matsui (1994)). Mass is normalized by the current Titan's mass. The *vertical lines* represent upper limits of the temperature where hydrated silicates and an ice-rock mixture can be maintained in the core (Fortes 2012)

less, its surface temperature would have reached $> 500$ K judging from accretion heat (Fig. 9.1) (Kuramoto and Matsui 1994). Then, the accretion heat would have caused large-scale vaporization of surface materials associated with a major rock-ice differentiation of the interior, resulting in the formation of a thick proto-atmosphere due to blanket effect of $H_2O$ vapor (Kuramoto and Matsui 1994). According to the results of satellite formation models (Lunine and Stevenson 1982; Mosqueira and Estrada 2003a, b), a typical timescale for Titan's accretion in a minimum mass disk is estimated to be $\sim 10^4$ years. Thus, it was generally believed that Titan would have had a hot and thick proto-atmosphere during accretion.

**Chemical composition of planetesimals:** The chemical composition of Titan's proto-atmosphere is determined by both those of planetesimals formed in the Saturnian subnebula and subsequent chemical reactions occurred in the proto-atmosphere. In order to explain a $CH_4$-rich and CO-poor atmosphere on present Titan, Prinn and Fegley (1981, 1989) propose that primordial CO and $N_2$ in the solar nebula would have been converted into $CH_4$ and $NH_3$ in the optically thick Saturnian subnebula. They suggest that the conversion would have readily proceeded in the subnebula via active heterogeneous catalytic reactions on the surface of metallic iron grains (Prinn and Fegley 1981, 1989), resulting in the formation of planetesimals in the Saturnian subnebula containing lots of $NH_3$ and $CH_4$ relative to $H_2O$. The early scenarios for generating a $N_2$ atmosphere on Titan (e.g., Atreya et al. 1978; McKay et al. 1988) considered the conversion of $NH_3$ to $N_2$ in the proto-atmosphere mainly composed of $NH_3$ and $CH_4$ based on the results of the optically thick subnebula model.

More recently, however, theoretical models and laboratory experiments question the idea of $CH_4$ and $NH_3$-rich planetesimals in the Saturnian subnebula. According

to the recent gas planet formation theory, satellite formation in a circumplanetary subnebula would have taken place in the late stage of gas planet formation (Canup and Ward 2002; Mousis et al. 2002). In this case, satellite formation would have occurred in an optically thin subnebula, which is supported in the radial dimension mostly by angular momentum (Wood 2000); whereas, Prinn and Fegley (1981, 1989) used the adiabatic relationship for an optically thick subnebula, which is valid for a pressure-supported atmosphere. Due to low pressures in the optically thin subnebula, the conversion of CO and $N_2$ into $CH_4$ and $NH_3$ would have been thermodynamically inhibited (Mousis et al. 2002). Moreover, laboratory experiments show that even if an optically thick subnebula was formed, conversion of CO into $CH_4$ would not have proceeded efficiently in the Saturnian subnebula (Sekine et al. 2005). This is due to loss of catalytic activity of metallic iron grains by the formation of graphitic carbon on the surface (so-called "poisoning" of metallic iron catalyst) (Sekine et al. 2005). The non-reactive graphitic carbon on the surface would have inhibited the absorption of nebular gases, severely limiting $CH_4$ production in the subnebula (Sekine et al. 2005, 2006). Even if the conversion of CO and $N_2$ into $CH_4$ and $NH_3$ in the Saturnian subnebula was not efficient, the chemical composition of the planetesimals would have been depleted in $N_2$ and CO. This is because primordial $N_2$ and CO were not substantially incorporated in planetesimals as clathrate hydrates due to the exhaustion of $H_2O$ by earlier clathrate formation (Mousis et al. 2002). Alternatively, the disk temperature of the Saturnian subnebula would not have dropped sufficient to form $N_2$ and CO clathrate hydrates (Mousis et al. 2002; Hersant et al. 2008).

If the chemical reactions in the Saturnian subnebula were inactive, primordial volatiles in the outer solar nebula (such as $CO_2$ and $CH_3OH$) also could have been incorporated in planetesimals that formed Titan as well as $NH_3$ and $CH_4$ (Sekine et al. 2005). In fact, both recent infrared observations of the interstellar ices (e.g., Gibb et al. 2000) and theoretical studies on cosmic-ray reactions in the outer solar nebula (e.g., Aikawa et al. 1999) suggest that the abundance of $CO_2$ would have reached 1–10 % relative to $H_2O$ in the Saturn-forming region of the solar nebula. The presence of $CO_2$ on accreting Titan should have affected the redox conditions of the proto-atmosphere and primordial warm water ocean; however, its effect has been poorly investigated (see below in the next Section).

**$N_2$ formation processes:** In the proto-atmosphere of Titan, it is suggested that shock heating (Jones and Lewis 1987; McKay et al. 1988) and photolysis (Atreya et al. 1978) have converted atmospheric $NH_3$ to $N_2$ efficiently. The strong UV flux and consequence effective atmospheric escape from Titan would have occurred in the first 500 Myrs after the formation of the solar system (e.g., Lammer et al. 2008; Penz et al. 2005). Thus, if Titan's $N_2$ was formed during and immediately after the accretion through shock heating and/or UV photolysis, formation of more than 10 bar of $N_2$ on early Titan would have been necessary to account for the current $N_2$ on Titan (Atreya et al. 2009).

Considering relatively high impact velocity of planetesimals due to the gravity of proto-Titan in the last stage of accretion (i.e., 2–4 km/s), shock heating induced by entry of these planetesimals into the proto-atmosphere would have thermally

dissociated $NH_3$ into $N_2$ (Jones and Lewis 1987; McKay et al. 1988). McKay et al. (1988) measured quantities of $N_2$ production by conducting laboratory experiments on a laser irradiation onto a gas mixture of $NH_3$ and $CH_4$. By applying their experimental results to a simple accretion model, they suggest that a total amount of $N_2$ produced by shock heating could have reached up to ∼25 bar during accretion (McKay et al. 1988). They also suggest that shock heating would have produced lots of $H_2$ and hydrocarbons, such as $C_2H_2$ and $C_2H_6$ (up to ∼100 bar of hydrocarbons), from $CH_4$ in the proto-atmosphere (McKay et al. 1988). Before the arrival of Cassini, Lunine et al. (1983) proposed that the presence of global hydrocarbon ocean on Titan as a possible replenishment source of atmospheric $CH_4$. Because a total amount of hydrocarbon was also comparable to that of putative ocean, McKay et al. (1988) imply that a hydrocarbon ocean also could have been produced on Titan during accretion. The major problem on the shock heating hypothesis is that any mechanisms cannot account for the escape of such large amounts of $H_2$ (up to ∼4 bar of $H_2$) from Titan's atmosphere, given strong UV flux from the young sun (Atreya et al. 2009).

Photolysis of $NH_3$ occurs at wavelength below 300 nm forming $N_2$ through $N_2H_4$ and $N_2H_3$ as intermediates (Atreya et al. 1978). The photochemical model of Titan's atmosphere found that there would be the ideal range of surface temperature (130–200 K) for production of $N_2$ from $NH_3$ (Atreya et al. 1978). At temperatures higher than 200 K, abundant $H_2O$ vapor co-existing with $NH_3$ in the proto-atmosphere produces OH radicals. The OH radicals react with $NH_2$ produced by $NH_3$ photolysis, preventing the formation of intermediate $N_2H_4$ and consequently $N_2$ (Atreya et al. 1978). On the other hand, atmospheric $N_2H_4$ would condensate at temperatures lower than 130 K, severely limiting the formation of $N_2$ (Atreya et al. 1978). Titan's surface temperature would have reached $>$ ∼300 K when accretion time is shorter than $10^5$ years (Kuramoto and Matsui 1994). As a consequence of cooling the surface in the end of accretion, Titan's surface temperature would have experienced the ideal temperature for $NH_3$ photolysis (i.e., 130–200 K) immediately after the accretion (Lunine and Stevenson 1985). In order to produce a sufficient amount of $N_2$ to explain the current $N_2$ atmosphere, it is required that Titan would have been in this ideal temperature for a prolonged time (∼30 Myr) (Adams 2006). If Titan formed within $\sim 10^4$ years, the surface temperature would have increased ∼500–600 K in the end of accretion stage (Kuramoto and Matsui 1994). In this case, Titan's surface could have experienced the ideal temperature for a prolonged time after accretion (e.g., ∼10–100 Myrs) (Atreya et al. 2009), although detailed thermal evolution of early Titan coupled with the atmospheric evolution have not been investigated.

Griffith and Zahnle (1995) propose an alternative idea of post-accretion $N_2$ formation on Titan. They consider that $N_2$ and N-bearing species contained in comets would have been supplied to Titan continuously after accretion (Griffith and Zahnle 1995). Based on the simple model of cometary impacts on Titan, Ganymede, and Callisto, they suggest that Titan and Callisto are likely to have a substantial atmosphere mainly due to their low impact velocities (Griffith and Zahnle 1995). Impacts of comets not only create an atmosphere but also erode

pre-existing atmospheric gas species, strongly depending on the impact velocity, size of impactor, and impact flux; however, these parameters are largely unknown, especially in the outer solar system.

In summary, the $N_2$ formation processes during accretion (i.e., shock heating and photolysis) require the presence of a thick and prolonged proto-atmosphere, which would have formed in association with a major differentiation of the interior due to a high level of accretion heat. If comets were the essential source of $N_2$, the isotopic abundances of major atmospheric constituents also should resemble to those of comets. The above three processes happened on Titan, regardless of whether they were effective to create the current atmosphere. In order to understand the responsible mechanism for the origin of $N_2$, we need to know on Titan's interior structure, the chemical composition of planetesimals, and the isotopic ratios of major atmospheric gas species. These observational data have been provided by the recent Cassini-Huygens mission.

## Clues and Problems Raised by Cassini-Huygens

**Titan's interior and the gas-starved subnebula model:** One of the most important clues for understanding the formation and evolution of Titan's atmosphere is a low-density core revealed by gravitational data (Iess et al. 2010). Based on Cassini's observations, it is considered that Titan's core consists of an ice-rock mixture (Iess et al. 2010) or hydrated silicates (Fortes et al. 2007; Castillo-Rogez and Lunine 2010; Fortes 2012), both of which imply that the interior has been colder than previously thought. In order to maintain an ice-rock mixture core, Titan must have been cold ($<$250 K) throughout its history. In this case, Titan should have been formed on the order of $10^6$ years in the subnebula to keep the interior temperature below this temperature (Fig. 9.1) (Barr and Canup 2010). On the other hand, if the core consists of hydrated silicates, Titan went through a warm and volatile melting phase (300–500 K) (Fortes 2012). However, the initial temperature of Titan's surface and interior must not have exceeded $\sim$500 K given long-lived radiogenic heating of the core; otherwise, the complete differentiation (i.e., dehydration of hydrated silicates) might have occurred in the core (Fortes 2012). According to the results of the accretion model (Kuramoto and Matsui 1994), such a warm (not cold but not hot) state of Titan would have been achieved when the accretion time is on the order of $10^5$ years (Fig. 9.1). Thus, Titan's interior structure infers that the plausible timescale of its accretion is $\sim 10^5$–$10^6$ years, which is significantly longer than the predictions of the minimum mass disk model of the Saturnian subnebula (i.e., $\sim 10^4$ years) (e.g., Lunine and Stevenson 1982; Mosqueira and Estrada 2003a, b).

Recently, the gas-starved model of a circumplanetary subnebula has been proposed (e.g., Canup and Ward 2002, 2006; Alibert and Mousis 2007; Sasaki and Stewart 2010). In this model, satellite growth in an actively supplied circumplanetary disk, sustained by an inflow from the solar nebula. Large satellites formed in the inflowing gas disk migrate inward by interaction with the gas and are eventually

lost to the gas planet (Canup and Ward 2006). The gas-starved model suggests that such growth and loss of large satellites continuously occur in the disk until the gas flow ends (Canup and Ward 2006). A Saturn-like satellite system can be produced when large inner satellites are lost by spiraling into the planet and another large outer satellite (i.e., Titan) remains in the disk as the gas inflow ends (Canup and Ward 2006). According to the gas-starved model, a typical timescale for accretion of Titan is on the order of $\sim 10^6$ years (Barr and Canup 2010; Sasaki and Stewart 2010), which is consistent with relatively cold interior of Titan inferred from gravitational data. Furthermore, the gas-starved models have succeeded to explain other characteristics of the Saturnian system revealed by Cassini (e.g., the formation of Saturn's $H_2O$-rich ring: Canup 2010; the wide variety in density of the Saturnian mid-sized satellites: Sekine and Genda 2012). Accordingly, the gas-starved disk is currently considered as the standard model for satellite formation in the Saturnian subnebula.

Although the new observations by Cassini seem to be consistent with the results of the gas-starved subnebula model, Titan's low density core raises a new question regarding the formation processes of $N_2$; that is, when Titan formed in $10^6$–$10^5$ years, its proto-atmosphere might have been only tenuous and short-lived (Kuramoto and Matsui 1994). This in turn means that it is unlikely that photolysis (and possibly shock heating) were responsible for producing more than 10 bar of $N_2$ during and immediately after the accretion. Based on the formation of Earth's atmosphere, we have generally considered that a massive secondary atmosphere forms only after a major differentiation, involving a high level of heat. Thus, a relatively cold Titan presents a dilemma on our view of how a massive atmosphere was formed on planets and satellites.

**Comet-like composition of planetesimals and CO formation during accretion:** Another important constraint for understanding the origin of Titan's $N_2$ is about the chemical compositions of planetesimals that formed the Saturnian satellites. One of the most remarkable findings by Cassini is perhaps water-rich plumes erupting from the south-pole region of Enceladus (Porco et al. 2006). The direct measurements of Enceladus' plume by Cassini indicate that the volatile composition of the plumes is similar to that in comets (Waite 2009), namely large amounts of $CO_2$ rather than $CH_4$. Because Titan is considered to have been formed in the Saturnian subnebula as well as Enceladus, the composition of Titan's planetesimals are also highly likely comet-like. These comet-like planetesimals are also consistent with the predictions by the optically thin disk models of the Saturnian subnebula, such as the gas-starved model (Canup and Ward 2006; Alibert and Mousis 2007). As described above, in the optically thick minimum mass disk, active chemical reactions would have converted CO and $CO_2$ into $CH_4$ (Prinn and Fegley 1981, 1989; Sekine et al. 2005). In contrast, the gas-starved model suggests that the chemical composition of planetesimals in the subnebula would have reflected that of the solar nebula due to inactive chemical reactions in the subnebula (Alibert and Mousis 2007). Thus, the comet-like composition of Enceladus' plume also supports the idea of the gas-starved disk for the Saturnian subnebula.

Given the chemical composition of Enceladus' plume, we need to revise the previous scenarios for generating a $N_2$ atmosphere on early Titan. Recently, Ishimaru et al. (2011) developed a new model of shock heating in planetary atmosphere, involving hydrodynamics of shock flow and kinetics of chemical reactions in blow shock around a planetesimal entering an atmosphere. They have investigated shock heating in Titan's proto-atmosphere for a wide range of redox states of atmospheric composition (Ishimaru et al. 2011). They have found that because atmospheric $CH_4$ is an efficient coolant in shock heating, $N_2$ production in a $NH_3 - CH_4$ atmosphere is highly inefficient (Ishimaru et al. 2011). In contrast, the presence of large amounts of $CO_2$ in a proto-atmosphere increases shock temperature, resulting in efficient $N_2$ production from $NH_3$ (Ishimaru et al. 2011). Although the presence of $CO_2$ in Titan's proto-atmosphere would have promoted the formation of $N_2$, they also pointed out that shock heating should have produced large amounts of CO from $CO_2$, which is comparable to that of $N_2$ (Ishimaru et al. 2011). They speculated that CO and $H_2$ produced by shock heating might have been recombined to $CH_4$ via catalytic reactions on the surface of metallic iron grains in turbulent wake behind a planetesimal entering the proto-atmosphere (Ishimaru et al. 2011). Nevertheless, Sekine et al. (2006) showed that the conversion rate of CO and $H_2$ into $CH_4$ via iron catalytic reactions is very low due to "poisoning" of catalysts (see section "Pre-Cassini View of the Origin of Titan's Atmosphere") under high temperatures and low pressures conditions, such as that in turbulent wake around planetesimals. Thus, abundant CO (e.g., $\sim$1 bar) might remain in the proto-atmosphere together with $N_2$, which is inconsistent with the present atmospheric composition.

The effect of the presence of $CO_2$ in Titan's proto-atmosphere on photochemical reactions has not been investigated. The presence of $CO_2$ in the proto-atmosphere may have promoted $NH_3$ photolysis. First, $CO_2$ would have reduced the abundances of H atom in the atmosphere by providing oxidants, such as O radical. The low concentrations of H atom imply that the intermediates of $NH_3$ photolysis (such as $NH_2$, $N_2H_4$, and $N_2H_3$) are not recycled back to $NH_3$ by the reactions with H atom. Additionally, the presence of abundant $CO_2$ would have prevented the formation of thick haze layer in the proto-atmosphere (Pavlov et al. 2001; Trainer et al. 2005). If the proto-atmosphere was mainly composed of $NH_3$ and $CH_4$, thick haze layer would have been produced and shielded $NH_3$ from solar UV light (Sagan and Chyba 1997; Wolf and Toon 2010). Thus, the presence of $CO_2$ could have accelerated the conversion of $NH_3$ to $N_2$ in the proto-atmosphere. However, given the formation of CO by $CO_2$ photolysis in planetary atmospheres composed of $CO_2$, $CH_4$, and $N_2$ (e.g., Pavlov et al. 2001), abundant CO is also highly likely produced in Titan's proto-atmosphere. In the proto-atmosphere, $CO_2$ and $CH_4$ are more thermodynamically stable than CO below the temperature of 600 K (Trigo-Rodriguez and Martin-Torres 2012). However, because of the very high activation energy of CO, conversion of CO into $CO_2$ and/or $CH_4$ requires the presence of effective catalysts in the atmosphere at the temperature $< 1{,}000$ K (Prinn and Fegley 1989). In the atmosphere of Mars, it is suggested that catalytic reactions on the surface of aerosols or ice cloud particles are essential to recycle photochemical products of CO back to $CO_2$, stabilizing a $CO_2$-rich atmosphere on Mars (e.g.,

Atreya and Gu 1994; Lefèvre et al. 2008). Nevertheless, it is uncertain whether such heterogeneous chemistry also could have played a key role in Titan's proto-atmosphere.

In conclusion, the comet-like composition of planetesimal inferred from the observations of Enceladus' plume (Waite 2009) raises a new question; that is the fate of abundant $CO_2$ and CO in the proto-atmosphere. The presence of such large amounts of $CO_2$ in the proto-atmosphere would have promoted $N_2$ production; however, it also should have resulted in the formation of abundant CO through all of the mechanisms that may have converted primordial $NH_3$ into $N_2$ during accretion. Given the long photochemical lifetime of CO in Titan's atmosphere ($\sim 10^9$ years: Yung et al. 1984; Wong et al. 2002), the lack of such abundant CO in the current atmosphere is apparently enigmatic.

**Post-accretion formation of $N_2$ :** The recent experimental studies have developed the idea of post-accretion formation of $N_2$ by focusing on the late heavy bombardment (LHB) of cometary bodies occurred around 4 billion years ago (Fukuzaki et al. 2010; Sekine et al. 2011). The LHB is known as a period of enhanced impact rates by asteroids and comets, revealed by analyzing Apollo samples from the large impact basins (e.g., Kring 2002). The new very successful "Nice" model and similar models have proposed that dynamic and orbital changes in the outer gas giants would have interacted with remaining icy planetesimals, triggering a temporal shower of cometary and asteriodal bodies onto the inner planets around 4 billion years ago (e.g., Gomes et al. 2005; Tsiganis et al. 2005). Such a bombardment of cometary bodies also would have occurred in the outer solar system. For the large icy satellites, including Titan, the LHB would have been one of the most energetic events (Barr and Canup 2010; Sekine et al. 2011). In hypervelocity impacts of comets during the LHB period, an impactor and part of the target material are vaporized, forming a hot impact vapor. In the impact vapor cloud, any $NH_{s_3}$ contained in Titan's crust and mantle would be thermally decomposed to $N_2$.

In order to evaluate this scenario, Sekine et al. (2011) determine the efficiency of impact-induced $N_2$ production by conducting laboratory experiments using the laser gun. The laser gun is a new and unique technique to determine impact chemistry (Fukuzaki et al. 2010; Sekine et al. 2011). Previous impact experiments usually used powder and light gas guns. However, these guns always produce lots of chemical contaminations, such as gun debris and combustion gases. In contrast, the laser gun uses a high energy laser irradiation to accelerate a projectile (e.g., Sekine et al. 2011). This chemically clean acceleration technique allows us to measure directly gas species formed by actual impacts.

Figure 9.2 shows $N_2$ production efficiency of $NH_3 - H_2O$ ice as a function of the impact velocity and the peak shock pressure achieved by the impact given by Sekine et al. (2011). These results indicate that $N_2$ production begins around 8 GPa and increases with the peak shock pressure (Fig. 9.2). This figure also shows that the shock pressure for complete $N_2$ degassing is about 23 GPa. These results suggest that $N_2$ formation does not occur efficiently in the impacts of satellitesimals during accretion and impacts onto Pluto, Charon, and other icy dwarf

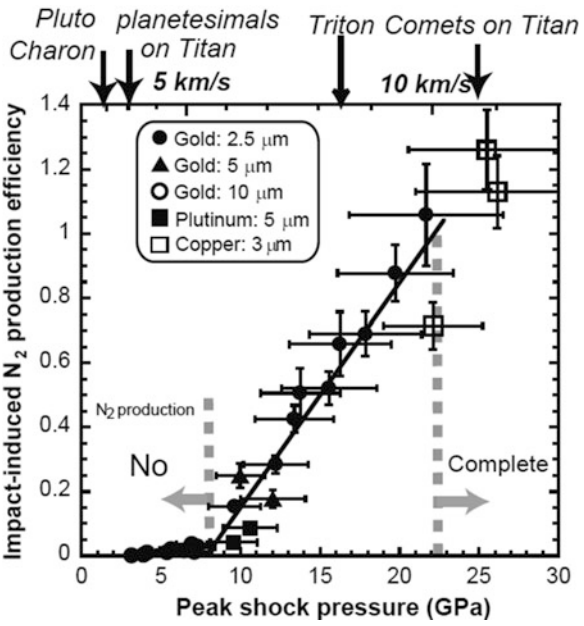


**Fig. 9.2** Efficiency of impact-induced $N_2$ production from $NH_3$-$H_2O$ ice target as a function of impact velocity of comets and peak shock pressure achieved by the impacts (original data from Sekine et al. (2011)). The *symbols* represent the material and thickness of the projectile used in the experiments (Sekine et al. 2011). *Arrows* in the upper horizontal axis represent the average impact velocities onto icy satellites and dwarf planets (Zahnle et al. 2003)

planets (Fig. 9.2). However, the conversion to $N_2$ proceeds efficiently in cometary impacts after accretion on Titan, Triton, and other icy moons because of their high impact velocities (Fig. 9.2). These results suggest that the evolution of $N_2$ on Triton is fundamentally different from that of Pluto depending on the impact velocity, although these have apparently similar $N_2$-dominated atmospheres.

Sekine et al. (2011) introduced the experimental results into a hydrodynamic impact simulation model. Using a simple model of $N_2$ inventory on Titan based on hydrodynamic simulations of hypervelocity impacts, Sekine et al. (2011) obtain a total $N_2$ production during the LHB based on the impact flux given by the Nice model (Barr and Canup 2010). They found that even if Titan starts with an airless body, it could have indeed acquired the current amount of $N_2$ during the LHB when Titan's interior contains 1–2% of $NH_3$ relative to $H_2O$ (Sekine et al. 2011). When Titan had possessed a significant atmosphere (e.g., 1–2 bar) before the LHB, most of it would have been replaced by impact-induced $N_2$ during the LHB on volatile-rich, low-gravity Titan (Sekine et al. 2011). These results imply that even if photolysis and shock heating produced a CO-rich atmosphere during accretion, most of it would have been replaced by an impact-induced atmosphere. However, if Titan's crust contains lots of $CO_2$ ice as implied by Enceladus' observations (Waite 2009), cometary impacts also would have led to the formation of CO (Fig. 9.3). The thermodynamic equilibrium calculation of impact vapor suggests that the major components of gas species in the final products of impact would be $H_2O$, $N_2$, $H_2$, and CO for a quenching temperature of 2,000 K (Fig. 9.3). In order to reduce the CO

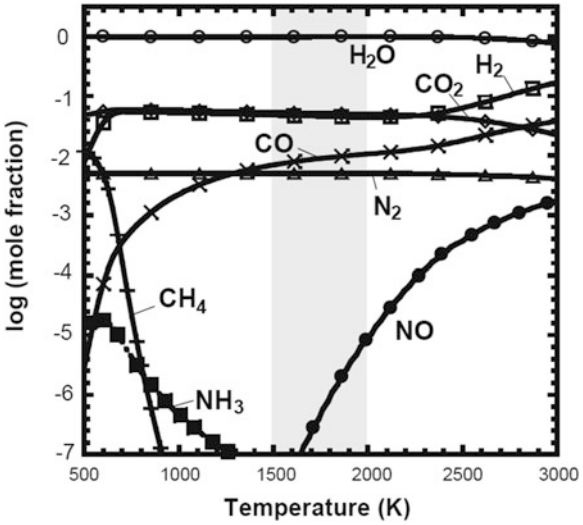


**Fig. 9.3** Equilibrium mole fractions of gas phase at 1 bar total pressures as a function of temperature, of the initial composition of Titan's crust ($H_2O = 100$; $CO_2 = 5$; $NH_3 = 1$, and $CH_4 = 1$, based on the composition of Enceladus' plume given by Waite (2009)). The *gray hatch* represents a proposed temperature range where gas-phase reactions are quenched (1,500–2,000 K; Ishimaru et al. 2011), resulting in a $CO/CO_2$ ratio in the final product as ∼0.1. Thermodynamic equilibrium calculations are conducted using software of the HSC chemistry Ver. 7

levels to the order of $10^{-5}$ of mole fraction (the current atmospheric level), the $CO_2$ concentration in the crust should be lower than $10^{-5}$–$10^{-4}$ relative to $H_2O$.

**Endogenic $N_2$ production:** Nitrogen would have been produced by thermal decomposition of $NH_3$ in the interior of Titan. Based on thermodynamic calculation, Matson et al. (2007) and Glein et al. (2009) suggest that if the interior temperature increased to ∼500–800 K, a significant amount of $NH_3$ is decomposed to $N_2$ and $H_2$. If such a high temperature is achieved during Titan's accretion, this should result in a full differentiation of the core in due to heating by long-lived radiogenic decay (Fortes 2012). In order to maintain a hydrated-silicate core, the initial temperature of the core should be less than 500 K. According to the thermal evolution model (Castillo-Rogez and Lunine 2010), high temperatures required for $NH_3$ decomposition could be achieved in the core in ∼1–3 billion years after the formation of the solar system. However, given the high solubility of $NH_3$ in water, it would have been partitioned mainly into the $H_2O$ mantle of Titan and highly depleted in the core. Thus, even if the core temperature has risen to the high temperatures, the $N_2$ production in the interior may not have been occurred.

## Summary and Future Perspectives

To summarize the clues and problems raised by Cassini, the gas-starved disk model of the Saturnian subnebula (Canup and Ward 2006; Alibert and Mousis 2007; Barr and Canup 2010) can account for many characteristics of Titan and other Saturnian satellites revealed by Cassini, such as a low density core of Titan (Iess et al. 2010), comet-like composition of Enceladus' plumes (Waite 2009), $H_2O$-rich Saturn's ring (Canup 2010), and the wide variety of the mid-sized satellites (Sekine and Genda 2012). Accordingly, it is now found to be the most plausible disk model for the Saturnian subnebula. However, the gas-starved model also predicts the accretion time of Titan as on the order of $10^6$ years (Canup and Ward 2006; Barr and Canup 2010) and the presence of lots of $CO_2$ in planetesimals that formed Titan (Alibert and Mousis 2007). The prolonged accretion of Titan should have prevented the formation of a thick and prolonged proto-atmosphere (Kuramoto and Matsui 1994), which is required for converting primordial $NH_3$ to $N_2$ through shock heating and/or photolysis (Atreya et al. 1978; McKay et al. 1988). The post-accretion cometary impacts during the late heavy bombardment can account for the formation of 1.5 bar of $N_2$ on Titan (Sekine et al. 2011). Nevertheless, large amounts of $CO_2$ in the proto-atmosphere and mantle of Titan should have led to the formation of abundant CO through all of the mechanisms that converted $NH_3$ to $N_2$, which is contradicted by the present atmospheric composition. Up to the present, there is no one model that can account for both the formation of Titan and other Saturnian satellites in the gas-starved disk and the origin of a $N_2$-dominated, thick atmosphere on Titan. In order to resolve the above dilemmas, the following future modeling, experiments, missions, and observations may become important:

1. **Modeling of Titan's accretion in the gas-starved disk and subsequence early thermal evolution:** Kuramoto and Matsui (1994) calculated the thermal evolution of accreting Titan by assuming gas-free accretion (Fig. 9.1). Given the gas-starved model, however, Titan was formed in the gas-starved disk. This implies that early Titan can capture $H_2$ and He from the disk, affecting thermal structure and chemical reactions in the proto-atmosphere, and volatile loss from early Titan (Okada and Kuramoto 2012).
2. **Examining the role of $CO_2$ in Titan's proto-atmosphere:** We need to revise the pervious scenarios for the origin of Titan's $N_2$ based on the realistic chemical composition of planetesimals inferred from Cassini's data. In especially, a photochemical model coupled with a haze-production microphysical model and a radiative transfer model would be required to examine the effect of $CO_2$ photolysis in Titan's proto-atmosphere. Although constructing such a self-consistent model of planetary atmosphere is still challenging, it is also useful to investigate climatic stability of planets that have a mildly reducing atmosphere, such as early Earth and super Earths. Furthermore, heterogeneous chemistry on the surface of aerosols and ice cloud particles may be essential to examine the fate of $CO_2$ and CO in Titan's proto-atmosphere.

3. **Space missions to comets and Enceladus for investigating isotopic compositions and abundances of both major volatiles noble gases:** The Cassini-Huygens mission has revealed that the $^{15}N/^{14}N$ ratio of Titan's $N_2$ ($\sim 5.5 \times 10^{-3}$: Niemann et al. 2005) is higher than that of Earth ($\sim 3.5 \times 10^{-3}$). The previous studies have interpreted the high nitrogen isotopic values as a result of fractionation due to hydrodynamic escape during and immediately after the accretion (Atreya et al. 2009). However, if post-accretion formation of Titan's atmosphere is correct, the high isotopic ratio in Titan's $N_2$ is primordial. This suggests that Titan's $N_2$ may have come from a different source in the solar nebula compared with the source of $N_2$ for the terrestrial planets, implying a large-scale isotopic heterogeneity of nitrogen between the inner and outer solar system as revealed by the Genesis mission (Marty et al. 2011). In order to test whether Titan's $N_2$ was produced during accretion or by post-accretion processes, measurements of the isotopic ratios of $^{15}N/^{14}N$ of $NH_3$ in comets and Enceladus with space missions and large telescopes are important.
4. **Partitioning and chemical evolution of primordial volatiles (such as $NH_3$, $CO_2$, and $CH_4$) in a warm water ocean formed on accreting Titan:** Removal processes of $CO_2$ from the surface would have been important in order to prevent the formation of abundant CO. If Titan was formed in $10^5$ years, it would have possessed a warm water ocean near the surface in the end of accretion, where $CO_2$ removal might have occurred. These processes may include $CH_4$ production associated with serpentinization and carbonate formation by reactions with cations leached from primitive minerals. Laboratory experiments to investigate the kinetics of these reactions are important to understand the fate of primordial $CO_2$ in Titan and other large icy satellites. In order to resolve the unresolved questions, it is important to consider Titan as an Earth-like system and learn more about how the atmosphere, mantle, and core evolved and interacted over its history.

**Acknowledgements** We greatly appreciate Josep M. Trigo-Rodriguez for the arrangements of this book and the meeting on "Nitrogen in Planetary Systems: the early evolution of the atmospheres of terrestrial planets" in Barcelona, September 2011. Support from Grants in Aid from Japan Society for the Promotion of Science is also acknowledged.

## References

Adams, E.Y.: Titan's thermal structure and the formation of a nitrogen atmosphere. PhD thesis, The University of Michigan (2006)

Aikawa, Y., Umebayashi, T., Nakano, T., Miyama, S.M.: Evolution of molecular abundances in proto-planetary disks with accretion flow. Astrophys. J. **519**, 705–725 (1999)

Alibert, Y., Mousis, O.: Formation of Titan in Saturn's subnebula: constraints from Huygens Probe measurements. Astron. Astrophys. **465**, 1051–1060 (2007)

Atreya, S.K., Gu, Z.G.: Stability of the Martian atmosphere: is heterogeneous catalysis essential? J. Geophys. Res. **99**(E6), 13133–13145 (1994)

Atreya, S.K., Donahue, T.M., Kuhn, W.R.: Evolution of a nitrogen atmosphere on Titan. Science **201**, 611–613 (1978)

Atreya, S.K., Lorenz, R.D., Waite, J.H.: Volatile origin and cycles: nitrogen and methane. In: Brown, R.H., Lebreton, J.-P., Waite, J.H. (eds.) Titan from Cassini-Huygens, pp. 177–199. Springer, New York (2009)

Barr, A.C., Canup, R.M.: Origin of the Ganymede-Callisto dichotomy by impacts during the late heavy bombardment. Nat. Geosci. **3**, 164–167 (2010)

Barr, A.C., Citron, R.I., Canup, R.M.: Origin of a partially differentiated Titan. Icarus **209**, 858–862 (2010)

Bockelée-Morvan, D., Crovisier, J., Mumma, M.J., Weaver, H.A.: The composition of cometary volatiles. In: Festou, M.C., Keller, H.C., Weaver, H.A. (eds.) Comets II, pp. 391–423. University of Arizona Press, Tucson (2004)

Canup, R.M.: Origin of Saturn's rings and inner moons by mass removal from a lost Titan-sized satellite. Nature **468**, 943–946 (2010)

Canup, R.M., Ward, W.R.: Formation of the Galilean satellites: conditions of accretion. Astron. J. **124**, 3404–3423 (2002)

Canup, R.M., Ward, W.R.: A common mass scaling for satellite systems of gaseous planets. Nature **441**, 834–839 (2006)

Castillo-Rogez, J.C., Lunine, J.I.: Evolution of Titan's rocky core constrained by Cassini observations. Geophys. Res. Lett. **37**, L20205 (2010)

Fortes, A.D.: Titan's internal structure and the evolutionary consequences. Planet. Space Sci. **60**, 10–17 (2012)

Fortes, A.D., Grindrod, P.M., Trickett, S.K., Voèadlo, L.: Ammonium sulfate on Titan: possible origin and role in cryovolcanism. Icarus **188**, 139–153 (2007)

Fukuzaki, S., Sekine, Y., Genda, H., Sugita, S., Kadono, T., Matsui, T.: Impact-induced $N_2$ production from ammonium sulfate: implications for the origin and evolution of $N_2$ in Titan's atmosphere. Icarus **209**, 715–722 (2010)

Gibb, E.L., et al.: An Inventory of interstellar ices toward the embedded protostar W33A. Astrophys. J. **536**, 347–356 (2000)

Glein, C.R., Desch, S.J., Shock, E.L.: The absence of endogenic methane on Titan and its implications for the origin of atmospheric nitrogen. Icarus **204**, 637–644 (2009)

Gomes, R., Levison, H.F., Tsiganis, K., Morbidelli, A.: A. Origin of the cataclysmic Late Heavy Bombardment period of the terrestrial planets. Nature **435**, 466–469 (2005)

Griffith, C.A., Zahnle, K.: Influx of cometary volatiles to planetary moons: the atmospheres of 1000 possible Titans. J. Geophys. Res. **100**, 16907–16922 (1995)

Hersant, F., Gautier, D., Tobie, G., Lunine, J.I.: Interpretation of the carbon abundance in Saturn measured by Cassini. Planet. Space Sci. **56**, 1103–1111 (2008)

Iess, L., et al.: Gravity field, shape, and moment of inertia of Titan. Science **327**, 1367–1369 (2010)

Iro, N., Gautier, D., Hersant, F., Bockelée-Morvan, D., Lunine, J.I.: An interpretation of the nitrogen deficiency in comets. Icarus **161**, 511–532 (2003)

Ishimaru, R., Sekine, Y., Matsui, T., Mousis, O.: Oxidizing proto-atmosphere on Titan: constraint from $N_2$ formation by impact shock. Astrophys. J. Lett. **741**, L10, 1–6. doi:10.1088/2041-8205/1/L10 (2011)

Jones, T.D., Lewis, J.S.: Estimated impact shock production of $N_2$ and organic compounds on early Titan. Icarus **72**, 381–393 (1987)

Kring, D.A., Cohen, B.A.: Cataclysmic bombardment throughout the inner solar system 3.9–4.0 Ga. J. Geophys. Res. **107**, 5009 (2002)

Kuramoto, K., Matsui, T.: Formation of a hot proto-atmosphere on the accreting giant icy satellite: implications for the origin and evolution of Titan, Ganymede, and Callisto. J. Geophys. Res. **99**, 21183–21200 (1994)

Lammer, H., Kasting, J.F., Chassefiere, Johnson, R.E., Kulikov, Y.N., Tian, F.: Atmospheric escape and evolution of terrestrial planets and satellites. Space Sci. Rev. **139**, 399–436 (2008)

Lefèvre, F., et al.: Heterogeneous chemistry in the atmosphere of Mars. Nature **454**, 971–975 (2008)

Lunine, J.I., Stevenson, D.J.: Formation of the Galilean satellites in a gaseous nebula. Icarus **52**, 14–39 (1982)

Lunine, J.I., Stevenson, D.J.: Thermodynamics of clathrate hydrate at low and high pressure with application to the outer solar system. Astrophys. J. Suppl. **58**, 493–531 (1985)

Lunine, J.I., Stevenson, D.J., Yung, Y.L.: Ethane ocean on Titan. Science **222**, 1229–1303 (1983)

Marty, B., Chaussidon, M., Wiens, R.C., Jurewicz, J.G., Burnett, D.S.: A$^{15}$N-poor isotopic composition for the solar system as shown by Genesis solar wind samples. Science **332**, 1533–1536 (2011)

Matson, D.L., Castillo, J.C., Lunine, J., Johnson, T.V.: Enceladus' plume: compositional evidence for a hot interior. Icarus **187**, 569–573 (2007)

Matsui, T., Abe, Y.: Evolution of an impact-induced atmosphere and magma ocean on the accreting Earth. Nature **322**, 526–528 (1986)

McKay, C.P., Scattergood, T.W., Pollack, J.B., Borucki, W.J., Ghyseghem, H.T.V.: High-temperature shock formation of $N_2$ and organics on primordial Titan. Nature **332**, 520–522 (1988)

Mosqueira, I., Estrada, P.R.: Formation of the regular satellites of giant planets in an extended gaseous nebula I: subnebula model and accretion of satellites. Icarus **163**, 198–231 (2003a)

Mosqueira, I., Estrada, P.R.: Formation of the regular satellites of giant planets in an extended gaseous nebula II: satellite migration and survival. Icarus **163**, 232–255 (2003b)

Mousis, O., Gautier, D., Bockelée-Morvan, D.: An evolutionary turbulent model of Saturn's subnebula: implications for the origin of the atmosphere of Titan. Icarus **156**, 162–175 (2002)

Niemann, H.B., et al.: The abundances of constituents of Titan's atmosphere from the GCMS instrument on the Huygens Probe. Nature **438**, 779–784 (2005)

Okada, H., Kuramoto, K.: Structure of the proto-atmosphere on Titan accreted in a gas-starved circumplanetary disk. In: Abstract of JpGU Meeting, PPS21-10, Makuhari, Japan (2012)

Pavlov, A.A., Brown, L.L., Kasting, J.F.: UV shielding of $NH_3$ and $O_2$ by organic hazes in the Archean atmosphere. J. Geophys. Res. **106**, E10, 23267–23287 (2001)

Porco, C.C., et al.: Cassini observes the active south pole of Enceladus. Science **311**, 1393–1401 (2006)

Penz, T., Lammer, H., Kulikov, Y.N., Biernat, H.K.: The influence of the solar particle and radiation environment on Titan's atmosphere evolution. Adv. Space Res. **36**, 241–250 (2005)

Prinn, R.G., Fegley, B. Jr.: Kinetic inhibition of CO and $N_2$ reduction in circumplanetary nebula: implications for satellite composition. Astrophys. J. **249**, 308–317 (1981)

Prinn, R.G., Fegley, B. Jr.: Solar nebula chemistry: origin of planetary, satellite, and cometary volatiles. In: Atreya, S.K., Pollack, J.B., Matthews, M.S. (eds.) Origin and Evolution of Planetary and Satellite Atmosphere. University of Arizona Press, Tucson (1989)

Sagan, C., Chyba, C.: The early faint sun paradox: organic shielding of ultraviolet-labile greenhouse gases. Science **276**, 1217–1221 (1997)

Sasaki, T., Stewart, G.R., Ida, S.: Origin of the different architectures of the Jovian and Saturnian satellite systems. Astrophys. J. **714**, 1052–1064 (2010)

Sekine, Y., Genda, H.: Giant impacts in the Saturnian system: a possible origin of diversity in the inner mid-sized satellites. Planet. Space Sci. **63–64**, 133–138 (2012)

Sekine, Y., Sugita, S., Shido, T., Yamamoto, T., Iwasawa, Y., Kadono, T., Matsui, T.: The role of Fischer-Tropsch catalysis in the origin of methane-rich Titan. Icarus **178**, 154–164 (2005)

Sekine, Y, Sugita, S., Shido, T., Yamamoto, T., Iwasawa, Y., Kadono, T., Matsui, T.: An experimental study of Fischer-Tropsch catalysis: implications for impact phenomena and nebular chemistry. Meteor. Planet. Sci. **41**(5), 715–729 (2006)

Sekine, Y., Genda, H., Sugita, S., Kadono, T., Matsui, T.: Replacement and late formation of atmospheric $N_2$ on undifferentiated Titan by impacts. Nat. Geosci. **4**, 359–362 (2011)

Smith, B.A., et al.: The Galilean satellites and Jupiter: Voyager 2 imagsing science results. Science **206**, 927–950 (1979)

Smith, B.A., et al.: Encounter with Saturn: Voyager 1 imaging science results. Science **212**, 163–191 (1981)

Tsiganis, K., Gomes, R., Morbidelli, A., Levson, H.F.: Origin of the orbital architecture of the giant planets of the solar system. Nature **435**, 459–461 (2005)
Trainer, M.G., et al.: Organic haze on Titan and the early Earth. PNAS **103**, 18035–18042 (2005)
Trigo-Rodriguez, J.M., Martin-Torres, F.J.: Clues on the importance of comets in the origin and evolution of the atmospheres of Titan and Earth. Planet. Space Sci. **60**, 3–9 (2012)
Waite, J.H., et al.: Liquid water on Enceladus from observations of ammonia and $^{40}$Ar in the plume. Nature **460**, 487–490 (2009)
Wolf, E.T., Toon, O.B.: Fractal organic hazes provided an ultraviolet shield for early Earth. Science **328**, 1266–1268 (2010)
Wong, A.-S., Morgan, C.G., Yung, Y.L.: Evolution of CO on Titan. Icarus **155**, 382–393 (2002)
Wood, J.A.: Pressure and temperature profiles in the solar nebula. Space Sci. Rev. **92**, 87–93 (2000)
Yung, Y.L., Allen, M., Pinto, J.P.: Photochemistry of the atmosphere of Titan: Comparison between model and observations. Astrophys. J. Supp. **55**, 465–506 (1984)
Zahnle, K.J., Kasting, J.F., Pollack, J.B.: Evolution of a steam atmosphere during earth's accretion. Icarus **74**, 62–97 (1988)
Zahnle, K., Schenk, P.M., Levision, H.F.: Cratering rates in the outer solar system. Icarus **163**, 263–289 (2003)

# Chapter 10
# Nitrogen in the Stratosphere of Titan from Cassini CIRS Infrared Spectroscopy

**Conor A. Nixon, Nicholas A. Teanby, Carrie M. Anderson, and Sandrine Vinatier**

**Abstract** In this chapter we describe the remote sensing measurement of nitrogen-bearing species in Titan's atmosphere by the Composite Infrared Spectrometer (CIRS) on the Cassini spacecraft. This instrument, which detects the thermal infrared spectrum from 10 to 1,500 $cm^{-1}$ (1,000–7 μm) is sensitive to vibrational and rotational emissions of gases and condensates in Titan's stratosphere and lower mesosphere, permitting the measurement of ambient temperature and the abundances of gases and particulates. Three N-bearing species are firmly detected: HCN, $HC_3N$ and $C_2N_2$, and their vertical and latitudinal distributions have been mapped. In addition, ices of $HC_3N$ and possibly $C_4N_2$ are also seen in the far-infrared spectrum at high latitudes during the northern winter. The $HC^{15}N$ isotopologue has been measured, permitting the inference of the $^{14}N/^{15}N$ in this species, which differs markedly (lower) than in the bulk nitrogen reservoir ($N_2$). We also describe the search in the CIRS spectrum, and inferred upper limits, for $NH_3$ and $CH_3CN$. CIRS is now observing seasonal transition on Titan and the gas

C.A. Nixon (✉)
Department of Astronomy, University of Maryland, College Park, MD 20742, USA
e-mail: conor.a.nixon@nasa.gov

N.A. Teanby
School of Earth Sciences, University of Bristol, Wills Memorial Building, Queen's Road, Bristol, BS8 1RJ, UK
e-mail: n.teanby@bristol.ac.uk

C.M. Anderson
Planetary Systems Laboratory, NASA Goddard Space Flight Center, Greenbelt, MD 20771, USA
e-mail: carrie.m.anderson@nasa.gov

S. Vinatier
LESIA, Observatoire de Paris, CNRS, 5 Place Jules Janssen, 92195 Meudon Cedex, France
e-mail: sandrine.vinatier@obspm.fr

J.M. Trigo-Rodriguez et al. (eds.), *The Early Evolution of the Atmospheres of Terrestrial Planets*, Astrophysics and Space Science Proceedings 35,
DOI 10.1007/978-1-4614-5191-4_10, 

abundance distributions are changing accordingly, acting as tracers of the changing atmospheric circulation. The prospects for further CIRS science in the remaining 5 years of the Cassini mission are discussed.

## Introduction

The two principal gaseous components of Titan's atmosphere are molecular nitrogen $N_2$ (98.5% in stratosphere) and methane $CH_4$ (1.4% in stratosphere) [1]. From just these two molecules and three elements a wealth of organic chemistry develops[1], resulting in a plethora of hydrocarbons and nitriles. The true chemical complexity of Titan's atmosphere was first revealed in 1980 with the Voyager encounter at Titan, during which a number of new molecular species were first detected through infrared spectroscopy by the IRIS (Infrared Interferometer Spectrometer) instrument: HCN, $C_2H_4$ and $C_2H_6$ [2]; $HC_3N$, $C_2N_2$ and $C_4H_2$ [3]; and the $C_3$ molecules $C_3H_4$ and $C_3H_8$ [4]. Further stratospheric species were found later: $CO_2$, CO, $CH_3CN$, $C_6H_6$ and $H_2O$ [5].

More recently, the NASA Cassini spacecraft entered Saturn orbit in July 2004, and has since made more than 80 close flybys of Titan at the time of writing. Equipped with an Ion and Neutral Mass Spectrometer (INMS) [6], Cassini has directly sampled the upper atmosphere of Titan, finding further chemical diversity, including ammonia ($NH_3$), amines ($-NH_2$) and imines ($-NH$), and heavier hydrocarbons such as toluene ($C_7H_8$) [7]. In the stratosphere, Cassini's infrared spectrometer CIRS (Composite Infrared Spectrometer) [8] has mapped the vertical, lateral and temporal variations of the stratospheric nitriles, which constitutes section "Nitrile Species in the Stratosphere" of this chapter. Later sections cover related topics: nitrile condensates and ices in section "Nitrile Condensables in Titan's Stratosphere", the isotopic ratio $^{14}N/^{15}N$ as measured in HCN in section "$^{15}N$ Isotopologues", and the search for molecules as yet undetected in the stratosphere in section "The Search for Further N-Bearing Molecules with CIRS".

We begin this chapter by briefly reviewing chemical processes from the break-up of $N_2$ to the formation of $H_xC_yN_z$ species, and also the CIRS instrument that is the source of the scientific information presented here.

### *Nitrogen Chemistry*

In Titan's upper atmosphere, nitrogen chemistry begins when molecular nitrogen is dissociated/ionized by solar UV radiation[2]:

[1] There are also some oxygen species, most notably CO at 50 ppm, which are not discussed here.

[2] The chemical discussion in this section follows the more detailed description in [9]

$$N_2 + h\nu \rightarrow N(^4S) + N^+ + e^- \qquad \lambda < 510\,\text{Å} \quad (10\%) \qquad (10.1)$$

$$\rightarrow N(^2D) + N^+ + e^- \qquad \lambda < 510\,\text{Å} \quad (90\%) \qquad (10.2)$$

$$\rightarrow N_2^+ + e^- \qquad 510 < \lambda < 796\,\text{Å} \qquad (10.3)$$

$$\rightarrow N(^2D) + N(^4S) \qquad 796 < \lambda < 1{,}000\,\text{Å} \qquad (10.4)$$

In addition, high-energy Galactic Cosmic Rays (GCRs, mainly protons and alpha particles) reach the lower atmosphere, where a second dissociation region occurs peaking near 100 km. To form nitriles or amines/imines, carbon and hydrogen are required, which are supplied by the solar photodissociation of methane:

$$CH_4 + h\nu \rightarrow CH + H + H_2 \qquad \lambda \leq 145\,\text{nm} \quad (7\%) \qquad (10.5)$$

$$\rightarrow {}^1CH_2 + H_2 \qquad \lambda \leq 145\,\text{nm} \quad (58.4\%) \qquad (10.6)$$

$$\rightarrow {}^1CH_2 + 2H \qquad \lambda \leq 145\,\text{nm} \quad (5.5\%) \qquad (10.7)$$

$$\rightarrow CH_3 + H \qquad \lambda \leq 145\,\text{nm} \quad (29.1\%) \qquad (10.8)$$

$$\rightarrow CH_3 + H \qquad \lambda > 145\,\text{nm} \qquad (10.9)$$

Nitriles arise when $CH_3$ reacts with N, either by:

$$N + CH_3 \rightarrow HCN + H_2 \qquad (10.10)$$

or

$$N + CH_3 \rightarrow H_2CN + H \qquad (10.11)$$

$$H_2CN + H \rightarrow HCN + H_2 \qquad (10.12)$$

which has the same net effect as reaction (10.10) but an overall faster rate. HCN may be photolyzed to H + CN, and the CN radical will then either (a) catalytically destroy unsaturated hydrocarbons and $H_2$ by H-abstraction, or (b) form heavier nitrile species by substitution of CN for H, e.g. $C_2H_4$ becomes $C_2H_3CN$ (acrylonitrile or vinyl cyanide).

The production of amines and imines begins when dissociated nitrogen atoms interact with methane:

$$N(^2D) + CH_4 \rightarrow NH + CH_3 \qquad (20\%) \qquad (10.13)$$

$$\rightarrow CH_2NH + H \qquad (80\%) \qquad (10.14)$$

The self-reaction of two imidogen radicals then leads to the amino radical, or alternatively atomic nitrogen plus molecular hydrogen leads to the same result:

$$2\mathrm{NH} \rightarrow \mathrm{NH_2} + \mathrm{N} \tag{10.15}$$

$$\mathrm{N} + \mathrm{H_2} + \mathrm{M} \rightarrow \mathrm{NH_2} + \mathrm{M} \tag{10.16}$$

Finally, ammonia is produced from the amino radical plus atomic hydrogen:

$$\mathrm{NH_2} + \mathrm{H} \rightarrow \mathrm{NH_3} \tag{10.17}$$

Other pathways are possible to these products: we have summarized only the (believed to be) principal pathways here. For a fuller description see [9]. In the following sections of this chapter, we will describe how the concentrations of various nitrile species have been measured by CIRS in the middle atmosphere, and on the search for ammonia in the stratosphere.

## *The Composite Infrared Spectrometer (CIRS)*

Cassini CIRS is a dual interferometer, comprised of separate far-infrared and mid-infrared spectrometers sharing a common telescope, foreoptics, reference laser, scan mechanism and other sub-systems to save mass and size. The telescope is a Cassegrain type, with 508 mm beryllium primary and 76 mm secondary mirrors. The incident beam is field-split and sent to either the far-IR or mid-IR interferometer. The far-IR interferometer is a Martin-Puplett (polarizing) type, using wire-grid polarizers to amplitude split radiation between 10 and 600 $\mathrm{cm^{-1}}$ (1,000–17 μm) in wavenumber (wavelength). The time-varying interferogram signal produced by the scanning of one retroreflector is afterwards detected by a thermopile (bolometer) detector known as FP1 (Focal Plane 1), which is 1 mm in size and has apparent field-of-view projected on the sky plane of 2.5 mrad FWHM (full-width to half-maximum of Gaussian response).

The mid-IR interferometer is a standard Michelson type covering the spectral range 600–1,400 $\mathrm{cm^{-1}}$ (17–7 μm), and the signal is detected by one of two arrays. CIRS FP3 (Focal Plane 3) consists of a $1 \times 10$ array of photoconductive (PC) detectors sensitive from 600 to 1,100 $\mathrm{cm^{-1}}$ (17–9 μm), while FP4 (Focal Plane 4) is a similar $1 \times 10$ array of photovoltaic detectors sensitive from 1,100 to 1,400 $\mathrm{cm^{-1}}$ (9–7 μm). Pixels of both arrays have square-shaped projected fields-of-view 0.273 mrad in width. By varying the travel distance (or scan time) of the mirror carriage, spectral resolutions varying from 0.5 to 15.5 $\mathrm{cm^{-1}}$ are possible, after application of Hamming apodization to reduce the ripples/ringing caused by the finite Fourier Transform.

The FP1 detector is held at 170 K, identical to the rest of the instrument optics and mechanical assembly, while FP3/FP4 are cooled to an operating temperature

of ~75 K via a 30-cm radiator pointed at cold space. For calibration therefore, the FP1 detector needs only one temperature reference target (space at 2.73 K), while FP3/FP4 require both reference scans of deep space and also an internal warm shutter at ~170 K. A more detailed overview of the instrument can be found in the literature [8, 10], while more detailed descriptions of the FP1 far-IR interferometer and the FP3/FP4 mid-IR interferometer have been separately published [11, 12].

As Cassini approaches Titan, CIRS performs different science observations depending on distance, based on the differing capabilities of the mid-IR and far-IR spectrometers. At large distances (380,000–260,000 km, 19–13 h from closest approach), the mid-IR arrays are typically used in nadir-scanning mode, where the arrays are 'combed' across Titan's visible disk. Closer in (260,000–180,000 km, 13–9 h), the FP1 detector is placed on the disk and long-integrations are made at a fixed location, to build up high S/N at the highest spectral resolution (0.5 $cm^{-1}$) to search for/measure weak species in the far-IR. At medium distances (180,000–100,000 km, 9–5 h), the mid-IR detectors acquire sufficient spatial resolution to resolve the limb of Titan's atmosphere (defined by the atmospheric scale height, about 50 km), and are used for limb mapping or integrating. Less than 5 h (100,00 km) from Titan, the far-IR channel again takes precedence, used first in nadir mapping mode (100,000–45,000 km, 5:00–2:15 h) and finally in limb mode (45,000–5,000 km, 2:15–0:15 h), when the spatial resolution becomes sufficient to resolve the limb using the large FP1 detector. Further details of the Titan science strategy can be found in existing publications [8, 13, 14].

## Nitrile Species in the Stratosphere

The three major nitrile species in Titan's atmosphere are HCN, $HC_3N$, and $C_2N_2$, and all are spectroscopically detected and measured by CIRS – see Fig. 10.1. Through modeling these emissions, and assuming the atmospheric temperature is independently known, the abundances can be measured. In this section we discuss the inferred global distribution of these nitriles and consider what this tells us about nitrogen-species chemistry on Titan.

### *Vertical Profiles at Low Latitudes*

Nitrile species are produced by photochemical reactions in Titan's upper atmosphere at altitudes above 500 km (section "Nitrogen Chemistry"). This is above the region that is observable with Cassini CIRS. However, these species are transported into the lower mesosphere and stratosphere by vertical mixing processes, which allow them to be observed. At altitudes of approximately 100–150 km in the lower stratosphere, temperatures become cold enough to allow condensation and rain-out of nitrile species. This source-sink arrangement sets up positive vertical concentration gra-

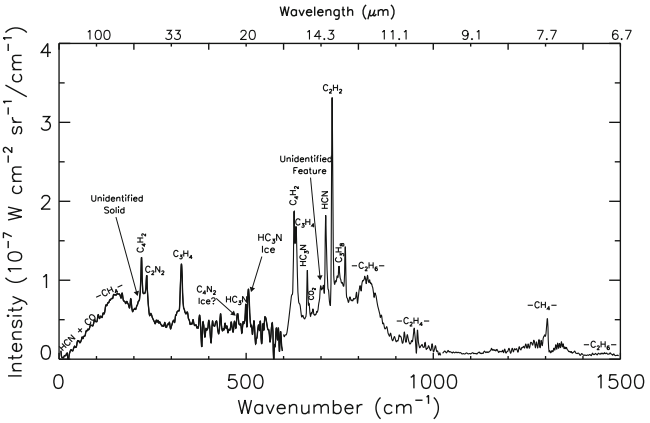


**Fig. 10.1** Sample CIRS limb spectrum of Titan at 70°N, 125–160 km altitude from August 2007. Vibrational bands of HCN, $HC_3N$ and $C_2N_2$ are labeled, along with an $HC_3N$ ice signature (Adapted from Anderson and Samuelson [15])

dients where the relative abundance increases with altitude. Photochemical models predict that vertical gradients are steeper for species with shorter photochemical lifetimes (e.g. $HC_3N$) as they have less time to mix into lower atmospheric levels before being destroyed by photolysis.

Shortly after Cassini's arrival at the Saturnian system in July 2004, CIRS limb sounding observations from the early flybys gave the first detailed vertical profiles of nitriles in Titan's atmosphere [16, 17] (Fig. 10.2). The CIRS results confirm earlier ground based sub-millimeter work [18–20] based on high-resolution measurements of the lineshape of nitrile rotational lines. Both HCN and $HC_3N$ were observed to have steep vertical gradients – in broad agreement with photochemical models. Titan's equatorial abundances had the best agreement with the Earth-based results because of the sampling bias towards low latitudes in disk-averaged ground-based spectra. Equatorial latitudes also bear the most resemblance to photochemical model predictions, as the equator is closest to equilibrium conditions in terms of minimal atmospheric motion and ambient solar flux. The abundance of $C_2N_2$ at the equator was measured to be 0.055 ppb at 125 km [21]. Comparisons with photochemical models [22] suggests an abundance this high is most consistent with $N_2$ dissociation by cosmic rays in the lower stratosphere.

Interestingly, early results showed that the gradient for HCN was steeper than predicted by the current photochemical models. This suggests an additional sink for nitriles in lower atmosphere, effectively reducing their atmospheric lifetimes compared to photochemical model predictions.

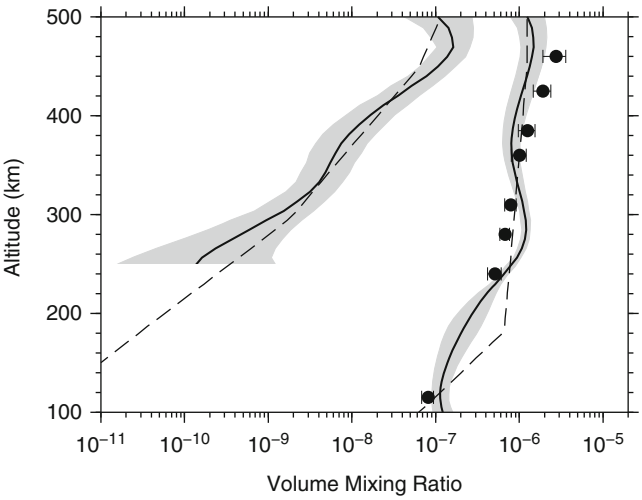


**Fig. 10.2** Profiles of HCN and $HC_3N$ from Teanby et al. [16] (*solid line* with grey error envelope) and Vinatier et al. [17] (*filled circles* with error bars) derived from CIRS limb observations in December 2004 (Tb flyby) at a latitude of 15°S. *Dashed lines* show the previous estimates from ground-based work [19]. Agreement between studies is good and shows a steep gradient for HCN and a very steep gradient for $HC_3N$

## *Global Variation of Abundances*

The early CIRS results suggest that Titan's nitriles are more complex than previously thought. Further insight into the chemical processes can be obtained by considering the distribution of nitriles across Titan's globe – a feat now possible because of the spatial sampling ability of CIRS.

At the start of the mission in 2004 Titan was experiencing early northern winter. The resulting differential heating between southern and northern hemispheres gives rise to large convection cells – analogous to the Hadley cells on Earth – which causes upwelling in the south and subsidence in the north. These vertical atmospheric motions have the ability to modify the equilibrium photochemical profiles [23, 24]. Where subsidence is occurring, the entire vertical profile is advected downwards. As a consequence of the positive vertical gradient, this leads to increased abundances at each altitude. Conversely, upwelling causes a decrease in abundance at each altitude. This phenomenon helps us in two ways:

1. By observing the increase and decrease in abundances across Titan's globe, we are able to map out vertical circulation patterns.
2. By looking at variations in subsidence-induced enrichment between different gases we can learn about the relative vertical gradients – as steeper vertical gradients will result in greater enrichment. This in turn informs us about the relative lifetimes of the different species.

The best way to map the global distribution of the different gases is by using nadir (downward looking) observation sequences. CIRS medium spectral resolution mapping scans are particularly useful for this as they observe an entire hemisphere at once and are taken on nearly every flyby. High spectral-resolution north-south swaths, although less numerous, are also extremely useful as they provide better signal-to-noise and spectral discrimination between different gases. Nadir datasets were used early in the mission [25–27] to map out the global distribution of many of Titan's trace species – including the nitriles. The early studies have subsequently been expanded [21, 24, 28–33] and the northern winter distribution of most trace species is now well understood. Figure 10.3 shows the distribution of HCN and $HC_3N$ from a typical northern winter flyby.

A large enrichment of most trace species – including nitriles – is observed at the north pole compared to the rest of the planet – indicating a large single south-to-north circulation cell with subsidence in the north, consistent with the winter season. Detailed studies of the north pole have shown there to be a strong circumpolar vortex [25, 29, 34]. The vortex is produced by a combination of poleward transport of air by the atmospheric circulation cells and conservation of angular momentum, which causes a spin up of stratospheric and mesospheric air masses. Vortex wind speeds were determined using the thermal wind equation, which implied wind speeds of nearly 200 m/s in the stratosphere at around 30–60°N. Across the vortex boundary at 60°N, there is a strong potential vorticity gradient, which indicates that a significant mixing barrier exists separating polar and non-polar air masses. Enhanced infrared emission from large abundances of trace gases such as HCN then act as an effective cooling mechanism, which further reinforces the general circulation. The chemistry and dynamics in this region are thus intimately linked.

Figure 10.3 shows that north-polar $HC_3N$ enrichment is much greater than that of HCN. This is consistent with the much shorter photochemical lifetime of $HC_3N$ (0.8 years) compared to HCN (44 years) [22]. $HC_3N$ is also confined much more closely to the north polar region than HCN. This confinement is due to the mixing barrier caused by the north polar vortex, which effectively prevents cross latitude mixing and confines species within the vortex core. Other short lifetime gases (e.g. $C_4H_2$) are also observed to be largely confined to the vortex core. HCN has a more complex behaviour, i.e. a gradual south-to-north gradient. This is largely explicable by a combination of HCN's long photochemical lifetime and steep vertical gradient. The steep gradient means it is sensitive to vertical motion – including upwelling in the southern summer hemisphere – whereas its long lifetime means it has time to escape the vortex mixing barrier and be transported to lower latitudes.

The high enrichment of many trace species within the polar vortex provides the possibility of unique chemistry, as in Earth's antarctic vortex, however this has so far been difficult to observe with CIRS due to the (assumed) complexity of any chemical products and cold temperatures. However, it is possible to use observed polar enrichments to probe the relative lifetimes of many species. If the only processes occurring are known photochemical reactions and vertical atmospheric motion, then the observed north polar enrichment should be proportional to the predicted vertical gradient, i.e. inversely proportional to the predicted species lifetime.

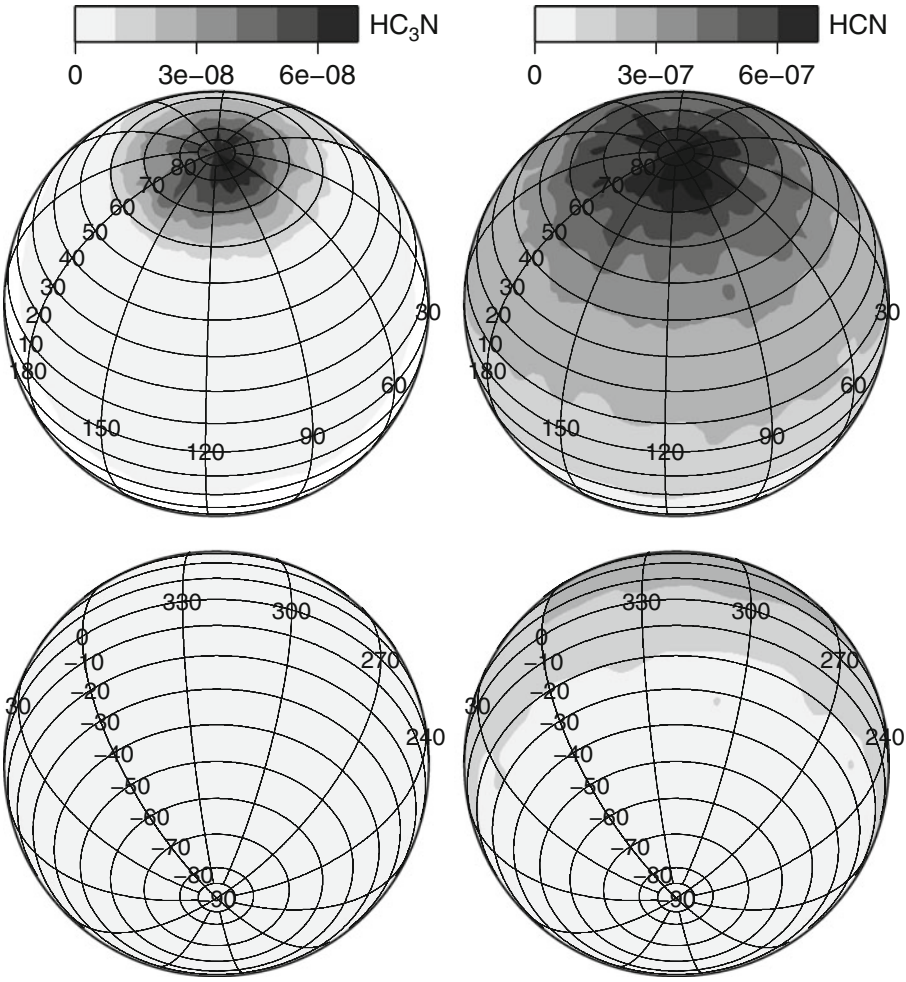


**Fig. 10.3** Maps of HCN and $HC_3N$ derived for the northern and southern hemispheres. $HC_3N$ is greatly enriched at high northern latitudes, but decreases sharply south of 60°N and is present at very low levels elsewhere. HCN is also enriched in the north, but has a more gradual variation from south to north. These observations suggest subsidence at the north pole and are consistent with the presence of a polar vortex (Redrawn from Teanby et al. [28])

Figure 10.4 shows there is indeed such a relation, but surprisingly the nitrile trend appears separate to that for hydrocarbons. This suggests that there is some additional sink mechanism causing the vertical gradient of nitriles to be steeper than expected from photochemical models. The cause of this is currently unknown, but could include incorporation of nitriles into photochemical hazes or polymerisation [31].

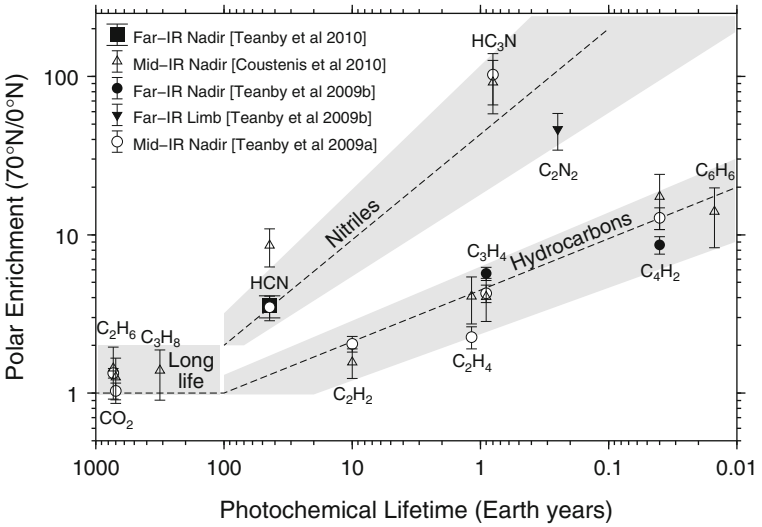


**Fig. 10.4** Observed polar enrichment as a function of predicted photochemical lifetime from Wilson and Atreya [22]. Shorter lifetime species are typically more enriched, although nitriles appear to be anomalously enriched compared to hydrocarbons. This suggests an additional loss mechanism for nitrile species (Redrawn from Teanby et al. [31])

## *Nitrile Profiles in the Northern Winter Polar Vortex*

Specific to the north polar regions are large amplitude composition layers in most trace gases, especially in the nitriles (Fig. 10.5). These layers are somewhat puzzling and could be linked to discrete haze layers observed by Cassini's Imaging Science Sub-System [35]. Suggested causes of these layers include: chemical sinks, gravity waves, incorporation into haze layers, or dynamics.

The most plausible of these is a possible dynamical origin. Teanby et al. [36] proposed that the layering was caused by cross vortex mixing, which allows polar and non-polar air masses to mix. A similar process occurs for ozone at the boundary of Earth's polar vortices [37]. In this scenario the high wind shear in the vortex causes instabilities and trace-gas poor air is transported across the vortex boundary. Conversely, displaced trace-gas rich air escapes the vortex and is mixed to non-polar atmosphere latitudes. Because the stratosphere is stably stratified, the resulting layers can be fairly long lived and persist long enough to be observed by CIRS limb observations.

If this mechanism is correct then we would expect gases with the most polar enrichment to have the largest amplitude layers, and all the gas layers for the same observation to have similar altitudes, which both appear to be the case (Fig. 10.5). This would not be the case if a chemical sink were responsible, unless it acted on all gases similarly, which seems unlikely. Also, a gravity wave origin does not seem to provide large enough amplitude to explain up to 50-fold layer amplitudes for $HC_3N$.

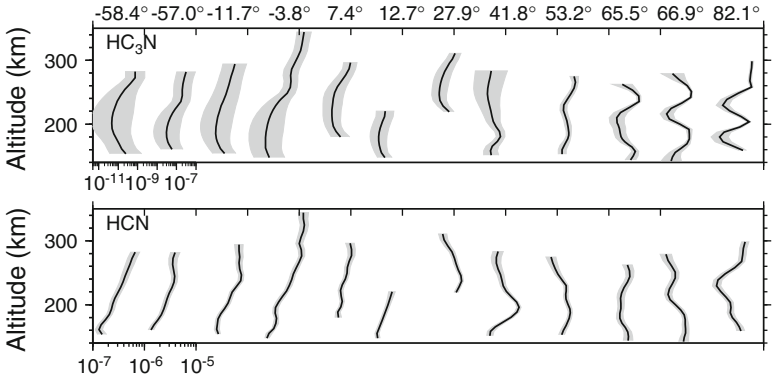


**Fig. 10.5** Profiles of HCN and $HC_3N$ derived from high spatial resolution limb data. Latitudes are given at the top and profiles from different observations are offset horizontally for clarity. North of 60°N – within the north polar vortex – large amplitude composition layers are evident. These could suggest mixing/instabilities on the vortex boundary allowing mixing of polar and non-polar airmasses (Redrawn from Teanby et al. [36])

However, it is thought that gravity waves play a role in eroding the vortex wall and contributing to the cross latitude mixing [29]. It can be seen that nitrile chemistry and atmospheric dynamics appear to be inextricably intertwined on Titan. Further insight will be possible as the Cassini mission progresses.

## Nitrile Condensables in Titan's Stratosphere

In this section, we discuss the detection of nitrile ices observed in Titan's stratosphere by CIRS. Given that CIRS is the successor to the IRIS instrument onboard Voyager, we will provide a brief overview of the ices observed by IRIS, which motivated the continued search for stratospheric ices with CIRS, nearly one Saturn year (∼30 terrestrial years) later.

### *Nitrile Ice Cloud Characteristics in the Thermal Infrared*

There are two distinct types of cloud systems in Titan's atmosphere. The first is condensed $CH_4$, typically found in Titan's troposphere and similar to water clouds in Earth's troposphere. The second type of ice cloud arises in Titan's much more dynamically stable stratosphere and is composed of condensed nitriles and/or hydrocarbons. The latter type are the clouds that CIRS detects in Titan's stratosphere.

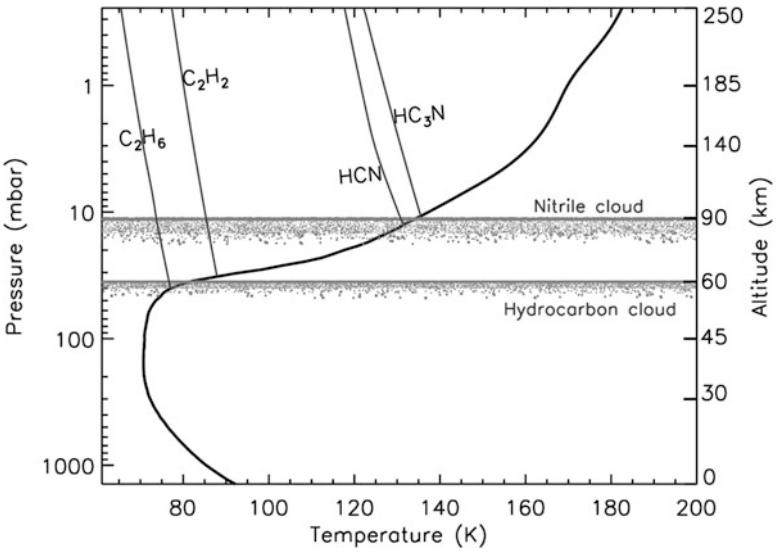


**Fig. 10.6** Figure from West et al. [38]. Temperature dependence of Titan's pressure-altitude relation (*thick black curve*) at latitude 15°S in mid-2006 [15, 34]. Superimposed are the derived saturation vapor pressure curves for the four most abundant trace organics (*dark grey curves*). Vertical distribution of vapor abundances for hydrocarbons and nitriles were patterned after [33] and [16], respectively. Condensation is expected to occur at altitudes below the intersection of the saturation vapor pressure curves with Titan's temperature structure. The *two narrow layers* represent the altitude locations of generic nitrile and hydrocarbon cloud regions where saturation can occur

The fate of most organic vapors in Titan's lower stratosphere is condensation, forming sharply layered upper boundaries near the altitude location where condensation is expected. Figure 10.6, originally published in [38], illustrates the altitude locations that are expected for such ice clouds, when using the temperature structure at 15°S during mid northern winter on Titan (circa 2006).

Whereas the IRIS low wavenumber cut-off occurred at 200 $cm^{-1}$, CIRS extends further to 10 $cm^{-1}$, covering a significant portion of the sub-millimeter spectrum that turns out to be extremely important and uniquely qualified for the detection of ice signatures from nitriles. In the far-IR between 70 and 270 $cm^{-1}$, nitrile ices reveal numerous overlapping broad-emission features caused by low-energy lattice vibrations [39]. CIRS is able to detect these signatures due to (1) its excellent signal-to-noise in this part of the far-IR spectrum and (2) the Planck intensity is quite strong in this spectral region. Hydrocarbon ices have very small absorption cross-sections in this part of the far-IR, since they tend to not have strong spectral features in this region. This hinders CIRS from detecting hydrocarbon condensate signals, even though their abundances are larger than those of condensed nitriles [27].

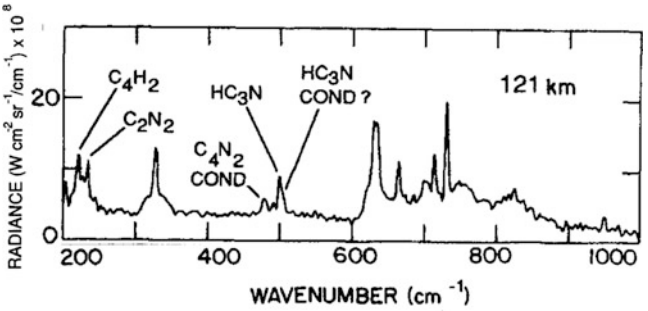


**Fig. 10.7** Figure adapted from Samuelson et al. [40]. Titan's radiance spectrum as observed by IRIS. The spectrum is an average of 3 spectra and was recorded at an altitude of 121 km above Titan's surface horizon (limb-viewing mode). The discovery of the $\nu_6$ band of crystalline $HC_3N$ at 506 $cm^{-1}$ and the putative $\nu_8$ band of crystalline $C_4N_2$ at 478 $cm^{-1}$ are easily seen

## *CIRS Observations of Nitrile Ices*

Sharp ice emission features above Titan's thermal-IR continuum are the easiest to detect provided the abundances are sufficiently large. These features point uniquely to a specific, isolated pure ice (no mixtures). Examples of such features are the $\nu_6$ band of crystalline $HC_3N$ at 506 $cm^{-1}$ and the $\nu_8$ band of crystalline $C_4N_2$ at 478 $cm^{-1}$, both of which have been observed and identified in Titan's atmosphere from first Voyager IRIS then Cassini CIRS. Figure 10.7 is an IRIS spectrum depicting both the $HC_3N$ condensate at 506 $cm^{-1}$ and the $C_4N_2$ condensate at 478 $cm^{-1}$ [40]. Since the IRIS spectral resolution of 4.3 $cm^{-1}$ was too low to spectrally separate the $HC_3N$ condensate at 506 $cm^{-1}$ from the vapor at 499 $cm^{-1}$, an abundance and particle size determination was not possible. However using the higher spectral discrimination of CIRS, both particle size and abundance were determined from observations of Titan at 70°N and 62°N during northern winter [41]. Regarding the feature at 478 $cm^{-1}$ observed by both IRIS and CIRS, and tentatively attributed to $C_4N_2$ ice based on spectral location [42], there is a caveat that the vapor has never been observed in Titan's atmosphere, which is an absolute requirement for the ice to form.[3] This is a mystery that is still being addressed today.

In contrast to the sharp ice emission features that are spectrally easy to detect, ice signatures exist in Titan's far-IR spectrum that are spectrally very broad due to low-energy lattice vibrations (librations), and are comprised of numerous overlapping emissions that are impossible to isolate individually. Even though these types of composite features are intrinsically much stronger than those due to pure ices, they are much more difficult to detect and identify because of their quasi-continuum nature. Thus, the spectral dependence must be derived from a full radiative analysis [15, 44]. An example of this type of identification is the CIRS-discovered nitrile composite ice feature that peaks at 160 $cm^{-1}$, labeled (2) in Fig. 10.8 (after [38].)

[3] An upper limit of 9 ppb for $C_4N_2$ gas was determined by de Kok et al. [43].

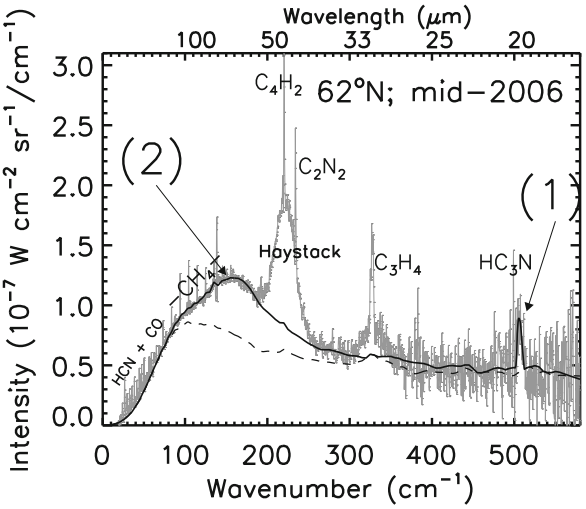


**Fig. 10.8** Figure and caption from West et al. [38]. CIRS spectrum of Titan at 62°N (*thin black curve*). Various organic vapors are labeled as is the unknown solid material has been termed the 'haystack.' The sharp 506 $cm^{-1}$ $HC_3N$ ice emission feature is labeled (1) and the broad 160 $cm^{-1}$ composite ice feature is labeled (2). The *solid* and the *dashed black curves* are respectively synthetic spectra with and without the ice contribution, fit to the data with a radiative transfer analysis. Notice that feature (1) is easily distinguished from the continuum whereas feature (2) is indistinguishable from the continuum and would not be identified as such without a radiative transfer analysis

The CIRS-derived vertical and spectral dependence of this ice feature at 160 $cm^{-1}$ is illustrated in Fig. 10.9 at latitude 15°S. This ice feature is thought to be comprised of a mix of nitrile ices based on the altitude location of the cloud (see Fig. 10.6) and the spectral dependence of the observed ice feature spans wavenumbers where nitriles have numerous overlapping absorption features [15, 39].

Our analyzes to date [15, 38, 41, 44] indicate that during mid to late northern winter on Titan (during the Cassini prime and extended missions) a system of thin nitrile ice clouds extend globally from 85°N to at least 55°S. These clouds are tentatively assigned to composites of HCN and $HC_3N$, but most likely contain additional trace nitrile ices, based on the broad emission feature seen by CIRS centered at 160 $cm^{-1}$. These ice clouds are found at altitudes around 90 km at equatorial and southern latitudes, and increase in altitude as Titan's temperature structure cools in the stratosphere, and most organic vapor abundances increase during northern winter. We expect these clouds to maintain a global distribution but the abundances will change as functions of latitude as Titan changes season.

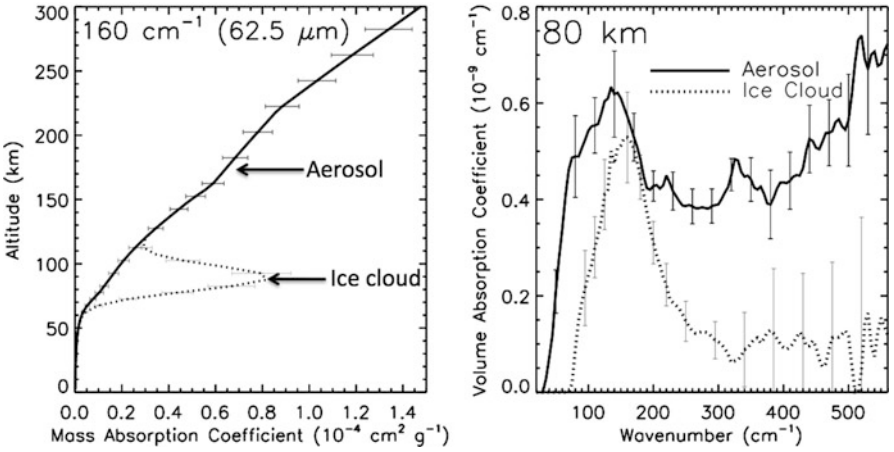


**Fig. 10.9** Figures and caption adapted from Anderson and Samuelson [15]. *Left side*: Derived vertical distributions of mass absorption coefficient at 160 $cm^{-1}$ at 15°S with 1$\sigma$ uncertainties shown. The model assumes a single aerosol and a single ice cloud component. Absorption coefficients are for aerosol only (*solid curve*) and aerosol plus ice (*dotted curve*). *Right side*: Derived spectral dependence of volume absorption coefficient at the 80 km altitude level at 15°S with 1$\sigma$ uncertainties shown. Absorption coefficients are for aerosol plus ice (*solid curve*) and ice only (*dotted curve*)

## Other N-Bearing Species and Isotopes

In this section, we discuss the search for, and measurement of, very low mixing ratio nitrogen-bearing species: the $HC^{15}N$ isotopologue of HCN, and the species $NH_3$ and $CH_3CN$ that have not yet been detected by CIRS in Titan's atmosphere, although detected previously by other techniques.

### $^{15}N$ *Isotopologues*

The study of isotopic ratios in Titan's main molecular reservoirs of nitrogen and carbon, namely $N_2$ and $CH_4$, bring information on the origin and evolution mechanisms of the atmosphere. In contrast, the study of the isotopic ratios in HCN, which is a product of the photodissociation of $CH_4$ and $N_2$ (see section "Nitrogen Chemistry"), gives us information on the atmospheric chemistry. $HC^{15}N$ was first detected from ground-based millimeter telescopes [18–20] from the 88.6 and 258.16 GHz lines. The inferred $^{14}N/^{15}N$ disk averaged isotopic ratios varied between 60.5 and 94. Subsequently CIRS detected for the first time the 711 $cm^{-1}$ band of $HC^{15}N$ [45]. Limb observations were used to constrain the $^{14}N/^{15}N$ isotopic ratio in HCN at 15°S and 83°N for altitudes between 150 and 400 km. Using a constant-with-height vertical isotopic ratio in model calculations allowed the CIRS observations to be

reproduced with values of $56^{+16}_{-13}$ and $56^{+10}_{-9}$ at 15°S and 83°N respectively. As the isotopic ratio does not vary with latitude, it is possible to derive a mean isotopic ratio of $56 \pm 8$.

This derived isotopic ratio in HCN from CIRS data is substantially lower than that measured for $N_2$ ($^{14}N/^{15}N = 167.7 \pm 0.6$) in situ with the Huygens Gas Chromatograph/Mass Spectrometer (GCMS) [1], implying that HCN is enriched in $^{15}N$ compared to $N_2$. As $N_2$ is the main nitrogen reservoir in Titan's atmosphere, its greater $^{14}N/^{15}N$ ratio compared to HCN suggests the existence of a fractionation process in the formation of HCN (daughter) from $N_2$ (parent) preferring $^{15}N$ over $^{14}N$.[4] A likely explanation has been posited [46] involving isotope-selective $N_2$ photodissociation. This process occurs at wavelengths shorter than 100 nm, mainly through predissociation transitions toward Rydberg and valence states [47–49]. These states have long enough lifetimes to display rotational and vibrational structures. The vibrational bands of the two isotopes $^{14}N^{15}N$ and $^{15}N^{15}N$ can be shifted by tens of wavenumbers compared to the $^{14}N_2$ bands [48, 50]. As $^{14}N_2$ is the most abundant isotope, it absorbs most of the solar radiation in the high atmosphere, while the radiation able to photodissociate $^{14}N^{15}N$ and $^{15}N^{15}N$ will penetrate at deeper levels. Therefore, $^{14}N^{15}N$ and $^{15}N^{15}N$ can be photo-dissociated at deeper levels than most of $^{14}N_2$ . This process can therefore greatly increases the $^{14}N/^{15}N$ isotopic ratio in HCN compared to $N_2$.

## *The Search for Further N-Bearing Molecules with CIRS*

In this subsection we discuss the search for $NH_3$ and $CH_3CN$ in Titan's stratosphere, both of which are expected to be present at low levels from photochemical models. Both ammonia and acetonitrile have been directly detected in Titan's ionosphere by the Cassini mass spectrometer (INMS) [7]. However, only acetonitrile has been previously detected in the stratospheric/mesospheric region of the atmosphere sensed by CIRS, and using ground-based sub-millimeter telescopes [19] rather than the infrared spectral region.

Therefore, a recent study by the CIRS team attempted to search rigorously for these species in the high S/N limb spectra of Titan acquired specifically for the purpose [5]. Data from long limb integrations (4 h) from two flybys (T55 at 25°S, and T64 at 76°N) were originally analyzed: since then one further observation has been analyzed as described below. The bands used were located in the 9–11 μm spectral region, where Titan's infrared spectrum is relatively uncluttered by the strong alkane and alkyne bands seen elsewhere, and CIRS has high sensitivity. For $NH_3$ , the $\nu_2$ band centered at 950 $cm^{-1}$ was employed, while the $\nu_7$ band of $CH_3CN$ at 1,041 $cm^{-1}$ was likewise selected.

[4] Or the reverse: preferential destruction of $^{14}N$-bearing HCN.

**Table 10.1** Upper limits on the abundances of $NH_3$ and $CH_3CN$ in Titan's atmosphere

| Gas | Flyby | Date | Lat. | Pressure | VMR upper limit (ppbv) | | |
|---|---|---|---|---|---|---|---|
| name | no. | | (°) | (mbar) | $1-\sigma$ | $2-\sigma$ | $3-\sigma$ |
| $NH_3$ | T55 | 22-MAY-09 | 25°S | 7.6 | 0.59 | 0.88 | 1.3 |
| | T64 | 28-DEC-09 | 76°N | 0.26 | 2.0 | 6.4 | 14 |
| $CH_3CN$ | T55 | 22-MAY-09 | 25°S | 0.27 | 49 | 78 | 109 |
| | T64 | 28-DEC-09 | 76°N | 0.018 | 660 | 830 | 1,000 |
| | T72 | 24-SEP-10 | 76°N | 0.30 | 53 | 70 | 89 |

The line list for ammonia was already available in a standard atlas (HITRAN 2008) [51], while the requisite line list for acetonitrile was created for the study. Using these line lists, synthetic Titan spectra were calculated, incrementally adding quantities of each gas to the model atmosphere, until the gas emission signature exceeded the noise threshold by 1, 2, and 3-$\sigma$ amounts. The results table of [5] is reproduced here, adding an additional data line for acetonitrile, by analysis of spectra acquired during the more recent T72 flyby (September 24th 2010) that has been computed since the 2010 publication. This adds additional constraint for $CH_3CN$ at 0.30 mbar in the stratosphere at 76°N, a lower altitude than previously (Table 10.1).

## Conclusions and Future Directions

In this chapter we have described the chemical origin and stratospheric distributions of nitrogen-bearing molecules in Titan's stratosphere as observed by Cassini CIRS, focusing on the infrared-detected nitrile gases HCN, $HC_3N$ and $C_2N_2$. Measurements of the abundances of these gases is important not only for constraining and improving models of the chemistry, but also because their different lifetimes allow us to track atmospheric motions.

At the beginning of the Cassini era in 2004, all three nitriles exhibited steep positive vertical gradients of abundance at low latitudes. In contrast, at the high northern latitudes then experiencing winter, the profiles were more nearly constant with height implying that strong subsidence was occurring – firm evidence of the large global Hadley circulation cell that had been predicted by dynamical models. The details differed for the three gases, with the longer-lived HCN showing positive enhancement even at low altitudes towards the mid-latitudes: evidence of the returning branch of the circulation cell.

The long duration of the Cassini mission (8 years in Saturn orbit and counting) is now permitting us to observe the turning of Titan's long seasons, as the northern enrichments have begun to exhibit fading, even as abundance enhancements have begun to emerge in Titan's far south. We may look forward to witnessing further details of this changing circulation during the latter years of the Cassini mission – hoped to last until 2017 near the time of northern summer solstice.

Even as we now gain some confidence in our growing knowledge of this picture, mysteries remain that continue to elude our understanding. In particular, we remark on the curious difference in the trends of enhancement versus lifetime for the nitriles shown in Fig. 10.4 compared to the hydrocarbons – with the implication that there are processes occurring that are not yet included in our models. To this list we could add the current non-detection of $CH_3CN$ in the stratosphere by CIRS (but seen by ground-based telescopes), or the similar elusiveness of $NH_3$ – firmly detected in the upper atmosphere. New missions and instruments may be required to finally resolve these and other riddles.

## References


1. Niemann, H.B., Atreya, S.K., Demick, J.E., Gautier, D., Haberman, J.A., Harpold, D.N., Kasprzak, W.T., Lunine, J.I., Owen, T.C., Raulin, F.: Composition of Titan's lower atmosphere and simple surface volatiles as measured by the Cassini-Huygens probe gas chromatograph mass spectrometer experiment. J. Geophys. Res. (Planets) **115**, 12006–+ (2010). doi:10.1029/2010JE003659
2. Hanel, R., Conrath, B., Flasar, F.M., Kunde, V., Maguire, W., Pearl, J.C., Pirraglia, J., Samuelson, R., Herath, L., Allison, M., Cruikshank, D.P., Gautier, D., Gierasch, P.J., Horn, L., Koppany, R., Ponnamperuma, C.: Infrared observations of the Saturnian system from Voyager 1. Science **212**, 192–200 (1981). doi:10.1126/science.212.4491.192
3. Kunde, V.G., Aikin, A.C., Hanel, R.A., Jennings, D.E., Maguire, W.C., Samuelson, R.E.: $C_4H_2$, $HC_3N$ and $C_2N_2$ in Titan's atmosphere. Nature **292**, 686–688 (1981). doi:10.1038/292686a0
4. Maguire, W.C., Hanel, R.A., Jennings, D.E., Kunde, V.G., Samuelson, R.E.: $C_3H_8$ and $C_3H_4$ in Titan's atmosphere. Nature **292**, 683–686 (1981). doi:10.1038/292683a0
5. Nixon, C.A., Achterberg, R.K., Teanby, N.A., Irwin, P.G.J., Flaud, J.M., Kleiner, I., Dehayem-Kamadjeu, A., Brown, L.R., Sams, R.L., Bézard, B., Coustenis, A., Ansty, T.M., Mamoutkine, A., Vinatier, S., Bjoraker, G.L., Jennings, D.E., Romani, P.N., Flasar, F.M.: Upper limits for undetected trace species in the stratosphere of Titan. Faraday Discuss. **147**, 65–+ (2010). doi:10.1039/c003771k
6. Waite, J.H., Lewis, W.S., Kasprzak, W.T., Anicich, V.G., Block, B.P., Cravens, T.E., Fletcher, G.G., Ip, W.H., Luhmann, J.G., McNutt, R.L., Niemann, H.B., Parejko, J.K., Richards, J.E., Thorpe, R.L., Walter, E.M., Yelle, R.V.: The Cassini Ion and Neutral Mass Spectrometer (INMS) Investigation. Space Sci. Rev. **114**, 113–231 (2004). doi:10.1007/s11214-004-1408-2
7. Vuitton, V., Yelle, R.V., McEwan, M.J.: Ion chemistry and N-containing molecules in Titan's upper atmosphere. Icarus **191**, 722–742 (2007). doi:10.1016/j.icarus.2007.06.023
8. Flasar, F.M., Kunde, V.G., Abbas, M.M., Achterberg, R.K., Ade, P., Barucci, A., Bézard, B., Bjoraker, G.L., Brasunas, J.C., Calcutt, S., Carlson, R., Césarsky, C.J., Conrath, B.J., Coradini, A., Courtin, R., Coustenis, A., Edberg, S., Edgington, S., Ferrari, C., Fouchet, T., Gautier, D., Gierasch, P.J., Grossman, K., Irwin, P., Jennings, D.E., Lellouch, E., Mamoutkine, A.A., Marten, A., Meyer, J.P., Nixon, C.A., Orton, G.S., Owen, T.C., Pearl, J.C., Prangé, R., Raulin, F., Read, P.L., Romani, P.N., Samuelson, R.E., Segura, M.E., Showalter, M.R., Simon-Miller, A.A., Smith, M.D., Spencer, J.R., Spilker, L.J., Taylor, F.W.: Exploring The Saturn System In The Thermal Infrared: The Composite Infrared Spectrometer. Space Sci. Rev. **115**, 169–297 (2004). doi:10.1007/s11214-004-1454-9
9. Lavvas, P., Coustenis, A., Vardavas, I.: Coupling photochemistry with haze formation in Titan's atmosphere, part I: Model description. Planet. Space Sci. **56**(1), 27–66 (2008). doi:10.1016/j.pss.2007.05.026. http://www.sciencedirect.com/science/article/B6V6T-4PN05S4-2/2/

2f028ed3f317ff898f73c50d4b73fb21. Surfaces and Atmospheres of the Outer Planets, their Satellites and Ring Systems: Part III, European Geosciences Union General Assembly – Sessions PS3.02 and PS3.03

10. Kunde, V.G., Ade, P.A., Barney, R.D., Bergman, D., Bonnal, J.F., Borelli, R., Boyd, D., Brasunas, J.C., Brown, G., Calcutt, S.B., Carroll, F., Courtin, R., Cretolle, J., Crooke, J.A., Davis, M.A., Edberg, S., Fettig, R., Flasar, M., Glenar, D.A., Graham, S., Hagopian, J.G., Hakun, C.F., Hayes, P.A., Herath, L., Horn, L., Jennings, D.E., Karpati, G., Kellebenz, C., Lakew, B., Lindsay, J., Lohr, J., Lyons, J.J., Martineau, R.J., Martino, A.J., Matsumura, M., McCloskey, J., Melak, T., Michel, G., Morell, A., Mosier, C., Pack, L., Plants, M., Robinson, D., Rodriguez, L., Romani, P., Schaefer, W.J., Schmidt, S., Trujillo, C., Vellacott, T., Wagner, K.,Yun, D.: Cassini infrared Fourier spectroscopic investigation. In: Horn L. (ed.) Society of Photo-Optical Instrumentation Engineers (SPIE) Conference Series, vol. 2803, pp. 162–177, Denver, Colorado (1996)
11. Brasunas, J.C., Lakew, B.: Long-term stability of the Cassini Fourier Transform spectrometer en route to Saturn. Recent Res. Dev. Opt. **4**, 95–113 (2004)
12. Nixon, C.A., Teanby, N.A., Calcutt, S.B., Aslam, S., Jennings, D.E., Kunde, V.G., Flasar, F.M., Irwin, P.G., Taylor, F.W., Glenar, D.A., Smith, M.D.: Infrared limb sounding of Titan with the Cassini Composite InfraRed Spectrometer: effects of the mid-IR detector spatial responses. Appl. Opt. **48**, 1912–+ (2009). doi:10.1364/AO.48.001912
13. Nixon, C.A., Achterberg, R.K., Flasar, F.M.: Infrared Limb Sounding With Cassini CIRS: Optimal Viewing Strategy Using Horizon Nodes. IEEEAC 1174 (2010)
14. Nixon, C.A., Ansty, T.M., Flasar, F.M., Achterberg, R.K.: Designing infrared observations of Titan's atmosphere with Cassini CIRS. IEEEAC 1633 (2012)
15. Anderson, C.M., Samuelson, R.E.: Titan's aerosol and stratospheric ice opacities between 18 and 500 μm: Vertical and spectral characteristics from Cassini CIRS. Icarus **212**, 762–778 (2011)
16. Teanby, N.A., Irwin, P.G.J., de Kok, R., Vinatier, S., Bézard, B., Nixon, C.A., Flasar, F.M., Calcutt, S.B., Bowles, N.E., Fletcher, L., Howett, C., Taylor, F.W.: Vertical profiles of HCN, $HC_3N$, and $C_2H_2$ in Titan's atmosphere derived from Cassini/CIRS data. Icarus **186**, 364–384 (2007)
17. Vinatier, S., Bézard, B., Fouchet, T., Teanby, N.A., de Kok, R., Irwin, P.G.J., Conrath, B.J., Nixon, C.A., Romani, P.N., Flasar, F.M., Coustenis, A.: Vertical abundance profiles of hydrocarbons in Titan's atmosphere at 15°S and 80°N retrieved from Cassini/CIRS spectra. Icarus **188**, 120–138 (2007)
18. Hidayat, T., Marten, A., Bézard, B., Gautier, D., Owen, T., Matthews, H., Paubert, G.: Millimeter and submillimeter heterodyne observations of Titan, retrieval of the vertical profile of HCN and the $C^{12}/C^{13}$ ratio. Icarus **126**(1), 170–182 (1997)
19. Marten, A., Hidayat, T., Biraud, Y., Moreno, R.: New millimeter heterodyne observations of Ttan: vertical distributions of nitriles HCN, $HC_3N$, $CH_3CN$, and the isotopic ratio $^{15}N/^{14}N$ in its atmosphere. Icarus **158**, 532–544 (2002)
20. Gurwell, M.A.: Submillimeter observations of Titan: global measures of stratospheric temperature, CO, HCN, $HC_3N$, and the isotopic ratios $^{12}C/^{13}C$ and $^{14}N/^{15}N$. Astrophys. J. **616**, L7–L10 (2004)
21. Teanby, N.A., Irwin, P.G.J., de Kok, R., Jolly, A., Bézard, B., Nixon, C.A., Calcutt, S.B.: Titan's stratospheric $C_2N_2$, $C_3H_4$, and $C_4H_2$ abundances from Cassini/CIRS far-infrared spectra. Icarus **202**, 620–631 (2009)
22. Wilson, E.H., Atreya, S.K.: Current state of modeling the photochemistry of Titan's mutually dependent atmosphere and ionosphere. J. Geophys. Res. **109**, E06002 (2004)
23. Lebonnois, S., Toublanc, D., Hourdin, F., Rannou, P.: Seasonal variations of Titan's atmospheric composition. Icarus **152**, 384–406 (2001)
24. Teanby, N.A., Irwin, P.G.J., de Kok, R., Nixon, C.A.: Dynamical implications of seasonal and spatial variations in Titan's stratospheric composition. Philos. Trans. R. Soc. Lond. A **367**, 697–711 (2009)

25. Flasar, F.M., Achterberg, R.K., Conrath, B.J., Gierasch, P.J., Kunde, V.G., Nixon, C.A., Bjoraker, G.L., Jennings, D.E., Romani, P.N., Simon-Miller, A.A., Bézard, B., Coustenis, A., Irwin, P.G.J., Teanby, N.A., Brasunas, J., Pearl, J.C., Segura, M.E., Carlson, R.C., Mamoutkine, A., Schinder, P.J., Barucci, A., Courtin, R., Fouchet, T., Gautier, D., Lellouch, E., Marten, A., Prange, R., Vinatier, S., Strobel, D.F., Calcutt, S.B., Read, P.L., Taylor, F.W., Bowles, N., Samuelson, R.E., Orton, G.S., Spilker, L.J., Owen, T.C., Spencer, J.R., Showalter, M.R., Ferrari, C., Abbas, M.M., Raulin, F., Edgington, S., Ade, P., Wishnow, E.H.: Titan's atmospheric temperatures, winds, and composition. Science **308**, 975–978 (2005)
26. Teanby, N.A., Irwin, P.G.J., de Kok, R., Nixon, C.A., Coustenis, A., Bézard, B., Calcutt, S.B., Bowles, N.E., Flasar, F.M., Fletcher, L., Howett, C., Taylor, F.W.: Latitudinal variations of HCN, $HC_3N$, and $C_2N_2$ in Titan's stratosphere derived from Cassini CIRS data. Icarus **181**, 243–255 (2006)
27. Coustenis, A., Achterberg, R.K., Conrath, B.J., Jennings, D.E., Marten, A., Gautier, D., Nixon, C.A., Flasar, F.M., Teanby, N.A., Bézard, B., Samuelson, R.E., Carlson, R.C., Lellouch, E., Bjoraker, G.L., Romani, P.N., Taylor, F.W., Irwin, P.G., Fouchet, T., Hubert, A., Orton, G.S., Kunde, V.G., Vinatier, S., Mondellini, J., Abbas, M.M., Courtin, R.: The composition of Titan's stratosphere from Cassini/CIRS mid-infrared spectra. Icarus **189**, 35–62 (2007)
28. Teanby, N.A., Irwin, P.G.J., de Kok, R., Nixon, C.A., Coustenis, A., Royer, E., Calcutt, S.B., Bowles, N.E., Fletcher, L., Howett, C., Taylor, F.W.: Global and temporal variations in hydrocarbons and nitriles in Titan's stratosphere for northern winter observed by Cassini/CIRS. Icarus **193**, 595–611 (2008)
29. Teanby, N.A., de Kok, R., Irwin, P.G.J., Osprey, S., Vinatier, S., Gierasch, P.J., Read, P.L., Flasar, F.M., Conrath, B.J., Achterberg, R.K., ezard, B., Nixon, C.A., Calcutt, S.B.: Titan's winter polar vortex structure revealed by chemical tracers. J. Geophys. Res. **113**, E12003 (2008)
30. Coustenis, A., Nixon, C., Achterberg, R., Lavvas, P., Vinatier, S., Teanby, N., Bjoraker, G., Carlson, R., Piani, L., Bampasidis, G., Flasar, F., Romani, P.: Titan trace gaseous composition from CIRS at the end of the Cassini-Huygens prime mission. Icarus **207**, 461–476 (2010)
31. Teanby, N.A., Irwin, P.G.J., de Kok, R., Nixon, C.A.: Mapping Titan's HCN in the far infrared: implications for photochemistry. Faraday Discuss. **147**, 51–64 (2010)
32. Teanby, N.A., Irwin, P.G.J., de Kok, R., Nixon, C.A.: Seasonal changes in Titan's polar trace gas abundance observed by Cassini. Astrophys. J. **724**, L84–L89 (2010)
33. Vinatier, S., Bézard, B., Nixon, C.A., Mamoutkine, A., Carlson, R.C., Jennings, D.E., Guandique, E.A., Teanby, N.A., Bjoraker, G.L., Flasar, F.M., Kunde, V.G.: Analysis of Cassini/CIRS limb spectra of Titan acquired during the nominal mission I. hydrocarbons, nitriles and $CO_2$ vertical mixing ratio profiles. Icarus **205**, 559–570 (2010)
34. Achterberg, R.K., Conrath, B.J., Gierasch, P.J., Flasar, F.M., Nixon, C.A.: Titan's middle-atmospheric temperatures and dynamics observed by the Cassini Composite Infrared Spectrometer. Icarus **194**, 263–277 (2008)
35. Porco, C.C., Baker, E., Barbara, J., Beurle, K., Brahic, A., Burns, J.A., Charnoz, S., Cooper, N., Dawson, D.D., Del Genio, A.D., Denk, T., Dones, L., Dyudina, U., Evans, M.W., Fussner, S., Giese, B., Grazier, K., Helfenstein, P., Ingersoll, A.P., Jacobson, R.A., Johnson, T.V., McEwen, A., Murray, C.D., Neukum, G., Owen, W.M., Perry, J., Roatsch, T., Spitale, J., Squyres, S., Thomas, P., Tiscareno, M., Turtle, E.P., Vasavada, A.R., Veverka, J., Wagner, R., West, R.: Imaging of Titan from the Cassini spacecraft. Nature **434**, 159–168 (2005)
36. Teanby, N.A., Irwin, P.G.J., de Kok, R.: Small-scale composition and haze layering in titan's polar vortex. Icarus **204**, 645–657 (2009)
37. Orsolini, Y.J.: On the formation of ozone laminae at the edge of the Arctic polar vortex. Quart. J. R. Meteorol. Soc. **121**, 1923–1941 (1995)
38. West, R., Lavvas, P., Anderson, C., Imanaka, H.: in Mueller-Wodarg, I., Griffith, C.A., Lellouch, E. & Cravens, T. (eds.) Titan: Surface, Atmosphere and Magnetosphere. Cambridge University Press/Cambridge Planetary Science Series (2013)
39. Moore, M.H., Ferrante, R.F., Moore, W.J., Hudson, R.: Infrared Spectra and Optical Constants of Nitrile Ices Relevant to Titan's Atmosphere. Astrophys. J. Suppl. **191**, 96–112 (2010)

40. Samuelson, R.E., Mayo, L.A., Knuckles, M.A., Khanna, R.J.: $C_4N_2$ ice in Titan's north polar stratosphere. Planet. Space Sci. **45**, 941–948 (1997)
41. Anderson, C.M., Samuelson, R.E., Bjoraker, G.L., Achterberg, R.K.: Particle size and abundance of $HC_3N$ ice in Titan's lower stratosphere at high northern latitudes. Icarus **207**, 914–922 (2010)
42. Masterson, C.M., Khanna, R.K.: Absorption intensities and complex refractive indices of crystalline HCN, $HC_3N$, and $C_4N_2$ in the infrared region. Icarus **83**, 83–92 (1990)
43. de Kok, R., Irwin, P.G.J., Teanby, N.A.: Condensation in Titan's stratosphere during polar winter. Icarus **197**, 572–578 (2008)
44. de Kok, R., Irwin, P.G.J., Teanby, N.A., Nixon, C.A., Jennings, D.E., Fletcher, L., Howett, C., Calcutt, S.B., Bowles, N.E., Flasar, F.M., Taylor, F.W.: Characteristics of Titan's stratospheric aerosols and condensate clouds from Cassini CIRS far-infrared spectra. Icarus **191**, 223–235 (2007). doi:10.1016/j.icarus.2007.04.003
45. Vinatier, S., Bézard, B., Nixon, C.A.: The Titan $^{14}N/^{15}N$ and $^{12}C/^{13}C$ isotopic ratios in HCN from Cassini/CIRS. Icarus **191**, 712–721 (2007). doi:10.1016/j.icarus.2007.06.001
46. Liang, M.C., Heays, A.N., Lewis, B.R., Gibson, S.T., Yung, Y.L.: Source of Nitrogen Isotope Anomaly in HCN in the Atmosphere of Titan. Astrophys. J. Lett. **664**, L115–L118 (2007). doi:10.1086/520881
47. Haverd, V.E., Lewis, B.R., Gibson, S.T., Stark, G.: Rotational effects in the band oscillator strengths and predissociation linewidths for the lowest $^1\Pi_u$-$X^1\Sigma_g^+$ transitions of $N_2$. J. Chem. Phys. **123**, 214304 (2005). doi:10.1063/1.2134704
48. Lewis, B.R., Gibson, S.T., Zhang, W., Lefebvre-Brion, H., Robbe, J.M.: Predissociation mechanism for the lowest $^1\Pi_u$ states of $N_2$. J. Chem. Phys. **122**, 144302 (2005). doi:10.1063/1.1869986
49. Stark, G., Huber, K.P., Yoshino, K., Smith, P.L., Ito, K.: Oscillator strength and linewidth measurements of dipole-allowed transitions in $^{14}N_2$ between 93.5 and 99.5 nm. J. Chem. Phys. **123**, 214303 (2005). doi:10.1063/1.2134703
50. Sprengers, J.P., Ubachs, W., Baldwin, K.G.H., Lewis, B.R., Tchang-Brillet, W.Ü.L.: Extreme ultraviolet laser excitation of isotopic molecular nitrogen: The dipole-allowed spectrum of $^{15}N_2$ and $^{14}N^{15}N$. J. Chem. Phys. **119**, 3160–3173 (2003). doi:10.1063/1.1589478
51. Rothman, L.S., Gordon, I.E., Barbe, A., Benner, D.C., Bernath, P.F., Birk, M., Boudon, V., Brown, L.R., Campargue, A., Champion, J.P., Chance, K., Coudert, L.H., Dana, V., Devi, V.M., Fally, S., Flaud, J.M., Gamache, R.R., Goldman, A., Jacquemart, D., Kleiner, I., Lacome, N., Lafferty, W.J., Mandin, J.Y., Massie, S.T., Mikhailenko, S.N., Miller, C.E., Moazzen-Ahmadi, N., Naumenko, O.V., Nikitin, A.V., Orphal, J., Perevalov, V.I., Perrin, A., Predoi-Cross, A., Rinsland, C.P., Rotger, M.,Šimečková, M., Smith, M.A.H., Sung, K., Tashkun, S.A., Tennyson, J., Toth, R.A., Vandaele, A.C., Vander Auwera, J.: The HITRAN 2008 molecular spectroscopic database. J. Quant. Spectrosc. Radiat. Transf. **110**, 533–572 (2009). doi:10.1016/j.jqsrt.2009.02.013

# Chapter 11
# Nitrogen in Titan's Atmospheric Aerosol Factory

**Nathalie Carrasco, Joseph Westlake, Pascal Pernot, and Hunter Waite Jr.**

**Abstract** Titan's organic aerosols are presumed to contain a large amount of nitrogen as inferred from the in situ measurements of the ACP instrument on board the Huygens probe. They show major emissions of ammonia and hydrogen cyanide after pyrolysis of the refractory nuclei of the atmospheric aerosols. Molecular nitrogen is a rather chemically inert molecule and the processes leading to the high nitrogen content of Titan's aerosols are far from being understood. Here we synthesize the results obtained on Titan's nitrogen composition from analysis of laboratory analogues produced with the PAMPRE experimental setup. These analogues are compared with the in situ measurements of the Cassini CAPS-IBS instrument.

## Introduction

Molecular nitrogen is the major component of Titan's dense atmosphere. This inert molecule is activated in the upper atmosphere by VUV radiations and particle impact ionization, causing its partial dissociation and ionization. Nitrogen radicals and ions further participate in the production of heavier nitrogen-containing species, as well as participate in reactions with methane that enable the initiation of the

N. Carrasco (✉)
LATMOS, UVSQ-UPMC-CNRS, Guyancourt, France
e-mail: nathalie.carrasco@latmos.ipsl.fr

J. Westlake
Applied Physics Laboratory, The Johns Hopkins University, Laurel, MD, USA

P. Pernot
Laboratoire de Chimie Physique, UMR8000 CNRS/Université Paris-Sud, Orsay, France

H. Waite Jr.
SwRI, San Antonio, TX, USA

J.M. Trigo-Rodriguez et al. (eds.), *The Early Evolution of the Atmospheres of Terrestrial Planets*, Astrophysics and Space Science Proceedings 35,
DOI 10.1007/978-1-4614-5191-4_11, 

complex organic chemistry in Titan's upper atmosphere. Instruments on board Cassini detected N-containing neutrals in the stratosphere (Coustenis et al. 2007; Teanby et al. 2007, 2010; Vinatier et al. 2010) and in the upper atmosphere (Magee et al. 2009) and N-containing ions in the ionosphere (Cravens et al. 2006; Vuitton et al. 2007, 2009; Yelle et al. 2010).

Titan is well known for its brownish photochemical haze hiding the surface of the satellite. One of the main results provided by the Cassini space mission was to reveal that the organic macromolecules that leads to Titan's aerosol formation are first primarily produced in the ionosphere (Waite et al. 2007), before sedimenting in lower atmospheric layers, and leading to a detached haze layer in Titan's stratosphere (Lavvas et al. 2009).

The efficient integration of nitrogen in the gas products, as observed by the CIRS and INMS instruments, encourages the development of models that incorporate nitrogen efficiently into the aerosols (Lebonnois et al. 2002; Wilson and Atreya 2003; Lavvas et al. 2008; Pernot et al. 2010). The Huygens descent in situ data confirm this idea: the refractory nuclei of Titan's aerosols samples were pyrolised by the ACP instrument during the descent of the Huygens probe in 2004 (Israel et al. 2005). The gas resulting from this combustion process contained large amounts of hydrogen cyanide (HCN) and ammonia ($NH_3$), which are tracers of significant nitrogen content in Titan's aerosols.

However, neither the precise content, nor the chemical form of nitrogen in Titan's aerosols is known yet. The exact composition and structure of this complex chemical matter remains an open question. To find some clues, several research teams carried out laboratory simulation activities.

To simulate Titan's upper atmosphere reactivity, reactive nitrogen has to be produced in the laboratory. This involves the use of energy wavelengths lower than 100 nm/12 eV. This VUV range is excluded by regular photolytic reactor because of their absorbing windows, but is accessible to windowless reactors coupled with synchrotron light sources (Imanaka and Smith 2007, 2010; Peng et al. 2013) and to plasma discharge sources (Khare et al. 1984; Coll et al. 1999; Somogyi et al. 2005; Szopa et al. 2006). These laboratory studies inform us of the possible mechanisms in competition in such complex ionized media, leading to aerosol nucleation. The present paper reports recent results obtained with the PAMPRE plasma experiment on nitrogen incorporation processes in Titan's aerosol analogues.

## The PAMPRE Experimental Setup

The PAMPRE set up is a plasma-based experiment, where a 13.56 MHz Radio Frequency Capacitively Coupled Plasma discharge is generated in a $N_2 - CH_4$ gaseous mixture (Fig. 11.1). Solid organic, negatively charged, particles are produced and maintained in levitation between the electrodes by electrostatic forces. The $N_2 - CH_4$ gaseous mixture is injected continuously into the plasma reactor, as a downward-oriented neutral flow. It produces a neutral drag force, which can eject the

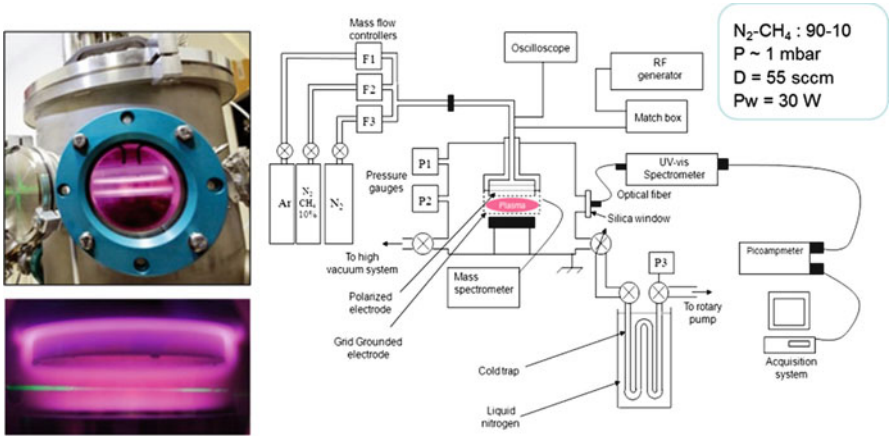


**Fig. 11.1** The PAMPRE setup. The *pink glow* is due to emission lines of molecular nitrogen, the *green line* corresponds to the light-scattering of a green laser (432 nm) by the aerosols in suspension in the reactive volume

solid particles out of the plasma discharge. The samples analyzed in the following were obtained in these operating conditions: room temperature, a total pressure of 0.9 mbar, a flow rate of $55.0 \pm 0.1$ sccm and an absorbed radio frequency power of $30 \pm 2$ W.

## Chemical Analysis of the Aerosols

PAMPRE aerosols were produced for different $N_2 - CH_4$ mixing ratios and characterized by a series of analytical methods.

***Elemental Analysis***

An elemental analysis of the aerosols was presented in Sciamma-O'Brien et al. (2010) from a determination of composition. The main results are presented in Fig. 11.2. The amount of carbon does not vary significantly with the amount of $CH_4$ injected in the plasma, and the nitrogen content remains high in all cases, from about 15 up to 30%. However, this analysis reveals a competition between hydrogen and nitrogen elements in the aerosol composition, the aerosols getting more hydrogen-rich and nitrogen-poor when the amount of injected $CH_4$ increases. As a consequence the N/C ratio decreases linearly from about 1 down to 0.5 with the initial methane amount.

To understand this nitrogen vs. hydrogen competition relative to carbon, several parameters were quantified and compared as a function of the initial content of methane in the gas mixture: atomic hydrogen density was quantified in the reactive medium by Carrasco et al. (2012); the aerosol production efficiency, defined as the mass of carbon incorporated in the aerosols divided by the mass of carbon consumed

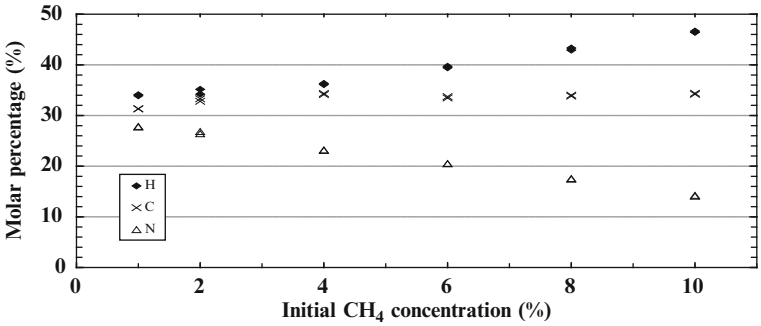


**Fig. 11.2** Elemental analysis of the Titan's aerosol analogues produced with initial methane amount varying from 1 to 10% (Adapted from Sciamma-O'Brien et al. (2010))

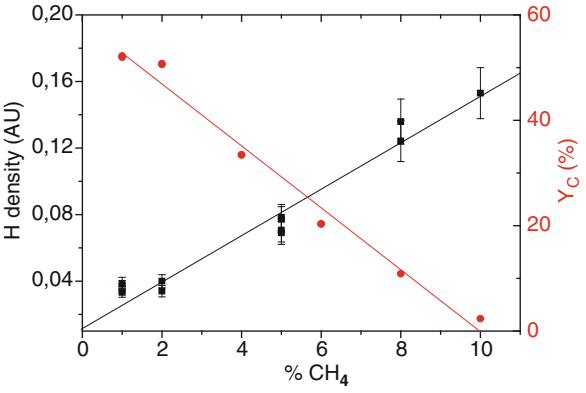


**Fig. 11.3** (*Black*) Atomic hydrogen density in arbitrary units measured by Optical Emission Spectroscopy (Carrasco et al. 2012).(*Red*) Aerosol production efficiency, $Y_C = m_{Caerosol}/m_{CH4consumed}$ (Sciamma-O'Brien et al. 2010)

by methane dissociation, was measured by Sciamma-O'Brien et al. (2010). A strong negative correlation is found between these two parameters (Fig. 11.3).

As atomic hydrogen is a well-known competitor for heterogeneous chemistry, able to saturate the adsorption sites of active surfaces, it appears that atomic hydrogen possibly inhibits the organic growth process. In the case of a gas mixture, with a 10% initial content of methane, products remain almost exclusively in the gas phase ($Y_C$ of a few%), whereas the gas-to-solid conversion increases up to 50% for gas mixtures with initial methane content lower than 2% (Fig. 11.3).

The organic growth process certainly involves additions on unsaturated functions. It is therefore favored by the abundant content of nitrogen-containing unsaturated functions, as shown by the high resolution mass analysis of Somogyi et al. (2005), and by the MSMS identification of the systematic $N \equiv C-NH-C \equiv N$ pattern in the molecules composing the aerosols (Carrasco et al. 2009).

### *High-Resolution Mass Spectrometry*

The chemical composition of aerosols has been studied in more details by extracting their soluble fraction in methanol. The extract of an aerosol prepared in a $N_2 - CH_{s4}$ 98–2% gas mixture, has been analyzed in Pernot et al. (2010) by

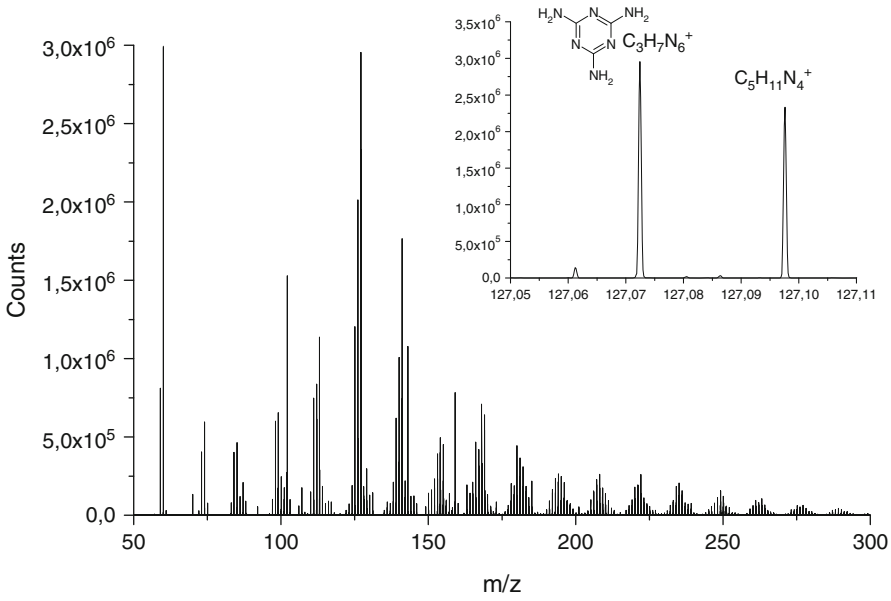


**Fig. 11.4** High resolution mass spectrum in the 50–300 m/z range of a PAMPRE aerosol prepared in a $N_2/CH_4$ 98–2% mixture, and extracted in methanol. A zoom on the 127.05–127.15 m/z range is given in the insert. The main ion detected at $m/z = 127.07$ is likely the protonated form of melamine, whose structure is plotted in the inset

ESI-FT-Orbitrap mass spectrometry, at a high resolving power of $M/\Delta M = 100,000$ at $m/z = 400$ (Fig. 11.4). High resolution enabled us to assign the composition of each peak (exact mass determination). As the extracted neutral species are softly singly protonated during the electrospray ionization step, the ions detected by this technique correspond actually to a $[M+H]^+$ structure, M being the native neutral.

Almost all identified compounds contain nitrogen, often in significant amounts. For example, a major peak at $m/z = 127.07$ exhibits the signature of a $C_3H_7N_6^+$ ion. The exact structure of the corresponding neutral is not provided by high resolution mass spectrometry, but this formula is consistent with melamine (structure in Fig. 11.4, inset). This structure alternates C and N in the skeleton of the molecule, which is in agreement with the systematic fragment NC-NH-CN detected by MSMS in Carrasco et al. (2009).

To analyze more globally the primary mass patterns constituting the soluble fraction of the aerosols, the analysis of the mass spectra can be carried out using van Krevelen diagrams, in which one plots the H/C ratio versus the N/C ratio for each molecule (Fig. 11.5). This diagram is rather symmetric, and presents an accumulation towards the point ($N/C = 0.5$; $H/C = 1.5$), in agreement with the global elemental analysis shown in Fig. 11.2, and therefore confirming the large incorporation of nitrogen into the aerosols.

The alternation of carbon and nitrogen in the structure of the molecules requires identifying gaseous precursors in agreement with this pattern. Vuitton et al. (2010)

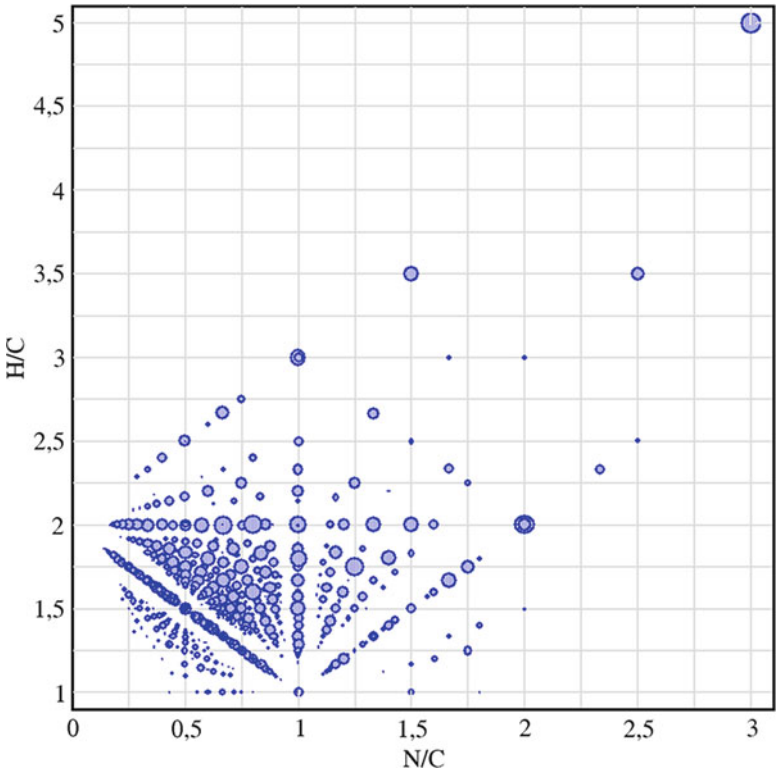


**Fig. 11.5** H/C vs. N/C van Krevelen diagram plotted from chemical formulae identified in the high resolution mass spectrum of Fig. 11.4. Each point is a species detected in the mass spectrum, and the size of the *circle* corresponds to the relative intensity of the peak (some points overlap)

have shown that PAMPRE aerosols are much more complex than a poly-HCN structure. Carrasco et al. (2012), in agreement with the model of Yelle et al. (2010) and the experimental study of Balucani et al. (2010), suggest a polymerization pathway through imine molecules, such as methanimine $CH_2 = NH$, and ethanimine $CH_3CH = NH$, which are detected as products in the plasma gas mixture.

## Comparison with CAPS Measurements

The Cassini Plasma Spectrometer (CAPS) onboard Cassini has measured large positive and negative ions through several flybys of Titan's ionosphere (Coates et al. 2007; Waite et al. 2007; Crary et al. 2009). The CAPS suite of instruments consists of the Ion Mass Spectrometer (CAPS-IMS), the Ion Beam Spectrometer (CAPS-IBS), and the Electron Spectrometer (CAPS-ELS). The CAPS-IBS has been used for its high energy resolution (0.014 $\Delta E/E$) as a rudimentary mass

spectrometer to measure heavy ions with masses reported above 250 Da. The CAPS-ELS is used in the same way with a more crude energy resolution. These two curved plate electrostatic analyzers function as mass spectrometers because of the large Mach number of the cold ionospheric ions rammed into the instrument during a pass (Cassini is generally moving around 6 km/s with respect to Titan's atmosphere resulting in a Mach number around 14 for a mass of 100 Da.). In this work we focus on the CAPS-IBS measurements of the large positive ions during the T40 dayside flyby and the T57 nightside flyby. The process of converting the energy per charge spectrum to a mass per charge spectrum utilizes a cross calibration between the CAPS-IBS and the Ion and Neutral Mass Spectrometer (INMS) that uses the spacecraft potential, ion temperature, relative amplitude, and along-track wind components as free parameters (Crary et al. 2009).

Studies with pure hydrocarbon plasmas at low pressures have shown that significant aromatic growth can occur in the absence of nitrogen. Deschenaux et al. (1999) used discharges in relatively low pressure (0.1 mbar) $CH_4$, $C_2H_2$, and $C_2H_4$, in order to study the effect of single, double, and triple carbon bonds on the production of aerosols. They found that molecular growth was fastest and achieved the largest growth with the (triply bonded) acetylene ($C_2H_2$) plasma. The ethylene ($C_2H_4$) plasma showed similar growth, but at a slower pace, while the methane plasma showed little growth and proceeded very slowly.

The positive ion spectra of these three experiments are compared with the T57 CAPS-IBS spectra within 50 km of closest approach in Fig. 11.6. The comparison is striking: the $CH_4$ plasma shows good correspondence up to the C5 group, while the $C_2H_2$ and $C_2H_4$ plasmas show nearly perfect correspondence throughout the spectra. The acetylene plasma has a clear even carbon number preference, as the triple bond is prevalent throughout the compounds. The ethylene plasma has a greater tendency to produce aliphatic compounds than the acetylene plasma, hence the wider peak groupings. From this comparison and the prevalence of acetylene and ethylene in the neutral atmosphere it is likely that the ion chemistry at Titan is proceeding through similar pathways. Of course, since these are hydrocarbon-only plasmas, there is a preference for odd masses. At Titan, the nitrogen-containing compounds fill in many of the even masses (Vuitton et al. 2007).

It is however to be noted that the positive ion hydrocarbon growth detected in pure hydrocarbon plasmas decreases rapidly for masses larger than 100 amu, which is in disagreement with the long tail observed in the CAPS-IBS mass distribution.

A comparison of the T40 and T57 CAPS-IBS mass spectra with the PAMPRE aerosols is presented in Fig. 11.6 (top). The high resolution mass spectrum shown Fig. 11.4 is reported in Fig. 11.6 as a high resolution spectrum and a low resolution spectrum, by convolution with the CAPS-IBS response function. Two aspects of this comparison are useful: (i) the peak locations of the C10 and heavier peaks occur at nearly the same location; and (ii) the falloff with mass and the observed peaks at the end of the spectrum are similar. In contrast with the pure hydrocarbon plasma ion mass spectra represented on Fig. 11.6, the PAMPRE aerosol mass spectrum is in excellent agreement with the heavier ions (masses larger than 100 amu) detected by CAPS-IBS.

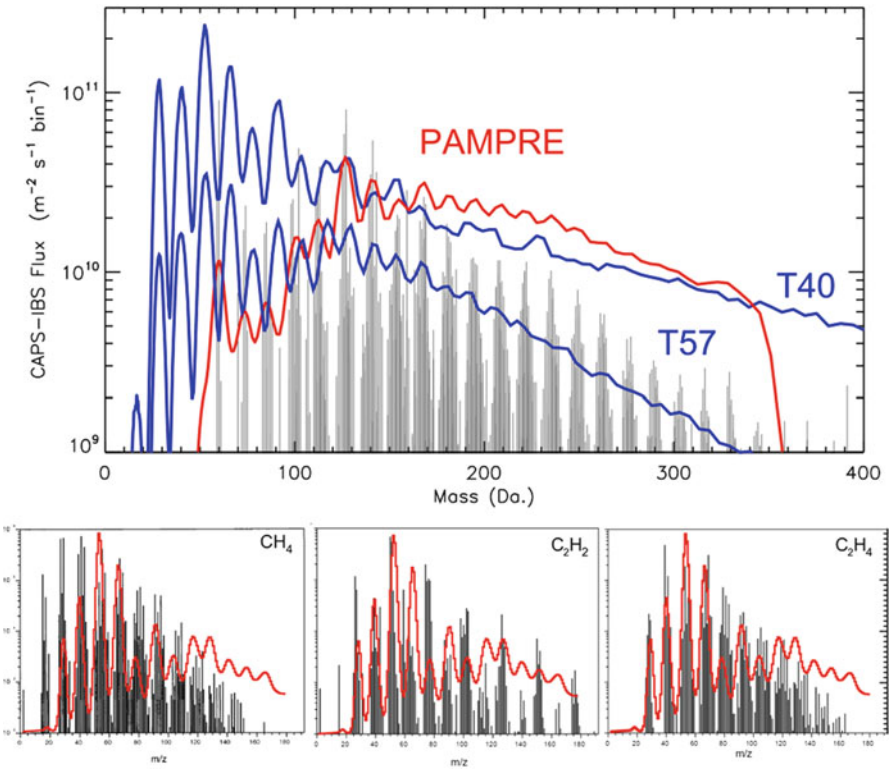


**Fig. 11.6** Shown are the T40 and T57 ion INMS spectra (*blue*) taken at 1,015 km (Westlake et al. 2012), compared to the degraded resolution (*red*) of a high resolution mass spectrum (*black*) of a $N_2 - CH_4$ 98:2% PAMPRE aerosol. The abundances of the PAMPRE high resolution mass spectrum are scaled such that a comparison with the CAPS-IBS fluxes is possible. The *bottom panels* compare $CH_4$, $C_2H_2$, and $C_2H_4$ laboratory plasmas of Deschenaux et al. (1999) to the T57 ion spectra at closest approach

Pernot et al. (2010) have shown that the composition of the compounds in the PAMPRE aerosols follow a $X - (CH_2)_m(HCN)_n$ copolymer structure, where the primary component has a symmetric composition $(m = n)$. In comparison, from the INMS low mass neutral spectrum, Titan is expected to have an elemental abundance represented by $C_{100}H_{157}N_{23}$. This roughly corresponds to a 3:1 $m$ to $n$ ratio, favoring the production of $(CH_2)_m$ type molecules over the $(HCN)_n$ type (Waite et al. 2008), i.e. an intermediate composition between pure hydrocarbons and the nitrogen-rich compounds composing PAMPRE aerosols.

**Acknowledgements** This work was financially supported by the ANR contract ANR-09-JCJC-0038.

## References


Balucani, N., Leonori, F., et al.: Formation of nitriles and imines in the atmosphere of Titan: combined crossed-beam and theoretical studies on the reaction dynamics of excited nitrogen atoms N(2D) with ethane. Faraday Discuss. **147**(0), 189–216 (2010)

Carrasco, N., Schmitz-Afonso, I., et al.: Chemical characterization of Titan's Tholins: solubility, morphology and molecular structure revisited. J. Phys. Chem. A **113**(42), 11195–11203 (2009)

Carrasco, N., Gautier, T., et al.: Volatile products controlling Titan's tholins production. Icarus **219**(1), 230–240 (2012)

Coates, A.J., Crary, F.J., Lewis, G.R., Young, D.T., Waite, J.H. Jr., Sittler, E.C. Jr: Discovery of heavy negative ions in Titan's ionosphere, Geophys. Res. Lett. **34**(22), L22103 (2007)

Coll, P., Coscia, D., et al.: Experimental laboratory simulation of Titan's atmosphere: aerosols and gas phase. Planet. Space Sci. **47**, 1331–1340 (1999)

Coustenis, A., Achterberg, R.K., et al.: The composition of Titan's stratosphere from Cassini/CIRS mid-infrared spectra. Icarus **189**(1), 35–62 (2007)

Crary, F., Magee, B., Mandt, K., Waite, J. Jr., Westlake, J., Young, D.: Heavy ions, temperatures and winds in Titan's ionosphere: combined Cassini CAPS and INMS observations. Planet. Space Sci. **57**(14–15), 1847–1856 (2009)

Cravens, T.E., Robertson, I.P., et al.: Composition of Titan's ionosphere. Geophys. Res. Lett. **33**, L07105 (2006)

Deschenaux, C., Affolter, A., et al.: Investigations of $CH_4$, $C_2H_2$ and $C_2H_4$ dusty RF plasmas by means of FTIR absorption spectroscopy and mass spectrometry. J. Phys. D **32**(15), 1876 (1999)

Imanaka, H., Smith, M.A.: Role of photoionization in the formation of complex organic molecules in Titan's upper atmosphere. Geophys. Res. Lett. **34**(2), L02204 (2007)

Imanaka, H., Smith, M.A.: Formation of nitrogenated organic aerosols in the Titan upper atmosphere. Proc. Natl. Acad. Sci. **107**(28), 12423–12428 (2010)

Israel, G., Szopa, C., et al.: Complex organic matter in Titan's atmospheric aerosols from in situ pyrolysis and analysis. Nature **438**(7069), 796–799 (2005)

Khare, B.N., Sagan, C., et al.: The organic aerosols of Titan. Adv. Space Res. **4**(12), 59–68 (1984)

Lavvas, P.P., Coustenis, A., et al.: Coupling photochemistry with haze formation in Titan's atmosphere, part II: results and validation with Cassini/Huygens data. Planet. Space Sci. **56**(1), 67–99 (2008)

Lavvas, P., Yelle, R.V., et al.: The detached haze layer in Titan's mesosphere. Icarus **201**(2), 626–633 (2009)

Lebonnois, S., Bakes, E.L.O., et al.: Transition from gaseous compounds to aerosols in Titan's atmosphere. Icarus **159**(2), 505–517 (2002)

Magee, B., Waite, J., Mandt, K., Westlake, J., Bell, J., Gell, D.: INMS-derived composition of Titan's upper atmosphere: analysis methods and model comparison. Planet. Space Sci. **57**(14–15), 1895–1916 (2009)

Peng, Z., Gautier, T., Carrasco, N., Pernot, P., Giuliani, A., Mahjoub, A., Correia, J.-J., Buch, A., Bénilan, Y., Szopa C., and Cernogora, G.: Titan's atmosphere simulation experiment using continuum UV-VUV synchrotron radiation. J. Geophys. Res. (In press, 2013)

Pernot, P., Carrasco, N., et al.: Tholinomics: chemical analysis of nitrogen-rich polymers. Anal. Chem. **82**(4), 1371–1380 (2010)

Sciamma-O'Brien, E., Carrasco, N., et al.: Titan's atmosphere: an optimal gas mixture for aerosol production? Icarus **209**(2), 704–714 (2010)

Somogyi, A., Oh, C.-H., et al.: Organic environments on Saturn's Moon, Titan: simulating chemical reactions and analyzing products by FT-ICR and ion-trap mass spectrometry. Am. Soc. Mass Spectrom. **16**, 850–859 (2005)

Szopa, C., Cernogora, G., et al.: PAMPRE: a dusty plasma experiment for Titan's tholins production and study. Planet. Space Sci. **54**, 394–404 (2006)

Teanby, N.A., Irwin, P.G.J., et al.: Vertical profiles of HCN, HC3N, and C2H2 in Titan's atmosphere derived from Cassini/CIRS data. Icarus **186**(2), 364–384 (2007)

Teanby, N.A., Irwin, P.G.J., et al.: Mapping Titan's HCN in the far infra-red: implications for photochemistry. Faraday Discuss. **147**(0), 51–64 (2010)
Vinatier, S., Bézard, B., et al.: Analysis of Cassini/CIRS limb spectra of Titan acquired during the nominal mission: I. Hydrocarbons, nitriles and CO2 vertical mixing ratio profiles. Icarus **205**(2), 559–570 (2010)
Vuitton, V., Yelle, R.V., et al.: Ion chemistry and N-containing molecules in Titan's upper atmosphere. Icarus **191**(2), 722–742 (2007)
Vuitton, V., Lavvas, P., et al.: Negative ion chemistry in Titan's upper atmosphere. Planet. Space Sci. **57**(13), 1558–1572 (2009)
Vuitton, V., Bonnet, J.-Y., et al.: Very high resolution mass spectrometry of HCN polymers and tholins. Faraday Discuss. **147**, 495–508 (2010)
Waite, J.H. Jr., Young, D.T., et al.: The process of Tholin formation in Titan's upper atmosphere. Science **316**, 870–875 (2007)
Waite, J.H., Young, D.T., et al.: The source of heavy organics and aerosols in Titan's atmosphere. Proc. Int. Astron. Union **4**(S251), 321–326 (2008)
Westlake, J.H., Waite, J.H. Jr., et al.: Titan's ionospheric composition and structure: photochemical modeling of Cassini INMS data. J. Geophys. Res. **117**, E01003 (2012)
Wilson, E.H., Atreya, S.K.: Chemical sources of haze formation in Titan's atmosphere. Planet. Space Sci. **51**, 1017–1033 (2003)
Yelle, R.V., Vuitton, V., et al.: Formation of $NH_3$ and $CH_2NH$ in Titan's upper atmosphere. Faraday Discuss. **147**(0), 31–49 (2010)

# Chapter 12
# Nitrogen Fixation by Photochemistry in the Atmosphere of Titan and Implications for Prebiotic Chemistry

**Nadia Balucani**

**Abstract** The observation of N-containing organic molecules and the composition of the haze aerosols, as determined by the Aerosol Collector and Pyrolyser (ACP) on-board Huygens, are clear indications that some chemistry involving nitrogen active forms and hydrocarbons is operative in the upper atmosphere of Titan. Neutral-neutral reactions involving the first electronically excited state of atomic nitrogen, $N(^2D)$, and small hydrocarbons have the right prerequisites to be among the most significant pathways to formation of nitriles, imines and other simple N-containing organic molecules. The closed-shell products methanimine, ethanimine, ketenimine, 2H-azirine and the radical products $CH_3N$, HCCN and $CH_2NCH$ can be the intermediate molecular species that, via addition reactions, polymerization and copolymerization form the N-rich organic aerosols of Titan as well as tholins in bulk reactors simulating Titan's atmosphere.

## Introduction

On Earth, atmospheric molecular nitrogen, $N_2$ (dinitrogen), is the most abundant source of nitrogen, but its chemical inertness is such that very few natural processes can convert it into its compounds. Nowadays, most $N_2$ is naturally fixed into its oxidized or reduced forms via nitrogen-fixing bacteria and lightning. We ignore, instead, the possible mechanisms of nitrogen fixation in the primordial terrestrial atmosphere, because neither biogenic $O_2$ (which is necessary to fix nitrogen into NO after lightning) nor nitrogen-fixing bacteria were present before the appearance of life. In addition, there is no geological record of what happened on our planet during the first half billion years after its formation and the origin of $N_2$ itself in

N. Balucani (✉)
Dipartimento di Chimica, Università degli Studi di Perugia, Perugia, Italy
e-mail: nadia.balucani@unipg.it

J.M. Trigo-Rodriguez et al. (eds.), *The Early Evolution of the Atmospheres of Terrestrial Planets*, Astrophysics and Space Science Proceedings 35,
DOI 10.1007/978-1-4614-5191-4_12, 

its present large amount is a matter of debate. Therefore, nitrogen fixation in an abiotic environment such as the primordial terrestrial atmosphere remains an open issue to be addressed. In the absence of information on the composition and chemical evolution of the primordial terrestrial atmosphere, a valid scientific approach relies on the study of the atmospheric chemistry of planets which share common characteristics with primitive Earth. Data on Earth-like exoplanets will probably be available in the near future, but in the meantime the best neighbour to consider is Titan, the massive moon of Saturn, because it has a dense $N_2$-dominated atmosphere with a very active chemistry (Vuitton et al. 2013). The atmosphere of Titan can be considered to be somewhat reminiscent of the primeval atmosphere of Earth (Coustenis and Taylor 1999). This working hypothesis can give valuable inputs in the understanding of the synthetic routes of N-containing prebiotic molecules on Earth before the emergence of life. Prebiotic molecules are those organic molecules which can be naturally synthesized in abiotic processes, but are characterized by some complexity and all the appropriate "ingredients" to function as precursors of biological molecules, that is, sugars, amino acids, nucleobases etc. (Balucani et al. 2009, 2012). According to the abiogenesis theory, Earth became rich enough in prebiotic molecules to have had the chance for life to spontaneously evolve from them. Two scenarios have been envisaged for the abiotic synthesis of prebiotic molecules: the endogenous and the exogenous synthesis theory (Chyba and Sagan 1992; Bernstein 2006). According to the endogenous vision, prebiotic species were synthesized directly on Earth from simple parent molecules (such as $N_2$ or $NH_3$, $H_2O$ or $H_2$, $CH_4$ or $CO_2$). The original atmosphere was in a reduced or oxidized (or intermediate) state and various sources of energy (intense lightning, energetic solar photons, radioactivity, intense volcanic activity, and shock waves of different kinds) could have induced its chemical transformation (Miller 1986) (an alternative endogenous synthesis theory, however, suggests that the organic synthesis of prebiotic molecules took place in the proximity of oceanic hydrothermal vents, see for instance Holm and Andersson 2005). According to the exogenous synthesis vision, instead, most of the organic molecules came from space, the carriers being comets, asteroids, meteorites and interplanetary dust particles. This vision gains support from the fact that prebiotic molecules have been observed in interstellar clouds, including star-forming regions, as well as in comets, asteroids, meteorites and interplanetary dust particles (Ehrenfreund et al. 2002). As we are going to see, in some way the case of Titan supports the theory of endogenous synthesis, since prebiotic molecules, such as nitriles and imines, are efficiently synthesized locally in the gaseous environment of the upper atmosphere (Vuitton et al. 2013; Balucani 2012).

## Nitrogen Chemistry in the Atmosphere of Titan

The atmosphere of Titan can be regarded as a giant photoreactor, where the energy deposited by solar photons, as well as cosmic rays and electrons from the magnetosphere of Saturn, induces numerous gas-phase reactions. The chemical

evolution of the atmosphere of Titan can be simulated in laboratory experiments (see, for instance Cable et al. 2012; Gautier et al. 2011; Imanaka and Smith 2010) which are similar, in their basic aspects, to that of Stanley Miller (1986). Using mixtures of nitrogen and methane reproducing the composition of the atmosphere of Titan, the formation of nitriles and other N-containing organic molecules is observed and a solid yellow/brown sticky residue (tholins) is formed (Cable et al. 2012; Gautier et al. 2011; Imanaka and Smith 2010; Sagan et al. 1992). Synthetic tholins should resemble the orange aerosols forming the haze of Titan, but the significant differences between a planetary atmosphere and a small laboratory reactor have to be considered (Cable et al. 2012). In particular, the composition of a planetary atmosphere is neither homogeneous nor constant and many physical parameters, such as vertical and wind transport or temperature and pressure gradients, cannot be reproduced in laboratory experiments. In addition, wall collisions typical of laboratory experiments, which are not present in a purely gaseous environment of the dimension of a planetary atmosphere, can affect the observed chemistry by favoring radical recombination. Recent experimental setups have been devised to reduce wall effects and measure the chemical products in situ (Gautier et al. 2011; Imanaka and Smith 2010). Nevertheless, these experiments and their results should only be considered indicative of the chemistry and aerosol composition of Titan (Cable et al. 2012). The best method to describe the chemistry of the atmosphere of Titan relies on a multidisciplinary approach where the observations are reproduced by photochemical models (Yung and DeMore 1998) that consider the physical conditions with their variations and complex networks of interconnected elementary chemical reactions (unimolecular, bimolecular and trimolecular). Various processes at the molecular level are involved, including photon/particle-induced ionization and ion-molecule reactions, photon/particle-induced dissociation and radical-molecule reactions, radiative association and recombination, aerosol heterogeneous or multi-phase processes (Vuitton et al. 2013). For an accurate modeling of these complex networks of elementary reactions, a number of experimental parameters are needed and the necessary molecular processes have to be investigated in laboratory experiments. Photochemical models of increasing complexity (Yung et al. 1984; Wilson and Atreya 2004; Lavvas et al. 2008) have been devised to describe the atmospheric composition of Titan and more stringent tests are now provided by the results of the Cassini-Huygens mission. In this respect, the discovery of an unexpectedly rich ionosphere, with large positive and negative ions (Waite et al. 2007; Coates et al. 2010) as well as the analysis of the aerosol composition by means of the Aerosol Collector and Pyrolyser (ACP) on-board Huygens (Israel et al. 2005) are among the most remarkable achievements of the Cassini-Huygens mission. In particular, according to the ACP results and consistently with the chemical composition of laboratory tholins, the aerosols are formed by N-rich organic macromolecules (Israel et al. 2005). The new challenges for the modeling of the atmosphere of Titan are: (a) to consider a strong coupling between ion and neutral chemistry and reproduce the amount of trace constituents observed towards the thermosphere (species such as benzene, ammonia or simple imines have been identified in the ionosphere and not in the stratosphere, see Vuitton et al. 2008;

Yelle et al. 2010); (b) to envisage haze formation mechanisms from the gaseous phase in the upper part of the atmosphere and (c) to conceive of mechanisms for significant incorporation of nitrogen into organic macromolecules. Since there are practically no radicals able to react with molecular nitrogen ($N_2$ has one of the strongest bonds in nature) at the temperature of Titan, the formation of N-containing species must initiate with the reactions of active forms of nitrogen, such as nitrogen atoms or ions, which are produced by several processes in the upper atmosphere of Titan (Vuitton et al. 2013). In particular, nitrogen atoms are produced by $N_2$ dissociation induced by electron impact and extreme ultra-violet photons or dissociative photoionization, galactic cosmic ray absorption, and $N_2^+$ dissociative recombination (Lavvas et al. 2011). All these processes lead to the formation of ground electronic state nitrogen atoms, $N(^4S_{3/2},)$, as well as nitrogen atoms in the first electronically excited, $N(^2D_{3/2,5/2})$ states (Lavvas et al. 2011). The radiative lifetimes of the metastable states $^2D_{3/2,5/2}$ are quite long ($6.1 \times 10^4$ and $1.4 \times 10^5$ s for the $^2D_{3/2}$, and $^2D_{5/2}$, respectively) and, therefore, the main fate of $N(^2D)$ is chemical reaction with other constituents of the upper atmosphere. Since $N(^4S)$ atoms are not reactive with singlet molecules and the probability of collision with another open-shell species is small, the production of $N(^2D)$ atoms is important because it can easily react with several relatively abundant molecules, such as $CH_4$, thus making an important contribution to the chemical evolution of the atmosphere and the formation of species containing a novel C-N bond.

## Formation of Nitriles and Imines Through the Reactions of $N(^2D)$ with Small Hydrocarbons

The reactions of atomic nitrogen in the first electronically excited state $^2D$ with hydrocarbons are believed to play an important role in the chemistry of the atmosphere of Titan. Since the early models, the reactions of $N(^2D)$ with $CH_4$ and $C_2H_2$ have been considered important steps towards the formation of HCN and $C_2N_2$ (Yung et al. 1984; Yung 1987), both observed in the atmosphere of Titan during the Voyager mission. The $N(^2D)$ reaction with ethylene was later invoked to account for the formation of acetonitrile detected in ground-based observations (Wilson and Atreya 2004). Reliable laboratory experiments on the kinetics of $N(^2D)$ reactions have become available only in the late 1990s, because of the experimental difficulties in studying those systems (Herron 1999). The reactions of $N(^2D)$ with small hydrocarbons have been found to be fast enough to be efficient under the conditions of Titan. In particular, the reactions with unsaturated hydrocarbons are faster than the ones involving methane, so they are important in the chemistry of Titan's atmosphere even though $C_2H_2$ and $C_2H_4$ are much less abundant than $CH_4$. The above mentioned kinetics experiments followed the $N(^2D)$ decay rate and no information was provided on the nature of the primary products. A complementary approach based on collision free experiments has been used to determine the nature

of the primary products and their branching ratios (Balucani et al. 2000a, b, 2009, 2010, 2012). As we are going to see, in all cases the primary reaction products are molecules containing a novel C-N bond.

***The Reaction $N(^2D) + CH_4$***

Because of the abundance of methane, this is the most important reaction involving $N(^2D)$. The room temperature rate constant is $k_{298} = 4.0 \times 10^{-12} cm^3 s^{-1}$ (Herron 1999) and the thermodynamically allowed channels are

$$N(^2D) + CH_4 \rightarrow CH_2 = NH + H \qquad \Delta H_0^0 = -321.2\,kJ/mol \quad (12.1a)$$

$$\rightarrow CHNH_2 + H \qquad \Delta H_0^0 = -172.0\,kJ/mol \quad (12.1b)$$

$$\rightarrow NH + CH_3 \qquad \Delta H_0^0 = -126.1\,kJ/mol \quad (12.1c)$$

$$\rightarrow CH_3N + H \qquad \Delta H_0^0 = -94.5\,kJ/mol \quad (12.1d)$$

where the enthalpies of the reaction channels reported are those calculated at the CCSD(T) level of calculations (Balucani et al. 2009). A first collision-free spectroscopic experiment established that the H-forming channels are dominant over the channel (12.1c) leading to NH (Umemoto et al. 1998). No information was given on the nature of the molecular co-product, even though methanimine ($CH_2 = NH$) formed in channel (12.1a) was suggested to be the most important molecular product. The reaction (12.1) was also investigated in crossed molecular beam (CMB) experiments with mass-spectrometric (MS) detection and time-of-flight (TOF) analysis (Balucani et al. 2009). In those experiments two distinct isomers were identified, that is methanimine (from channel 12.1a) and methylnitrene (from channel 12.1d). Their relative yield varied with the total available energy. The reaction micromechanisms, the product energy partitioning and the relative branching ratios of the competing reaction channels leading to the two isomers have been obtained. The interpretation of CMB-MS results was assisted by electronic structure calculations of stationary points and product energetics for the $CH_4N$ ground state doublet potential energy surface (Balucani et al. 2009). A comparison between experimental results on the two isomer branching ratios and statistical estimates based on the electronic structure calculations was performed, but the system was found to be highly nonstatistical, (the production of the less stable $CH_3N$ isomer is dominated by dynamical effects which cannot be accounted for in statistical calculations). As a consequence, the statistical branching ratio derived at the temperature of Titan cannot be used as such (Balucani et al. 2009).

***The Reaction $N(^2D) + C_2H_6$***

Ethane is the second most abundant hydrocarbon in the atmosphere of Titan. Many (22) reaction channels are thermodynamically allowed for the reaction $N(^2D) + C_2H_6$ (Balucani et al. 2010). Among them, those which have been found to make a contribution to the overall reaction are:

$$N(^2D) + C_2H_6 \rightarrow CH_2 = NH + CH_3 \qquad \Delta H_0^0 = -366.2\,kJ/mol \quad (12.2a)$$

$$\rightarrow CH_3CH = NH + H \qquad \Delta H_0^0 = -338.2\,kJ/mol \quad (12.2b)$$

$$\rightarrow CH_2 = CHNH_2 + H \qquad \Delta H_0^0 = -331.3\,kJ/mol \quad (12.2c)$$

$$\rightarrow CH_3CH_2 + NH \qquad \Delta H_0^0 = -135.6\,kJ/mol \quad (12.2d)$$

$$\rightarrow CH_2{=}\,NH(^3A'') + CH_3 \qquad \Delta H_0^0 = -94.4\,kJ/mol \quad (12.2e)$$

where the enthalpies of the reaction channels reported are those calculated at the CCSD(T) level of calculations (Balucani et al. 2010). The room temperature rate constant is $k_{298} = 1.9 \times 10^{-11}\,cm^3s^{-1}$ (Herron 1999).

The H-displacement channels were characterized in CMB-MS experiments and reaction (12.2) was found to behave statistically (Balucani et al. 2010). This is the ideal case to apply statistical theories for the estimates of the product branching ratio. According to these estimates, performed at the temperature relevant for the stratosphere of Titan, the C-C bond fission channel producing methanimine and $CH_3$ (channel 12.2a) is by far the dominant channel (79%), with the channel leading to ethanimine and H (channel 12.2c) accounting for 12.4% of the global reaction (Balucani et al. 2010). The other channels indicated make a minor (few percent) contribution.

### *The Reactions $N(^2D) + C_2H_4$ and $N(^2D) + C_2H_2$*

The reactions of $N(^2D)$ with acetylene and ethylene are also fast reactions ($k_{298} = 6.5 \times 10^{-11}$ and $4.3 \times 10^{-11} cm^3s^{-1}$, respectively; see Herron 1999) leading to the formation of new species containing a C-N bond (Balucani et al. 2000a, b, 2012). The open reaction channels are

$$N(^2D) + C_2H_2 \rightarrow HCCN + H \qquad \Delta H_0^0 = -211.3\,kJ/mol \quad (12.3a)$$

$$\rightarrow c - HC(N)C + H \qquad \Delta H_0^0 = -182\,kJ/mol \quad (12.3b)$$

and

$$N(^2D) + C_2H_4 \rightarrow CH_2NCH + H \qquad \Delta H_0^0 = -206.2\,kJ/mol \quad (12.4a)$$

$$\rightarrow c - CH_2(N)CH + H \qquad \Delta H_0^0 = -244.1\,kJ/mol \quad (12.4b)$$

$$\rightarrow CH_2 = C = NH + H \qquad \Delta H_0^0 = -329.5\,kJ/mol \quad (12.4c)$$

$$\rightarrow CH_3NC + H \qquad \Delta H_0^0 = -343.7\,kJ/mol \quad (12.4d)$$

$$\rightarrow CH_2NC + H_2 \qquad \Delta H_0^0 = -378.5\,kJ/mol \quad (12.4e)$$

$$\rightarrow c - CH(NH)CH + H \qquad \Delta H_0^0 = -107.4\,kJ/mol \quad (12.4f)$$

$$\rightarrow CH_3 + HNC \qquad \Delta H_0^0 = -403.3\,kJ/mol \quad (12.4g)$$

In the case of reaction (12.3), CMB-MS experiments, combined with electronic structure and statistical calculations, have established that channel (12.3a) is by

far the dominant one (Balucani et al. 2000a). The reaction (12.4) was instead established to produce the $CH_2NCH$ radical (channel 12.4a), 2H-azirine (channel 12.4b), ketenimine (channel 12.4c) and, with a small yield of 2–3%, isoacetonitrile (channel 12.4d) (Balucani et al. 2000b, 2012).

***Implications for the Modeling of the Atmosphere of Titan***

The detailed investigations of the reactions (12.1), (12.2), (12.3) and (12.4) in collision free experiments have allowed determining the reaction products for the most important $N(^2D)$ reactions in the atmosphere of Titan. Those results have somewhat changed the schemes of the photochemical models of the atmosphere of Titan. For instance, the assumption that only $NH + CH_3$ are the products of the reaction (12.1) (Yung et al. 1984; Krasnopolsky 2009) is not correct, as the reactive channel (12.1c) accounts at most for $\sim 30\%$ of the global reaction. The observation that the dominant channel is the one leading to methanimine, a closed-shell molecule containing a novel C-N bond, demonstrates that such a bond can be generated directly by a reaction involving an active form of nitrogen, the main constituent of the atmosphere of Titan, and $CH_4$, the second most abundant species. Therefore, nitrogen fixation can be achieved in the abiotic conditions of Titan's upper atmosphere starting from its main components (Balucani 2012). Methanimine has not been observed directly so far, but its protonated form, $CH_2NH_2^+$, is required to explain the peak at $m/z = 30$ in the mass spectrum recorded by the ion neutral mass spectrometer (INMS) on-board Cassini (Vuitton et al. 2006).

As for reaction (12.2), in the photochemical models of Titan it was either assumed (Wilson and Atreya 2004; Krasnopolsky 2009) to produce only $NH + C_2H_5$ (which is, instead, only a minor channel) or aziridine, $c - CH_2(NH)CH_2 + H$ (Lavvas et al. 2008). Neither of these suggestions is correct. As we have seen, methanimine from channel (12.2a) is also produced by the reaction $N(^2D) + CH_4$. Methane is more abundant than ethane by roughly three orders of magnitude, but the rate constant (at room temperature) of the reaction $N(^2D) + C_2H_6$ is one order of magnitude larger than that of methane. Therefore, the reaction of $N(^2D) + C_2H_6$ should contribute by a few percent to the global budget of methanimine (Balucani et al. 2010).

Methanimine is a very interesting compound in the context of the chemical evolution of the atmosphere of Titan. The presence of a double C = N bond makes it a very reactive molecule which easily undergoes polymerization, oxidation, and hydrolysis. We can speculate that, in a relatively dense medium such as the upper atmosphere of Titan (collision time $\sim 1$ s), methanimine reacts easily with radicals or undergoes polymerization and copolymerization. In addition, it can photodissociate to $HCNH/CH_2NH + H$ or $HCN/HNC + H_2$. The photodissociation product yield has not been characterized in laboratory experiments, but it is known that activated $CH_2 = NH$ can dissociate to $HCNH/H_2CN + H$ or $HCN/HNC + H_2$ (Arenas et al. 1999). These processes have been considered for the first time in the recent photochemical model by Lavvas et al. (2008), who were the first to consider the processes that $CH_2 = NH$ undergoes after its formation. The model by Lavvas et al., indeed, predicted a larger quantity of $CH_2 = NH$ than that inferred by INMS

but there is a lot of uncertainty on the possible fate of $CH_2 = NH$ in the upper atmosphere of Titan, because of a severe lack of knowledge on the possible chemical loss pathways of this species.

Growing evidence suggests that nitrogen chemistry contributes to the formation of the haze aerosols in the Titan upper atmosphere. In this respect, $CH_2 = NH$ is an excellent candidate to account for the formation of nitrogen-rich aerosols via polymerization or copolymerization with other unsaturated species or radical reactions. Ethanimine, the second most important molecular product of reaction (12.2), can also be a source of nitrogen-rich molecules and aerosols via addition reactions, polymerization and copolymerization. Ethanimine can also undergo UV photolysis forming reactive radicals that can further enhance the formation of nitrogen-rich complex species. A theoretical study (Arenas et al. 2000) has suggested that activated ethanimine can directly decompose to $CH_3CN + H_2$ and $CH_4 + HCN/HNC$. In this respect, activated ethanimine could be a source of acetonitrile and HCN/HNC.

The formation of HCCN in reaction (12.3) supports the mechanism of $C_2N_2$ formation suggested by Yung (1987). Interestingly, the HCCN radical has also been suggested to be an important precursor for nitrogenated organic solids obtained in the EUV irradiation of $N_2/CH_4$ mixtures (Imanaka and Smith 2010).

Finally, the main products of reaction (12.4) are a very reactive radical, $CH_2NCH$, the closed-shell species 2H-azirine and ketenimine. 2H-azirine is characterized by a strained ring and ketenimine has two double bonds: both species can easily be involved in polymerization processes.

## Conclusions

Detailed laboratory studies on the $N(^2D)$ reactions with methane and higher hydrocarbons, $C_2H_6$, $C_2H_2$ and $C_2H_4$, indicate that interesting N-containing species can be formed in neutral-neutral bimolecular reactions in the atmosphere of Titan, as well as in the atmospheres of other planets rich in molecular nitrogen and hydrocarbons. Only HCN, $CH_3CN$ and $CH_2 = NH$ have been identified in the atmosphere of Titan so far. These reactions can also make an important contribution in the formation of laboratory tholins in bulk experiments. Open-shell (such as $CH_3N$ and HCCN radicals) or highly unstable unsaturated N-compounds (including $CH_2 = NH$, $CH_3CH = NH$, $CH_2 = C = NH$ or $CH_2 = CH - NH_2$) are expected to undergo reactions with other species present in the atmosphere of Titan, possibly contributing to the growth of the N-rich macromolecules which form the haze aerosols. Therefore, reactions (12.1), (12.2), (12.3) and (12.4) can represent the first steps towards the formation of complex nitrogen macromolecules starting from a purely gas-phase environment. The aerosol macromolecules eventually deposit on the surface of Titan, where they accumulate because the low temperature does not allow further chemical evolution. If anything similar to Titan's haze has ever existed on our planet, it is reasonable to imagine that, once deposited on the surface of the

oceans, further chemical evolution might have transformed these molecules into the first building blocks of living entities. And, indeed, the laboratory analogs of the Titan aerosols (tholins) in the presence of liquid water are able to hydrolyze and produce prebiotic molecules including aminoacids.

**Acknowledgements** This work was partially supported by the COST Action CM 0805 *The Chemical Cosmos: Understanding Chemistry in Astronomical Environments*.

## References

Arenas, J.F., Marcos, J.I., Otero, J.C., Sanchez-Galvez, A., Soto, J.: A multiconfigurational self-consistent field study of the thermal decomposition of methyl azide. J. Chem. Phys. **111**, 551–561 (1999)

Arenas, J.F., Marcos, J.I., Lopez-Tocon, I., Otero, J.C., Soto, J.: Potential-energy surfaces related to the thermal decomposition of ethyl azide: the role of intersystem crossing. J. Chem. Phys. **113**, 2282–2289 (2000)

Balucani, N.: Elementary reactions and their role in gas-phase prebiotic chemistry. Int. J. Mol. Sci. **10**, 2304–2335 (2009). And references therein

Balucani, N.: Elementary reactions of N atoms with hydrocarbons: first steps towards the formation of prebiotic N-containing molecules in planetary atmospheres. Chem. Soc. Rev. **41**, 5473–5483 (2012)

Balucani, N., Alagia, M., Cartechini, L., Casavecchia, P., Volpi, G.G., Sato, K., Takayanagi, T., Kurosaki, Y.: Cyanomethylene formation from the reaction of excited nitrogen atoms with acetylene: a crossed beam and ab initio study. J. Am. Chem. Soc. **122**, 4443–4450 (2000a)

Balucani, N., Cartechini, L., Alagia, M., Casavecchia, P., Volpi, G.G.: Observation of nitrogen-bearing organic molecules from reactions of nitrogen atoms with hydrocarbons: a crossed beam study of $N(^2D)$ + ethylene. J. Phys. Chem. A **104**, 5655–5659 (2000b)

Balucani, N., Bergeat, A., Cartechini, L., Volpi, G.G., Casavecchia, P., Skouteris, D., Rosi, M.: Combined crossed molecular beam and theoretical studies of the $N(^2D) + CH_4$ reaction and implications for atmospheric models of Titan. J. Phys. Chem. A **113**, 11138–11152 (2009)

Balucani, N., Leonori, F., Petrucci, R., Stazi, M., Skouteris, D., Rosi, M., Casavecchia, P.: Formation of nitriles and imines in the atmosphere of Titan: combined crossed-beam and theoretical studies on the reaction dynamics of excited nitrogen atoms $N(^2D)$ with ethane. Faraday Discuss. **147**, 189–216 (2010)

Balucani, N., Skouteris, D., Leonori, F., Petrucci, R., Hamberg, M., Geppert, W.D., Casavecchia, P., Rosi, M.: Combined crossed beam and theoretical studies of the $N(^2D) + C_2H_4$ reaction and implications for atmospheric models of Titan. J. Phys. Chem. A **116**, 10467–10479 (2012). doi:10.1021/jp3072316

Bernstein, M.: Prebiotic materials from on and off the early Earth. Philos. Trans. R. Soc. B **361**, 1689–1702 (2006)

Cable, M.L., Horst, S.M., Hodyss, R., Beauchamp, P.M., Smith, M.A., Willis, P.A.: Titan tholins: simulating Titan organic chemistry in the Cassini-Huygens era. Chem. Rev. **112**, 1882–1909 (2012)

Chyba, C., Sagan, C.: Endogenous production, exogenous delivery and impact-shock synthesis of organic molecules: an inventory for the origins of life. Nature **355**, 125–132 (1992)

Coates, A.J., Wellbrock, A., Lewis, G.R., Jones, G.H., Young, D.T., Crary, F.J., Waite, J.H. Jr., Johnson, R.E., Hill, T.W., Sittler, E.C. Jr.: Negative ions at Titan and Enceladus: recent results. Faraday Discuss. **147**, 293–305 (2010)

Coustenis, A., Taylor, F.W.: Titan: The Earth-Like Moon. World Scientific, Singapore (1999)

Ehrenfreund, P., Irvine, W., Becker, L., Blank, J., Brucato, J.R., Colangeli, L., Derenne, S., Despois, D., Dutrey, A., Fraaije, H., Lazcano, A., Owen, T., Robert, F.: Astrophysical and astrochemical insights into the origin of life. Rep. Prog. Phys. **65**, 1427–1487 (2002)

Gautier, T., Carrasco, N., Buch, A., Szopa, C., Sciamma-O'Brien, E.: Nitrile gas chemistry in Titan's atmosphere. Icarus **213**, 625–635 (2011)

Herron, J.T.: Evaluated chemical kinetics data for reactions of $N(^2D)$, $N(^2P)$, and $N_2(A^3\Sigma_u^+)$ in the gas phase. J. Phys. Chem. Ref. Data **28**, 1453–1483 (1999)

Holm, N.G., Andersson, E.: Hydrothermal simulation experiments as a tool for studies of the origin of life on earth and other terrestrial planets: a review. Astrobiology **5**, 444–460 (2005)

Imanaka, H., Smith, M.A.: Formation of nitrogenated organic aerosols in the Titan upper atmosphere. PNAS **107**, 12423–12428 (2010)

Israel, G., Szopa, C., Raulin, F., Cabane, M., Niemann, H.B., Atreya, S.K., Bauer, S.J., Brun, J.F., Chassefiere, E., Coll, P., Conde, E., Coscia, D., Hauchecorne, A., Millian, P., Nguyen, M.J., Owen, T., Riedler, W., Samuelson, R.E., Siguier, J.M., Steller, M., Sternberg, R., Vidal-Madjar, C.: Complex organic matter in Titan's atmospheric aerosols from in situ pyrolysis and analysis. Nature **438**, 796–799 (2005)

Krasnopolsky, V.A.: A photochemical model of Titan's atmosphere and ionosphere. Icarus **201**, 226–256 (2009)

Lavvas, P., Coustenis, A., Vardavas, I.M.: Coupling photochemistry with haze formation in Titan's atmosphere, Part II: results and validation with Cassini/Huygens data. Planet. Space Sci. **56**, 67–99 (2008)

Lavvas, P., Galand, M., Yelle, R.V., Heays, A.N., Lewis, B.R., Lewis, G.R., Coates, A.J.: Energy deposition and primary chemical products in Titan's upper atmosphere. Icarus **213**, 233–251 (2011)

Miller, S.L.: Current status of the prebiotic synthesis of small molecules. Chem. Scr. **26B**, 5–11 (1986)

Sagan, C., Thompson, W.R., Khare, B.N.: Titan – a laboratory for prebiological organic-chemistry. Acc. Chem. Res. **25**, 286–292 (1992)

Umemoto, H., Nakae, T., Hashimoto, H., Kongo, K., Kawasaki, M.: Reactions of $N(^2D)$ with methane and deuterated methanes. J. Chem. Phys. **109**, 5844–5848 (1998)

Vuitton, V., Yelle, R.V., Anicich, V.G.: The nitrogen chemistry of Titan's upper atmosphere revealed. Astrophys. J. **647**, L175–L178 (2006)

Vuitton, V., Yelle, R.V., Cui, J.: Formation and distribution of benzene on Titan. J. Geophys. Res. **113**, E05007 (2008)

Vuitton, V., Dutuit, O., Smith, M.A., Balucani, N.: Chemistry of Titan's atmosphere, chapter 7. In: Mueller-Wodarg, I., Griffith, C., Lellouch, E., Cravens, T. (eds.) Titan: Surface, Atmosphere and Magnetosphere. Cambridge University Press (2013)

Waite, J.H. Jr., Young, D.T., Cravens, T.E., Coates, A.J., Crary, F.J., Magee, B., Westlake, J.: The process of tholin formation in Titan's upper atmosphere. Science **316**, 870–875 (2007)

Wilson, E.H., Atreya, S.K.: Current state of modeling the photochemistry of Titan's mutually dependent atmosphere and ionosphere. J. Geophys. Res.-Planets **109**, E06002 (2004)

Yelle, R.V., Vuitton, V., Lavvas, P., Klippenstein, S.J., Smith, M.A., Horst, S.M., Cui, J.: Formation of $NH_3$ and $CH_2NH$ in Titan's upper atmosphere. Faraday Discuss. **147**, 31–49 (2010)

Yung, Y.L.: An update of nitrile photochemistry on Titan. Icarus **72**, 468–472 (1987)

Yung, Y.L., DeMore, W.B.: Photochemistry of Planetary Atmospheres. Oxford University Press, New York (1998)

Yung, Y.L., Allen, M., Pinto, J.: Photochemistry of the atmosphere of Titan: comparison between model and observations. Astrophys. J. Suppl. Ser. **55**, 465–506 (1984)

# Chapter 13
# SNC Meteorites: Atmosphere Implantation Ages and the Climatic Evolution of Mars

**C.E. Moyano-Cambero, Josep M. Trigo-Rodríguez, and F. Javier Martín-Torres**

**Abstract** SNC meteorites are Martian rocks that provide valuable information about the atmospheric composition of Mars over time. These meteorites experienced significant shock during the impact that released them from Mars, and during the flight through the Martian atmosphere some of the gases were retained in the melted shock-altered glasses. As using different radiogenic systems can precisely date such shock processes, SNC achondrites can be considered time capsules capable of providing significant insight into the atmospheric evolution of Mars. Different SNCs were released by impacts at different times, having then different atmosphere-implantation ages, so in practice we can obtain clues on the composition of Mars' atmosphere at different times. Taking this information into account, we have developed a 1D model of the evolution of Martian Mars' atmosphere mass, near surface temperature and pressure.

## Introduction

Due to the complexity of in situ planetary exploration the only samples of Mars that are currently available to be studied in terrestrial laboratories are the Martian meteorites. Three main classes have been identified and named after the first identified meteorites of each class. These classes are: (i) shergottites (basaltic to lherzolitic igneous rocks, named after the Shergotty, India, fall of 1865); (ii) nakhlites (clinopyroxenites or wehrlites, formed as cumulate rocks and named after

C.E. Moyano-Cambero (✉) • Josep M. Trigo-Rodríguez
Facultat de Ciències, Institute of Space Sciences (CSIC-IEEC), Campus UAB, Torre C5-pares, 08193 Bellaterra, Barcelona, Spain
e-mail: moyano@ice.csic.es; trigo@ice.csic.es

F. Javier Martín-Torres
Centro de Astrobiología (CSIC-INTA), 28850 Torrejón de Ardoz, Madrid, Spain
e-mail: javiermt@cab.inta-csic.es

J.M. Trigo-Rodriguez et al. (eds.), *The Early Evolution of the Atmospheres of Terrestrial Planets*, Astrophysics and Space Science Proceedings 35,
DOI 10.1007/978-1-4614-5191-4_13, 

the Nakhla, Egypt, fall of 1911); and (iii) chassignites (dunitic cumulate rocks named after the Chassigny, France, fall of 1815). They are known by the acronym SNC (see e.g. the recent review by McSween and Huss (2010)). In the family of Martian meteorites we also have ALH 84001, an orthopyroxene-rich meteorite not assigned to any of the SNC types. Despite their unique and distinctive chemical and oxygen isotopic values, the SNC suite was not completely accepted as Martian in origin until that D.D. Bogard and P. Johnson noticed that some of them contain mineral phases with trapped gases that are consistent with Viking measurements (Bogard and Johnson 1983).

New measurement capabilities in the 1980s allowed analyzing tiny amounts of such gases that confirmed their Martian origin. The extraordinary compositional match was well exemplified with the study of the shergottite Elephant Moraine 79001 (EET 79001). This meteorite experienced a significant shock during the impact that released the original rock from Mars, and small samples of Martian atmosphere were retained during the ejection in the melted shock-altered glasses and the maskelynite that were formed in the shock veins (Bogard and Johnson 1983). A similar pattern was found later in Zagami (Fig. 13.1) shergottite (Marti et al. 1995). Using different radiogenic systems can precisely date such shock processes, so, in fact, meteorites can provide us information about Mars' atmosphere past. Many Martian meteorites could have been ejected by the same event, but even so there are enough meteorites released by impacts at different times, so as the ejection from Mars ages range from 1 to 20 Myr, in the practise we can obtain clues on the composition of Mars' atmosphere at different stages. For example, it is well known from isotopic studies that most shergottites reveal that were released from Mars at the time of the late Amazonian volcanism (Nyquist et al. 2001). It would also be desirable to obtain information about Mars' atmosphere at the epochs when Martian meteorites were formed, because it would cover a large part of the history of the red planet. In fact, preferred radiometric formation ages of basaltic and lherzolitic shergottites lie in the range $\sim$ 165–475 Myr, while nakhlites and chassignites are compatible with an average age of $\sim$ 1,300 Myr (Nyquist et al. 2001), and the oldest recognized Martian meteorite is ALH 84001 whose igneous crystallization date has been recently revised to be about 4,100 Myr (Lapen et al. 2010). Then, the method to analyze trapped gases in SNC meteorites is a way to corroborate accurate physical models dealing with the evolution of Mars' atmosphere over time. In this work we start a common project in order to analyze and characterize SNC meteorites that will be used to validate a model of Mars' atmospheric evolution from the beginning of the secondary atmosphere around 3.5 Gyr ago to our days (Martín-Torres et al. 2012).

The geological history of Mars can be split into three primary periods: Noachian (4.5 Gyr ago to 3.5 Gyr ago), Hesperian (3.5 Gyr ago to 2.9–3.3 Gyr ago), and Amazonian (2.9–3.3 Gyr ago to present). To understand paleoclimate and to correctly interpret the Mars meteorite record we need to understand two types of atmospheric conditions that may have occurred through the history of Mars: a dry, dusty situation similar to the current Mars and a warmer, wetter climate unlike any recent Martian conditions. For the first, the key difference between the current

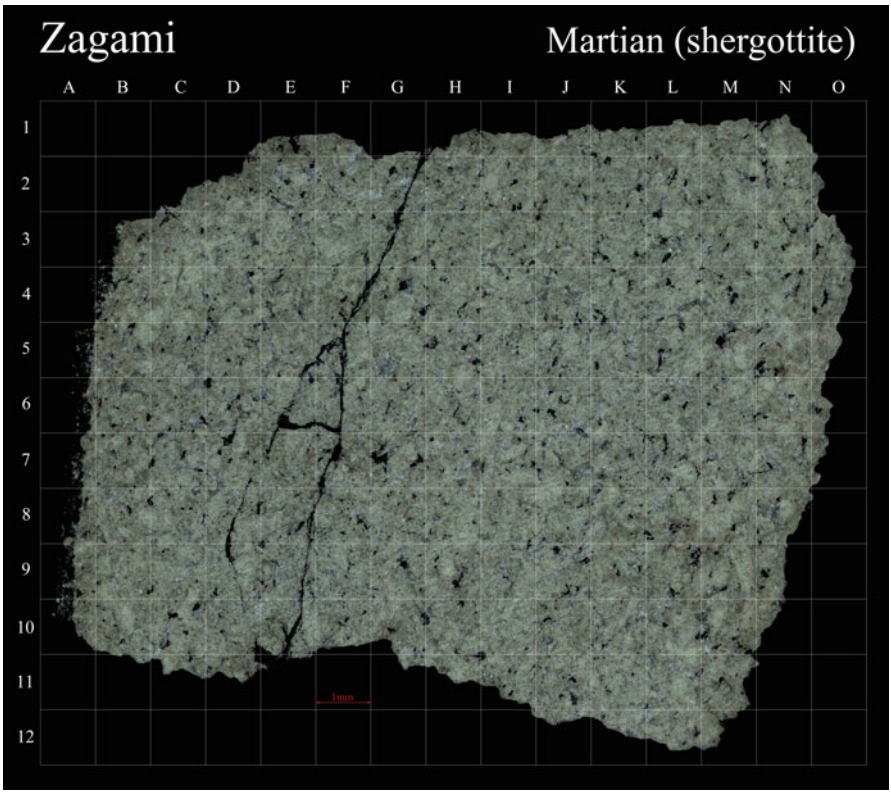


**Fig. 13.1** High-resolution mosaic of the Zagami shergottite, generated from separate reflection images taken with a Zeiss Scope petrographic microscope. Note the highly porous nature of this rock. The overlapped grid is 1 mm wide being used to locate features under study

climate and the paleoclimate is the possibility of a much thicker atmosphere. This kind of atmosphere leads to an increase in the atmospheric heat capacity, a change in the transmission of insolation and infrared energy through the atmosphere, and therefore a change in the general circulation and behavior of the atmosphere. For the second case the differences are more drastic. To achieve these globally "wet" conditions on ancient Mars requires a large global water inventory. To better understand these two possible paleoclimate states we have conducted several studies to examine the evolution of the Mars atmosphere bearing in mind these factors and deriving the expected mass, pressure, and temperature of the Mars atmosphere as a function of time. In the same way that Martian meteorites can help us to check this atmospheric evolution model, reciprocally the evolution derived from it will have an impact on the correct interpretation of the meteorites as will affect the environmental conditions in Mars. For example large atmospheric pressures in early Martian atmosphere would imply the existence of higher temperatures (through greenhouse effect with atmospheric $CO_2$) and, possibly, the existence of liquid water

on the surface. This view agrees with evidences of liquid water in past, like valley networks and outflow channels (McElroy et al. 1977; Clifford et al. 1988). This also fits with the only current evidence available of the oldest Martian meteorite known: ALH 84001 with secondary minerals produced by aqueous alteration and even a highly debated hosting of fossils of bacteria (Lapen et al. 2010).

## Mars Atmosphere Evolution Model

The model (Martín-Torres et al. 2012) we are going to use in the future together with the information from Martian meteorites begins considering the mass of Mars' atmosphere. At time t the amount of mass in the atmosphere is m(t). It depends of two variables: the degassed mass, $m_d(t)$, since the beginning of secondary atmosphere, and the mass lost, $m_l(t)$ by the atmosphere during the same period, i.e.:

$$m(t) = m_d(t) - m_l(t) \tag{13.1}$$

Periods of volcanism and calm made a non-continuous rate of degassing in time with, but we know that since the end of the accretion period (Noachian epoch) Mars was cooling. It is expected that this rate diminished as the planet aged and we assume that the degassing rate could be computed as follows:

$$m_d(t) = (A/B)\left[\exp[B(t-t_0)]-1\right] \tag{13.2}$$

where A is the degassing rate at time $t_0$ (1 Gyr, the beginning of secondary atmosphere) and B is a constant that controls the velocity of degassing.

There are several mechanisms of atmospheric mass loss, but the main ones are the drag of ions by the solar wind ($m_i(t)$), the dissociative recombination ($m_{dr}(t)$) and the oxidation of the surface rocks ($m_{ox}(t)$). Together, they can be expressed like:

$$m_l(t) = m_i(t) + m_{dr}(t) + m_{ox}(t) \tag{13.3}$$

These three mass terms contributing to the mass loss can be computed as follows:

1. **Material dragged by solar wind, $m_i(t)$**:
   We assume that the mass loss rate of ions is:

$$dm_i/dt = A \cdot \rho_S \cdot v^2 \cdot L/2 \tag{13.4}$$

   where A is a constant, $\rho_S$ is the solar wind density, L is the solar ultraviolet irradiance normalized to current values, and v is the solar wind velocity. Using current values of the solar ultraviolet irradiance (L = 1), a value of $v = 4 \times 10^5 m/s$, and $\rho_S = 7.15 \times 10^{-21} kg\ m^{-3}$, A should have a value between $-4.37 \times 10^8 s\ m$ and $-1.75 \times 10^9 s\ m$. Taking the following expression (Zahnle and Walker 1982):

$$L = C \cdot t^m \tag{13.5}$$

where $C = 1.898 \times 10^{21}\ s^{1.24}$ and m is a dimensionless constant with value -1.24. It also was established (Newkirk 1980) that:

$$v = D \cdot t^{r} \tag{13.6}$$

where $D = 5.27 \times 10^{12}\ m\ s^{-0.585}$ and r is an adimensional constant with a value of -0.415. With (13.5) and (13.6) it is possible to find the solution of Eq. (13.4):

$$m_i(t) = A \cdot r \cdot C \cdot D^2 \cdot \left(t^{m+2r+1} - t_0^{m+2r+1}\right) / [(m + 2r + 1)] \tag{13.7}$$

2. **Dissociative recombination, $m_{dr}(t)$**:
This is a mechanism by which an ionized molecule is recombined with an electron and then dissociated, producing fragments that may acquire velocities larger than the planetary escape velocity. We assume that its rate is proportional to the magnitude of the flux of incident solar ultraviolet radiation (McElroy and Yung 1976):

$$dm_{dr}/dt = b \cdot L \tag{13.8}$$

so that with Eq. (13.5) we obtain:

$$m_{dr}(t) = b \cdot C \cdot \left(t^{m+1} - t_0^{m+1}\right) / (m + 1) \tag{13.9}$$

3. **Oxidation of the surface rocks $m_{ox}(t)$:**
The rate $(dm_{ox}/dt)$ at which oxygen atoms may be trapped at the surface could be as large as $1.3 \times 10^{12}$ atoms $m^{-2} \cdot s^{-1}$ (Newkirk 1980), this is equivalent to a total mass loss of 5 kg/s in the whole surface. Assuming this rate as constant in time we get that:

$$m_{ox}(t) = 5(t - t_0) \tag{13.10}$$

**Total mass:**
Now we are able to calculate the total mass of the atmosphere. For the sake of clarity, avoiding confusion with the constant m, we are going to use M(t) as the total mass instead of m(t). From previous Eqs. (13.1), (13.3), (13.7), (13.9) and (13.10) the equation that describes the evolution of total atmospheric mass in time is:

$$\begin{aligned} M(t) = {} & (A/B)\left[\exp\left[B(t-t_0)\right] - 1\right] - A{\cdot}r{\cdot}C{\cdot}D^2{\cdot}\left(t^{m+2r+1} - t_0^{m+2r+1}\right) / [2(m+2r+1)] \\ & - bC\left(t^{m+1} - t_0^{m+1}\right) / (m+1) - 5(t-t_0) \end{aligned} \tag{13.11}$$

This equation depends on parameters A and B. Taking $t = t_P$, in which $t_P = 4.6$ Ga (present time), we can find A as a function of B:

$$\begin{aligned} A = {} & B\left[M(t_P) + A \cdot r \cdot C \cdot D^2\left(t_P^{m+2r+1} - t_0^{m+2r+1}\right) / [2(m + 2r + 1)]\right. \\ & \left. + bC\left(t_P^{m+1} - t_0^{m+1}\right) / (m + 1) + 5(t_P - t_0)\right] \setminus \left\{\exp\left[B(t_P - t_0)\right] - 1\right\} \end{aligned} \tag{13.12}$$

where B, explained before, becomes a free parameter of the model.

**Near Surface Temperature Modeling:**

At the planetary surface the temperature produced by the greenhouse effect is:

$$T^4(t) = T_e^4[1 + 3 \cdot \tau/4] \tag{13.13}$$

(Chamberlain and Hunten 1987) where $T_e$ is the mean planetary black body temperature and $\tau$ is the atmosphere optical thickness. After some studies (Zahnle and Walker 1982; Kasting and Grinspoon 1990; Gough 1981) $T_e$ can be written as:

$$T_e(t) = T_P\,[1 + 0.4(1 - t/t_P)]^{-1/4} \tag{13.14}$$

where $T_P$ is the present value of $T_e$, t is time, and $t_P$ is the age of the Sun. After the value of the total mass obtained in (13.11) the atmospheric temperature at the surface becomes:

$$T(t) = T_P\,[1 + 3t_P M(t)/4M_P]^{1/4}\,[1 + 0.4(1 - t/t_P)]^{-1/4} \tag{13.15}$$

**Surface Pressure Modeling:**

The atmospheric pressure P as function of time through the perfect gas equation normalized with respect to the present values ($P_P$, $M_P$, $T_a$) is given by

$$P(t) = M(t)T(t)P_P/M_P T_P \tag{13.16}$$

Using Eqs. (13.11), and (13.16) we evaluate P(t):

## Conclusions

We have developed a 1D model of the evolution of Martian mass, near surface temperature and pressure considering the main production and loss processes of Mars atmosphere and the radiative conditions on Mars (Fig. 13.2). SNC meteorites provide a complementary tool for atmospheric modeling and a straightforward method for model validation. The identification of the exact Mars surface region of SNC meteorites seems difficult, but they are still the only available samples of the red planet to test our climate evolution hypothesis (Moyano-Cambero et al. 2012). We plan to validate this atmospheric model with the clues obtained from Martian meteorites and tune the free parameters in our model. By now we have reached the following conclusions: (a) SNC meteorites provide valuable information about the atmospheric composition of Mars over time; (b) The three SNC classes are scattered in time and consequently are not homogeneously sampling Mars' atmospheric evolution, but it is obvious that they provide a complementary tool for atmospheric modeling as they contain tiny amounts of atmospheric constituents at the departure time from the red planet.

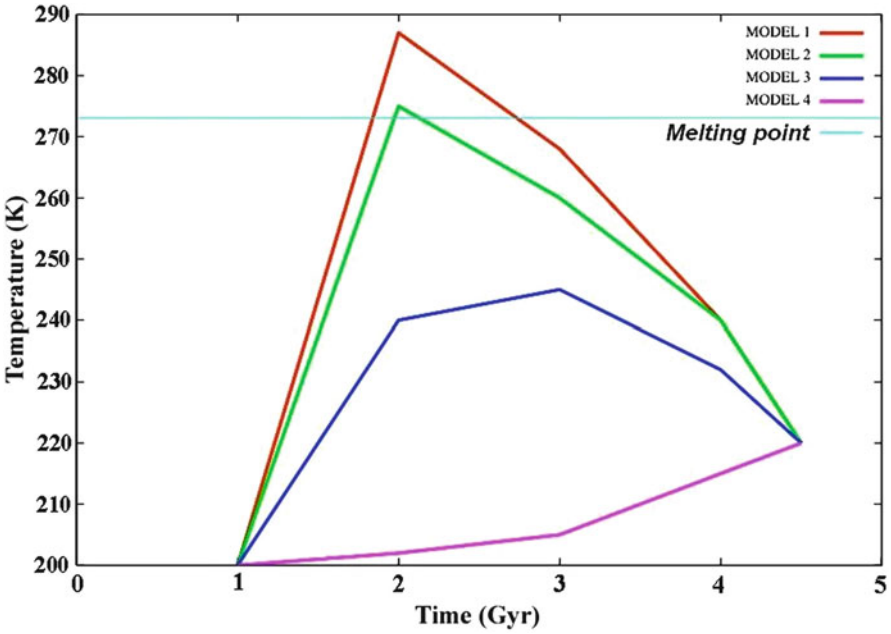


**Fig. 13.2** Near surface temperature as a function of time for different set of free parameters in the model. The melting point temperature is plotted for reference

**Acknowledgements** JMTR acknowledges CSIC grant #201050I043 and AYA2011-26522 grant.

## References

Bogard, D.D., Johnson P.: Martian gases in an Antarctic meteorite. Science **221**, 651–654 (1983)
Chamberlain, J.W., Hunten, D.M.: Theory of planetary Atmospheres (San Diego: Academic Press), esp. pp. 136–140 (1987)
Clifford, S.M., et al.: NASA Mars Project: evolution of climate and atmosphere. EOS Trans. AGU **69**, 1585 (1988)
Gough, D.O.: Solar interior structure and luminosity variations. Sol. Phys. **74**, 21–34 (1981)
Kasting, J.F., Grinspoon, D.H.: The Faint Young Sun Problem in The Sun in Time. University of Arizona Press, Tucson (1990)
Lapen, T.J., et al.: A younger age for ALH84001 and its geochemical link to shergottite sources in Mars. Science **328**, 347–351 (2010)
Marti, K., et al.: Signatures of the Martian atmosphere in glass of the Zagami meteorite. Science **267**, 1981–1984 (1995)
Martín-Torres, F.J., Moyano-Cambero, C.E., et al.: Evolution of Mars atmospheric pressure and temperature modeling and constrains from meteorites. LPS XLIII, abstract #2840 (2012)
McElroy, M.B., Yung, Y.L.: Oxygen isotopes in the Martian atmosphere: implications for the evolution of volatiles. Planet. Space Sci. **24**, 1107–1113 (1976)

McElroy, M.B., et al.: Photochemistry and evolution of Mars' atmosphere: a viking perspective. J. Geophys. Res. **82**, 4379 (1977)
McSween, H.Y., Huss, G.R.: Cosmochemistry. Cambridge University Press, Cambridge (2010)
Moyano-Cambero, C.E., Trigo-Rodríguez, J.M., et al.: Martian meteorites: reflectance properties, atmosphere-implantation ages, and the climatic evolution of Mars. LPS XLIII, abstract #1132 (2012)
Newkirk, G. Jr.: Solar variability on time scales of 105 years to 109.6 years. Geochi. Cosmochi. Acta Suppl. **13**, 293 (1980)
Nyquist, L.E., Bogard, D.D., et al.: Ages and geologic histories of Martian meteorites. Chronol. Evol. Mars **96**, 105–164 (2001)
Zahnle, K.J., Walker, J.C.G.: Evolution of solar ultravioleta luminosity. Rev. Geophys. **20**, 280–292 (1982)

# Glossary

**Compiled by Carles E. Moyano-Cambero, F. Javier Martín-Torres, María Serrano, and Josep M. Trigo-Rodríguez**

**Abiotic processes:** Non-biological factor (such as sunlight), material (such as sulfur dioxide), or process (such as hydrolysis) which can affect living or non-living constituents of an ecosystem.
**Ablation:** Removal of material from the surface of an object by vaporization, chipping, or other erosive processes.
**Absorption:** of electromagnetic radiation is the way in which the energy of a photon is taken up by matter, typically the electrons of an atom.
**Accretion:** The growth of a massive object by gravitationally attracting more matter, typically gaseous matter in an accretion disc
**Actinism:** The property of solar radiation that leads to the production of photochemical and photobiological effects.
**Achondrite:** A differentiated meteorite that exhibits no chondrules. Most achondrites are *igneous*↑ rocks coming from planetary bodies like e.g.: Mars, Moon or Vesta.
**Adiabatic:** Any process occurring without input or output of heat within a system (i.e. during the process the system is thermodynamically isolated- there is no heat transfer with the surroundings).
**Aerosol:** Suspension of fine solid particles or liquid droplets in a gas.
**Albedo:** The diffuse reflectivity or reflecting power of a surface
**Aliphatic compounds:** In organic chemistry, compounds composed of carbon and hydrogen are divided into two classes: aromatic compounds, which contain benzene or similar rings of atoms, and aliphatic which do not contain those rings.
Aliphatic compounds can be cyclic, like cyclohexane, or acyclic, like hexane. They also can be saturated, like hexane, or unsaturated, like hexene.
**Amazonian epoch:** The youngest epoch in the geologic history of Mars.
**Anaerobic bacteria:** Organism that does not require oxygen for growth.
**Andesite:** Extrusive *igneous*↑, volcanic rock, intermediate type between *basalt*↑ and dacite ranging from 57 to 63% $SiO_2$. Its typical mineral assemblage is

J.M. Trigo-Rodriguez et al. (eds.), *The Early Evolution of the Atmospheres of Terrestrial Planets*, Astrophysics and Space Science Proceedings 35,
DOI 10.1007/978-1-4614-5191-4, © Springer Science+Business Media New York 2013

dominated by *plagioclase*↑ plus *pyroxene*↑. Along with *basalts*↑ they are a major component of the Martian crust.

**Anoxic:** A total depletion in the level of oxygen, an extreme form of hypoxia or "low oxygen".

**Archean:** Geologic eon before the Proterozoic Eon, before 2.5 Ga (billion years, or 2,500 Ma) ago. The Archean era is generally agreed to have started at 3.8 billion years ago, but this boundary is informal. the earlier of two divisions of the Precambrian era, during whichthe earliest forms of life are assumed to have appeared.

**Augite:** Essential mineral in *mafic*↑ *igneous*↑ rocks and is also quite common in ultramafic rocks. It is a quite common *clinopyroxene*↑ rock with formula (Ca,Na)(Mg,Fe,Al,Ti)$(Si,Al)_2O_6$.

**Basalt:** General term referring to dark-coloured *mafic*↑ *igneous*↑ rocks, mostly composed of calcic *plagioclase*↑ and *clinopyroxene*↑; the fine-grained equivalent of *gabbro*↑.

**Biomarker:** Indicator of a biological state.

**Biosphere:** The global sum of all ecosystems. It can also be called the zone of life on Earth, a closed (apart from solar and cosmic radiation), and self-regulating system. is the global ecologicalsystem integrating all living beings and their relationships, including their interaction with the elements of the lithosphere, hydrosphere, and atmosphere.

**Birefrigence:** The optical property of a material having a refractive index that depends on the polarization and propagation direction of light.

**Bolometric luminosity:** A measurement of brightness. The difference in bolometric magnitude is related to the luminosity ratio

**Branching ratios:** In particle physics and nuclear physics, the branching fraction for a decay is the fraction of particles which decay by an individual decay mode with respect to the total number of particles decaying

**Breccia:** A coarse-grained clastic rock, composed of angular broken rock fragments held together by a mineral cement or in a fine-grained *matrix*↑.

**Calcite:** A common rock-forming mineral with a perfect rhombohedral cleavage, and general formula: $CaCO_3$.

**Cambrian explosion:** The relatively rapid appearance, around 530 million years ago, of most major animal phyla, as demonstrated in the fossil record, accompanied by major diversification of organisms including animals, phytoplanckton and calcimicrobes.

**Chondrite:** Primitive meteorites with contain glassy spherules or chondrules mostly composed of silicates in their inner structure.

**Chromite:** A mineral of the spinel group of general formula: $(Fe,Mg)(Cr,Al)_2O_4$. It could consist of iron: $FeCr_2O_4$ or magnesium $MgCr_2O_4$. When Al substitutes Cr, it is called hercynite: $FeAl_2O_4$

**Clinopyroxene:** A group name for *pyroxenes*↑ crystallizing in the monoclinic system and sometimes containing Ca with or without Al and the alkalies.

**Collisional excitation:** In astronomy, collisional excitation gives rise to spectral lines in the spectra of astronomical objects such as planetary nebulae and H

II regions. In these objects, most atoms are ionised by photons from hot stars embedded within the nebular gas, stripping away electrons. The emitted electrons, (called photoelectrons), may collide with atoms or ions within the gas, and excite them. When these excited atoms or ions revert to their ground state, they will emit a photon.

**Crossed molecular beam:** Chemical experiments where two beams of atoms or molecules are collided together to elucidate the dynamics of the chemical reaction, and can detect individual reactive collisions.

**Cumulate rock:** An *igneous*↑ rock formed by the accumulation of crystals that settle out from a magma by the action of gravity. Cumulate rocks are named according to their texture, and acumulate texture is diagnostic of the conditions of formation of this group of *igneous*↑ rocks.

**Cyanobacteria:** Phylum of bacteria that obtain their energy through photosynthesis. The name "cyanobacteria" comes from the color of the bacteria (blue).

**Degassing:** The removal of dissolved gases from liquids, especially water or aqueous solutions.

**Diabase:** An intrusive rock whose main components are labradorite and *pyroxene*↑ and which is characterized by having an *ophitic*↑ texture.

**Diaplectic:** Glasslike mineralogic features produced by shock waves in such a way that the characteristics of the liquid state are lacking. A diaplectic mineral has been disordered and deformed crystals have been modified by shock waves propagating into the mineral.

**Diffusion:** One of several transport phenomena that occur in nature. A distinguishing feature of diffusion is that it results in mixing or mass transport without requiring bulk motion.

**Dunite:** A periodotite in which the *mafic*↑ mineral is almost entirely *olivine*↑, with accessory *chromite*↑.

**Dwarf stars:** A star, such as the sun, having relatively low mass, small size, and average or below average luminosity.

**Eccentricity:** The orbital eccentricity of an astronomical object is a parameter that determines the amount by which its orbit around another body deviates from a perfect circle.

**Effective temperature:** The temperature of a black body that would emit the same total amount of electromagnetic radiation.[1] Effective temperature is often used as an estimate of a body's temperature when the body'semissivity curve (as a function of wavelength) is not known.

**Electrospray ionization (ESI):** Technique used in mass spectrometry to produce ions.

**Endogenous:** Proceeding from within; derived internally.

**Endothermic reactions:** A process or reaction in which the system absorbs energy from the surroundings in the form of heat.

**Enstatite:** A common rock-forming mineral of the *orthopyroxene*↑ group and general formula: $MgSiO_3$

**Enthalpy:** A measure of the total energy of a thermodynamic system.

**Entropy:** A thermodynamic property that is the measure of a system's thermal energy per unit temperature that is unavailable for doing useful work.
**Escape velocity:** The speed at which the kinetic energy plus the gravitational potential energy of an object is zero.[nb 1] It is the speed needed to "break free" from a gravitational field without further propulsion.
**Euhedral:** A mineral grain that is completely bounded by its own rational faces, and whose growth during crystallization was not interfered by adjacent grains.
**EUV irradiation:** Extreme ultraviolet radiation (EUV or XUV) is high-energy ultraviolet radiation, generally defined to be electromagnetic radiation in the part of the electromagnetic spectrum spanning wavelengths from 120 nm down to 10 nm, and therefore (by the Planck–Einstein equation) having photons with energies from 10 eV up to 124 eV (corresponding to 124–10 nm respectively). EUV is naturally generated by the solar corona and artificially by plasma and synchrotron light sources.
**Excited state:** Any quantum state of the system that has a higher energy than the ground state(that is, more energy than the absolute minimum)
**Exogenous:** Caused by factors or an agent from outside the organism or system
**Exoplanet:** Usual term to design an extrasolar planet, i.e. a planet found around a star different to our Sun.
**Exosphere:** The uppermost layer of Earth's atmosphere. In the exosphere the density is so low that particles collide only rarely.
**Exothermic reaction:** Chemical reaction that releases energy in the form of light or heat.
**Faint young Sun paradox:** Describes the apparent contradiction between observations of liquid water early in the Earth's history and the astrophysical expectation that the Sun's output would be only 70% as intense during that epoch as it is during the modern epoch. The issue was raised by astronomers Carl Sagan and George Mullen in 1972.[1] Explanations of this paradox have taken into account greenhouse effects, astrophysical influences, or a combination of the two.
**Fayalite:** A brown to black mineral of the *olivine*↑ group: $Fe_2SiO_4$.
**Feldspar:** A group of abundant rock-forming minerals of general formula: $Mal(Al,Si)_3O_8$, where M = K,Na,Ca,Ba,Rb,Sr, and Fe. Feldspars are the most widespread of any mineral group and constitute about 60% of the crusts of rocky planets.
**Fischer-Tropsch reaction:** Chemical process for the prouction of liquids hydrocarbons (gasolina, kerosene, gasoil and lubricants) from synthesis gas (CO and H2).
**Forsterite:** A white or yellow mineral of the *olivine*↑ group: $Mg_2SiO_4$. Use to be isomorphous with *fayalite*↑.
**Fusion crust:** A glassy thin layer produced by the cooling of viscous minerals produced by the ablation of a meteorite during its deceleration in the atmosphere of a planet. Its thickness constrains the outer region affected by the temperature peak induced by friction to less than one millimeter due to the low thermal conductivity of *chondrites*↑ or *achondrites*↑.
**Gabbro:** A group of basic intrusive *igneous*↑ rocks composed principally of basic *plagioclase*↑ and *clinopyroxene*↑, with or without *olivine*↑ and *orthopyroxene*↑.

**Gas giant:** Large planet that is not primarily composed of rock or other solid matter.
**Geo-corona:** The luminous part of the outermost region of the Earth's atmosphere, the exosphere. It is seen primarily via far-ultraviolet light (Lyman-alpha) from the Sun that is scattered from neutral hydrogen. It extends to at least 15.5 Earth radii.
**Gibbs energy:** A thermodynamic potential that measures the "useful" or process-initiating work obtainable from a thermodynamic system at a constant temperature and pressure (isothermal, isobaric)
**Glacial era:** A period of long-term reduction in the temperature of the Earth's surface and atmosphere, resulting in the presence or expansion of continental ice sheets, polar ice sheets and alpine glaciers.
**Haber process:** The industrial implementation of the reaction of nitrogen gas and hydrogen gas. It is the main industrial route to ammonia
**Hadean:** The first geologic eon of Earth and lies before the Archean
**Helioseismology:** The study of the propagation of wave oscillations, particularly acoustic pressure waves, in the Sun.
**Hematite:** A common Fe mineral with general formula: $\alpha - Fe_2O_3$
**Hollandite:** A silvery-gray to black mineral of general formula: $Ba(Mn^{+2}, Mn^{+4})_8O_{16}$.
**Homopause:** The level of transition between the homosphere and the heterosphere; it lies about 50–56 miles (80–90 km) above the earth. Also known as turbopause.
**Hot-jupiters:** A class of extrasolar planets whose characteristics are similar toJupiter, however, with high surface temperatures because they orbit very close to their parentstars,[6] between approximately 0.015 and 0.5 astronomical unit ($2.2 \times 10^6$ and $75 \times 10^6$ km) of their parent stars,[7] while Jupiter orbits its parent star (the Sun) at 5.2 astronomical units($780 \times 10^6$ km), causing low surface temperatures.
**Hydrolysis:** Cleavage of chemical bonds by the addition of water.
**Hydrosphere:** In physical geography describes the combined mass of water found on, under, and over the surface of a planet.
**Iddingsite:** A mixture of silicates (of ferric iron, calcium, and magnesium) formed by the alteration of *olivine*↑. It basically consists of a mixture of clay minerals, and iron oxides. As it has been found on Martian meteorites, its ages have been calculated to obtain absolute ages when liquid water was at or near the surface of Mars. Iddingsite forms from the weathering of *basalt*↑ in the presence of liquid water and can be described as a *phenocrist*↑, i.e. it has megascopically visible crystals in a fine-grained groundmass of a *porphyritic*↑ rock. Because iddingsite is constantly transforming it does not have a definite structure or a definite chemical composition. The chemical formula for iddingsite has been approximated as $MgO \cdot Fe_2O_3 \cdot 4H_2O$ where CaO can be substituted by MgO.
**Igneous rock:** Rocks that solidified from molten or partly molten material.
**Ilmenite:** An iron-black, opaque, and rhombohedral mineral with general formula: $FeTiO_3$.
**Interferometry:** A family of techniques in which waves, usually electromagnetic, are superimposed in order to extract information about the waves.

**Ionosphere:** A part of the upper atmosphere, from about 85 to 600 km altitude, comprising portions of the mesosphere,thermosphere and exosphere, distinguished because it is ionized by solar radiation. It plays an important part in atmospheric electricityand forms the inner edge of the magnetosphere.
**Isomers:** Compounds with the same molecular formula but different structural formulas.
**Isotopologues:** Molecules that differ only in their isotopic composition. Simply, the isotopologue of a chemical species has at least one atom with a different number of neutrons than the parent.
**Large convection cells:** A system in which a fluid is warmed, loses density and is forced into a region of greater density.
**Late heavy bombardment (LHB) period:** A period of time approximately 4.1 to 3.8 billion years ago (Ga) during which a large number of impact craters were formed on the Moon, and by inference on Earth, Mercury, Venus, and Mars as well.
**Lherzolitic:** Peridotite mainly composed of *olivine*↑, *orthopyroxene*↑, and *clinopyroxene*↑.
**Line-by-line radiative transfer model: LBLRTM** is an accurate, efficient and highly flexible model for calculating spectral transmittance and radiance.
**Lithosphere:** The rigid outermost shell of a rockyplanet. On Earth, it comprises the crust and the portion of the uppermantle that behaves elastically on time scales of thousands of years or greater.
**Lyman-$\alpha$ line:** A spectral line of hydrogen, or more generally of one-electron ions, in the Lyman series, emitted when the electron falls from the $n = 2$ orbital to the $n = 1$ orbital, where $n$ is the principal quantum number.
**Mafic:** An *igneous*↑ rock mainly composed of one or more ferromagnesian minerals.
**Magnetite:** A black, strongly magnetic, opaque mineral of the spinel group with general formula: (Fe,Mg)$Fe_2O_4$. The formula for magnetite may also be written as $FeO \cdot Fe_2O_3$, which is one part wüstite (FeO) and one part *hematite*↑ ($Fe_2O_3$).
**Magnetosphere:** Layer of the atmosphere formed when a stream of charged particles, such as the solar wind, interacts with and is deflected by the magnetic field of a planet or similar body. Earth is surrounded by a magnetosphere, as are the other planets with intrinsic magnetic fields: Mercury, Jupiter, Saturn, Uranus, and Neptune.
**Maskelynite:** Thetomorphic *plagioclase*↑ glass; common as meteorite mineral consisting of a shock-formed noncrystalline phase that results from vitrification of *plagioclase*↑ in rocks transfigured by shock waves and that retains the external features of crystalline *plagioclase*↑.
**Mass Independent Fractionation (MIF):** Any chemical or physical process that acts to separate isotopes, where the amount of separation does not scale in proportion with the difference in the masses of the isotopes.
**Matrix:** The finer-grained material enclosing, or filling the interstices between the larger grains or particles of a sedimentary rock, or meteorite.
**Merrilite:** A mineral with general formula: $Ca_9(Mg,Fe)Na(PO_4)_7$.

**Mesosphere:** Layer of the Earth's atmosphere that is directly above the stratosphere and directly below the thermosphere.
**Mesostasis:** The last formed interstitial materials, either glassy or aphanitic of an *igneous*↑ rock.
**Metasomatism:** The process of practically simultaneous capillary solution and deposition by which a new mineral of partly or wholly different chemical composition may grow in the body of an old mineral or mineral aggregate.
**Metastable states:** States of certain physical systems that can exist in long lived states that are less stable than the system's most stable state
**Metazoan:** A major group of multicellular, eukaryotic organisms of the kingdom Animalia or Metazoa.
**Methanogens:** Microorganisms that produce methane as a metabolic byproduct in anoxic conditions.
**Microphenocryst:** A small, conspicuous crystal present in a *porphyritic*↑ rock.
**Mixing ratio:** The abundance of one component of a mixture relative to that of all other components.
**M-star:** The spectral class of a star is a designated class of a star describing the ionization of its photosphere (what atomic excitations are most prominent in the light), giving an objective measure of the photosphere's temperature. Stars of spectral class M (M-star) have such low luminosities; there are none bright enough to see with the unaided eye.
**Nadir:** The direction pointing directly *below* a particular location; that is, it is one of two vertical directions at a specified location, orthogonal to a horizontal flat surface there
**Nebula:** An interstellar cloud of dust, hydrogen, helium and other ionized gases.
**Nitrogen fixation:** A process by which nitrogen $(N_2)$ in the atmosphere is converted into ammonia $(NH_3)$. Atmospheric nitrogen or elemental nitrogen is relatively inert: it does not easily react with other chemicals to form new compounds. Fixation processes free up the nitrogen atoms from their diatomic form $(N_2)$ to be used in other ways.
**Noachian epoch:** The oldest epoch in the geologic history of Mars. It extends back in time to the beginnings of the planet, and ended sometime between 3.8 and 3.5 billion years ago (according to accepted models)
**Olivine:** An orthorhombic magnesium iron mineral with general formula: $(M,Fe)_2SiO_4$. It is a common mineral in the Earth's subsurface but weathers quickly on the surface. It consists of the isomorphous solid-solution series *forsterite*↑-*fayalite*↑. The ratio of magnesium and iron varies between the two endmembers of the solid solution series: forsterite (Mg-endmember) and fayalite (Fe-endmember). Compositions of olivine are commonly expressed as molar percentages of *forsterite*↑ (Fo) and *fayalite*↑ (Fa) (e.g., $Fo_{70}Fa_{30}$). The melting temperature varies smoothly between the two endmembers, as do other properties.
**Olivine-phyric:** An *olivine*↑ formed by large crystals in a *porphyritic*↑ way.
**Ophitic:** A granular texture of an igneous rock in which lath-shaped *plagioclase*↑ crystals are partially or completely included in *pyroxene*↑ crystals, typically *augite*↑.

**Orbital periods:** The time taken for a given object to make one complete orbit about another object.
**Orthoclase:** A color-less, white, cream, or grey mineral of the alkali *feldspar*↑ group with general formula: $KalSi_3O_8$.
**Orthopyroxene:** A group name for *pyroxenes*↑ crystallizing in the orthorhombic system and usually containing no Ca and little or no Al.
**Outgassing:** The release of a gas that was dissolved, trapped, frozen or absorbed in some material.
**Palagonite:** An alteration product from the interaction of water with volcanic glass of chemical composition similar to basalt. Palagonite can also result from the interaction between water and basalt melt.
**Paleoclimatology:** The study of changes in climate taken on the scale of the entire history of Earth.
**Paleosol:** In Paleoclimatology refers to "fossil" soils buried within sedimentary or volcanic deposits from which we can infer valuable information of the environment in which such materials formed.
**Peridotite:** A general term for a coarse-grained *plutonic*↑ rock composed mainly of *olivine*↑ with or without other *mafic*↑ minerals like e.g. *pyroxenes*↑, amphiboles and micas.
**Phenocryst:** A relatively large, conspicuous crystal in porphyritic rock.
**Phosphate:** A mineral compound containing tetrahedral $PO_4^{-3}$ groups. Pyromorphite is a quite common example: $Pb_5(PO_4)_3Cl$
**Photolysis:** Photodissociation, photolysis, or photodecomposition is a chemical reaction in which a chemical compound is broken down by photons. It is defined as the interaction of one or more photons with one target molecule.
**Photoionization:** The physical process in which an incident photon ejects one or more electrons from an atom, ion or molecule
**Photon:** An elementary particle, the quantum of light and all other forms ofelectromagnetic radiation, and the force carrier for the electromagnetic force, even when static via virtual photons
**Pigeonite:** A mineral of the *clinopyroxene*↑ group with general formula: $(Mg,Fe^{+2},Ca)(Mg,Fe^{+2})Si_2O_6$. It is an intermediate in composition between clinoenstatite and diopside, and has little Ca, little or no Al, and less ferrous Fe than Mg.
**Plagioclase:** A group of triclinic *feldspars*↑ of general formula: (Na,Ca)Al(Si,Al) $Si_2O_8$. Rather than referring to a particular mineral with a specific chemical composition, plagioclase is a solid solution series of different compositional members. The series ranges from albite to anorthite endmembers (with respective compositions $NaAlSi_3O_8$ to $CaAl_2Si_2O_8$), where soNa and Ca can substitute for each other in the mineral's crystal lattice structure. Plagioclase is a major constituent mineral in the Earth's crust, and a major constituent of rock highlands on the Moon.
**Planetesimals:** Solid objects thought to exist in protoplanetary disks and in debris disks.
**Plutonic:** An *igneous*↑ rock formed at great depth.

**Polarizers:** An optical filter that passes light of a specific polarization and blocks waves of other polarizations
**Polymorph:** A crystal form of a substance that displays polymorphism.
**Porphyritic:** The texture of a rock in which larger crystals are set in a finer-grained groundmass, which may be crystalline, or glassy or both.
**Potencial vorticity:** A quantity which is proportional to the dot product of vorticity and stratification that, following a parcel of air or water, can only be changed by diabatic or frictional processes.
**Precambrian epoch:** The epoch that describes the large span of time in Earth's history before the current Phanerozoic Eon, and is a Supereon divided into several eons of the geologic time scale. It spans from the formation of Earth about 4,570 Ma (million years) ago to the beginning of the Cambrian Period, about 542 Ma, when macroscopic hard-shelled animals first appeared in abundance.
**Pressure gradient:** A physical quantity that describes which direction and at what rate the pressure changes the most rapidly around a particular location (Pa/m).
**Primordial terrestrial atmosphere, primeval atmosphere or protoasmosphere:** The primeval atmosphere was composed mostly of water ($H_2O$), carbon dioxide ($CO_2$) and monoxide (CO), molecular nitrogen ($N_2$) and molecular hydrogen ($H_2$), and hydrogen chloride (HCl) outgassed from molten rock, with only traces of reactive molecular oxygen ($O_2$)
**Prokaryotes:** A group of organisms whose cells lack a cell nucleus(karyon), or any other membrane-bound organelles.
**Proterozoic:** A geological eon representing the time just before the proliferation of complex life on Earth.
**Protoplanetary disk:** A rotating circumstellar disk of dense gas surrounding a young newly formed star, a T Tauri star, or Herbig Ae/Be star. The protoplanetary disk may be considered an accretion disc because gaseous material may be falling from the inner edge of the disk onto the surface of the star, but this process should not be confused with the accretion process thought to build up the planets themselves
**Pyrite:** A common isometric mineral that has general formula: $FeS_2$. It is dimorphous with marcasite and often contains small amounts of other metals.
**Pyrolisis:** A thermochemical decomposition of organic material at elevated temperatures without the participation of oxygen.
**Pyroxene:** A group of dark rock-forming silicate minerals, closely related in crystal form and composition and having the general formula: ABSi2O6, where $A = Ca$, Na, Mg or $Fe^{+2}$, and $B = Mg$, $Fe^{+2}$, $Fe^{+3}$, Fe, Cr, Mn or Al.
**Pyrrhotite:** A common red-brown to bronze pseudohexagonal mineral: $Fe_{1-x}S$ that has a defect structure in which some of the ferrous ions are lacking.
**Radiative transfer analysis:** It describes the way in which radiation is affected as it travels through a material medium.
**Radiative transfer model:** Code or simulator calculates radiative transfer of electromagnetic radiation through a planetary atmosphere, such as the Earth's.

**Radioisotopes:** An atom with an unstable nucleus, characterized by excess energy available to be imparted either to a newly created radiation particle within the nucleus or via internal conversion.
**Rate coefficient:** In chemical kinetics a reaction rate coeffient $k$ or $\lambda$ quantifies the speed of a chemical reaction.·
**Rayleigh scattering:** Named after the British physicist Lord Rayleigh,[1] is the elastic scattering of light or other electromagnetic radiation by particles much smaller than the wavelength of the light.
**Rocky planets:** A planet that is composed primarily of silicate rocks or metals. Within the Solar System, the terrestrial planets are the planets closest to the Sun.
**Rydberg state:** An electronically excited state of an atom with energy that follow the Rydberg formula as they converge on an ionic state with an ionization energy.
**Sedimentary rock:** A rock formed by the deposition of sediment by a geologic process: vulcanism, erosion, etc.
**Sensitivity:** A measure of the proportion of actual positives which are correctly identified as such.
**Serpentine:** A rock consisting almost wholly of serpentine-group minerals like e.g. antigorite and chrysotile or lizardite, derived by alteration of ferromagnesian silicate minerals.
**Serpentinisation:** The process of hydrothermal alteration by which Mg-rich silicate minerals like e.g. *olivine*↑, *pyroxenes*↑ and amphiboles in ultrabasic rocks are converted into or replaced by *serpentine*↑ minerals
**Shale:** Fine-grained, *clastic*↑ sedimentary rock composed of mud that is a mix of flakes of clay minerals and tiny fragments of other minerals.
**Siderite:** A rhombohedral mineral of the calcite group with general formula: $FeCO_3$.
**Silica:** The chemically resistant dioxide of silicon that is omnipresent in *achondritic*↑ meteorites, and has the general formula: $SiO_2$.
**S/N:** Signal-to-noise ratio
**Spectrum:** A condition that is not limited to a specific set of values but can vary infinitely within a continuum.
**Stochastic processes:** A collection of random variables; this is often used to represent the evolution of some random value, or system, over time.
**Stoichiometry:** A branch of chemistry that deals with the relative quantities of reactants and products in chemical reactions. In a balanced chemical reaction, the relations among quantities of reactants and products typically form a ratio of whole numbers.activation energy of the reaction
**Stratosphere:** The second major layer of Earth's atmosphere, just above the troposphere, and below the mesosphere
**Stromatolite:** Layered accretionary structures formed in shallow water by the trapping, binding and cementation of sedimentary grains by biofilms of microorganisms, especially cyanobacteria (commonly known as blue-green algae). Stromatolites provide some of the most ancient records of life on Earth by fossil remains which date back more than 3.5 billion years ago.

**Sulfide:** A mineral compound characterized by the sulfate radical $SO_4$. Two main types exist: anhydrous sulfates as barite $BaSO_4$ or hydrous ones like e.g. gypsum: $CaSO_4 \cdot 2H_2O$

**Thermal escape:** The loss of planetary atmospheric gases to outer space.

**Thermosphere (exobase):** The layer of the Earth's atmosphere directly above the mesosphere and directly below theexosphere. Within this layer, ultraviolet radiation (UV) causes ionization

**Tholins:** A heteropolymer molecule formed by solar ultraviolet irradiation of simple organic compounds such as methane or ethane. Tholins do not form naturally on modern-day Earth, but are found in great abundance on the surface of icy bodies in the outer solar system. They usually have a reddish-brown appearance.

**Tides:** The rise and fall of sea levels caused by the combined effects of the gravitational forces exerted by theMoon and the Sun and the rotation of the Earth.

**Trace specie:** A specie that has an average concentration of less than 100 parts per million measured in atomic count or less than 100 micrograms per gram.

**Troposphere:** The lowest portion of Earth's atmosphere. It contains approximately 80% of the atmosphere's mass and 99% of its water vapor and aerosols

**Ultramafic rock:** Igneous and meta-igneous rocks with very low silica content (less than 45%), generally $> 18\%$ MgO, high FeO, low potassium, and are composed of usually greater than 90% mafic minerals (dark colored, high magnesium and iron content). The Earth's mantle is composed of ultramafic rocks.

**Uraninite:** A radioactive, uranium-rich mineral and ore with a chemical composition that is largely $UO_2$, but also contains $UO_3$ and oxides of lead, thorium, and rare earth elements. It is most commonly known as **pitchblende.**

**Valence state:** The number of valence bonds[1] a given atom has formed, or can form, with one or more other atoms.

**Vertical circulation patterns:** The general geometric configuration of atmospheric circulation usually applied, in synoptic meteorology, to the large-scale features of synoptic charts and mean charts.

**Volatiles:** Chemical elements exhibiting low boiling points.

**Vortex core line:** A line-like feature tracing the center of a vortex within a velocity field.

**VUV radiation:** Vacuum UltraViolet radiation.

**Wavenumber (wavelength):** The spatial frequency of a wave. It can be envisaged as the number of waves that exist over a specified distance

**Wehrlite:** A *plutonic*↑ rock, typically a *peridotite*↑ composed of *olivine*↑ and *clinopyroxene*↑ with common accessory opaque oxides.

**Zenith angle:** An imaginary point directly "above" a particular location, on the imaginary celestial sphere. "Above" means in the vertical direction opposite to the apparent gravitational force at that location.

**Zircon:** A mineral belonging to the group of nesosilicates. Its chemical name is zirconium silicate and its corresponding chemical formula is $ZrSiO_4$.

# About the Editors

Josep M. Trigo-Rodriguez started at Castelló Planetarium in 1990, and he spent thirteen years working in the development of programs and public outreach. The last four years he has spent as associate professor at University Jaume I of Castelló, giving lectures on Thermodynamics and Physics. In the meantime, Dr. Trigo-Rodriguez obtained his degree in Physics from the University of Valencia in 1997 and his Ph.D. in Theoretical Physics (Astrophysics) in 2002 under the direction of Prof. Jordi Llorca (UPC) and Prof. Juan Fabregat (UV). In 2003 he obtained a Spanish grant that allowed him to continue his career in a postdoctoral position at the Institute of Geophysics & Planetary Physics of UCLA. After almost three years working on primitive meteorites he returned to Barcelona in 2006 with a JdC grant in order to join the Institute of Space Sciences (CSIC-IEEC). In 2009, he won his position as Tenured Scientist of the Consejo Superior de Investigaciones Cientificas (CSIC) at that research institute. (http://www.spmn.uji.es/ESP/trigo.html)

François Raulin received his diploma from the Ecole Supérieure de Physique et Chimie Industrielles de la Ville de Paris in 1969, and a Doctorat d'Etat (on the role of sulfur in prebiotic chemistry) from the Université Paris 6 in 1976. He was research fellow at Carl Sagan's Laboratory, Cornell University, in 1970–71, assistant Professor at University Paris Val de Marne until 1978 and CNRS/NSF post-doctoral fellow at Cyril Ponnamperuma's Laboratory of Chemical Evolution, University of Maryland. F. Raulin is the Co-I of CIRS (Cassini), ACP and GC-MS (Huygens). He is also IDS of the Cassini-Huygens mission (Titan's Chemistry and Exobiology) and Col.I of the COSAC and COSIMA experiments of the Rosetta European cometary mission. He is Deputy team leader of the MOMA experiment of the ExoMars mission.

Conor Nixon holds a B.A. in Natural sciences from the University of Cambridge and a Doctorate in Planetary Science from the University of Oxford, where his thesis was entitled 'Remote Sounding of the Atmosphere of Titan.' Since graduating he has worked on the science team of the Cassini spacecraft CIRA instrument at NASA Goddard Space Flight Center in Greenbelt, Maryland. His research interests are

J.M. Trigo-Rodriguez et al. (eds.), *The Early Evolution of the Atmospheres of Terrestrial Planets*, Astrophysics and Space Science Proceedings 35,
DOI 10.1007/978-1-4614-5191-4, © Springer Science+Business Media New York 2013

focused on understanding the chemistry, dynamics, origin, and evolution of outer planetary atmospheres, in particular Jupiter, Saturn, and Titan.

Christian Muller is a science coordinator and knowledge manager at B.USOC (Belgium Users Support and Operation Center). The B.USOC specializes in support to manned space flight and also supports BELSPO, the Belgian Science Policy Office. In the near future, B.USOC support will be extended to international treaties, including treaties on environment, Antarctica, the ocean and other federal Belgian federal matters. He received his Ph.D. in 1976 under the direction of Prof. Baron Nicolet.

The volume editors have all been involved in planetary science and astrobiology research for several decades. Additionally, the workshop participants contributing to this book have remarkable careers, having produced a good number of high-quality written papers under peer-review process, and also provided excellent talks during the workshop.